



# HHS Public Access

Author manuscript

*Chem Rev.* Author manuscript; available in PMC 2023 January 26.

Published in final edited form as:

*Chem Rev.* 2022 January 26; 122(2): 2353–2428. doi:10.1021/acs.chemrev.1c00444.

## Strategies to Generate Nitrogen-Centered Radicals That May Rely on Photoredox Catalysis: Development in Reaction Methodology and Applications in Organic Synthesis

Kitae Kwon, R. Thomas Simons, Meganathan Nandakumar, Jennifer L. Roizen

Duke University, Department of Chemistry, Box 90346, Durham, NC, 27708-0354, United States

### Abstract

For more than seventy years, nitrogen-centered radicals have been recognized as potent synthetic intermediates. This review is a survey designed for use by chemists engaged in target-oriented synthesis. This review summarizes the recent paradigm-shift in access to and application of *N*-centered radicals enabled by visible-light photocatalysis. This shift broadens and streamlines access to many small molecules because the conditions are mild. Explicit attention is paid to innovative advances in N–X bonds as radical precursors, where X = Cl, N, S, O, and H. For clarity, key mechanistic data is noted, where available. Synthetic applications and limitations are summarized to illuminate the tremendous utility of photocatalytically-generated nitrogen-centered radicals.

### Graphical Abstract

---

j.roizen@duke.edu .

Author Contributions

All authors provided initial drafts of their biographies and contributed to all sections of the manuscript.

Jennifer L. Roizen provided extensive feedback on and revised all sections of the manuscript.

Initial figures and text were authored by:

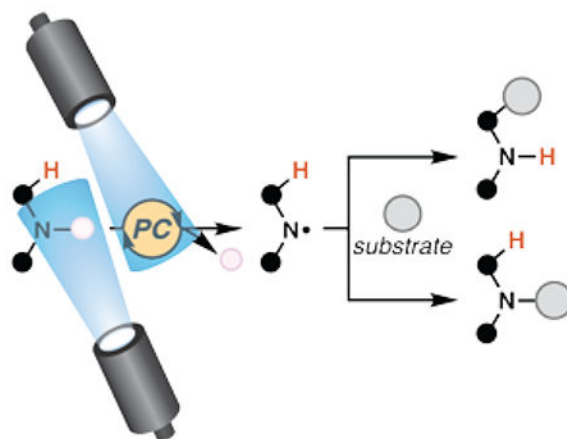
Kitae Kwon for Sections 1, 5, 7 and TOC graphic;

R. Thomas Simons for Sections 1–4, 6.1 and 6.3–6.4;

Meganathan Nandakumar for Sections 6.2, 6.5, photocatalyst figures for Section 1, and the abbreviations.

The authors declare no competing financial interest.

A version of Sections 1–4, 6.1, 6.3–6.4, and 7 have been included in R. Thomas Simons' Thesis following initial submission of this manuscript.<sup>401</sup>



## 1. INTRODUCTION

Nitrogen-centered radical species are highly reactive, promising synthetic intermediates.<sup>1</sup> Given their potential, Zard remarked that paucity in early reports detailing the use of nitrogen-centered radical species as synthetic tool can be attributed to “... a dearth of convenient routes for generating these reactive species and a lack of awareness concerning their reactivity.”<sup>1</sup> Indeed, harsh thermal or photonic reaction conditions, or a toxic radical initiator were necessary to generate these intermediates. In the late 2000s, investigations into reactions that rely on nitrogen-centered radical species underwent a tectonic shift when organic chemists adopted visible light-mediated photocatalysis as a practical strategy to construct organic molecules.<sup>2</sup>

Reactions involving photocatalytically-generated, nitrogen-centered radicals may proceed mechanistically through: a closed, formal catalytic cycle where each molecule of product formed requires direct interaction with a photocatalyst and may include a second interaction for closure of the photocatalytic cycle (Scheme 1, path A), a radical chain where the radical of one molecule of substrate engages another to perpetuate a chain reaction (Scheme 1, path B), or some combination thereof.<sup>3,4</sup> To distinguish between these processes, measurements of a reaction’s quantum yield can provide evidence supporting some extent of radical chain propagation.<sup>5</sup> Evidence for or against the kinetic feasibility of a given reaction step can be derived from characterization of the excited state photocatalyst and its interactions with reaction components, often by transient absorption spectroscopy (TAS) and Stern-Volmer quenching experiments.<sup>6,7</sup> Additional data can support or refute proposed mechanistic steps based on electrochemical measurements of oxidation and reduction potentials for reaction components. Published values for a broad array of organic molecules are available; a compilation has been included of known ground and excited state potentials for relevant photocatalysts (Figures 1–4). In many cases, data is unavailable to distinguish between these processes. So several processes described herein as “photoredox catalyzed”<sup>47,48</sup> may not technically be catalyzed, but instead simply depend on the combination of visible light irradiation and inclusion of low- to sub-mol-percent amounts of photocatalysis-capable compound.

Regardless of their role in a particular reaction, photocatalysis-capable compounds have broadly enabled both novel reactivity and new pathways to known reactivity. Often capable of serving as potent oxidants, reductants, and energy-transfer agents, photocatalysts are generally bench-stable with little to no toxicity and available for commercial purchase. Moreover, photocatalytic reactions are applicable in a vast array of settings, from process-scale and flow-reactor syntheses<sup>2,9,43</sup> to picomolar high-throughput screening.<sup>44,45</sup> Development of these technologies continues to accelerate their broader adoption.

Ultimately, the glow of photoredox catalysis has illuminated new corridors through which the energy of visible-light can be used to mediate access to versatile nitrogen-centered radical intermediates. Photocatalysis has enabled otherwise rare reaction manifolds, including: the C–H functionalization of (hetero)arenes (Section 2, Section 5, Section 6.3), intermolecular, anti-Markovnikov amino-difunctionalization of alkenes (Sections 2–6.3, Section 6.5), and guided, intermolecular Giese conjugate addition reactions (Section 5.5, Section 6.2, Section 6.4). Furthermore, the array of new bond disconnections leading to nitrogen-centered radicals enabled by photoredox catalysis (Section 4, Section 5, Section 6) has generated a veritable menu of options for viable precursors, each with unique properties capable of enabling reactivity in diverse reaction environments, while tremendous strides have been made in the fundamental understanding of processes such as proton-coupled electron transfer (PCET) (Sections 6.2–6.3). As reports of this type continue to proliferate, they further catalyze interest and innovation in the important field of photocatalysis.

This review constitutes a survey of transformations that may capitalize on visible-light photoredox catalysis to access nitrogen-centered radical intermediates through the direct interaction of an excited-state photosensitizer and a substrate. The reactions discussed throughout this review are selected to include those expected to generate nitrogen-centered radicals under conditions requiring both visible light irradiation and catalytic quantities of a photocatalysis-capable compound. Generally, manuscripts where fulfillment of these criteria is ambiguous or contradicted by the available data are not included. The photochemical and photophysical underpinnings of these processes have been well-reviewed by others,<sup>2,46,47,48</sup> so, when available, mechanistic data has been included to allow readers to understand the strength of associated mechanistic proposals.

This review is organized by radical precursor, focusing on the pioneering inventions of viable precursors that rely on cleavage of N–Cl, N–S, N–N, N–O or N–H bonds to generate the critical putative nitrogen-centered radical intermediates. For each addressed technology, attention is paid to the process of nitrogen-centered radical generation, any information that can be used to distinguish between radical-chain propagation processes and truly catalytic processes, and the synthetic advantages and limitations afforded by the associated method. This review focuses principally on reactions that are thought to initially rely on free-radical intermediates, and, for the most part, does not discuss photosensitized or photocatalyzed nickel-mediated transformations,<sup>49,50</sup> many of which appear to rely on nitrogen-centered radicals as intermediates.<sup>51,52,53,54,55,56,57</sup> Additionally, it does not address photoredox-mediated reactions that employ tertiary amines as reagents.<sup>58,59</sup> Notably, related, focused review articles cover a subset of similar topics;<sup>60, 61, 62, 63, 64, 65</sup> however, there is no

comprehensive review article that unites these topics. Accordingly, this review aims to deliver a comprehensive overview of investigations on this topic.

## 2. NITROGEN-CENTERED RADICALS CAN BE GENERATED FROM NITROGEN–CHLORINE BONDS IN THE PRESENCE OF PHOTOREDOX CATALYSTS

For more than a hundred years, nitrogen–halogen bonds have been known precursors to  $\delta$ -functionalized products as in the course of Hofmann–Löffler–Freitag (HLF) reactions.<sup>66,67</sup> Investigations into the mechanism of this class of reactions were not reported until the mid-twentieth century with the work of Wawzonek and Thellan, who proposed a radical mechanism based on the importance of radical initiators like hydrogen peroxide or visible light irradiation.<sup>68</sup> Their proposal of a radical-chain propagation mechanism was later confirmed through extensive investigations by Corey and Hertler.<sup>69</sup> While HLF reactions have found broad synthetic utility, the ability to derive the key nitrogen-centered radical under neutral and room temperature conditions has been the subject of continuing research in the intervening decades. Pre-installation of the nitrogen-halogen bond has allowed for solely visible-light-initiated HLF-type reactions for a variety of nitrogen-containing functional groups, including amides and sulfamate esters.<sup>70, 71, 72</sup> Other functional groups, such as *N*-chlorosulfonamides, are not reactive under the same room temperature, solely visible-light-initiated conditions, instead requiring ultraviolet irradiation to induce photolysis.<sup>70, 73, 74</sup> In 2015, S. Yu and Qin disclosed a system for  $\delta$ -C(sp<sup>3</sup>)–H chlorination (Scheme 2) that relies on a mild light source and iridium photocatalyst, and may be photoredox-initiated or mediated.<sup>75</sup> Indeed, in the presence of visible light irradiation, the photoexcited iridium catalyst [Ir(ppy)<sub>2</sub>bpy]PF<sub>6</sub> can be quenched by *N*-chlorosulfonamide **1** to produce a chloride anion, oxidized Ir(IV), and *N*-centered radical intermediate **3**. After this point, the *N*-centered radical intermediate **3** is expected to rapidly proceed through a 1,5-HAT to give the carbon-centered radical intermediate **4**, which can feasibly engage in one or more productive reaction pathways depending on the particular substrate. From the carbon-centered radical intermediate **4**, the reaction can proceed directly to the chlorinated product **2** by radical-chain propagation (Scheme 2, path a)<sup>69</sup> through abstraction of the chlorine present in another molecule of substrate **1**. While “light-on, light off” experiments conducted by Qin and Yu showed light to be required for significant reaction progress, it is noteworthy that this does not preclude a radical chain propagation mechanism.<sup>3</sup> With more oxidatively labile carbon-centered radical intermediates, a mechanistic scenario has not been excluded: it may be theoretically possible that these alkyl radicals are oxidized to cations, which are then trapped by chloride in radical-polar crossover process. Specifically, both reaction pathways are plausible in the production of  $\delta$ -chlorinated product **2a**, as the resonance stabilization afforded by the benzylic position should result in a relatively low oxidation potential (oxidation of secondary benzylic radical PhCH•CH<sub>3</sub> E<sub>p/2</sub><sup>ox</sup> = +0.37 V vs SCE).<sup>76</sup> By contrast, the demonstrated reactivity under the same conditions to give the primary  $\delta$ -chlorinated product **2b** could indicate an efficient radical chain propagation mechanism, as the oxidation of primary alkyl radical of type **4** where R = H would be thermodynamically challenging.

Subsequent research from other laboratories suggests a radical chain propagation mechanism in photoredox-mediated, sulfonamide-guided chlorination reactions (Scheme 3).<sup>77</sup> In W. Yu and co-workers recent disclosure of a procedure for *in situ*-generation the nitrogen-chlorine bond, the quantum yield of the sulfonamide-guided chlorination when employing a preformed N–Cl bond was found to be  $(\phi) = 3.23$ , meaning an average of 3.23 molecules of product were formed per absorbed photon. This result provides substantial evidence for a radical-chain propagation mechanism in sulfonamide guided-chlorination reactions.

*N*-chlorosulfonamides have also been employed to chlorosulfonamidate unactivated terminal olefins (Scheme 4).<sup>78</sup> Under visible-light irradiation and in the presence of an iridium photocatalyst, *N*-chloro-*N*-methyl toluenesulfonamide **9** engages in chlorosulfonamidation of terminal olefins **8** and ind-1-ene, with sulfonamidation occurring exclusively at the terminal carbon. Some variation in substitution at the olefin is tolerated, with styrene yielding chlorosulfonamidated product **10a** in 78% yield and oct-1-ene yielding product **10b** in 64% yield. This reaction, however, relies on secondary *N*-chlorosulfonamide substrates, and does not engage electron-deficient olefins. As will be observed in numerous examples throughout this review, amidyl radicals, and the electronically similar sulfonamidyl radicals, are electrophilic, which influences reaction selectivity, particularly when engaged in intermolecular 1,2-difunctionalization of alkenes. The electrophilic character of amidyl radicals has been investigated by Newcomb and co-workers, and the reality of this character is borne out through the complete regioselectivity reported in this investigation and others like it.<sup>79,80</sup>

While *N*-chlorosulfoximines have long been known to engage in intermolecular 1,2-difunctionalization of electron-rich olefins *via* UV-irradiation or radical initiators,<sup>81</sup> recent methods employing photoredox catalysts have enabled similar reactivity under room-temperature, visible-light irradiation (Scheme 5).<sup>82</sup> Using a photo-excited ruthenium complex and organic base in acetonitrile, *N*-chlorosulfoximine **II** reacts with an excess of styrene **12** to furnish 1,2-difunctionalized products, like **13a**. Across substrates **13a–13c**, reaction efficiency decreases in parallel with the extent of alkane fluorination, underscoring the apparent necessity of an *S*-fluoroalkyl substituent for efficient application of this process.

Photoredox-capable complexes appear important to a visible light-induced *N*-arylation utilizing *N*-chloroamines as substrates and benzoxazoles as radical trapping agents (Table 1).<sup>83</sup> The mechanism for this reaction is not well explored.

Photoredox catalysis driven by visible light irradiation has also been implemented to convert *N*-chlorophthalimides **14** to imidyl radicals for use in an arene imidation reaction (Table 2, entries 1–2).<sup>84</sup> The conditions can be adapted to permit *in situ* formation of *N*-chlorophthalimide (entries 3–4) with a slightly diminished yield. This use of *N*-chlorophthalimide was disclosed within months of analogous methods for arene imidation that rely on an *N*-trifluoroacetoxyphthalimide<sup>85</sup> and an *N*-succinimidyl perester<sup>86</sup> under photoredox and electrochemical regimes, respectively. Consistent with other investigations, *N*-acetoxyphthalimide is an inefficient nitrogen source under these reaction conditions (entry

5).<sup>85</sup> Similarly, sulfonate-based leaving groups (entries 6–8), as well as other halides (entries 9–10), are inferior substitutes for the chlorine atom.

These reactions<sup>84, 85</sup> are proposed to rely on strongly reducing photocatalyst Ir(dFppy)<sub>3</sub> or Ir(ppy)<sub>3</sub> to access critical phthalimidyl radical **17** with a chloride or trifluoroacetoxy anion as a byproduct (Scheme 6). With *N*-chlorophthalimide (**14a**), the viability of this mechanistic step is supported by data showing that *N*-chlorophthalimide (**14a**) quenches the photoexcited [Ir<sup>III</sup>]<sup>\*</sup> in a concentration dependent manner ( $K_q = 2.6 \times 10^8 \text{ M}^{-1} \text{ s}^{-1}$ )<sup>84</sup> and is thermodynamically feasible ( $E_{p/z}(\text{Ir}^{\text{IV}}/\text{Ir}^{\text{III}*}) = -1.57 \text{ V vs SCE}$ ; <sup>17</sup>  $E_p(\text{14a}) = -0.45 \text{ V vs SCE}$  in CH<sub>3</sub>CN<sup>87</sup>). Resultant *N*-centered radical **17** is proposed to add into the arene's  $\pi$ -system. Additional support for this mechanism comes from kinetic isotope experiments employing a 1:1 ratio of C<sub>6</sub>H<sub>6</sub>:C<sub>6</sub>D<sub>6</sub> which gave a kinetic isotope effect measurement of  $K_{H/D} = 1.13$ ;<sup>84</sup> this value is consistent with those measured in electrophilic aromatic substitution and related radical aromatic substitution reactions, indicating the deprotonation step likely occurs after the rate-determining step.<sup>88</sup> The authors propose the photocatalytic cycle to be closed by oxidation of the resonance-stabilized, carbon-centered radical **18** to give cationic Wheland intermediate **19**, which is poised for deprotonation to give desired product **16** in modest to good yields. Absent iridium catalyst and acetic acid, only 8% yield of the desired product is isolated, indicating that use of a photoredox catalyst is necessary to access the desired product in synthetically useful yields.

Whereas substrates such as *N*-chlorosulfonamides were previously only engaged under ultraviolet irradiation, with the introduction of photocatalysts to initiate and perpetuate reactions, similar transformation can be affected at ambient temperature and with visible light irradiation. Owing to these mild conditions, radical-mediated reactions have become more broadly synthetically viable. Under visible light, photosensitized or catalyzed processes harness *N*-chlorinated precursors to nitrogen-centered radicals in alkene 1,2-chloroamination reactions, directed C–H functionalization reactions of alkanes, and intermolecular C–H imination of arenes. These constitute a small subset of the technologies unlocked through photocatalytic or photosensitized generation of nitrogen-centered radicals.

### 3. NITROGEN-CENTERED RADICALS CAN BE GENERATED FROM NITROGEN–NITROGEN BONDS WITHIN *N*-AMINOPYRIDINIUM SALTS IN THE PRESENCE OF PHOTOREDOX CATALYSTS<sup>89,90</sup>

Nitrogen–nitrogen bonds are not often formed or cleaved in fine chemical synthesis, yet nitrogen–nitrogen bond cleavage is a viable path to a variety of *N*-centered radicals. In 2005, Studer and co-workers reported carbamate-masked 3-amino-1,4-cyclohexadienes **20** as stable precursors to nitrogen-centered radicals (Figure 5).<sup>91</sup> These were further developed into 1-amino-Hantzsch-type dihydropyridine esters **21**.<sup>92</sup> Both of these were, however, employed using traditional radical initiators. Photosensitizers were used to engage this category of nitrogen-radical precursor by the 2015 development of aminopyridinium salts **22a**.

In one of the first known examples of photoredox-driven generation of a nitrogen-centered radicals from N–N bond cleavage, *N*-aminopyridinium salts **14b** serve as precursors for radical C–H amination of (hetero)arenes (Scheme 7–8).<sup>93</sup> These salts have a relatively low reduction of potential ( $E_{\text{p}}^{\text{red}}(\mathbf{14b}) = -0.75 \text{ V vs SCE}$ ) and their reduction by photoexcited ruthenium catalyst ( $E_{1/2}(\text{Ru}^{\text{II}*}/\text{Ru}^{\text{III}}) = -0.81 \text{ V vs SCE}$ ) is thermodynamically favorable.<sup>94</sup> Under visible, blue light irradiation, slightly elevated temperatures, and in the presence of 4 Å molecular sieves, amino-pyridinium salt **14b** can be reduced, releasing 2,4,6-collidine and phthalimide radical **17**. Radical species **17** can then react with the excess benzene **15**, as had already been observed in related systems with *N*-acyloxyphthalimides (vide infra)<sup>85,95</sup> and *N*-chlorophthalimides (vide supra),<sup>84</sup> to access dearomatized radical species **18**. Subsequent oxidation to **19** and deprotonation, likely by 2,4,6-collidine, provides *N*-phenylphthalimide (**16**) in modest yield. A unique benefit of this approach is the concurrent, stoichiometric production of pyridyl base, which eliminates the need to add exogenous base in this reaction (compare to Scheme 6).<sup>84</sup>

Under related conditions, Studer and co-workers extended their *N*-aminopyridinium salt-generated radicals to engage in direct C(2)-amidation of *N*-methyl indoles and pyrroles (Scheme 8).<sup>93</sup> Employing the same ruthenium photocatalyst in acetonitrile, use of two equivalents of *N*-aminopyridinium salts based on *N*-(methyl)toluenesulfonamide or *N*-methyl-*Boc*-amine to give indole-derived products **24a** and **24c**, as well as pyrrole-derived **24b**. These reactions (Scheme 7–8) are the first reported example of photoredox-enabled generation of nitrogen-centered radicals from the controlled, unsymmetric breaking of N–N bonds. Moreover, the successful use of an *N*-*Boc*-amine as a nitrogen-centered radical agent was unprecedented in photoredox chemistry prior to this publication.

Nitrogen-centered radicals, derived from aminopyridinium salts engage in regioselective aminohydroxylation of olefins in the presence of visible light and a photosensitizer, with amination occurring at the less substituted carbon of the parent olefin, yielding products **25**. (Scheme 9).<sup>96</sup> With a slight excess of aminopyridinium salt **22b** and in a 9:1 mixture of acetone and water, photoexcited iridium species is proposed to engage in a single-electron reduction of the *N*–*N* bond to produce sulfamyl radical **26** and pyridine. This step is both thermodynamically feasible ( $E_{\text{p}}^{\text{red}}(\mathbf{22b}) = -0.80 \text{ V vs SCE}$ ) for photoexcited iridium ( $E_{1/2}(\text{Ir}^{\text{III}*}/\text{Ir}^{\text{IV}}) = -1.73 \text{ V vs SCE}$ )<sup>16</sup> and kinetically feasible ( $K_{\text{q}} = 6.0 \times 10^3 \text{ M}^{-1}\text{s}^{-1}$ ) based on Stern-Volmer quenching analysis. The nitrogen-centered radical then adds to the less-substituted carbon of the olefin to give carbon-centered radical intermediate **27**. Benzylic radical **27** may then be converted by oxidized iridium species to aromatic-stabilized carbocation intermediate **28**. In the presence of pyridine and water, a combination of nucleophilic attack by water or hydroxide and deprotonation by pyridine yields desired product **25** in 85% yield.

Expanding from this reaction (Scheme 9), amidohydroxylation is feasible using amidopyridinium salts **29** as nitrogen sources to furnish amide- and carbamate-functionalized products, **30a** and **30b**, respectively. (Scheme 10).<sup>97</sup> These nitrogen sources are viable owing to inclusion in the reaction of a catalytic amount of scandium (III) triflate, which is proposed to act as a Lewis acid, complexing with amidopyridines **29** and lowering the thermodynamic barrier for reduction of the nitrogen–nitrogen bond. The reaction does

not proceed in the absence of light, iridium photocatalyst, or scandium (III) triflate, which is consistent with the proposed roles of these reagents and conditions in the reaction.

In 2018, Xu, Hu, and co-workers disclosed a set of conditions for aminohalogenation of styrenes employing sulfonamide-based aminopyridinium salt **22b** and nucleophilic halogen sources (Scheme 11). Under blue light irradiation at room temperature, the photoexcited iridium catalyst ( $[\text{Ir}(\text{ppy})_2\text{dtbbpy}]\text{PF}_6$ ) can generate intermediates analogous to those described above (Scheme 9, intermediates **26**, **27**, and **28**). In the presence of nucleophilic halides, such as Olah's reagent (pyridine $\cdot$ 9(HF)), aminofluorination product **31a** can be produced in very good yields; while similarly, pyridine $\cdot$ (HCl) reacts to give aminochlorination product **31b** in a somewhat reduced 66% yield. Substitution of the halide sources with pyridine $\cdot$ (HBr) does produce aminobromination product **31c**, however only at a heavily reduced 17% yield

Under related conditions, aminopyridinium salt **22b** engages in diastereoselective aziridination of  $\beta$ -methylstyrenes **32** (Scheme 12).<sup>98</sup> Using a modest excess of dibasic potassium phosphate and aminopyridinium salt **22b** in dichloromethane with an iridium photocatalyst under blue light irradiation, mixtures of *E*- and *Z*-styrenes are aziridinated in good yields with >20:1 dr for *trans*-aziridines containing an inductively deactivating group (i.e., **33a** and **33b**). Somewhat unexpectedly, a product derived from styrenes bearing an inductively donating tolyl group (**33c**), however, does not react as readily, with substantially reduced yields and a modest 1.5:1 dr biased toward the *cis*-aziridine product instead.

Aminopyridinium salts have also been employed to produce  $\alpha$ -sulfamyl-containing carbonyl compounds from *O*-protected enolates (Scheme 13).<sup>99</sup> Using primarily *O*-acyl enolates **34**, the reaction proceeds with photoexcited  $\text{Ir}(\text{ppy})_3$  in acetonitrile under blue light irradiation, providing access to the title compounds. A variety of aromatic ketones can be synthesized in good to excellent yield, including those bearing potentially reactive aryl substituents, such as aryl iodide-containing product **35a** at 83% yield. Aliphatic ketones are produced, including ketone **35b** containing a newly-formed quaternary sulfamyl center in 52% yield, and cyclic ketone **35c**, which, impressively, contains two unreacted alkenes. Finally, several aldehydes are synthesized, including  $\alpha$ -sulfamyl undec-10-enal **35d** which is produced at 66% yield.

Leveraging the pyridine liberated from this class of reactants as a heteroarene source rather than as a base, Hong and co-workers have recently disclosed a series of reactions which produce new pyridyl-C(sp<sup>2</sup>)-C(sp<sup>3</sup>) bonds, beginning with an aminopyridylation of vinyl ethers and amides (Scheme 14–15).<sup>100</sup> Mechanistically, to initiate the reaction, photoexcited eosin Y reacts with an excess of aminopyridinium salt **37a** in a thermodynamically and kinetically feasible single-electron reduction ( $E_{p/2}(\mathbf{37a}) = -0.62 \text{ V vs SCE in CH}_3\text{CN}$ ;  $E_{1/2}(\text{PC}^*/\text{PC}^{*+}) = -1.11 \text{ V vs SCE in 1:1 H}_2\text{O:CH}_3\text{CN}$ ;<sup>101</sup> Stern-Volmer experiments found  $K_q(\tau) = 11.87 \text{ M}^{-1}$ ) to release pyridine and produce nitrogen-centered radical intermediate **39**. As noted previously (*vide supra*, Scheme 4),<sup>79,80</sup> electrophilic sulfamyl radical intermediate **39** adds to more electron-rich terminal carbon of vinyl ether **36a** to give intermediate **40**. Carbon-centered, nucleophilic radical intermediate **40** then likely adds to the C(4) position of another equivalent of aminopyridinium salt **37a** to give radical, cationic species **41**. This readily is deprotonated by the excess of tribasic phosphate which



can undergo radical decomposition to produce another equivalent of **39** and final product **38a**. This reaction proceeds through a radical chain mechanism, consistent with a quantum yield ( $\phi$ ) of 33.5, which suggests that on average each absorbed photon of light results in formation of thirty-three and a half equivalents of product. For this transformation, DFT calculations suggest that position selectivity may arise from non-covalent interactions between the negatively-charged sulfamyl oxygens and positively-charged aminopyridinium nitrogen–nitrogen bond, which are spatially proximal when intermediate **41** forms by reaction at C(4) but not at C(2).<sup>102</sup>

This reaction tolerates variations in both the vinyl component **36** and the pyridyl-component of **37** (Scheme 15). Pyridyl C(4)-selectivity is degraded by substitution to the pyridyl C(3)-position, with 3-methoxy-4-pyridyl product **38b** synthesized with a 2.5:1 C(4):C(2) selectivity. Functionalization at C(2) of the pyridine group is frequently beneficial to yields and selectivity with product **38c** synthesized in >98% yield. Limited diastereoselectivity is observed in stereocenter-containing vinyl-substrates, such as serine-derived product **38d** which is obtained with a 1.1:1 dr. *N*-vinyl acetamide is also successfully employed under the same reaction conditions to give amide-containing product **38e** in 70% yield.

In order to modulate the previously demonstrated C(4)-selectivity (vide supra, Scheme 14–15), Hong and co-workers turned to amidopyridinium reagent **42a** and strongly oxidizing mesityl acridinium photocatalyst, which could generate a nitrogen-centered radical without initial loss of the pyridyl group, in an overall process that induces C(2)-selectivity by radical formal 1,3-dipolar cycloaddition (Scheme 16–17).<sup>103</sup> The photocatalytic oxidation of amidopyridinium **42a** to nitrogen-centered radical intermediate **44** is kinetically feasible ( $K_q \cdot \tau = 370.43 \text{ M}^{-1}$ ). While some of the alkenes used could be directly oxidized by photocatalyst ( $E_{1/2}(\text{PC}^*/\text{PC}^{\bullet-}) = +2.09 \text{ V vs SCE in CH}_3\text{CN}$ ), such as **32** ( $E_{p/2}^{\text{ox}}(\text{32}) = +1.74 \text{ V vs SCE in CH}_3\text{CN}$ )<sup>104</sup>, the relatively lower oxidation potential of amidopyridinium **42a** ( $E_{p/2}^{\text{ox}}(\text{42a}) = +1.58 \text{ V vs SCE in CH}_3\text{CN}$ ) makes the desired pathway highly competitive, if not dominant. Once formed, electrophilic amidyl radical intermediate **44** adds to the more electron-rich carbon of the alkene to give stabilized carbon-centered radical intermediate **45**. In a radical formal 1,3-dipolar cycloaddition process, carbon-centered radical **45** transiently produces 5-membered radical cation intermediate **46**; this step proceeds with complete diastereoselectivity in all reported instances for an *anti*-relationship between substituents of unsymmetric alkenes (as well as a 1,2-*syn*-relationship between the amide and pyridine in the final products). The stereochemical preference is understood to arise from steric interactions between the alkene substituents in the transition state between **45** and **46** (calculated as 2.7 kcal/mol by DFT).<sup>105</sup> The final reaction steps, including *N*–*N* bond scission, deprotonation of the pyridine C(2), and protonation of the amide, are likely rapid and are proposed to proceed through amidyl radical intermediate **47**. Quantum yield experiments ( $\phi = 0.141$ ) don't directly implicate a radical chain propagation mechanism, and kinetic isotope effect for pyridine-*d5*-derived **42a** ( $K_{H/D} = 1.01$ ) is negligible, indicating the deprotonation of **46** is not rate-limiting. This amidopyridylation reaction engages an array of activated and unactivated alkenes alike, maintaining pyridine C(2)-selectivity throughout (Scheme 17).

By employing phosphonate-quinolinone photocatalyst,<sup>32</sup> Hong and co-workers convert amino- and amidopyridinium salts *via* 1,5-HAT process to alkyl pyridines **50**, with complete selectivity for addition at pyridine C(4) (Scheme 18).<sup>106</sup> The reaction employs blue light irradiation in DMSO at room temperature and is reported to be complete within 30 minutes. Likely beginning with a reduction of starting material **49** ( $E_{p/2}^{\text{red}}(\mathbf{49}) = -0.82$  V vs SCE in CH<sub>3</sub>CN) by excited-state photosensitizer ( $E_{1/2}(\text{PC}^*/\text{PC}^{*\text{+}}) = -1.29$  V vs SCE in CH<sub>3</sub>CN), pyridine is released to form nitrogen-centered radical intermediate **3c**. This initial step is further supported by a demonstrated quenching of excited state photosensitizer by starting material **49** (Stern-Volmer experiments found  $K_q \cdot (\tau) = 6.98$  M<sup>-1</sup>). The subsequent 1,5-HAT process furnishes carbon-centered radical intermediate **4c**. This intermediate is proposed to engage in nucleophilic attack of another molecule of aminopyridinium salt **49**, which occurs selectively at the pyridinium group's C(4)-position. Pyridyl-radical intermediate **51** is likely then deprotonated and the *N-N* bond is broken to produce another molecule of nitrogen-centered radical intermediate **3c**. The precise mechanism of deprotonation in this step is unclear; however, addition of base slightly decreased NMR yields of the optimization substrate. Quantum yield experiments ( $\phi = 41.2$ ) support a proposed radical chain propagation mechanism.

With higher concentrations of phosphonate-quinolinone photosensitizer (Scheme 18) and modulating the pyridinium salt's anion, Hong and co-workers are able to extend their reaction protocol to include amidopyridinium salts, such as **52** (Scheme 19). Reacting at a lower overall concentration and on a longer timescale, pyridylation products **53a** and **53b** are synthesized with a bias toward pyridine C(4)-selectivity, albeit with meaningful amounts of C(2) minor products. Yields are generally higher for pyridylation at tertiary alkyl radicals, with a stronger bias toward pyridine C(4)-selectivity for these more sterically-hindered radicals as well. Quantum yield experiments ( $\phi = 12.7$ ) implicate an analogous radical chain propagation process to that proposed for the sulfonamide-guided pyridylation above (Scheme 18).

Introduction of *N-N*<sup>+</sup> salts and *N*<sup>•</sup>-*N*<sup>+</sup> zwitterionic species has enabled guided- and unguided-amination reactions. Loss of pyridine from the starting salts upon single-electron reduction by photocatalysts results in the slow addition of a weak base to the reaction, which has simplified systems that might otherwise require an exogenous base (Table 1 and Scheme 6). Moreover, the metered generation of nitrogen-centered radicals, through direct SET or radical chain propagation mechanisms, affords additional control over reaction progress and, in many cases, obviates potential overreaction by preventing *N*-centered radical generation on the same molecule after its initial reaction. These benefits must be measured against cost of additional steps required to access substrates bearing the requisite *N-N* bond, and, in instances where these benefits are greater, this method of nitrogen-centered radical generation will surely enable innovative chemistry for years to come.

#### 4. NITROGEN-CENTERED RADICALS MAY BE GENERATED FROM NITROGEN–SULFUR BONDS

Few reports document photocatalyst-mediated reactions that utilize nitrogen–sulfur bonds as precursors to nitrogen-centered radicals; however, a recent example was disclosed in 2018 by Bolm and co-workers (Scheme 20A).<sup>107</sup> The dearth of examples may be due in part to N–S bonds with low oxidation-state sulfur groups being relatively labile to direct photolysis, as demonstrated in recent C–H xanthylation reactions.<sup>108,109,110</sup> In the presence of Ir(ppy)<sub>3</sub>, under blue light irradiation, thiocyanate substrates react with an excess of styrene to give good yields of desired, difunctionalized products (Scheme 20A). Though mechanistic information about this reaction is sparse, the observed regioselectivity, lack of additives, and lack of reaction absent photocatalyst implicate a photoredox- or photosensitizer-generated, nitrogen-centered radical mechanism.

Radical reactions have been described in the presence of a photocatalysis-capable compounds that involve N–S bonds, where the sulfur atom is in higher oxidation state (Scheme 20B–C).<sup>111, 112</sup> These detosylation processes differ in terms of substrate applications and conditions. In initial disclosures by Lu, Xiao and co-workers, *N,N*-disubstituted sulfonamides rely on iridium photocatalyst to reduce the substrate, and Hantzsch ester as a reductant and hydrogen atom source in the course of detosylation. This protocol can enable selective detosylation of a fully-substituted nitrogen centers bearing an aryl amide in the presence of a secondary nitrogen bearing a tosyl group (Scheme 20B).<sup>111</sup> More recently, an organic photocatalyst has been applied to affect detosylation of *N*-aryl, *N,N*-diaryl and *N,N*-dialkyl sulfonamides (Scheme 20C). In the presence of an (Mes-PhAc)–based to mediate substrate reduction and base oxidation, with Hünig's base as a reductant and hydrogen atom source, detosylation proceeds selectively on a substrate bearing a pendant methylsulfonamide (Scheme 20C).<sup>112</sup> Under the standard reaction conditions, detosylation of amidyl **56c** furnishes protonated **57c** (Scheme 20D). This same substrate provides limited evidence that these reactions may proceed via nitrogen-centered radical intermediates. Specifically, absent water, amidyl **56c** furnishes both protonated **57c** and cyclized **57d** (Scheme 20D). This byproduct is suggestive of the presence of a nitrogen-centered radical as a putative reaction intermediate.

#### 5. NITROGEN-CENTERED RADICALS CAN BE GENERATED FROM NITROGEN–OXYGEN BONDS

Nitrogen-centered radicals are accessible from the nitrogen–oxygen bonds within oximes, oximides, oxyamides, benzenesulfonamides, amidoximes and imidates. The generated nitrogen-centered radicals participate in bond-forming reactions with appropriate radical trapping agents. This section summarizes reactions that propose neutral nitrogen-centered radical species as intermediates. Many complementary reactions are outside of the scope of this review, including promising transformations that rely on photocatalyst-mediated N–O bond cleavage with pyridinium salts to generate pyridyl radical cation intermediates.<sup>113, 114</sup>

## 5.1. Iminyl Radicals Can Be Generated from *O*-Aryl and *O*-Acyl Oxime Analogues

**5.1.1 Radicals Prepared from *O*-Aryl or *O*-Acyl Oximes Can Add Across Olefins**—Iminyl radicals are important synthetic intermediates,<sup>115</sup> and are accessible from *O*-aryloximes. When incorporated into  $\gamma,\delta$ -unsaturated ketoximes, these *O*-aryloxime precursors can be converted into 1-pyrroline analogues<sup>116,117</sup> via iminyl radical intermediates. Within substrate *O*-aryloximes, a weak N–O bond is amenable to homolytic fission to reveal the corresponding nitrogen-centered iminyl radical.<sup>118</sup> The bond homolysis event can be triggered thermally, photochemically, or in the presence of single-electron reductants such as phenolate, Fe- and Cu-salts, SmI<sub>2</sub> and SnBu<sub>3</sub>H.<sup>119</sup>

At the end of the 20<sup>th</sup> century, Narasaka and co-workers discovered that iminyl radicals could be generated from *O*-aryloximes *via* single-electron reduction.<sup>120,121,122</sup> The accessed iminyl radical intermediate is poised to undergo 5-*exo-trig* cyclization with a pendant olefin to deliver a nucleophilic carbon-centered radical.<sup>122</sup> Subsequent trapping of the radical with a hydrogen atom or other electrophile provides 1-pyrroline derivative. Uncovering this photochemical process propelled Narasaka and co-workers to develop a photocatalyst-mediated strategy to convert *O*-aryloximes to 1-pyrrolines.<sup>122</sup> In 2001, Mikami and Narasaka disclosed photoredox catalysis as a tactic to transform  $\gamma,\delta$ -unsaturated *O*-aryl oximes to pyrrolines (Scheme 21A).<sup>123,124,125</sup> In this transformation, following photoexcitation of 1,5-dimethoxynaphthalene (1,5-DMN,  $E_{1/2}(\text{DMN}^+/*\text{DMN}) = -2.5 \text{ V vs. SCE (CH}_3\text{CN)}$ )<sup>a</sup> the excited state photocatalyst is proposed to reduce an *O*-aryl oxime to furnish a phenolate and the putative iminyl radical intermediate. The generated iminyl radical intermediate undergoes 5-*exo-trig* cyclization, and, in more efficient reactions, the resultant carbon-centered radical intermediate is quenched using 1,4-cyclohexadiene as a hydrogen atom source.

Reaction efficiency is sensitive to the wavelength of the engaged light source, as substrate **58** absorbs irradiation beneath 320 nm. Consequently, absent photosensitizer, *O*-aryl oxime **58** undergoes homolytic cleavage to generate undesired ketone byproduct **61**, along with pyrroline **60** (entry 2). Pyrroline **60** forms more efficiently when light below 320 nm is excluded from the reaction (entry 3), and with *O*-aryl oxime **58**. With more effective *O*-aryl oximes, lower catalyst loadings can prove equally efficient (entry 7). Ultimately, this practical reaction highlights the promise of photoredox catalysis as a tactic to use *O*-aryl oximes as stable precursors to iminyl radical intermediates.

Leonor and co-workers<sup>126</sup> advanced the technology from Misaka and Narasaka with a synthetic protocol that relies on an *O*-aryloxime as iminyl radical precursor but requires a lower photocatalyst loading and irradiation using a less intense light source (Scheme 21B). Instead of 1,5-dimethoxynaphthalene, eosin Y (EY) is employed as the photocatalyst, which elicits the desired transformation at 2 mol % catalyst loading. Leonor and co-workers are able to replace the use of a specialized Hg(Xe) lamp, and employ less intense visible light sources. In their research, photoexcitation of eosin Y prompts SET between \*EY and *O*-aryl

<sup>a</sup>The  $E_{1/2}(\text{DMN}^+/*\text{DMN})$  was calculated from the Rehm-Weller equation, where  $E_{1/2}(\text{DMN}^+/*\text{DMN}) = E_{1/2}(\text{DMN}^+/\text{DMN}) - E_{0-0}$ . The  $E_{1/2}(\text{DMN}^+/\text{DMN})$  and  $E_{0-0}$  values were obtained from Reference 31.

oxime **62** to generate iminyl radical that participates in a 5-*exo-trig* hydroiminium reaction to furnish 1-pyrroline **63** in 78% yield.

In conjunction with these tactical modifications, Leonori and co-workers evaluated a similar range of aryl groups within the precursor oxime to permit efficient conversion of the *O*-aryl oxime to the product. Oximes **64a–64d** possess the appropriate reduction potential ( $E_p^{\text{red}}$ ) to be irreversibly reduced by eosin Y ( $E_{1/2}[\text{EY}^+/*\text{EY}] = -1.11 \text{ V vs. SCE in CH}_3\text{CN}$ ). 2,4-Dinitroaryl oximes, such as **64a**, were chosen for more extensive explorations due to their relatively low  $E_p^{\text{red}}$ , which favor irreversible SET between eosin Y and oxime, and because these oximes are relatively easy to purify.

The method advanced by Leonori and co-workers is similar to the method developed by Misaka and Narasaka inasmuch as this reaction is sensitive to the wavelength of the light source. When comparing the efficiency of a reaction under blue, green, or red LEDs, the most efficient process relies on green LEDs ( $\lambda = 530 \text{ nm}$ ), which promote the reaction of starting material **62** to 1-pyrroline **63** in 95% yield. This improvement in efficiency might be predicted, as eosin Y is known to absorb green light ( $\lambda_{\text{abs}} = 539 \text{ nm}$ )<sup>127</sup> optimally to yield \*EY. Consequently, the result from the experiment allows the authors to suggest that the data are consistent with reaction mechanism that is initiated by SET between EY\* and *O*-aryl oxime **62**.

Nearly concurrently, a similar cascade sequence was described that, relies on the conversion of *O*-acyloximes *via* single-electron reduction through iminyl radical intermediates and 5-*exo-trig* cyclization onto a pendant olefin to afford a nucleophilic carbon-centered radical. At this point do the processes diverge – the *generated* radical can be trapped by an electron-rich olefin to furnish pyrroline products with pendant ketones (Scheme 22A).<sup>128</sup> This transformation is highly sensitive to the reaction solvent. Broadly, while polar protic and amine solvents (excepting pyridine) greatly hinder or arrest reactivity, polar aprotic solvents are required for product formation. Of these, DMF was chosen as the optimal solvent. Solvents such as DMA and NMP also displayed high conversion of starting material, but favor formation of undesired **67** over desired **66**. This reaction manifold is robust to variety of aryl-substituted oximes, such *E*- and *Z*-configured 2-thiophenyl oximes. The reaction is ineffective with styrenyl or phenylacetylnyl oximes, and with tri-substituted and sterically congested silyl enol ethers (not depicted). This reaction is suitable for downstream derivatization of pyrrolines to pyrrolizidine alkaloids (Scheme 22B).<sup>128</sup>

Insofar as an iminyl-radical-generation / 5-*exo-trig* cyclization cascade permits rapid access to pyrroline scaffolds, by analogy, use of an oxime imidate substrate decorated with pendant olefin should provide an oxazoline. This recognition makes the reaction cascade exponentially more powerful than initially envisioned: a masked allyl alcohol can serve as an imidate radical precursor to provide access to oxazolines and masked 1,2-amino alcohols (Scheme 23).<sup>129</sup> These reactions rely on an intramolecular cyclization / radical trapping cascade to achieve net aminoalkylation, aminoarylation, and hydroamination reactions. A subsequent acidic work-up can reveal 1,2-amino alcohol products, providing efficient access to high-value targets.

### 5.1.2 Radicals Prepared from *O*-Acyl Oximes Can Cyclize onto Arenes or Vinyl Arenes

As a complement to these approaches, iminyl radicals derived from oximes with conjugated  $\pi$ -systems engage in 6-*endo-trig* cyclization reactions to provide *N*-heterocycles such as phenanthridines, quinolines, and pyridines (Scheme 24).<sup>120,121,130</sup> To access this reactivity, Yu and Zhang activate *O*-acyl oxime substrates by photoirradiation with visible light in the presence of Ir(ppy)<sub>3</sub> photoredox catalyst, ultimately furnishing a series of heterocyclic products.<sup>131</sup> These transformations rely on irreversible reduction of starting *O*-acyl oximes **72** by the photocatalyst ( $E_{1/2}[\text{Ir}^{\text{IV}}/\text{Ir}^{*\text{III}}] = -1.73$  V versus SCE)<sup>16</sup> to reveal iminyl radicals, a process that benefits from the selection of an appropriate acyl precursor (Scheme 24A). Electron-deficient benzoyl groups **72a–72c** affect the conversion of *O*-acyl oximes **72** to phenanthridines **73** in 91% to quantitative yield. By contrast, phenanthridines are not isolated from reactions that rely on more electron-rich, less readily reduced substrates that incorporate benzoyl groups, aryloxy carbonates, or an acetoxy group (i.e., **72d–72h**). Presumably, variations in ease of reduction reflect the electronic influence of *O*-acyl groups on the  $\sigma^*_{\text{N-O}}$  orbital energy of *O*-acyl **72**.<sup>132</sup> While pentafluoro-substituted substrate **72b** delivers the desired product in quantitative yield, *p*-trifluoromethyl **72a** is an attractive redox-active handle over **72b** due to its slightly lower molecular weight.

The transformation is robust to a wide variety of *O*-acyl oximes to provide differentially substituted phenanthridines, quinolines, and pyridines (Scheme 24B–C). Notably, with *meta*-substituted arene substrates **74a** and **74b**, accessed iminyl radical intermediates add across the aromatic  $\pi$ -systems at two sites competitively to deliver mixtures of positional isomers as products (i.e., **75a** and **75b**, Scheme 24B). Importantly, this strategy has been applied to improve access to noritidine, a benzo[*c*]phenanthridine derivative with anti-tumor properties (Scheme 25). With these technologies, noritidine can be accessed in five steps and 55% overall yield, a considerable advance over a previous 11-step route (20% overall yield).<sup>133</sup> This achievement underscores the powerful potential of photoredox catalyst and nitrogen-centered radicals for organic synthesis.

This general approach to preparing quinolines and phenanthridines would be more powerful if it were to rely directly on readily available aldehydes as starting materials, rather than on aldehyde-derived *O*-acyl oximes. Consequently, Yu and co-workers have disclosed a one-pot protocol to convert aldehydes *via* *O*-acyl hydroxylamines into quinolines and tetrahydrophenanthridines (Scheme 26).<sup>134</sup> With this method, an aldehyde condenses with an *O*-acyl hydroxylamine with a 4-cyanobenzoyl group, and the intermediate *O*-acyl oxime then proceeds through a 6-*endo-trig* cyclization reaction, obviating the syntheses and isolations of requisite *O*-acyl oximes. This protocol depends on blue LEDs as the reaction light source, as undesired side products form when a light source is used that emits light across a broader wavelength range. This approach has been employed with biaryl aldehydes and *O*-4-cyanobenzoyl hydroxylamine to afford phenanthridines, as exemplified by a two-step gram-scale synthesis of trisphaeridine, an alkaloid possessing antitumor and antiretroviral properties (Scheme 27).<sup>135,136,137</sup> This procedure represents an improvement over the previous best-in-class synthetic route to trisphaeridine, which requires four synthetic steps from the same aryl bromide **89** and provides trisphaeridine (**92**) in 29% overall yield.<sup>138</sup>

### 5.1.3 Radicals Prepared from *O*-Acyl Oximes Can Abstract Hydrogen Atoms

—In addition to adding across olefins, or aromatic rings, iminyl radicals can affect C–H abstraction, typically by way of 1,5-hydrogen atom transfer (HAT) based on a six-membered transition state. Indeed, oximes have been used as precursors for iminyl radicals that engage in 1,5-HAT prior to addition across an arene (Scheme 28). These technologies build on seminal research by Forrester and co-workers.<sup>139,140</sup> In these reactions, thermolysis of the oxyacetic acid **93** under basic and oxidative conditions triggers a cascade sequence to form iminyl radical **95**, which affects 1,5-HAT to generate carbon-centered radical **96**. Once formed, this nucleophilic radical adds across an aromatic  $\pi$ -bond to deliver a cyclic imine (not depicted). Upon rearomatization and *in situ* hydrolysis, this sequence affords 1-tetralone product **94** (Scheme 28). Considering the allure of 1-tetralones as monoamine oxidase inhibitors for Parkinson's disease therapy<sup>141</sup>, milder photoredox methods to generate 1-tetralones from oxyacetic acid derivatives have emerged.

Inspired by this transformation, Nevado and co-workers developed the first photoredox catalyst-mediated process that harnesses this strategy with *O*-acyl oxime substrates (i.e., **97**, Scheme 29).<sup>142</sup> To date, the transformation of *O*-acyl oximes to 1-tetralones only proceeds in the presence of water as co-solvent, and is most effective in the presence of an acid additive (AcOH), which is thought to facilitate a reversible and rate-determining HAT event (Scheme 29A).<sup>140</sup> Competent substrates range from those containing electron-deficient to electron-dense arenes as oxime substituents, benzofurans, or pendant aliphatic rings sizes (not shown). To add complexity to this advance, under basic conditions, in the presence of light, photocatalyst and in a non-aqueous solvent system, these same *O*-acyl oxime substrates undergo homolytic cleavage and 1,5-HAT, but then subsequently react to provide 1-pyrrolines (Scheme 30). Reaction diastereoselectivity is limited when not reinforced by a cyclic ring.

## 5.2. Hydroxyacid-Derived Oximes Are Appropriate Precursors to Iminyl Radicals

### 5.2.1 These Iminyl Radicals Can Serve as Intermediates in

**Iminofunctionalization Reactions**—While *O*-acyl oximes serve as efficient precursors to iminyl radical intermediates, many similar transformations can be achieved using hydroxyacid-derived oximes. Indeed, nearly fifty years ago, Forrester and co-workers discovered that hydroxyacid-derived oximes are appropriate precursors to iminyl radicals.<sup>143,144</sup> Building on this research, thirty years ago, Boivin, Zard and co-workers employ a thusly-derived iminyl radical intermediate in a 5-*exo-trig* cyclization. The resultant carbon-centered radical reacts with methyl acrylate in a Giese-type reaction to afford alkylated 1-pyrroline.<sup>145, 146, 147</sup> These pivotal findings set the stage for analogous technologies that employ milder photoredox-catalyst conditions to streamline access to functionalized 1-pyrroline (Scheme 31–32).

In 2017, Studer, Leonori, and co-workers developed photoredox catalyst-mediated tactics to convert hydroxyacid-derived  $\gamma,\delta$ -unsaturated ketoximes, such as **105**, to iminyl radicals.<sup>148, 149</sup> Following intramolecular 5-*exo-trig* cyclization, the resultant radicals can be trapped by olefin in intermolecular Giese reactions.<sup>145</sup> In Jiang and Studer's cascading Giese-type reaction,  $\gamma,\delta$ -unsaturated ketoxime **105** is transformed to desired product **106a**

in 68% yield when  $[\text{Ir}(\text{dF}(\text{CF}_3)\text{ppy}_2)(\text{dtbbpy})]\text{PF}_6$  is employed as photosensitizer and CsF as a base (Scheme 31). Using this strategy, a wide catalogue of Michael acceptors participates in the Giese reaction to access alkylated 1-pyrrolines. For example, thiophene-substituted ketoxime and a pendant piperidine are carried through the reaction to furnish pyrrolines. Furthermore, under these conditions a cascading cyclization reaction proceeds with excellent diastereoselectivity to generate a [5-6]-fused bicyclic system (i.e., **106d**).

By contrast, Leonori and co-workers rely on  $[\text{Mes-Acr}]\text{ClO}_4$  to affect their iminofunctionalization reactions (Scheme 32). Concurrent with Jiang and Studer's disclosure, Leonori and co-workers disclosed a very similar approach to iminofunctionalization reactions – one that proceeds through an identical iminyl radical intermediate (Scheme 33). To design an optimal iminyl radical precursor, Leonori and co-workers analyzed the electrochemical half potentials for a series of carboxylates, and determined that  $\alpha,\alpha$ -dimethylated carboxylates,<sup>150</sup> such as **107**, are more readily oxidized than their less substituted analogues (i.e., **111a–111d**). Consequently, Leonori and co-workers rely on these more substituted analogues as precursors to their iminofunctionalization reactions. Leonori and co-workers anticipated that these carboxylates would be oxidized in the presence of light by excited state  $^*[\text{Mes-Acr}]\text{ClO}_4$  ( $E^*_{1/2} = +2.08$  V vs. SCE in  $\text{CH}_3\text{CN}$ ),<sup>27</sup> a process that is reported to be infeasible with excited state  $^*[\text{Ir}(\text{dF}(\text{CF}_3)\text{ppy}_2)(\text{dtbbpy})]\text{PF}_6$  ( $E^*_{\text{ox}} = +0.89$  V vs. SCE in  $\text{CH}_3\text{CN}$ ).<sup>8</sup> Upon decarboxylation and loss of acetone, an iminyl radical would form, poised for cyclization onto a pendant olefin. Following cyclization, the resultant carbon-centered radical could trap a broad array of radical electrophores.

Like Jiang and Studer, Leonori and co-workers evaluate  $\alpha,\beta$ -unsaturated electrophiles with their novel iminyl radical precursors (Scheme 33). Cascading cyclization reactions proceeded with modest diastereoselectivity to generate a [5-6]-fused bicyclic system (i.e., **113a**). Moreover, the reaction tolerates a range of  $\alpha,\beta$ -unsaturated carbonyl electrophiles, including cyclohexenone and diethyl (*E*)-diazene-1,2-dicarboxylate, to form products such as **113b** and **113c**, respectively.

Leonori and co-workers' iminofunctionalization strategy can be generalized to affect iminohalogenation, iminochalcogenation, hydroimination, iminoazidation, and iminoolefination processes by varying the solvent, base, and employed atom- or group-transfer agent (Scheme 34). These reactions rely on a hydroxyacid-handle as an iminyl radical precursor, and  $[\text{Mes-Acr}]\text{ClO}_4$  as a photosensitizer. Halogenated 1-pyrrolines are accessed when NFSI<sup>151</sup>, NCS<sup>152</sup>, diethyl bromomalonate<sup>153</sup>, and NIS<sup>154</sup> are employed as halogen-transfer agents. In this context, one limitation is well documented: the iminoiodination reaction results in synthetically useful yields when a terminal olefin is engaged but is not efficient when di- and trisubstituted olefins are targeted as the sites for installation of a relatively weak carbon–iodine bond (not shown). Stronger  $\text{C}(\text{sp}^3)\text{–S}$  and  $\text{C}(\text{sp}^3)\text{–Se}$  bonds can be accessed when benzosuccinimide derivatives are used as chalcogen group-transfer agents.<sup>155,156</sup> Furthermore, azides can be installed through the use of arylsulfonfyl azide as a group-transfer agent.<sup>157</sup> If a reductively neutral process is targeted, hydroimination processes proceed in the presence of aryl disulfide, a known catalytic hydrogen-atom donor.<sup>158</sup> Alternatively, iodine (V) sources are appropriate precursors to



enable group-transfer in the course of carbon–carbon bond-forming reactions.<sup>159,160,161</sup> Ultimately, this is a versatile approach to enable targeted iminofunctionalization reactions.

Moreover, this approach to iminofunctionalization can enable late-stage reactions with synthetically useful efficiencies. In the late 20<sup>th</sup> century, Zard and co-workers used a thevinone (**117**) derivative to showcase an intramolecular hydroiminaton reaction (Scheme 35A). Zard and co-workers converted thevinone to oxime **118**, which, following homolysis of the weak N–O bond, cyclizes to furnish imine **119**.<sup>162</sup> Building upon this precedent, Leonori and co-workers employ thevinone derivative **117** as a precursor for a series of photoredox mediated iminoazidation, iminoamidation and iminoselenylation reactions to access polycyclic imines **121a–121c**, respectively (Scheme 35B).<sup>149</sup>

Similarly designed iminyl-radical precursors can, upon radical-addition to a pendant olefin, be intercepted by a cobalt complex en route to an intramolecular Aza Heck-type cyclization reaction to provide pyrrolines (Scheme 36A).<sup>163</sup> In the presence of a [Mes-Acr]ClO<sub>4</sub> photoredox catalyst and Co(dm<sub>g</sub>H)(dmH<sub>2</sub>)Cl<sub>2</sub> complex, oxime ester **122** undergoes cyclization reaction to provide organocobalt intermediate **124**, which is poised for β-hydride elimination to furnish product **123**. Previously, this pyrroline scaffold was accessed *via* the Narasaka–Heck cyclization between oxime ester and pendant olefin with a palladium catalyst.<sup>164,165</sup> Photocatalytic conditions are relatively mild, so the dual photoredox/Co catalysis manifold offers advantage over the Narasaka–Heck reaction by tolerating oxime esters bearing substituents that are sensitive to Pd or Cu complexes. For example, an oxime ester bearing aryl iodide participates in the reaction to provide pyrroline **123a** in 53% yield. This reaction enables rapid construction of polycyclic scaffolds, such as *cis*-fused tetracyclic product **123b** in 49% yield in 1:1 dr. Modifying reaction condition and employing Co(dm<sub>g</sub>H)<sub>2</sub>(4-CN-Py)Cl<sub>2</sub> complex permits radical Aza-cyclization / intermolecular Heck-type reaction cascade with oxime ester **122** and olefin **125** to provide pyrroline motif **126** (Scheme 36B). Similarly powerful examples come from the synthesis of thiophene-decorated pyrroline **126a** and pyrroline bearing 1,1,2-trisubstituted internal olefin **126b** in moderate yields and with high selectivity for (*E*)-isomer.

**5.2.2 Hydroxyacid-Derived Iminyl Radicals Can React with Chalcogens to Install New Chalcogen–Nitrogen Bonds**—A mechanistically analogous iminyl radical formation / intramolecular *N*-radical addition cascade can be intercepted by a pendant thioether to furnish an isothiazole (Scheme 37).<sup>166</sup> In the propose reaction mechanism, generation of radical species **130** triggers intramolecular annulation reaction *via* *N*-radical addition to sulfur. Upon thioether fragmentation, this event would provide desired product **129** and methyl radical, which would be oxidized under aerobic condition to provide formaldehyde as a byproduct. During the course of reaction optimization, the net transformation of oxime **127** to isothiazole **129** is viable in presence of photocatalyst with excited oxidation potential lower than the irreversible oxidation potential of sodiated oxime salt **128a** ( $E_{p/2}^{ox} = +1.58$  V versus SCE in acetone). Strongly oxidizing [Mes-Acr]ClO<sub>4</sub> ( $E_{1/2}[PC^-/PC^*] = +2.08$  V versus SCE in CH<sub>3</sub>CN)<sup>27</sup> is empirically identified as the optimal photosensitizer for the reaction. The reaction is less efficient in presence of photosensitizers that are more oxidizing than [Mes-Acr]ClO<sub>4</sub>. Equally pertinent to the

reaction efficiency is the thioether group of  $\alpha$ -imino-oxy acid. Within a series of thioethers (i.e., **128b–128e**), which all have compatible  $E_{p/2}^{ox}$  values with respect to [Mes-Acr]ClO<sub>4</sub>, benzyl thioether **128d** reacts with the highest efficiency, presumably due to formation of resonance-stabilized benzylic radical en route to product **129**. This is a viable strategy to generate varied arenes, including tricyclic 1,3-benzodioxole-containing isothiazole **132a**, methylated isothiazolo[5,4-*b*]pyridine **132b**, and furan- (**132c**) and thiophene-embedded isothiazole (**132d**) scaffolds (Scheme 38).

### 5.3. Ketoximes and Aldoximes Can Serve as Precursors to Persistent Iminyl Radical Intermediates

Furthermore, with ketoximes such as those derived from acetophenone and benzophenone, conversion to an iminyl radical can proceed based on an energy transfer mechanism involving photosensitizer, and thereby prompt an array of radical reactions. This iminyl radical generation strategy was first documented by Glorius and co-workers in 2019 in a reaction in which electron-deficient *O*-acyl oxime **133** undergoes energy transfer-triggered decarboxylation to provide aryl radical (not depicted) and iminyl radical **135a** (Scheme 39A).<sup>167</sup> The aryl radical is trapped by iodine-transfer reagent (CH<sub>2</sub>I<sub>2</sub>) to provide aryl iodide **134**. Based on the electrochemical potentials of starting material **133** ( $E_{p/2}^{red} = -2.00$  V versus SCE) and photosensitizer ( $E_{1/2}[*Ir^{III}/Ir^{IV}] = -0.89$  V vs. SCE,  $E_{1/2}[Ir^{III}/Ir^{II}] = -1.37$  V vs. SCE), a SET pathway is excluded as a mechanistic possibility because it would be a thermodynamically unfavorable process. By contrast, photosensitizer possesses appropriate triplet energy ( $E_T = 60.8$  kcal•mol<sup>-1</sup>) to sensitize oxime **133** ( $E_T = 46.4$  kcal•mol<sup>-1</sup>). Notably, this reaction gives rise to byproducts imine **136**, ketone **137**, and hydrazine **138a**, which are likely to originate from iminyl radical **135a**. In fact, these byproducts provide evidence that iminyl radical **135a** is a persistent radical species — otherwise, byproducts **136–138a** would be unlike to form. Consistent with this hypothesis, under deuterium-transfer conditions, *O*-acyl oxime **139** produces deuterated arene **140** and 6-phenylphenanthridine **141**, presumably by way of intramolecular radical addition of the nitrogen-centered radical to a neighboring  $\pi$ -system (Scheme 39B).

A net intramolecular decarboxylative C–N bond forming reaction can be used to access an aliphatic primary amine surrogate, such as alkyl amine **143a**, from aliphatic *O*-acyl oxime **142a** (Scheme 40A).<sup>18</sup> Mechanistically, this reaction appears to rely on energy transfer between oxime **142a** and triplet excited-state iridium photosensitizer to afford triplet excited-state oxime **144** via triplet-triplet energy transfer (TTEP), en route to critical iminyl radical **135b** (Scheme 40B). Steady-state and transient electronic transition spectroscopy experiments revealed that the rate of triplet-triplet energy transfer between oxime **142a** and photosensitizer ( $k_{ET} = 1.1 \times 10^8$  s<sup>-1</sup>) is faster than the rates of radiative ( $k_r = 3.8 \times 10^5$  s<sup>-1</sup>) and non-radiative decays ( $k_{nr} = 3.8 \times 10^4$  s<sup>-1</sup>) of excited photosensitizer. So, triplet-triplet energy transfer between the two species occurs before the decay of excited photosensitizer back to singlet ground-state. A number of standard methods to access iminyl radical intermediates from *O*-acyl oxime esters are not viable when using benzophenone-derived *O*-acyl oxime esters **142a** as substrates. For example, Förster-type resonant energy transfer is unlikely, given negligible spectral overlap between the absorption spectrum for oxime **142a** and the phosphorescence spectrum for several excited-state iridium (III) complex

(Scheme 40C). Additionally, a single electron transfer mechanism is excluded because it is not thermodynamically favorable, based on the electrochemical potentials of oxime **142a** ( $E_p^{\text{red}} = -1.83$  V versus SCE,  $E_p^{\text{ox}} = +2.35$  V versus SCE, Scheme 40D). Ultimately, once iminyl radical forms, recombination with alkyl radical is proposed to deliver primary amine surrogates.

A similar energy transfer mechanism is proposed as the basis for the position-selectivity of a photosensitizer-enabled carboimination reaction between benzophenone-derived *O*-acyl oxime esters **142b** and unactivated olefins **146** to afford  $\alpha$ -iminonitriles (Scheme 42).<sup>168</sup> Consistent with previous findings,<sup>18</sup> a number of standard methods to access iminyl radical intermediates from *O*-acyl oxime esters are not viable when using benzophenone-derived *O*-acyl oxime esters **142b** as substrates. So, a triplet–triplet energy transfer mechanism is proposed between oxime **142b** and photoexcited iridium complex to furnish excited oxime **148**, which gives way to persistent<sup>169</sup> iminyl radical **135b** upon decarboxylation. The position-selectivity of this carboimination reaction is predicted to originate from the persistent radical effect<sup>169</sup> (Scheme 42B). Relying on long lifetime of iminyl radical **135b**, more transient alkyl radical **149** escapes the solvent cage to undergo radical addition to terminal site of olefin **146**. In keeping with this hypothesis, radical crossover experiments with oximes **142b**, **151a** and acrylonitrile **146** furnish non-crossover  $\alpha$ -iminonitrile products **147a**, **152a** and hydrazines **138b**, **153**, crossover  $\alpha$ -iminonitrile products **152b**, **147b** and hydrazine **154** as detected by GC-MS. This protocol offers position-selectivity that complements that available from previous intermolecular carboamination reactions that were initiated by nitrogen-centered radicals,<sup>170</sup> presumably because they did not rely on persistent benzophenone imine radicals.

Intermolecular, radical-radical cross-coupling reactions that rely on a persistent benzophenone iminyl radical as a precursor to a transient alkyl radical can be extended to synthesize 1,2-amino alcohol surrogates (Scheme 42).<sup>171</sup> Specifically, oxime carbonates **155** react with olefins **156** in net oxyimination processes, mediated by a thioxanthone organic photosensitizer. This protocol permits highly atom-economical assembly of 1,2-amino alcohol analogues as every atom of oxime carbonate and mono-, di-, and trisubstituted olefin feedstocks are utilized. Control experiments suggest that chemoselectivity may arise due to the low rate of radical recombination between alkoxy-carbonyloxy and iminyl radicals (Scheme 42B), thereby affording 1,2-aminoalcohol surrogates efficiently.

Intermolecular, radical-radical cross-coupling reactions have been disclosed between a persistent benzophenone iminyl radical and an aryl-derived radical, also based on a proposed energy transfer mechanism, and can be used to assemble primary amines bearing tetrasubstituted  $\alpha$ -carbon centers (Scheme 43A).<sup>172</sup> For example, amine product **164a** is isolated in 86% yield upon reaction of acetophenone-derived oxime **162** and 4-cyanopyridine **163** in presence of an iridium photosensitizer, diisopropylamine as a reductant and benzoic acid as a soluble proton source (Scheme 43A). This reaction protocol provides access to primary amines adjacent to a sterically bulky <sup>t</sup>Bu-substituent (**164b**), and medically-relevant cyclopropyl<sup>173</sup> (**164c**) and F<sub>3</sub>C<sup>174</sup> (**164d**) groups. The transformation is largely restricted to cyanopyridines, which can be more readily reduced to critical radical intermediates (i.e., **172**). For example, non-heteroaromatic cyanoarene such as 1-

naphthonitrile does not engage in two-component coupling reaction with iminyl radical to provide amine **164g**.

The reaction is proposed to proceed based on initial energy transfer between photoexcited  $^*[\text{Ir}^{\text{III}}]$  and oxime **162** to provide triplet excited-state oxime **165**. Stern-Volmer analysis reveals that bimolecular quenching of  $^*[\text{Ir}^{\text{III}}]$  by oxime **162** is kinetically favorable ( $K_{\text{ET}} = K_{\text{q}} \approx 2.6 \times 10^7 \text{ M}^{-1} \cdot \text{s}^{-1}$ ) and proceeds faster than decay of  $^*[\text{Ir}^{\text{III}}]$  back to ground-state  $[\text{Ir}^{\text{III}}]$  ( $k_{\text{r}} = 2.0 \times 10^5 \text{ s}^{-1}$ ,  $k_{\text{nr}} = 6.4 \times 10^5 \text{ s}^{-1}$ ).<sup>175</sup> Indeed, oxime **162** undergoes facile N–O bond cleavage to generate persistent iminyl radical **166** that is poised to abstract hydrogen-atom from DIPA to form closed-shell imine **167** and carbon-centered radical **168**. It is proposed that imine is protonated by benzoic acid to generate iminium benzoate **169**, which engages in exergonic single-electron reduction with radical **168** to provide 1-phenylethaneaminyl radical **170** and diisopropylmimium benzoate **171** ( $G = -7.4 \text{ kcal} \cdot \text{mol}^{-1}$ ). Alternatively, 1-phenylethaneaminyl radical **170** can be generated from single-electron transfer between iminium benzoate **169** ( $E_{\text{red}} \approx -0.8 \text{ V}$  versus SCE in DMSO) and  $[\text{Ir}^{\text{II}}]$  ( $E_{1/2}^{\text{red}} = -1.42 \text{ V}$  versus SCE in MeCN). Concurrently, 4-cyanopyridine **163** undergoes PCET with  $[\text{Ir}^{\text{II}}]$  and proton source to generate persistent radical **172** that undergoes radical-coupling with 1-phenylethaneaminyl radical **170** to afford intermediate **173**. Ultimately, rearomatization of intermediate **173** expels hydrogen cyanide and delivers product **164a**.

Remarkably, nitrogen-centered radicals can be either nucleophilic or electrophilic, based in part on the pendant functionality, and this polarity influences reaction kinetics. This is the chemical basis for the reaction of sulfonamide **174** with hydrazone **175** to provide hydrazonamide **176** (Scheme 44).<sup>176</sup> This  $\text{C}(\text{sp}^2)\text{--N}$  bond-forming reaction is initiated by photoredox-mediated generation of sulfonamidyl radical species **177**, which undergoes radical-addition across  $\text{C}=\text{N}$  bond to provide nitrogen-centered radical intermediate **178**. In fact, the unpaired electron and adjacent lone-pair stabilizes the intermediate through three-electron  $\pi$ -bonding interaction.<sup>177</sup> Single-electron oxidation of intermediate **178** by  $[\text{Ir}^{\text{IV}}]$  complex regenerates ground-state photocatalyst and resonance-stabilized diazenium cation **179** / **180**. Ultimately, deprotonation of diazenium cation furnishes desired product **176**. Through this reaction, hydrazonamide bearing quinoline **176a** and phenyl-enriched hydrazonamide **176b** form in 88% yield, and 76% yield, respectively. By contrast, *N*-Boc and *N*-Bs hydrazones do not participate in reactions with sulfonamidyl radical intermediates – events that would give rise to products **176c** and **176d**, respectively.

## 5.4 Iminyl Radicals That Are Generated from Strained Cyclic Oximes Can Engage in Ring-Opening Cascade Reactions

**5.4.1 These Ring-Opening Cascades Are Well-Established Strategies to Affect Distal Carbofunctionalization Reactions Involving Olefins**—When the accessed iminyl radicals are substituents on strained cyclic oximes,  $\beta$ -scission can occur to furnish an alkyl radical that is available for subsequent reactions. Zard and co-workers discovered that under visible light, photoreactive cyclobutanone-derived oxime substrate **181** partakes in a  $\beta$ -scission / radical conjugate addition / chalcogenation cascade with a radical trapping agent such as methyl acrylate (Scheme 45).<sup>178</sup> The operative mechanism in this transformation is posited to involve activation of cyclic oxime **181** via net photolysis

of N–O bond to reveal iminyl radical species **183**. Subsequently,  $\beta$ -scission of iminyl radical **183** generates  $\gamma$ -cyanoalkyl radical **184**. This radical intermediate is poised for the Giese reaction with methyl acrylate to provide electrophilic radical intermediate **185** that is ultimately sequestered by 2-pyridinethiyl group to give rise to chalconized indane **182**. Torsionally strained four-membered cyclic oximes are generally employed as substrates where the ring-opening steps are considerably exothermic ( $G \approx -26.3 \text{ kcal}\cdot\text{mol}^{-1}$  for cyclobutane).<sup>179</sup> Five-membered cyclic oximes, which have less exothermic ring-opening steps ( $G \approx -6.2 \text{ kcal}\cdot\text{mol}^{-1}$ )<sup>179</sup> than their four-membered congeners, are reactive substrates under certain reaction conditions, and they typically require further driving force, such as that available when a resonance- or inductively stabilized alkyl radical species forms through iminyl radical  $\beta$ -scission.

#### 5.4.2 By Using Hydroxyacid-Derived Oxime Substrates, Ring-Opening Cascades Can Result in Direct Atom- or Group-Transfer Processes—

Leonori, Sheik and co-workers recognized hydroxyacid-derived oximes as iminyl radical precursors amenable to photoredox-mediated iminyl radical formation/  $\beta$ -scission / fluorine-, chlorine- and azide-transfer cascades.<sup>180</sup> Formally, oximes **186** react with electrophilic atom- or group-transfer agents “X–Y”, where X is partially positive atom or group, to furnish distal functionalized aliphatic nitriles **187** (Scheme 46A). The initial reaction mechanism is analogous to the tactics disclosed by Leonori and Sheik to affect intramolecular cyclization of an iminyl radical onto an olefin (Scheme 21B).<sup>149</sup> In one plausible mechanism, acid **186** is a precursor to  $\alpha,\alpha$ -dimethylhydroxycarboxylate (not depicted), which can reductively quench an excited state photocatalyst to initiate the sequence that forms iminyl radical **188** and triggers  $\beta$ -scission to unveil 3° cyanoalkyl radical intermediate **189**. The nucleophilic carbon-centered radical engages in atom- or group-transfer reaction with X–Y to yield desired products **187**. Electrophilic reaction byproduct Y• readily accepts an electron from photocatalyst to generate closed-shell species Y and regenerate the ground-state photocatalyst. In fact, the single-electron reduction of electrophilic Y• by photocatalyst is speculated to be exergonic, which could prevent premature oxidation of 3° carbon-centered radical **189**. Using this approach, fluorination, chlorination and azidation of aliphatic nitriles are realized (Scheme 46A). Under the appropriate reaction conditions, Selectfluor®<sup>181</sup> serves as a competent fluorine-transfer agent to yield fluorinated products, while NCS<sup>152</sup> can serve as appropriate chlorine-transfer agent to afford chlorinated products. Furthermore, arylsulfonyl azide traps the putative cyanoalkyl radicals to deliver azide products.<sup>157</sup>

Even though this distal fluorination reaction of aliphatic nitriles hinges on productive photocatalyst turnovers by the substrates, a quantum yield experiment indicates that this fluorine-atom transfer process proceeds predominantly *via* radical chain propagation mechanism ( $\phi = 2.8$ ), albeit in tandem with the photoredox reaction manifold (Scheme 46B). To gauge the propensity for substrates to participate in the fluorination reaction,

$G^0$  values of the conversion of iminyl radical **188** to alkyl radical **189** are approximated by DFT calculations (Scheme 46C). The quantum mechanical investigation suggests that “experimentally successful” fluorination reaction is broadly driven by thermodynamically favorable ring-strain release of the iminyl radical and the radical stabilizing effects of substituents. Cyclobutanone-derived oximes are speculated to engage in facile fluorination

reaction due to the exergonic ring-strain release, while larger cyclic oximes (ring size = 5–7) partake in the reaction if they possess substituents that stabilize the concomitant alkyl radicals.

Furthermore, hydroxy acid-derived oximes engage in potentially mechanistically analogous group-transfer reactions with other electrophilic group-transfer agents. Similar to photoredox-mediated alkynyl transfer reaction with hypervalent iodine (V) reagent and unsaturated oxime by Leonori and co-workers,<sup>149</sup> Waser and co-workers reported that alkynyl transfer reaction with  $\alpha,\alpha$ -dimethylhydroxyacid-derived oxime **186a** and ethynyl benziodoxolone-based alkynyl transfer agent<sup>160</sup> **191a** provides alkynylated product **192a** (Scheme 47).<sup>40</sup> The reaction is not optimal with conventional photocatalysts such as  $[\text{Ir}(\text{dFCF}_3\text{ppy})_2\text{dtbbpy}]\text{PF}_6$ , 4-CzIPN,  $[\text{Mes-Acr}]\text{ClO}_4$  and 9,10-dicyanoanthracene, presumably because they possess excited state potentials that result in inefficient oxidation of oxime **190**, or undesirably efficient oxidation of product. Nevertheless, this reaction proceeds in the presence of more oxidizing 4-CzIPN analogues. Among the 4-CzIPN derivatives, 4-ClCzIPN most effectively converts **190** to **192a**, presumably because its oxidation potential is appropriate to oxidize substrate **190** without promoting product oxidation. With this catalyst, diastereoenriched product **192b** is accessed in 65% yield, and electron-deficient alkyne **192c** is isolated in 71% yield (Scheme 48). In fact, other hypervalent iodine (V) reagents can be employed to permit styrene-transfer reactions (cf. **192d**) with good stereoselectivity, as well as nitrile-transfer (cf. **192f**) and silyl alkyne-transfer (cf. **192e**) reactions, albeit with diminished product yields. Togni's reagent is found to be the exception, as it does not promote trifluoromethyl-transfer reaction to furnish  $\alpha$ -trifluoromethylated amine **192g**.

### 5.4.3 Ring-Opening Cascades Can Trigger Alkene Carbofunctionalization Reactions

$\beta$ -Scission/ring-opening cascade sequences can be intercepted by iminyl radicals derived from cyclic oximes with readily oxidizable electron-dense methoxybenzyl groups, much as  $\gamma,\delta$ -unsaturated oximes with PMP handles template iminyl radical generation / intramolecular annulation upon reductive quenching of photocatalyst.<sup>34</sup> Indeed, cyclic oximes with PMB ethers engage in the Giese reactions with an array of electron-deficient olefins to furnish alkylated products **193a** under UV irradiation with organic photosensitizer 2-Cl-AQN (Scheme 49).<sup>182</sup> To activate cyclic oxime **193a**, reactions involve a net hydrogen-atom abstraction to furnish benzylic/ $\alpha$ -ethereal radical **195** that fragments *via*  $\beta$ -scission to unveil iminyl radical **196** and *p*-tolualdehyde. The generation of iminyl radical is speculated to involve benzylic hydrogen-abstraction of **193a** by \*2-Cl-AQN,<sup>183</sup> a postulate that is consistent with KIE experiments ( $k_{\text{H}}/k_{\text{D}} = 2.13\text{--}2.18$ ). In this reaction, efficiency is correlated with the thermodynamic stability of the generated benzylic radical across a series of readily reducible oximes **193b–193d** ( $E_{\text{p}/2} = +1.37$  to  $+1.86$  V versus SCE in  $\text{CH}_3\text{CN}$ ,  $E_{1/2}^{\text{ox}} = +2.3$  V versus SCE in  $\text{CH}_3\text{CN}$ ).<sup>34,182</sup> Once generated,  $\beta$ -scission of iminyl radical **196** provides alkyl radical intermediate **197** that is trapped by olefin to provide ester-stabilized  $\alpha$ -radical species **198**. Finally, ester-stabilized radical **198** is converted to desired product **194** through two possible mechanisms. First, radical **198** could engage in direct solvent hydrogen-atom abstraction with 2-butanone to provide **194**. Second, radical **198** ( $E_{\text{p}/2} \approx -0.63$  V versus SCE in  $\text{CH}_3\text{CN}$ )<sup>184</sup> could be reduced by

2-Cl-AQN ( $E_{1/2}$  [AQ/AQ<sup>•-</sup>] = -0.96 V versus SCE in CH<sub>3</sub>CN)<sup>35</sup> to provide enolate (not depicted) that undergoes solvent deprotonation to afford **194**. Indeed, deuterium labeling experiments suggest that the latter mechanism should prevail over the hydrogen-atom abstraction mechanism.

Zhou and co-workers developed a related approach to assemble *gem*-difluoroalkenes from hydroxy-acid-derived oxime **199** and  $\alpha$ -trifluoromethyl alkene (Scheme 50).<sup>185</sup> Using this approach, a variety of (hetero)aryl-derived  $\alpha$ -trifluoromethyl alkenes can engage in the reaction, as exemplified by synthesis of *gem*-difluoroalkene with 2-methoxypyridine substituent in 80% yield. While larger cyclic oximes tend to be unresponsive to radical cascade reaction paradigm, this reaction condition renders six-membered cyclic oxime reactive to provide the corresponding product **201e** in 75% yield with 5:1 dr. Remarkably congested compounds can be assembled efficiently, including *gem*-difluoroalkene product **201f**, which contains two contiguous quaternary centers, and is accessed in 77% yield with 15:1 dr.

To the best of knowledge, prior to 2019, there were no photo-mediated strategies to allow the productive and direct use of hydroxyoximes as iminyl radical precursors. Hydroxyoximes are used directly with arylsulfinyl chlorides in the Hudson reaction to generate *N*-sulfonylimines that results in N–O bond fragmentation, and this approach has been leveraged to convert hydroximes to iminyl radicals.<sup>186,187</sup> Nevertheless, photo-irradiative reactions of hydroxyoximes have remained unexplored due to unproductive and competitive O–H bond cleavage that arise from weak O–H BDEs of hydroxyoximes.<sup>188</sup> In 2019, Xiang, Chen, Yang and co-workers addressed this gap in the literature (Scheme 51).<sup>189</sup> Building on the recognition by the Xie and Zhu research groups that triphenylphosphine-derived phosphoranyl radicals<sup>190</sup> could be used to directly activate strong C–O bonds,<sup>191, 192, 193</sup> these researchers determined that the N–O bond of hydroxyoximes could be activated to homolytic cleavage by reaction with these phosphoranyl radicals (Scheme 51). Specifically, these researchers accomplish two-component coupling with hydroxime **204** as an iminyl radical precursor, and  $\alpha,\alpha$ -diaryl- or  $\alpha$ -trifluoromethyl-substituted alkenes as radical trapping agents en route to installation of *bis*-aryl or *gem*-difluoroalkene groups under the aegis of Ph<sub>3</sub>P additive. Triphenylphosphine enjoys a pivotal role in the reaction as an activating group by forming phosphonyl radical,<sup>194</sup> Ph<sub>3</sub>P<sup>•+</sup> ( $E_{1/2}$ [Ph<sub>3</sub>P<sup>•+</sup>/Ph<sub>3</sub>P] = +0.98 V versus SCE),<sup>195</sup> which arises from thermodynamically favorable reductive quenching of the photocatalyst ( $E_{1/2}^{\text{red}}$  [\*Ir<sup>III</sup>/Ir<sup>II</sup>] = +1.21 V versus SCE).<sup>8</sup> Indeed, Stern-Volmer analysis confirms that the photocatalyst can be reductively quenched by Ph<sub>3</sub>P. The generated phosphonyl radical reacts with hydroxime **204** to furnish phosphoranyl radical **205**.<sup>196</sup> Thermodynamically driven  $\beta$ -scission<sup>197</sup> is followed by radical addition to an alkene form carbon-centered radical **206**. The radical is poised for reduction by photocatalyst ( $E_{1/2}$  [Ir<sup>III</sup>/Ir<sup>II</sup>] = -1.37 V versus SCE)<sup>8</sup> to generate carbanion **207**. For example, reduction of diphenyl-stabilized methinyl radical species ( $E_{1/2}$ [R<sup>•</sup>/R<sup>-</sup>]  $\approx$  -1.34 V versus SCE)<sup>204</sup> is achieved by strong reductant [Ir<sup>II</sup>] to provide the desired carbanion intermediate. At this stage, protonation or  $\beta$ -fluoride elimination from anion **207** give rise to diaryl **208** or difluorinated **209**, respectively. Thereby, hydroxyoximes can serve as direct precursors to iminyl radicals in productive synthetic transformations.

Using this approach, extremely electronically varied olefins constitute appropriate radical trapping agents (Scheme 51).  $\alpha$ -Trifluoromethylated alkenes participate in the coupling reaction to access *gem*-difluorinated alkenes with resonance donating and electron-withdrawing aryl substituents (i.e., **209a** and **209b**, respectively).<sup>198, 199</sup> Unsurprisingly, a Giese reaction with chalcone proceeds under this reaction conditions, furnishing Giese reaction product **208a** in 92% yield. With  $\alpha,\alpha$ -diarylolefins, the reaction tolerates pendant quaternary carbon center **208b**, and carbamate **208c**, and can install alkenes with pendant heterocycles to furnish products such as 2-thiophenyl **208d**. Interestingly, *bis-p*-methoxyphenyl groups prompt the formation of olefinated product **208e** as the major product rather than the anticipated net-alkylated product (not depicted). Logically, this reaction pathway could result if generate radical intermediate **206** is more amenable not to the depicted reduction to anion **207**, but, instead, to oxidation to a cationic intermediate (not shown), with subsequent base-mediated elimination to install the olefin. Recognizing this minor limitation, this process offers a step-economical approach to directly engage cyclic hydroxyoximes in  $\beta$ -scission / Giese-type reactions with electron-deficient olefins without pre-installing redox-active handle.

#### 5.4.4 Ring-Opening Cascades Can Be Intercepted by Transition-Metal Mediated Bond-Forming Processes—

Oximes can be used as alkyl radical precursors in nickel-mediated cross-coupling reactions (Scheme 52),<sup>200</sup> merging the above-described approach with known nickel- and photosensitizer-driven processes.<sup>146</sup> A process that relies on oxime precursors may entail photocatalyst activation of oxime **186** to reveal cyanoalkyl radical **189**, which is speculated to undergo C–C cross-coupling reaction with nickel complex and carbon group transfer agent. Highly related reaction conditions furnish arylated-, alkylated-, and vinylated aliphatic nitriles. (Hetero)arylated aliphatic nitriles are easily installed with an array of (hetero)aryl bromides, as exemplified by cross-coupling reactions with caffeine-derived aryl bromide. Alkyl bromide such as L- $\beta$ -bromoalanine can be trapped to afford an unnatural amino acid product. Terminal alkynes as trapping agents promotes a net vinylation reaction that delivers *gem*-disubstituted terminal olefin, as demonstrated with *N*-(3-butynyl)phthalimide as reaction partner to afford an 1,4-diamine product. These photoredox-mediated nickel-catalyzed cross-coupling reactions provide an approach to access (hetero)arylated, vinylated and alkylated alkanes.

An alternative strategy to intercept this photoredox-mediated ring opening cascade sequence takes precedent from a photoredox-mediated and Co-catalyzed vinylation reaction between oxime esters and alkenes<sup>163</sup> to affect olefination (Scheme 53).<sup>201</sup> Indeed, this transformation permits assembly of a diverse catalogue of alkenes from a range of cyclic oxime esters and styrene derivatives. For example, azetidine-derived oxime ester and styrene react to give allylic amine **211a** in 63% yield with high stereoselectivity (>20:1 *E/Z*). This reaction is more broadly relevant, as 2-vinylbenzothiophene is a viable substrate to provide (*E*)-isomer-enriched desired product **211c** in 72% yield. Interestingly, when benzyl methacrylate is subjected to the reaction conditions, a mixture of internal and terminal alkene products **211d** and **211e** are generated. This observation suggests that  $\beta$ -hydride elimination step of organocobalt complex is not regioselective in the presence of multiple  $\beta$ -hydrogen atoms. Unfortunately, this transformation is not suitable for use with 1,2-disubstituted



styrenes or aliphatic olefins. Nevertheless, dual photoredox- and Co-catalyzed Heck-type reactions between cyclic oxime esters and styrenes constitutes complimentary reaction to dual photoredox- and Ni-catalyzed cross-coupling processes that engage cyclic oximes and terminal alkynes to access internal alkenes.

#### 5.4.5 Ring-Opening Cascades Can Rely on *O*-Acyl Cyclic Oxime Substrates to Affect Alkene Carboetherification Reactions

—In a seminal report by Uemura, Nishimura and co-workers, cyclobutanone-derived *O*-benzoyloxime engage in thermally-mediated and iridium-catalyzed N–O bond cleavage to form a nitrogen-centered iminyl radical intermediate.<sup>202</sup> This high-energy radical species is predisposed to undergo  $\beta$ -scission to furnish carbon-centered alkylnitrile radical, which is sequestered by a hydrogen-atom source or group-transfer agent to provide a series of aliphatic nitriles. This reaction cascade is mechanistically analogous to the process that engages  $\alpha$ -hydroxy acid-derived cyclic oximes as substrates. In principle, *O*-acyl cyclic oximes should generate iminyl radicals in presence of photoredox-active molecules. More than a decade after the pioneering disclosure, Zhou and co-workers have hypothesized *O*-acyl cyclic oxime as photoredox-active substrate that undergoes iminyl radical formation /  $\beta$ -scission cascade under photoredox manifold.<sup>203</sup>

A Giese-type reaction constitutes a complementary strategy to introduce new alkyl groups to alkyl chains, using olefin electrophiles and cyclic oximes as alkylnitrile precursors. Within this broader reaction manifold, Zhou and co-workers have developed a photoredox catalyst-mediated approach to utilize cyclobutanone-derived *O*-acyl oxime **212a** as a precursor to an iminyl radical, which enters a cascade sequence involving  $\beta$ -scission and addition across a styrenyl olefin with high electron density to provide linear alkane **213a** (Schemes 54).<sup>203</sup> This strategy relies on a strongly reducing photocatalyst for optimal reaction efficiency: only Ir(ppy)<sub>3</sub> and eosin Y deliver the desired product **213a** in synthetically relevant yields, and each of these photocatalysts possesses excited reduction potentials that are compatible with the reduction potential of oxime **212a** ( $E_p^{\text{red}} = -0.99$  V vs. SCE in CH<sub>2</sub>Cl<sub>2</sub>, Scheme 54).

This approach enables three-component coupling reactions that engage cyclobutanone-derived *O*-acyloximes **212a** as iminyl radical precursors and styrenyl derivatives as radical trapping agents. Following radical trapping, generated radical intermediate **215** is presumed to undergo in situ oxidation furnish a cationic intermediate, which is trapped by the third reaction component: a nucleophilic solvent (Scheme 55). Indeed, the oxidation of benzyl radical **215** ( $E_{p/2} = +0.73$  V versus SCE)<sup>204</sup> to benzyl cation **216** is thermodynamical feasible with Ir(ppy) ( $E_{1/2}[\text{Ir}^{\text{IV}}/\text{Ir}^{\text{III}}] = +0.77$  V versus SCE).<sup>16</sup> In methanol, this process can provide synthetically useful access to  $\beta$ -alkoxyester derives, a class of compounds that is typically accessed *via* aldol addition reactions, based on use of the 1,2-disubstituted olefin, ethyl cinnamate as a radical trapping agent. Alternatively, this process can be used to install a tetrasubstituted distal center based on the use of a 1,1-disubstituted alkene, such as isopropenylbenene, as a radical trapping agent. Furthermore, 1,3-amino alcohol analogues may be accessed using a 3-azetidinone-derived oxime as a substrate. To target formation of more complex ethers, other nucleophilic alcoholic solvents can be employed, such as propargylic alcohol and ethylene glycol. Alternatively, to form simpler benzyl alcohols, water is a suitable nucleophilic solvent.

#### 5.4.6 Ring-Opening Cascades Can Rely on *O*-Acyl Cyclic Oxime Substrates in Net Vinylation Processes

In principle, many alternative approaches could be used to productively engage intermediates generated from cyclobutanone-derived *O*-acyl oxime **212** through two-component cascades involving iminyl radical formation /  $\beta$ -scission, and addition across a  $\pi$ -system. Specifically, Yu has demonstrated that if the engaged olefin is a styrylboronic acid, the generated benzylic radical **219** is proposed to be oxidized to benzylic carbocation **220**, and this intermediate cation can be quenched through deborylation to furnish an (*E*)-1,2-disubstituted olefin (Scheme 56).<sup>205</sup> This strategy permits assembly of biologically relevant scaffolds such as 4,4-disubstituted piperidine,<sup>206</sup> which is prepared in 83% yield and in modest stereoselectivity. Additionally, 1,2-disubstituted allylether and 1,3-diarylpropene are accessed in synthetically relevant yield with high stereoselectivity. As such, this type of reactivity can be harnessed to forge new C(sp<sup>2</sup>)-C(sp<sup>3</sup>) bonds with appropriate olefin coupling partners.

A vinylation reaction is also feasible based on initial cyclobutanone-derived *O*-acyl oxime substrates **221**, while relying on the same initial two-component cascade involving iminyl radical formation /  $\beta$ -scission, and addition across an olefin. Indeed, Chen, Xiao and co-workers intercept these cascades to affect several complementary reactions (Schemes 57–58). In a net vinylation sequence, following radical trapping by an olefin, oxidation of a putative benzylic radical provides a benzylic cation, which undergoes base-mediated elimination reaction of the homobenzylic proton to furnish the olefin (Scheme 57A).<sup>207</sup> Intriguingly, this reaction manifold is robust to silyl enol ether as radical acceptors (Scheme 57B). For example, *O*-acyloxime **212a** reacts with tri-substituted silyl enol ether to provide the  $\alpha$ -substituted ketone **227**, a class of radical acceptor that was not previously viable within the context of another iminyl radical cascade.<sup>128</sup>

#### 5.4.7 Ring-Opening Cascades Can Rely on *O*-Acyl Cyclic Oxime Substrates to Trigger Ring-Expansion Processes

Furthermore, a mechanistically analogous initial two-component cascade can be proposed wherein cyclobutanone-derived *O*-acyl oxime substrates **212** react to trigger ring expansion of vinyl cyclobutanol radical trapping agents **228** and furnish  $\alpha$ -arylated cyclopentanone products **229** (Scheme 58).<sup>208</sup> A plausible mechanism to explain this reactivity involves a familiar cascade sequence of iminyl radical formation /  $\beta$ -scission / addition across an olefin / radical oxidation that can furnish a cation that is vicinal to a fully-substituted alcohol. This intermediate would trigger a 1,2-alkyl shift in a process that is analogous to type-1 semipinacol rearrangement and furnish  $\alpha$ -arylated cyclopentanone products **229**. Consistent with the proposed reaction mechanism, these reactions are more efficient when they engage electron-dense vinyl arenes, which are better poised to resonance stabilize an intermediate cation (i.e., **231**). So, anisole-substituted product **229a** forms more efficiently (in 92% yield) than 4-fluorophenyl-substituted analogue, which is isolated in 54% yield. An appropriately positioned ester could stabilize radical intermediate **230** (Y = CH<sub>2</sub>, R<sup>1</sup> = CO<sub>2</sub>Me), and does not appreciably affect the reaction outcome, furnishing ester-substituted **229d** in 90% yield in 1:1 dr. By contrast, oxetane-derived oxime reacts to form ether **229c** in 54% yield. In this case, it is possible that ring-opening to relatively stable  $\alpha$ -oxygenated radical **230** (Y = O, R<sup>1</sup> = H) could slow olefin trapping en route to ether **229c**, which could be the origin of depressed reaction

efficiencies. Oxetanes themselves do not poison the reaction: vinyl oxetanes can engage in the reaction as radical trapping agents, as evidenced by production of dihydrofuranone **229e** in 83% yield. Additionally, while this process is sensitive to substrate substitution, this reaction can engage less strained cyclopentanol-derived terminal olefin **232** as viable coupling partner with oxime **212a** to deliver cyclohexanone **233** in 69% yield.

#### 5.4.8 Ring-Opening Cascades Can Rely on *O*-Acyl Cyclic Oxime Substrates to Affect Alkene Carbofunctionalization Reactions—

A more practical strategy to introduce carbonyl group to alkyl nitriles from ketone feedstocks is through a radical-polar crossover cascade that couples *O*-acyloxime **212a** and more readily accessible olefin trapping agents (i.e., aryl olefins) in the presence of DMSO to affect a radical addition / Kornblum oxidation cascade.<sup>209,210</sup> This reaction is presumed to proceed through a cascade involving iminyl radical formation /  $\beta$ -scission, and addition across a  $\pi$ -system, yet, the thusly generated intermediate cation (i.e., **236**) is expected to be intercepted intermolecularly by DMSO, with generated cation **237** serving as a viable intermediate in a formal Kornblum oxidation (Scheme 59). While the traditional Kornblum oxidations requires exogenous base to convert alkoxy-sulfonium intermediates to ketones, this reaction does not require exogenous base to obtain the desired ketone product. In fact, the use of base diminishes the reaction performance.<sup>b</sup> The operative oxidation process is speculated to arise from a photoredox-mediated process.<sup>211</sup> Specifically, this research relies on the recognition by Akita and co-workers that an alkoxy-sulfonium intermediate, such as **237**, can be reduced by a photocatalyst in the key step of a radical-mediated formal Kornblum oxidation reaction.<sup>211, 212</sup> This mechanistic hypothesis is consistent with the detection by HRMS of dibenzylsulfide in a crude reaction mixture (Scheme 59B). Furthermore, oxygen-isotope labeling experiment with Me<sub>2</sub>S<sup>18</sup>O (89% <sup>18</sup>O incorporated) delivers unlabeled and labeled products **238a** and **238b** in 23:73 ratio.<sup>210</sup> This mechanistic proposal is also consistent with the reaction outcome when  $\alpha$ -arylated oxime **212c** is used as a substrate. Specifically, oxime **212c** is expected to react through thermodynamically stable benzylic radical **240**, which does not trap olefin, and therefore does not form three component coupling product **241**, but instead forms ketone **239** directly in 60% yield (Scheme 59C).<sup>209</sup>

While the Kornblum oxidation cascade constitutes a viable strategy to incorporate ketone functionality, sulfonylation can proceed when an SO<sub>2</sub> surrogate is included in the reaction. In fact, 1,4-diazabicyclo[2.2.2]octane disulfate (DABSO) has been employed as SO<sub>2</sub> surrogates to affect visible-light mediated sulfonylation cascade with *O*-aryl  $\gamma,\delta$ -unsaturated oximes and silyl enolates.<sup>213,214</sup> Less expensive, commercially abundant potassium metabisulfite can also be used as an SO<sub>2</sub> surrogate to affect sulfonylation<sup>215</sup> under photoredox-mediated conditions.<sup>216</sup> *O*-acyl oximes **212**, K<sub>2</sub>S<sub>2</sub>O<sub>5</sub>, olefins and alcohols participate in multi-component coupling reactions to provide aliphatic sulfones **242** (Scheme 60). This reaction is speculated proceed through trapping of cyanoalkyl radical **189** by SO<sub>2</sub> to provide sulfonyl radical **243**, which is trapped by olefin to deliver radical species **244**. Subsequent oxidation of benzylic radical **244** to carbocation **245** and nucleophilic attack

<sup>b</sup>The reaction mass balance was not disclosed to contextualize the investigation of base, so it is unclear whether diminished yields in reactions involving exogenous base result owing to a competitive unproductive elimination reaction to furnish alkene byproducts, which are the dominant reaction products generated in reference 207 under similar reaction conditions.

by alcohols ultimately produces product **242**. Presumably, oxidation of the benzylic radical occurs at a rate faster than  $k \approx 8.8 \times 10^7 \text{ s}^{-1}$ , as a cyclopropyl radical is expected to undergo ring-opening at this rate,<sup>217</sup> and product **242a**, with an intact cyclopropane forms in 45% yield. This result is difficult to interpret as it is unclear whether cyclopropyl ring-opening products have been detected in this reaction. Reaction conditions are sufficiently mild to enable conversion of 1-methyleneindane to elimination-prone tertiary ether product **242b**, without generating potential indene byproduct.<sup>216</sup> The reaction benefits from strain-release during cyclobutane opening, as less-strained cyclopentanone-derived *O*-acyl oxime is an ineffective substrate that does not provide the product **242c**. In terms of nucleophiles, while *tert*-butanol is not an effective trapping agent in this reaction, presumably owing to steric encumbrance, the reaction is flexible enough to allow the use of water and CD<sub>3</sub>OD as nucleophiles, paving the way to deliver tertiary alcohol **242d**, or to assemble deuterium-incorporating sulfones.

The cascade sequence involving iminyl radical generation /  $\beta$ -scission and SO<sub>2</sub> trapping can be invoked to generate alkylsulfonyl radical **243**, which can be intercepted by aryl-substituted methylenecyclopropanes **246** to provide 3,4-dihydronaphthalenes **247** (Scheme 61).<sup>218</sup> Plausibly, the initial three-component iminyl radical generation /  $\beta$ -scission and SO<sub>2</sub> trapping cascade furnishes carbon-centered radical intermediate **248** that undergoes  $\beta$ -scission to form homoallylic radical species **249**. This homoallylic radical is trapped intramolecularly by a pendant arene and re-aromatization (not depicted) ultimately yields product **247**. Higher yields are observed when methylenecyclopropanes incorporate electron-dense arenes, such as anisole analogues, rather than electron-deficient arenes, such as benzonitrile derivatives **247b** and **247f**. Sterically, *ortho*-substituted aryl methylenecyclopropanes (**247a** and **247b**) are the least responsive olefin substrates in the reaction. Aryl methylenecyclopropanes with *meta*-substitution are more reactive but suffer because radical-addition to arene is not position-selective. For example, the reaction product with *meta*-substituted benzylic ether is isolated as a mixture of positional isomer, favoring A<sup>1,3</sup>-strain minimized product **247c** over A<sup>1,3</sup>-strained product **247d**. Not surprisingly, *para*-substituted aryl methylenecyclopropanes (**247e** and **247f**) are the most reactive among the arene series. This three-component coupling reaction is not effective with phenyl-substituted methylelecyclobutane **250** as a radical trapping agent, presumably because it is expected to undergo net endergonic cyclobutyl-ring-opening / seven-membered ring formation sequence ( $G \approx +4.9 \text{ kcal}\cdot\text{mol}^{-1}$ ).<sup>179</sup> This reaction is not effective when the iminyl radical is generated from heterocyclic oximes, such as azetidine and oxetane derivatives (**212d** and **212e**). Lastly, but not surprisingly, less torsionally strained five-membered cyclic oxime **212f** does not furnish product under the reaction conditions.

By extension, the iminyl radical generation /  $\beta$ -scission / addition to SO<sub>2</sub> cascade sequence can be used to generate alkylsulfonyl radical **243**, which can be intercepted by cyclic vinyl sulfone **252**, which can serve as both an “SO<sub>2</sub>”-source and radical trapping agent in the preparation of  $\beta$ -ketosulfones **253** (Scheme 62).<sup>219</sup> Mechanistically, this transformation leverages organic triflate’s propensity to fragment towards F<sub>3</sub>C• and SO<sub>2</sub><sup>220</sup> and relies on chemoselective alkyl radical addition to SO<sub>2</sub> to generate alkylsulfonyl radical species.<sup>221</sup> To initiate the reaction, literature precedent suggests that energy transfer between

photosensitizer and vinyl sulfone **252** generates enol radical **254** and  $\text{CF}_3\text{SO}_2^\bullet$ .<sup>222</sup> A net radical  $\alpha$ -trifluoromethylation of **254** liberates  $\text{SO}_2$ , which is poised to react with radical species **189** to form alkylsulfonyl radical **243**. Intermolecular trapping of alkylsulfonyl radical **243** by another molecule of cyclic vinyl triflate **252** delivers *O*-stabilized enol radical **257**. This enol radical is poised for  $\beta$ -scission to deliver  $\beta$ -ketosulfone **253** and  $\text{F}_3\text{CSO}_2^\bullet$ , which can fragment into  $\text{F}_3\text{C}^\bullet$  and  $\text{SO}_2$  to propagate another cycle of product formation. This transformation tolerates oximes with synthetically useful functional groups, such as ester and nitrile; however, yields erode with phenyl-substituted oxime substrates, unless the benzylic carbon is fully substituted. Branched  $\beta$ -ketosulfones such as **253e** and **253f** can be synthesized, albeit with reduced isolated yields. Unlike the aforementioned sulfonylation reactions, this reaction renders five-membered cyclic oxime to provide the product **253f** in 42% yield.

#### 5.4.9 Ring-Opening Cascades Can Rely on *O*-Acyl Cyclic Oxime Substrates in (Hetero)arylation Reactions—

The related Minisci-type reactions<sup>223, 224</sup> permit synthetic chemists to formally alkylate heteroarenes and electron-deficient arenes with alkyl radical species *via*  $\text{C}(\text{sp}^2)\text{-H}$  alkylation process. Thus, Minisci-type reactions between cyanoalkyl radicals generated from cyclic oximes and heteroarenes should be possible. In 2017, the Guo laboratory demonstrated that such cyanoalkyl radicals effect Minisci-type reactions with heteroarenes under thermally- and nickel-mediated process.<sup>225</sup> The aforementioned research begat a series of milder photoredox-mediated Minisci-type reactions with cyclic oximes as alkyl radical precursors and heteroarenes (Scheme 63).<sup>226, 227, 228</sup> Research laboratories led by Kong, Xu, and Wang have disclosed that *O*-acyloxime **212a** reacts with quinoxalinone **258a** to deliver alkylated quinoxalinone product **259**, with DMF or  $\text{CH}_2\text{Cl}_2$  as a reaction solvent (Scheme 63A).<sup>226, 227</sup> Shortly thereafter, Xiang, Yang and co-workers document that perfluoropyridin-4-ol-derived oxime **260** is an appropriate precursor to generate the same product *via* a Minisci-type reaction with the same quinoxalinone (i.e., **259**, Scheme 63B).<sup>228</sup> Collectively, this transformation depends on strongly reducing  $\text{Ir}(\text{ppy})_3$  photocatalyst ( $E_{1/2} [^*\text{Ir}^{\text{III}}/\text{Ir}^{\text{IV}}] = -1.73$  versus SCE)<sup>16</sup> to cleave the redox-active handles to reveal the iminyl radical. The *O*-perfluoropyridinyl-derived oxime **260** ( $E_{\text{p}/2} = -1.49$  V versus SCE)<sup>227</sup> can be cleaved by oxidative quenching of  $^*\text{Ir}(\text{ppy})_3$ , and by thermal N–O bond cleavage in dark. Indeed, the reaction without light furnished the desired product **259** in 60% yield. *Sans*  $\text{Ir}(\text{ppy})_3$ , the reaction yields trace quantities of product **259**. At this point, the role of  $\text{Ir}(\text{ppy})_3$  is unclear, but, in a less mechanistically ambiguous scenario, the perfluoropyridin-4-ol handle offers additional opportunity to trigger Minisci-type reactions with heteroarenes under thermally mediated conditions.<sup>228</sup> Following iminyl radical formation and  $\beta$ -scission, cyanoalkyl radical species **189** is poised to undergo radical addition to quinoxalinone to generate *N*-centered radical intermediate **261**, which is oxidized by photocatalyst to generate highly reactive ammoniumyl species that is poised for base-mediated re-aromatization to give the alkylated quinoxalinone **263** (Scheme 63C).

Each of these disclosures about potentially photo-mediated Minisci reactions documents reactivity that is distinct. Wang and co-workers show that less-strained  $\alpha$ -phenyl substituted six-membered cyclic oxime reacts with quinoxalinone **258a** to provide a less compact

product **264** in 42% yield (Scheme 64A).<sup>227</sup> Concurrently, Kong and Xu laboratories show that chromenone **265** can engage in Minisci-type reaction with oxime **212a** to yield the alkylated product **266** in 46% yield,<sup>226</sup> which can be thought of as a base-free alternative that compliments the technology pioneered by Chen, Xiao and co-workers (Scheme 57).<sup>207</sup>

Quinoxalinones are not unique as viable heteroarene radical trapping agents, the Minisci-type reaction can engage other heteroarenes to provide isoquinoline **268** in 37% yield (Scheme 65A).<sup>227</sup> The sluggish reaction performance is improved by the addition of triflic acid, which presumably protonates isoquinoline to generate a more reactive radical acceptor poised, after radical addition, to undergo single electron oxidation and subsequent elimination, ultimately generating isoquinoline **268** in 94% yield.<sup>229</sup> While many heteroarenes are viable, unsubstituted quinoline **269** and 2-phenylpyridine **271**, which have an additional electrophilic carbon-center, produce regioisomeric mixtures of products **270a**, **270b** and **272a**, **272b**, respectively (Scheme 65B). These photo-mediated reactions compliment a silver-catalyzed process.<sup>230</sup>

#### 5.4.10 Ring-Opening Cascades Can Rely on O-Acyl Cyclic Oxime Substrates in Annulation Processes

—Logically, these approaches can be extended to allow for net annulation cascades. The laboratories of Zhao, Chen and Xiao, recognized the viability of annulation cascades involving *N*-phenylacrylamide (**273**) as a radical trapping agent to assemble 3,3-dialkyloxindole derivative **274** (Scheme 66).<sup>203,207</sup> Furthermore, both publications document isonitriles as radical trapping agents in the course of annulation reactions (Scheme 66).<sup>203,207</sup> As a complement to these sp-hybridized  $\pi$ -systems, Chen, Xiao and co-workers demonstrated that phenylacetylene derivative **277** traps intermediates arising from 3-phenyl-*O*-acyl oxime **212g** in a net iminyl radical formation/ $\beta$ -scission / radical formal [4+2]-cycloaddition reaction to access nitrile-decorated 1,2-dihydronaphthalene derivative **278**. (Scheme 66).<sup>207</sup> These photoredox-mediated radical annulation cascades prompted development of synthetic strategies to assemble polycyclic scaffolds.

The net iminyl radical formation/ $\beta$ -scission / radical formal [4+2]-cycloaddition reaction of 3-phenyl-*O*-acyl oxime **212g** and phenylacetylene derivative **277** relies on a pendant arene within cyclobutanone-derived *O*-acyl oxime **212g** for annulation (Scheme 66, third reaction).<sup>207</sup> Chen and Xiao laboratories have developed complementary synthetic protocol that employs 3-naphthyl-substituted *O*-acyl oximes **212** and electron-deficient olefins as coupling partners to build 1,2,3,4-tetrahydrophenanthrene derivatives **279** (Scheme 67A).<sup>231</sup> The efficiency of this protocol depends on specific nature of the electron-deficient olefin radical trapping agent. These reaction conditions do not efficiently engage  $\beta$ -substituted methyl acrylate, dimethyl fumarate,  $\alpha,\beta$ -unsaturated amide, or styrene in the desired reactions. Fortunately, sterically encumbered 3-methylene-dihydrofuran-2-(3*H*)-one proves to be a viable radical trapping agent and provides spirocyclic product **279b** in 27% yield. Furthermore, reactions with  $\alpha,\alpha$ -disubstituted acrylates furnish 1,2,3,4-tetrahydrophenanthrenes with tetrasubstituted carbon-centers. Notably, this strategy affects position-selective radical addition to arenes and avoids the production of site-isomeric product. Site-selectivity may prove to be predictable: DFT calculations are consistent with

the hypothesis that kinetically originated selectivity reflects the relative stabilities of the two penultimate carbon-centered radical species **281a** and **281b** leading to the two positional isomers (Scheme 67B). Indeed, the desired carbon-centered radical **281a** is estimated to be 7.0 kcal•mol<sup>-1</sup> more stable than its site-isomer **281b**.

In the absence of an  $\alpha$ - or  $\beta$ -aryl substituent on the cyclobutanone-derived *O*-acyl oxime, annulation reactions have been reported with aryl isonitriles as radical trapping agents, once again relying on net iminyl radical formation/  $\beta$ -scission cascades to furnish cyclopenta[*b*]quinoxalines (Scheme 68).<sup>232</sup> Previously, tin-based radical initiator had been used to synthesize cyclopenta[*b*]quinoxalines from aryl isonitrile and iodonitrile.<sup>233,234</sup> The photoredox manifold obviates the use of toxic stannane reagents. In this transformation, the addition of *O*-acyl oxime **212**-derived cyanoalkyl radical **189** to aryl isonitriles **282a** forms carbon-centered radical **284**, which is poised to engage in the first annulation sequence (Scheme 68A). In the event, ring closure furnishes iminyl radical **285**, which cyclizes onto a well-positioned arene. Rearomatization reveals cyclopenta[*b*]quinoxaline products **283a**. In these reactions, arene substitution pattern impacts regio- and chemoselectivity. For example, *meta*-substituted aryl isonitriles such as **282b** and **282c** produce regioisomeric mixture of products **283b**, **283c** and **283d**, **283e**, respectively (Scheme 68B). Reasonably, under the reaction conditions, *o*-thiomethyl substituted **282d** delivers alkylated benzothiazole product **286** instead of anticipated product, suggesting that the radical-addition to SMe is favored over the radical-addition to nitrile (Scheme 68C).

#### 5.4.11 Ring-Opening Cascades Can Rely on *O*-Acyl Cyclic Oxime Substrates to Affect Atom- and Group-Transfer and -Trapping Processes—

Furthermore, group-transfer agents (Y–X–X–Y) such as disulfides, diphenyldiselenide and diboronates have been identified as radical trapping agents that partake in the cascadic two-component coupling reactions with *O*-acyl cyclic oximes (Scheme 69).<sup>235</sup> These group-transfer agents are electronically compatible *O*-acyl cyclic oximes because electron-rich radical byproduct Y–X• can reduce oxidized photocatalyst. Thiolation reactions with azetidine-derived oximes are viable with dimethyldisulfide and a variety of electronically perturbed diaryldisulfides to provide amine-substituted sulfides (**288a–288c**) in good yields. Analogous selenylation reaction with the same oxime substrate and diphenyldiselenide provides amine **288d** in 49% yield. *O*-acyl cyclic oximes respond to borylation reaction with diboronic acid and subsequent reaction work-up with pinacol affords easily isolatable boronic ester product. For example, benzyl ether substituted oxime is transformed to **288e**, which is a scaffold could be carried further to access 1,2-diols, highlighting the broad variety that can be introduced into a molecular scaffold using this approach.

Another two-component coupling cascade that begins with *O*-acyl cyclic oxime substrates involves reductive carboxylation with carbon dioxide.<sup>236</sup> Carbon dioxide is an inexpensive feedstock that is poised for nucleophilic attack by carbanion generated from iminyl radical formation /  $\beta$ -scission / single-electron reduction cascade. This type of reactivity is difficult to access from with *O*-acyl cyclic oximes because substrate reduction by the photocatalyst outcompetes reduction of corresponding alkyl radical to the critical carbanion intermediate. Zhang, Yu and co-workers used this challenge as a testing ground to convert *O*-acyl cyclic oxime to carbanion using exogenous reductant (Scheme 70).<sup>237</sup> Mechanistically, it is

proposed that upon excitation of  $[\text{Ir}^{\text{III}}]$  to  $[\text{Ir}^{\text{III}*}]$ , Hünig's base ( $E_p^{\text{ox}} = +0.68$  V versus SCE in benzene)<sup>238</sup> triggers reductive quenching of  $[\text{Ir}^{\text{III}*}]$  to  $[\text{Ir}^{\text{II}}]$  ( $E_{1/2}[\text{Ir}^{\text{II}}/\text{Ir}^{\text{III}}] = +0.68$  V versus SCE in MeCN).<sup>8</sup> Resultant  $[\text{Ir}^{\text{II}}]$  complex is poised to reduce oxime **289** to generate radical anion **291**. In fact, Stern-Volmer analysis reveals that Hünig's base reductively quenches  $[\text{Ir}^{\text{III}*}]$  more quickly ( $K_q = 3.3 \times 10^8 \text{ M}^{-1} \cdot \text{s}^{-1}$ ) relative to oxime **289**.  $\beta$ -scission of the radical anion species reveals iminyl radical **292**, which undergoes a second  $\beta$ -scission process to furnish benzylic radical species **293**. It is speculated that  $[\text{Ir}^{\text{II}}]$  generated from reductive quenching of  $[\text{Ir}^{\text{III}*}]$  by Hünig's base reduces **293** to carbanion **294**. Indeed, the generation of carbanion is supported by deuterium incorporation with  $\text{D}_2\text{O}$  in the reaction of substrate **289** to afford product **296** with 95% deuterium incorporation. Presuming an intermediate radical anion forms, nucleophilic attack on  $\text{CO}_2$  would occur to deliver carboxylate **295**, which could be protonated upon acidic work-up to provide carboxylic acid **290** and complete the ring-opening cascade sequence. Under optimal reaction conditions, oxime **289** is transformed to carboxylic acid **290** in 93% yield. This reaction does not proceed in the absence of light and furnishes trace product absent  $\text{Ir}(\text{ppy})_3$ . In absence of  $\text{CO}_2$ , product **290** is detected in 35% yield, which suggests that sodium carbonate plays dual role of minor source of  $\text{CO}_2$  source and reaction base. Removing sodium carbonate from the reaction yields product **290** in 70%, which establishes  $\text{CO}_2$  as the major  $\text{CO}_2$  source. Intriguingly, absence of Hünig's base nevertheless affords product **290** in 34% yield. So, many of the reaction components serve multiple roles in the reaction.

Through iminyl radical formation /  $\beta$ -scission cascades, other nucleophiles can be incorporated under the assistance of copper catalyst. This process is exemplified by non-photo-mediated copper catalyzed radical cross-coupling reactions of cyanoalkyl radicals generated from *O*-acyl oximes and terminal alkynes.<sup>239</sup> With the rise in utility of copper under photo-mediated manifolds,<sup>240</sup> analogous photo-mediated strategies employing copper catalysts have emerged. It is worth underscoring that despite ongoing discussions on copper's dual role as a photocatalyst and a transition-metal catalyst,<sup>240</sup> dark reactions are viable reaction pathways to elicit desired transformations. The complexity in reaction mechanisms involving copper arises in part because of the redox properties of copper.<sup>241</sup> Notwithstanding the mechanistic uncertainty, irradiation with visible light nevertheless imparts improvement on reaction performance within the context of multicomponent coupling reactions involving cyclic oximes, radical trapping agents and organocuprate intermediates.<sup>242, 243</sup> For these reactions, reaction efficiency improves in the presence of visible-light. This suggests that either a) the copper catalyst participates in photoredox process in tandem with light-independent pathways or, b) visible-light (blue light  $\approx 450$  nm or  $63.5 \text{ kcal} \cdot \text{mol}^{-1}$ ) promotes oxidation of the copper catalyst by N–O bond scission (N–O BDE  $\approx 57 \text{ kcal} \cdot \text{mol}^{-1}$ ).<sup>244</sup> In light of these phenomenon, the upcoming discussions will include reactions that are speculated to involve photoredox events and may note reaction mechanisms that occur in the absence of light.

As an alternative strategy to intercept an iminyl radical formation/  $\beta$ -scission cascade and to install an alkyne, copper catalyst can affect alkynylation in the presence of a terminal alkyne (Scheme 71). Without light, this reaction is possible under thermally mediated conditions.<sup>239</sup> Alternatively, Shi and co-workers report a two-component coupling reaction



between *O*-acyloxime **212a** and terminal alkyne **297** with Cu(OTf)<sub>2</sub> under visible-light irradiation to deliver alkynyl nitrile **298**.<sup>245</sup> This strategy can be employed to convert sterically encumbered cyclic oxime to the alkynyl nitrile **298a** in 77% yield, as well as alkynyl nitrile with quaternary carbon-center **298b** in 59% yield. This reaction also permits terminal alkynes such as indole-derived alkyne to provide the corresponding product **298c** in 55% yield and can render diacetone D-glucose-derived terminal alkyne susceptible to the desired transformation to access complex alkynyl nitrile in 43% yield. Control experiments reveal that this reaction does not proceed in the absence of light, which suggests that light is critical to the operative reaction mechanism. The authors suggest that the benefits of light to the reaction suggest that the copper catalyst is an active photoredox catalyst<sup>240</sup> or that photo-irradiation promotes oxidation of the copper catalyst by N–O bond scission.<sup>244</sup>

An alkyl radical, generated from an *O*-acyl oxime can react with an enantioenriched cyanocuprate complex in a process that ultimately forges a new C(sp)–C(sp<sup>3</sup>) bonds enantioselectively (Scheme 72).<sup>246,247</sup> In the presence of amino indanol-derived chiral spirobisoxaoline ligand<sup>248</sup> **299**, enantioselective cyanation proceeds efficiently between five-membered cyclic oxime **212i** and TMSCN, in the presence of blue light and Ir(ppy)<sub>3</sub> photocatalyst to deliver (*R*)-nitrile **300a** in 78% yield with 96:4 er. This reaction proceeds inefficiently absent light, or absent photocatalyst. Absent copper pre-catalyst, this reaction affords the racemic product in 14% yield, which confirms that bond-formation is mediated by chiral copper complex. In a concurrently developed reaction, *ent*-ligand **299** (*ent*-**299**) and an organic photocatalyst Ph-PTZ react under purple light to furnish product **300b** in (*S*)-enantiomer quantitatively in 95.5:4.5 er (Scheme 72B). Interestingly, this reaction does not proceed without light and the photocatalyst, although trace product is detected when the copper pre-catalyst is omitted.

Mechanistically, both transformations are initiated by generation of nitrogen-centered iminyl radical **301** from photoredox-mediated N–O bond scission involving oxime **212b** (Scheme 72B). Indeed, the reduction of oxime **212b** ( $E_p = -1.69$  V versus SCE in DMA) by both Ir(ppy)<sub>3</sub> ( $E_{1/2} [\text{Ir}^{\text{IV}}/\text{Ir}^{\text{III}}] = -1.77$  V versus SCE in CH<sub>3</sub>CN) and Ph-PTZ ( $E_{1/2} [\text{Ph-PTZ}^+/\text{Ph-PTZ}^*] = -2.1$  V versus SCE in CH<sub>3</sub>CN) are thermodynamically favorable.<sup>247</sup> Stern-Volmer experiments indicate that the oxidative quenching of Ir(ppy)<sub>3</sub> by oxime **212b** is kinetically feasible ( $K_{q,212b} = 4.7 \times 10^7 \text{ M}^{-1}\cdot\text{s}^{-1}$  in PhMe).<sup>c</sup>,<sup>249</sup> The experiments further reveals that (*ent*-**299**)Cu<sup>n</sup>(CN) complex can oxidatively quench the photocatalyst ( $K_{q,[\text{Cu}]} = 1.4 \times 10^7 \text{ M}^{-1}\cdot\text{s}^{-1}$  in PhMe)<sup>c</sup> to potentially generate the corresponding reduced [Cu]<sup>n-1</sup> species. After the photoredox-mediated activation of oxime, it is proposed that the expelled carboxylate liberates cyanide anion from TMSCN through nucleophilic substitution reaction, a hypothesis that is consistent with the detection of trimethylsilyl carboxylate in reaction mixture by GC-MS analysis.<sup>247</sup> The liberated cyanide anion is hypothesized to serve as a counteranion for oxidized photocatalyst. Thermodynamically favorable single-electron oxidation of (*ent*-**299**)Cu<sup>n</sup>(CN) ( $E_{1/2} [\text{Cu}^{\text{I}}/\text{Cu}^{\text{II}}] = +0.36$  V versus SCE in CH<sub>3</sub>CN)<sup>226</sup> by photocatalyst ( $E_{1/2} [\text{Ir}^{\text{IV}}/\text{Ir}^{\text{III}}] = +0.83$  V versus SCE in CH<sub>3</sub>CN,  $E_{1/2} [\text{Ph-PTZ}^+/\text{Ph-PTZ}^*] = +0.68$  V versus SCE in CH<sub>3</sub>CN)<sup>16, 226</sup> provides (*ent*-**299**)Cu<sup>n+1</sup>(CN)<sub>2</sub>.<sup>247</sup> This

<sup>c</sup>The  $K_q$  was calculated from  $d(F_0/F)/d[\text{quencher}]$  values obtained from reference 247 and phosphorescence lifetime of Ir(ppy)<sub>3</sub> in toluene obtained from reference 247.

copper complex is poised to trap alkyl radical species **203** generated from the  $\beta$ -scission of **301** to access organocupric intermediate **303**. The ultimate reductive elimination step establishes new C(sp<sup>3</sup>)–C(sp) bond to provide enantioenriched dinitrile **300b** and regenerate (*ent*-**299**)Cu<sup>II</sup>CN complex. It should be underscored that under the optimal reaction developed by Xiao, Chen and co-workers, this reaction possesses low quantum yield ( $\phi = 0.509$ ). So, the possibility of this transformation proceeding through radical chain propagation mechanism cannot be ruled out. Overall, these enantioselective two-component coupling reactions between cyclic oximes and TMSCN constitute an example from a collection of strategies to affect enantioselective bond-forming reactions through the union of photoredox catalysis with chiral transition-metal catalysis.

#### 5.4.12 Absent an Exogenous Radical-Trapping Agent, Ring-Opening Cascades That Rely on *O*-Acyl Cyclic Oxime Substrates Engage in Migration/Elimination Sequences, or Trap *In Situ*-generated Carboxylate Anions—*O*-Acyl

cyclic oxime substrates can engage in a photoredox-mediated reaction cascade in the absence of radical or nucleophilic trapping agents. For example, 3,3-diaryl-substituted *O*-acyl cyclic oxime **212** is converted to  $\alpha,\beta$ -unsaturated nitrile under the aegis of Ir(ppy)<sub>3</sub> photocatalyst and DABCO as exogenous base (Scheme 73).<sup>250</sup> Photoredox-mediated N–O bond scission /  $\beta$ -scission cascade of oxime **212** ultimately reveals 1° alkyl radical intermediate **305**, which undergoes 1,2-aryl migration to form a secondary benzylic radical. Oxidation of benzylic radical **306** to carbocation **307** and elimination of acidic benzylic proton by DABCO furnishes (*E*)-alkene **304** as the major product. For oximes with different aryl substituents, the migratory aptitude of aryl group appears to be dictated by stereoelectronic considerations. For example, a more electron-rich thiophene moiety migrates more readily than a phenyl substituent to deliver thiophenyl **304a**. Unfortunately, non-selective aryl migration occurs when two differently substituted arenes possess similar electronic and steric profiles. In the case of phenyl and *o*-xylenyl bearing oxime, both arenes rearrange competitively to provide a mixture of products. Ultimately, this reaction affords  $\alpha,\beta$ -unsaturated nitriles and  $\beta$ -functionalized nitriles under mild reaction conditions.

Absent diaryl-substituents, *O*-acyl oxime **212** engages in  $\beta$ -scission / aryl acetate coupling cascade through intermediacy of benzyl radical **309** and benzyl cation **310** to furnish benzoate **308**,<sup>251</sup> which opens possibilities for downstream functionalization reactions with nitrile- or benzoate-groups (Scheme 74). Remarkably, compact to large cyclic oximes ( $n = 1$ – $5$ ) engage in this transformation productively. Strained 4- and 5-membered cyclic oximes proceed through the reaction cascade to provide corresponding desired products **308a** and **308b** in 54% and 81% yields, respectively. Despite the diminished isolated yield, 6-membered cyclic oxime reacts to provide product **308c** in 48% yield. Slightly more strained 7- and 8-membered cyclic oximes are amenable to the reaction, and provide products **308d** and **308e** in 63% and 69% yield, respectively. This reaction cascade can be applied to acyclic oxime, in which ketoxime **311** was converted to ester **312** in 51% yield.

Broadly, reactions with *O*-acyl cyclic oximes as *N*-centered radical precursors rely on oxidative quenching of photocatalyst to affect  $\beta$ -scission / radical addition cascades. These sequences terminate based on oxidation to form a carbocation intermediate, which is

quenched by a nucleophile to foment new C–C or C–heteroatom bonds, or with exogenous base to affect elimination to establish new C=C bonds. Alternatively, by switching the redox-active handles to those that rely on reductive quenching, new reaction modes become available. Specifically, the  $\beta$ -scission / radical addition cascade can be followed directly or indirectly by reduction to install a carbanionic intermediate, and involving electrophilic radical or anion trapping agents, or Brønsted acids. In principle, this approach should enable atom- and group-transfer reactions with electrophilic atom- and group-transfer agents and Giese-type reactions with electron-deficient olefins.

### 5.5. Iminyl Radicals Guide C–H Functionalization Reactions

Notably, iminyl radical intermediates can induce C–H functionalization reactions, which are expected to proceed through 1,5-hydrogen atom transfer (HAT) processes, prior to trapping a halogen atom to generate a 3° alkyl fluoride or chloride. This is remarkable as intramolecular 1,5-HAT process are not likely to be induced by an iminyl radical, and gas-phase DFT calculations performed at the UB3LYP/6–31+G(d,p) level of theory suggest that this abstraction event is an endergonic process (Scheme 75A).<sup>180</sup> Theoretical calculations estimate that the hydrogen-atom abstraction by iminyl radical **313** to generate carbon-centered radical **314** is endergonic by  $G = 4.2 \text{ kcal}\cdot\text{mol}^{-1}$ . Fortunately, Forrester and co-workers<sup>139</sup> envisioned that this process could be energetically favorable under acidic conditions. In acid, the iminium radical cation generated would be more electrophilic than neutral iminyl radical and would favor hydrogen-atom abstraction.<sup>252</sup> Indeed, gas-phase DFT calculations at the same level of theory reveal that the HAT event that converts **315** to **316** is exergonic by  $G = -24.9 \text{ kcal}\cdot\text{mol}^{-1}$ . These calculation results suggest that acidic reaction condition could deliver a highly effective reaction system. Unfortunately, traditional protic conditions are incompatible with the mildly basic photoredox-mediated decarboxylative conditions that furnish access to iminyl radical intermediates.<sup>253</sup>

To overcome this tactical limitation, Leonori and co-workers identified photo-aided conditions to promote decarboxylative fluorination and chlorination reactions (Scheme 75B–C).<sup>180</sup> These photo-mediated fluorination conditions benefit from the addition of a silver salt, which is presumed to facilitate C–F bond formation.<sup>254</sup> The fluorination process proceeds less rapidly in the absence of photocatalyst. Under the optimal conditions, the reaction relies on a radical chain propagation mechanism, as indicated through quantum yield ( $\phi = 4.8$ ) experiments, which suggest that at least 4.8 equivalents of product form per photon of light absorbed. Nevertheless, at least one product suggests that these reaction conditions overcome the site-selectivity that would be achieved through an unguided reaction. The reaction tolerates pendant esters, phenyl substituents, bromides, azides, nitriles, ethers, and thioethers, and has not been described with heteroaromatic substituents. Surprisingly, the developed chlorination conditions tolerate pendant heteroaromatic substituents, including a chloropyridyl unit and a furan, which is prone to undesired electrophilic aromatic chlorination reactions, and would be expected to react directly with the employed chlorinating agent, *N*-chlorosuccinimide (NCS), under highly related conditions (Scheme 75C). These guided chlorination reaction conditions, like the  $\gamma$ -fluorination process conditions, have been applied to two substrates that could be used

to highlight guided site-selectivity. Subjecting a 4,8-dimethyl-1-phenylnonan-1-one-derived oxime to the reaction condition affords chlorinated product **321c** in 34% yield.

Concurrently, Jiang and Studer<sup>148</sup> developed an oxime-guided Giese reaction at tertiary and benzylic C(sp<sup>3</sup>)–H centers (Scheme 76).<sup>255</sup> Following hydrolytic aqueous work-up, a C(4)-functionalized ketone is revealed. This process transforms wide scope of oximes to their corresponding functionalized ketones, and suitable radical trapping agents include  $\alpha,\beta$ -unsaturated esters and ketones. The reaction tolerates aryl and heteroaryl-substituted oximes, as demonstrated with thiophenyl-substituted oxime. Furthermore, if the reaction is worked-up with benzoyl chloride and triethylamine, the product incorporates an activated imine handle that is poised for further functionalization.<sup>256</sup>

Aliphatic *O*-acyl oximes **324** can induce guided net C–H vinylation reactions with styrenyl boronic acids **217a** as radical trapping agents under photoredox-mediated conditions to afford aliphatic ketones **325** (Scheme 77).<sup>205</sup> The most efficient vinylation reactions rely on tertiary radicals as intermediates. So, when a substrate can undergo competitive reactions at secondary or tertiary centers, vinylation proceeds at the tertiary center. Nevertheless, vinylation of a secondary carbon is possible when the engaged center is stabilized by an adjacent heteroatom (cf. **325b**), and even at primary benzylic centers (cf. **325c**).

A directed vinylation reaction proceeds between *O*-acyl oxime **326** and olefin **327** to afford vinylated aliphatic ketone **328** by way of proposed intermediate cation **330**, which is more readily accessible in the presence of an acidic additive (Scheme 78A).<sup>257</sup> Not surprisingly, this transformation exhibits more facile vinylation reactions at tertiary centers relative to secondary centers, where reactions proceed more readily than at primary centers, presumably based on the relative stability of the requisite intermediate radicals. Interestingly, with  $\alpha$ -methyl styrene as a radical trapping agent, terminal alkene product **328d** predominates relative to internal alkene product (not depicted) in 92% yield and in >99:1 *t.i.* With coumarin as a radical trapping agent, C–C bond formation proceeds at the  $\alpha$ -carbon rather than the  $\beta$ -carbon. Indeed, electron-deficient olefins prove challenging as radical trapping agents, including benzyl acrylate, benzyl crotonate, acrylonitrile, and electron-deficient styrenes. Presumably these electron-withdrawing groups should less readily form requisite carbocation intermediates. Notably, the critical carbocationic intermediate can be trapped by water or a nucleophilic alcohol to afford alcohol or ether products (Scheme 78B).<sup>258</sup> In these reactions, when 1,3-diene is used as a radical trapping agent, reactions proceed preferentially at C(2) to provide alcohol **329a**, based on the formation of stable benzylic carbocation en route to product. Ultimately, this approach can furnish either vinylation or oxygenation products.

Iminyl radicals are powerful reaction intermediates that can be harnessed to affect position-selective C(sp<sup>3</sup>)–H functionalization reactions through the intramolecular 1,5-HAT / alkyl radical trap cascade. Logical future directions for reaction development involve enantio- and position-selective C(sp<sup>3</sup>)–H functionalization reactions. These formidable processes are challenging because enantiodetermining steps involving alkyl radicals must be faster than unproductive reaction pathways that lead to enantioerosion.<sup>259</sup>

Fortunately, Nagib and co-workers have reported a guided enantioselective intramolecular C(sp<sup>3</sup>)-H amination reaction that transforms closely related imidates to enantioenriched oxazolines (Scheme 79). These transformations are proposed to involve initial coordination of the iminyl nitrogen to a chiral Cu-complex. This coordination facilitates N-O bond reduction by a photoexcited iridium complex. The resultant imidate radical is poised for 1,5-HAT to direct formation of an alkyl radical. In the critical bond-forming step, the chiral ligand is able to induce enantioselective C-N bond formation.<sup>260</sup> This imidate radical-guided enantioselective C(sp<sup>3</sup>)-H functionalization could set the stage for the invention of iminyl radical-guided enantioselective C(sp<sup>3</sup>)-H functionalization reactions that rely on exogenous radical trapping agents.

## 5.6. Nitrogen-Centered Radicals Can Be Generated from Oxyimides, Oxyamides, and Benzenesulfonamides

### 5.6.1 Radicals Prepared from Oxyimides, Oxyamides, and Benzenesulfonamides Can Engage in *N*-(Hetero)arylation Reactions—

Oxyimides are useful synthetic precursors to imidyl radicals by N-O bond reduction, which can be mediated by visible light photocatalysts. In a pioneering research by Sanford and co-workers, *N*-acyloxyphthalimide **334** bearing an electron-withdrawing trifluoromethyl group engages in *N*-(hetero)arylation reaction with (hetero)arenes in presence of Ir(ppy)<sub>3</sub> photoredox catalyst (Scheme 80).<sup>85</sup> The electron-withdrawing trifluoroacyl group is critical to this reaction. In an earlier investigation led by Okada and Oda, *N*-acyloxyphthalimide with a less electron-deficient acyl group preferentially fragments to imidyl anion and alkyl radical upon photoredox-mediated decarboxylation reaction (Scheme 80A).<sup>95</sup> By contrast, with a more electron-deficient trifluoroacyl substituent, excited state [Ir<sup>III</sup>] catalyst is oxidized to [Ir<sup>IV</sup>] complex, with concomitant reduction of imidate **334** to afford trifluoroacetate **336** and critical imidyl radical **17**. The accessed electrophilic imidyl radical **17** is poised to add to arene **15** to afford radical **18**, which can be oxidized by the [Ir<sup>IV</sup>] complex to provide Wheland intermediate **19** and regenerate ground-state Ir-photocatalyst. Ultimately, re-aromatization of intermediate **19** by trifluoroacetate **336** yields product **16** and trifluoroacetic acid. Generally, addition of imidyl radical to arene follows position-selectivity and reactivity patterns that have been associated with electrophilic aromatic substitution reactions. For example, *p*-anisole reacts to provide predominantly *ortho*-substituted product **335a**, along with less significant amounts of *meta*-substituted and *para*-substituted products. Similarly, α,α,α-trifluoromethylbenzene reacts to furnish *meta*-substituted product **335b** as the major product. More electron-rich arenes are viable substrates for the reaction, as are 2,6-dichloropyridine and 2,6-dibromopyridine. As the process tolerates halogenated arenes, reaction products can be poised for subsequent manipulations in cross-coupling reactions.

While initially these *N*-arylation technologies relied on imidyl radical intermediates, this approach has become more versatile. A similar reaction mechanism can be invoked to rationalize photoredox-mediated reactions between hydroxylamine analogue **337** and heteroarenes, such as indole derivative **338** to yield C(2)-functionalized product **339** (Scheme 81A).<sup>261</sup> Indeed, this reaction also follows general reactivity patterns previously observed in electrophilic aromatic substitution reactions. Indoles with electron-donating

groups are more reactive (**339a**, 94% yield) than those with electron-withdrawing groups. The power of this process is showcased using a melatonin derivative that can be transformed into product **339f** in 97% yield. With more recent advances in nitrogen-source designs, varied electron-deficient *O*-aryloxy amides **340** can be employed as aminating reagents (Scheme 81B).<sup>262</sup>

### 5.6.2 Radicals Prepared from Oxyimides or Oxyamides Can Add Across Double Bonds<sup>263</sup>

—This approach has been extended to enable intramolecular carboamination reactions to access pyrroloindolines (Scheme 82).<sup>264,265</sup> In fact, this strategy has been exploited for rapid synthesis of (±)-flustramide B (Scheme 82A) and (±)-flustraminol B (Scheme 82B). To access (±)-flustramide B,<sup>264</sup> *N*-prenylated *O*-aryloxy amide **346** can be prepared in two steps from brominated indole-3-acetic acid **342** and prenyl bromide **343**. Indeed, *O*-aryloxy amide **346** engages in photoredox-mediated alkylation with  $\alpha$ -sulfonyl acrylate **347** to provide alkylated pyrroloindoline **348** in 76% yield. Subsequent vinyl sulfone reduction and cross-metathesis deliver (±)-flustramide B. This strategy has been applied to prepare (±)-flustraminol B,<sup>265</sup> albeit with a critical difference. The key transformation converts *O*-aryloxy amide **346** to tertiary alcohol **352** based on trapping of an alkyl radical intermediate by O<sub>2</sub> in air in a net hydroxyamination reaction. In this sequence, amide reduction leads to (±)-flustraminol B. As an alternative, it is possible to intercept the key radical cascade sequence to affect net intramolecular hydroamination, as a powerful approach to access other pyrroloindoline cores (Scheme 82C).<sup>265</sup>

Amidyl radicals generated upon N–O bond cleavage can add across electron-dense olefins in the course of diamidation and aminooxygenation reactions (Scheme 83).<sup>266</sup> One mechanistic proposal to explain the net diamination of styrene begins with conversion of *O*-aryloxy amide **356a** to amidyl radical, possibly based on oxidative quenching of excited Ir-photocatalyst. The resultant electrophilic amidyl radical **357a** is poised to add to styrene **359** to furnish benzylic radical **360**. Benzylic radicals ( $E_p \approx +0.73$  V versus SCE in CH<sub>3</sub>CN)<sup>267</sup> undergo thermodynamically favorable oxidation by [Ir<sup>IV</sup>] complexes ( $E_{1/2}$  [Ir<sup>IV</sup>/Ir<sup>III</sup>] = +0.77 V versus SCE in MeCN)<sup>16</sup> to provide carbocation **361** and ground-state Ir(ppy)<sub>3</sub>. At this stage, carbocation **361** could engage in a Ritter-type reaction with acetonitrile to generate nitrilium ion **362** and it is attacked by carboxylate **358** to yield intermediate **363**. As an alternative, DMSO is another solvent that can serve as carbocation trapping agent, and can be used to affect Kornblum oxidation reaction to afford  $\alpha$ -amino ketone **365** from *O*-aryloxy amide **356b** and styrene **359** (Scheme 83B).<sup>266</sup> The roles of solvents in these reactions are supported by experiments using isotopically labeled solvents. In both reactions, a variety of styrenes are viable olefin radical trapping agents. In contrast to the diamidation reaction, this Kornblum oxidation reaction can engage heteroarenes such as thiophene, so this value-adding process is more versatile than the mechanistically related diamination reaction.

Several complementary mechanisms underpin strategies to induce radical-mediated addition across an olefin. For example, an amidyl radical can be generated from *N*-phthalimide derivative by way of an energy transfer event between appropriate photosensitizer. Such an energy transfer process is expected to be the basis for a reaction between

*O*-vinylhydroxylamine **366** and alkene **368** in presence of Ir-photosensitizer and H<sub>2</sub>O to provide ketone **367** (Scheme 84).<sup>170</sup> This intermolecular carboamination reaction is promoted by fragmentation of substrate **366** to oxygen-centered radical species **369** and imidyl radical **370** upon energy transfer. At this point, imidyl radical **370** engages in radical addition to alkene **368** at the sterically uncongested carbon-atom to deliver carbon-centered radical intermediate **371**. Radical **371** engages in a second radical addition with starting material **366**. Finally, β-scission of intermediate **372** affords product **367** and regenerating phthalimidyl radical **370**. As corroboration for this proposed radical chain propagation mechanism, the quantum yield of this reaction is greater than 1 ( $\phi = 12.9$ ). Through this methodology an array of ketones is constructed. For example, 1,2-diamine decorated ketone **367a** is synthesized in 47%. In contrast to reactions mediated by transition-metal catalysts, substrates containing Lewis basic functional groups are compatible in this photosensitized multi-component carboamination reaction. This benefit is evident when an alkene with pendant free-hydroxyl group is subjected to the reaction to provide amino alcohol derivative **367b** in 55% yield.

In an effort to identify easily accessible precursors to amidyl radicals, Studer and co-workers identified α-amido oxyacids **373a** as amidyl radical precursors (Scheme 85).<sup>268</sup> Using these amidyl radical precursors, a cascade sequence involving addition to an olefin can be intercepted by an atom-transfer reagent. To affect fluorination, α-amido oxyacid **373a** is proposed to give way to amidyl radical, which can add across olefin **368**. The resultant benzylic radical reacts with Selectfluor as a fluorine-atom donor to afford β-fluoroamide **374**. This reaction tolerates free hydroxyl groups, as well as bromides (**374b**), nitro groups (**374c**), and protected amines (**374d**). Interestingly, under similar reaction conditions, tetrasubstituted olefin **380a** engages in an ene-type fluorination reaction with Selectfluor to provide allylic fluoride **381**, which then participates in the amidofluorination reaction with amidyl radical and a second equivalent of Selectfluor to provide difluorinated amide **382** in 85% yield.

An analogous reaction cascade can be extended to trigger anti-Markovnikov hydro- and deuterioamidation reactions that engage olefins **380** and α-amido oxyacids **373a** under conditions that may enable dual photoredox and thiol catalysts in the presence of water or heavy water (Scheme 86).<sup>269</sup> In the proposed reaction mechanism, following activation of α-amido oxyacid **373b** towards amidyl radical **357b** via reductive quenching of a photocatalyst, amidyl radical **357b** would react with olefin **380** to form a new C–N bond, and provide carbon-centered radical **364**. Concurrently, carbonate or carbonic acid undergoes proton- or deuterium-exchange with H<sub>2</sub>O or D<sub>2</sub>O to provide carbonic acid that transfers a proton or deuteron to thiolate **387** to provide thiol or deuterated thiol **385**. Hydrogen- or deuterium-atom abstraction delivers hydro- or deuterioamidated product **383**. Remarkably, this reaction is so mild that it tolerates pendant trimethylsilyl ethers, as well as free primary alcohols, and can be used to access a range of selectively deuterated products.

It is possible to engage amidyl radical precursors in enantioselective reactions with 2-acyl imidazoles **389**, which form chiral-at-rhodium complex (–RhO) to provide enantioenriched α-aminated product **390** (Scheme 87).<sup>20</sup> This enantioselective transformation relies on –RhO complex to behave as both reaction photosensitizer and enantioselective

catalyst, analogous to  $\text{-Ir}$  complexes employed by Meggers and co-workers to affect enantioselective alkylation between 2-acyl imidazole and alkyl bromides.<sup>270</sup> In this enantioselective C–N bond-forming reaction,  $\text{-RhO}$  complex serves as both photosensitizer to generate amidyl radical **391** from precursor **388** and as an enantio-inducing Rh-catalyst to promote the formation of chiral Rh-enolate **392**. Subsequently, amidyl radical **391** undergoes radical-addition to chiral Rh-enolate **392** at *si*-face to provide Rh-ketyl **393**. Ligand-exchange involving starting material **389** ultimately releases product **390** and reforms Rh-activated 2-acyl imidazole complex **395**. Interestingly, this reaction proceeds *via* radical chain propagation ( $\phi = 13.6$ ). It is likely that Rh-enolate **392** behaves as initiator and reinitiator, or “smart initiator”.<sup>271</sup> To re-initiate the reaction *via* radical chain propagation mechanism, electron-rich Rh-ketyl complex **393** is poised for single-electron reduction with carbamate **388** to provide amidyl radical **391** and Rh-complex **393**. Ultimately, this is a powerful approach to enantioselective photosensitized reactions.

**5.6.3 Radicals Prepared from Oxyimides or Oxyamides Can Affect C–H Functionalization Reactions**—Amidyl radicals can engage in intermolecular C–H functionalization reactions. With the identification of  $\alpha$ -amido oxy acids **396** as amidyl radical precursors, an opportunity has emerged to take advantage of the propensity of [1.1.1]propellanes **397** to undergo strain-release reactions with nitrogen-centered radicals, and thereby reveal bicyclo[1.1.1]pentylamines, historically challenging to access motifs that are less readily oxidizable bioisosteres of anilines (Scheme 88).<sup>272</sup> This reaction involves mechanistically familiar kinetically feasible reductive quenching of excited state photocatalyst by  $\alpha$ -amido oxy acetate **399** ( $K_q = 3.6 \times 10^6 \text{ M}^{-1}\cdot\text{s}^{-1}$ ) to furnish amidyl radical **401**. Once formed, amidyl radical **401** is trapped by [1.1.1]propellane **397** *via* strain-releasing transition-state geometry **402** to furnish carbon-centered radical **403**. DFT calculations estimates this initial two-component coupling step to possess energy barrier of  $G^\ddagger = 15.3 \text{ kcal}\cdot\text{mol}^{-1}$  and is exergonic by  $-12.4 \text{ kcal}\cdot\text{mol}^{-1}$ . The formed carbon-centered radical can engage in chlorine-atom transfer to provide chlorinated bicyclo[1.1.1]pentylamine **398a**. Alternatively, carbon-centered radical **403** can unproductively react with another molecule of [1.1.1]propellane **397** to provide radical species **408** and undergo oligomerization. Kinetically, the chlorine-atom transfer reaction is predicted to have a lower energy barrier than oligomerization by  $0.8 \text{ kcal}\cdot\text{mol}^{-1}$ , thereby favoring formation of the desired product. Given the relevance of bicyclo[1.1.1]pentane derivatives in medicinal chemistry, chlorinated bicyclo[1.1.1]pentylamine with heteroaryl groups can be incorporated. Indeed, chlorinated bicyclo[1.1.1]pentylamine decorated with 2-chloropyridyl group **398b** is synthesized in 64% yield, as well as tolerating furanyl group to access product **398c** in 59% yield. As exemplified by product **398d**, this reaction can incorporate electron-deficient imidyl group in assembly of chlorinated bicyclo[1.1.1]pentylamine derivative. Unfortunately, primary chlorinated bicyclo[1.1.1]pentylamine **398e** cannot be assembled through this reaction protocol. Instead, the reaction with NH-amidyl radical provides complex mixtures of compounds.

Notably, other atom- and group-transfer reactions can be triggered with appropriate reagents (Scheme 89).<sup>272</sup> Brominated bicyclo[1.1.1]pentylamine **409a** is accessed with bromotrichloromethane as bromine-atom transfer agent, albeit in 20% yield due to



oligomerization. Chalcogenation reactions employs phthalimide derivatives as sulfide- and selenyl-transfer agents, providing sulfides **409b** and **409c** in 66–77% yields and selenylated bicyclo[1.1.1]pentylamine **409d** in 72% yield. 2-phenylmalononitrile serves as hydrogen-atom transfer agent to deliver bicyclo[1.1.1]pentylamine **409e** in 49% yield. Ultimately, this approach provides access to a broad variety of bicyclo[1.1.1]pentylamines, which are promising aniline isosteres.

Amidyl radicals can guide C-H functionalization reactions through intramolecular 1,5-HAT events. Accordingly, photoredox-mediated reaction conditions have been developed to transform oxime esters **401** to functionalized amides **411** with atom- or group-transfer agents through the intermediacy of amidyl radical poised for 1,5-HAT reaction (Scheme 90).<sup>273</sup> To induce productive 1,5-HAT / guided atom- or group-transfer reaction cascade a variety of nitrogen-centered radical species (**413–412d**) have been examined through theoretical investigations of local electrophilicity of nitrogen-centered radical ( $\omega_k^+$ ), N–H and C–H BDEs, as well as  $G^\ddagger$  and  $G$  of 1,5-HAT processes. Not surprisingly, iminyl radical **413** ranks lowest in electrophilicity ( $\omega_k^+ = 0.77$  eV) and 1,5-HAT event is endergonic by 4.2 kcal•mol<sup>-1</sup> with energy barrier of 13.7 kcal•mol<sup>-1</sup>. Carbamoyl radicals **412a**, **412b** and amidyl radical **412c** are more electrophilic than iminyl radical **413** and are estimated to proceed through exergonic 1,5-HAT events with lower energy barriers. Amidyl radical **412d** is ranked as the most electrophilic radical intermediate ( $\omega_k^+ = 1.38$  eV) and is expected to undergo facile 1,5-HAT with estimated  $G^\ddagger = 5.7$  kcal•mol<sup>-1</sup> and  $G = -16.6$  kcal•mol<sup>-1</sup>. Note that for these nitrogen-centered radicals, the difference in BDEs ( $\text{BDE} = \text{BDE}_{\text{N-H}} - \text{BDE}_{\text{C-H}}$ ) correlates to  $G$  values of 1,5-HAT events. Relying on previously employed atom- and group-transfer agents and a permutation of photocatalyst, reaction base and solvent, fluorine-,<sup>181</sup> chlorine-,<sup>152</sup> thiol-,<sup>155</sup> cyano-<sup>161</sup> and alkynyl-transfer<sup>160</sup> reactions are accomplished to provide functionalized amides. For all functionalization reactions under each optimized reaction condition, low quantum yields were observed ( $\phi = 0.02 - 0.08$ ). While these low quantum yields suggest closed radical cycle mechanism, they do not rule out the possibility of radical chain propagation mechanism.

### 5.7. Nitrogen-Centered Radicals Can Be Generated from Amidoxime Esters

In 2003, Zard and co-workers found that amidinyl radicals could be employed as intermediates to construct imidazolines and imidazoles, albeit with use of a stannane-diazo initiator at reflux.<sup>274</sup> Since this disclosure, various reports have described annulation reactions involving amidinyl radical generation, which include iron-<sup>275</sup> and nickel-catalyzed<sup>276</sup> radical annulations, iodine(III)-mediated C(sp<sup>2</sup>)-H imidation of *N*-arylamidines<sup>277,278</sup> and electrolytic N–H bond scission of dihydroquinazoline-derived imines under reflux conditions.<sup>279</sup> Drawing inspirations from pivotal discoveries by Zard co-workers, a collaborative effort from the Wang, Liu and Wang research groups developed a mild photoredox-mediated protocol that converts *N*-aryloxime esters to 2-substituted benzimidazoles (Scheme 91).<sup>280</sup> The reaction suffers predictable substrate scope limitations. For example, *tert*-Butyl substituted *N*-aryloxime ester do not engage in the reaction to furnish the product **415c**, presumably due to kinetically unfavorable steric repulsion in the transition-state geometry of intramolecular annulation event. Further, when the aniline portion of the substrate contains *meta*-substituted OMe (**414a**) and Cl groups

(**414b**), regioisomeric mixtures of corresponding products **415d**, **415f** and **415e**, **415g** are obtained, respectively. Nevertheless, this reaction protocol offers mild and benign reaction condition to productively transform *N*-aryloxime esters to benzimidazoles.

## 6. NITROGEN-CENTERED RADICALS CAN BE GENERATED FROM NITROGEN–HYDROGEN BONDS

### 6.1 Nitrogen-Centered Radicals Can Be Generated by Direct Oxidation of Amines

**6.1.1 Nitrogen-Centered Aminium Radical Cations That Are Generated from Amines Can Add to Olefins**—Nearly 60 years ago, Robert Neale and Richard Hinman disclosed one of the first productive reactions involving the addition of an aminium radical cation across an olefin (Scheme 92).<sup>70, 281, 282</sup> This invention relied on a step to stoichiometrically *N*-halogenate an amine, followed by a second step to process the *N*-halogenated amine through protonation with a strong Brønsted acid and photolysis with ultraviolet light. Under these conditions, light homolyzes the relatively weak *N*-X bond (X = halogen or nitrosyl<sup>283</sup> groups are among the most common). The generated aminium radical cation is poised to form a C–N bond upon radical addition across an olefin. This process exhibits reliable anti-Markovnikov selectivity, as a consequence of both the positive charge and highly electrophilic nature of the aminium radical cation.<sup>281</sup> During the intervening decades, a wide array of methods have been developed for accessing aminium radical cations; none of these reactions, however, enabled direct access to anti-Markovnikov olefin hydroamination without prefunctionalization of amines, forcing reaction conditions, or both.<sup>63, 281, 283, 284</sup>

Fortunately, Knowles and co-workers have streamlined the reaction and liberated it from relatively harsh reaction conditions. They have developed the first general, aminium radical-based, photocatalyst-driven process for anti-Markovnikov, olefin hydroamination (Schemes 92–93).<sup>285, 286</sup> In the presence of light and an iridium photocatalyst, *N*-aryl-*N*-alkyl amines **416** engage pendant aryl olefin acceptors in 5- and 6-*exo-trig* cyclization reactions to furnish cyclic *N*-aryl pyrrolidine, piperidine, morpholine, and piperazine products **417**. This advance permits the transformation to generate products that would not be expected to form under traditional conditions, including 3-pyridinyl **417a**, which forms in 86% yield, as well as furan- and thiophene-containing products (not depicted). In these types of transformations, 6-*exo-trig* cyclization reactions to form piperidine products exhibit greater diastereoselectivity than 5-*exo-trig* cyclization to form pyrrolidine products (cf. **417d** vs. **417e**). Importantly, this transformation provides access to *N*-tosyl piperazine **417f** and morpholine **417g**, albeit in slightly diminished 58% and 44% yields, respectively. This broad substrate tolerance is a testament to the relatively mild and direct conditions that enable this net redox-neutral reaction to proceed.

Knowles and co-workers have proposed a photoredox-catalyzed mechanism for this transformation that is supported by physicochemical measurements. In the proposed reaction mechanism, initial one-electron oxidation of neutral aniline **416** could generate an aminium radical cation **418**, with concurrent reduction of an excited state iridium photocatalyst. Consistent with this proposal, amine **416** has a peak potential ( $E_p$ ) of +0.83

V versus saturated calomel electrode (SCE), indicating that strongly oxidizing iridium(III) photocatalyst ( $E_{1/2}[\text{Ir}^{\text{III}*}/\text{Ir}^{\text{II}}] = +0.66 \text{ V vs. SCE}$ )<sup>8</sup> may be slightly thermodynamically disfavored. Nevertheless, electron transfer between substrate **416** and excited state iridium(III) photocatalyst is kinetically facile, as demonstrated by luminescence quenching assays ( $K_q = 3.1 \times 10^9 \text{ M}^{-1} \text{ s}^{-1}$ ).<sup>12</sup> This oxidation is seemingly reversible, as the relative rate constants for two substrates differ when they are measured in reactions run as experiments with substrate competition or as independent transformations. Cyclization of the thusly generated aminium radical cation onto the olefin would produce benzylic radical species **419**. This C–N bond-forming step is proposed to be the rate-limiting step, an observation that is supported by Hammett analysis, with a linearly correlated  $\sigma_p$  ( $R^2 = 0.96$ ) and a negative  $\rho$  ( $\rho = -0.56$ ). Whereas, if the rate-determining step proceeds through addition of a neutral aminyl radical, a positive  $\rho$ -value would be expected.<sup>287</sup> Moreover, in the subsequent steps, the reaction exhibits a modest, kinetic isotope effect ( $k_H/k_D = 1.1$ , in  $\text{CH}_3\text{OH}$  vs.  $\text{CH}_3\text{OD}$ ), which is consistent with a mechanism in which a new benzylic C–H bond forms to furnish product **417** after the rate-limiting step of the reaction.

In principle, two alternative reaction sequences could convert radical **419** to product: the operative electron-transfer / proton-transfer sequence, or a direct C–H abstraction pathway, a process that is not consistent with deuterium labeling experiments. If the product were to form based on C–H abstraction by radical **419** from the solvent, reactions in  $\text{CD}_3\text{OH}$  would be expected to result in benzylic deuteration; however, these experiments do not result in product deuteration. By contrast, an electron-transfer / proton-transfer sequence is consistent with experimental evidence. Initial reduction should be thermodynamically favorable and allow an aryl-stabilized radical ( $E^0[\text{R}\cdot/\text{R}^-] \approx -1.45 \text{ V versus SCE}$ ),<sup>288</sup> such as **419**, to engage a strong reductant ( $E_{1/2}[\text{Ir}^{\text{II}}/\text{Ir}^{\text{III}}] = -1.51 \text{ V versus SCE}$ )<sup>8</sup> to furnish carbon anion **420**. Following electron-transfer, a proton-transfer step is consistent with reactions carried out in  $\text{CH}_3\text{OD}$ , which result in benzylic deuteration.

Overall, this transformation constitutes a mechanistic complement to the hydroamination system developed by Nicewicz and co-workers, which relies on an organic photocatalyst to oxidize an olefin as the starting point for a net hydroamination reaction.<sup>289</sup>

Building on the development of this technology, Knowles and co-workers advanced the first general method for the intermolecular, anti-Markovnikov hydroamination of unactivated alkenes with secondary alkyl amines (Scheme 94).<sup>290</sup> Investigating dialkyl amine substrates was inspired by research from Luszyk and co-workers, who observed that piperidine-derived radical cations added to unactivated, internal alkenes with a rate more than 100-fold that of the aniline derivatives previously used by Knowles and co-workers.<sup>291, 285</sup> Employing the more strongly oxidizing  $[\text{Ir}(\text{dF}(\text{Me})\text{ppy})_2(\text{dtbbpy})]\text{PF}_6$  (2 mol%) ( $E_{1/2}(\text{Ir}^{\text{III}*}/\text{Ir}^{\text{II}}) = 0.99 \text{ V vs SCE (MeCN)}$ ), secondary dialkyl amines (**421a**), such as piperidine ( $E_p^{\text{ox}} = 0.94 \text{ V vs SCE (MeCN)}$ ),<sup>104</sup> undergo a single electron transfer to furnish aminium radical cations (**424**) which engage in facile addition to olefins (**422a**) resulting in ammonium and radical-carbon bearing intermediate (**425**). Piperidine was found to quench the photoexcited iridium complex in a concentration-dependent manner ( $K_q = 1.7 \text{ M}^{-1} \text{ s}^{-1}$ ),<sup>12, 290</sup> while among a representative set of alkenes, only *N*-Boc-2,3-dihydropyrrole was observed to quench the iridium complex ( $k\tau = 160 \text{ M}^{-1}$ ), thus differentiating this method from those developed by

Nicewicz and co-workers.<sup>289</sup> In order to close the catalytic cycle and access the neutral, hydroamination product (**423a**), Knowles and co-workers found it necessary to include 2,4,6-triisopropylphenyl (TRIP) thiol (50 mol%). The thiol likely facilitates both hydrogen abstraction by the carbon-centered radical and the deprotonation of the ammonium ion. Furthermore, the resultant thiol radical can function as an effective electron sink for closing the catalytic cycle and regenerating the Ir(III) photocatalyst. This critical, double role for TRIP thiol is supported by control reactions finding no reaction occurs in its absence, as well as a complete lack of deuterium incorporation when using deuterated solvents indicating that the solvent is like uninvolved in the transfer of protons.

A broad variety of substituted alkenes can be aminated by secondary amines with 47–98% yield (43 examples) and complete anti-Markovnikov selectivity. Monosubstituted alkene products (**423b**), cyclic and acyclic disubstituted alkene products (**423c** and **423d**), tri-, and tetra-substituted alkene products (**423e**, **423f**, and **423g**) were all accessed in 60–96% yields (Scheme 95). The least effective of these was mono-substituted alkene product (**423b**) which was isolated with 60% yield only after reaction at 45 °C. Conversely, TMS-enol ethers were found to be particularly effective at engaging in this transformation (**423d**) with a 95% yield. A linalool-derived substrate bearing both a trialkyl-alkene and a terminal allylic alcohol was hydroaminated selectively at the trialkyl alkene in 96% yield (**423e**). The tetra-substituted alkene 2,3-dimethyl-but-2-ene was aminated (**423g**) at an impressive 91% yield. The reaction is still effective in the presence of other, potentially reactive heteroatoms on the amine or alkene, including alcohols (**423e** and **423i**), Boc-amines (**423f**), primary amines (**423h**), or spirocyclic amides (**423l**). The benzylic hydroxyl group of a precursor to the antidepressant fluoxetine did result a diminished yield (**423j**, 55% yield), but was unaffected by the aryl ether present in the API (**423k**, 80% yield).

As a further extension of this technology, Knowles and co-workers recently disclosed a new protocol which enables primary amines to engage in intermolecular, anti-Markovnikov hydroamination of unactivated alkenes with 47–98% yields to give secondary amines (Scheme 96).<sup>292</sup> Remarkably, overalkylation to give quaternary amines is not observed, and tertiary amines are barely detectable (< 30:1). In terms of position-selectivity, apart from reactions using dihydropyran as a radical trapping agent, Markovnikov products are not observed. Once again, TMS-enol ethers are effective radical trapping agents, giving 80% yield of 1,2-amino alcohol **428a** upon acidic workup. Furthermore, a product derived from cumylamine (**428b**) is synthesized in 69% yield, which is significant because, with an acidic workup, the cumyl group can be removed to give a primary amine at the site of hydroamination. A terminal, primary olefin reacts to furnish primary amine **428c**, albeit at reduced yield. The reaction does tolerate other potentially reactive functional groups, such as amides **428d**, and engages both *cis*- and *trans*-oct-4-ene with a marginally higher yield of desired product **428e** when beginning from the *cis*- isomer.

Aminium radical cations generated by photoredox catalysis have enabled anti-Markovnikov hydroamination of alkenes both inter- and intramolecularly. Distinct procedures, as developed by Knowles and co-workers, are applicable to primary and secondary amines for intermolecular hydroamination and without meaningful amounts of over-reaction, produce secondary and tertiary amine products, respectively. Mechanistic insights gained from these

developments suggest that the reversal of site-selectivity from that typically observed in transition metal-catalyzed processes arises from the electrophilic nature of the radical cation.

**6.1.2. Nitrogen-Centered Aminium Radical Cations That Are Generated from Amines Are Proposed Intermediates in Arylation Reactions**—Building off a related photoredox platform that engages direct oxidation of arenes for C–H functionalization,<sup>293</sup> Nicewicz and co-workers have disclosed a photo-driven strategy for (hetero)arene C–H amination that is particularly effective with more electron-dense arenes (Scheme 97).<sup>294</sup> Employing a powerfully oxidizing mesityl acridinium photocatalyst under blue light irradiation, a broad array of amines can react productively. The position-selectivity of these reactions depends on the arene substituent: isoleucine methyl ester reacts with anisole to form *ortho*-substituted product preferentially and reacts with an aryl silyl ether to forms *para*-substituted product preferentially. Interestingly,  $\alpha$ -chiral amine products **431a–431d** fully retain enantioenrichment during the reaction, suggesting that the reaction does not transiently generate an  $\alpha$ -aminyl radical. Notably, this process tolerates sterically encumbered amines, such as adamantylamine, and electron-dense heteroarenes, consistent with the broad substrate scope anticipated for reactions under mild conditions.

In order to interrogate the mechanism of this reaction, benzene was employed as a co-solvent and coupling partner for the valine methyl ester **429a** (Scheme 98A). This simplifies mechanistic investigations, as benzene oxidation by the excited state photocatalyst is not expected to be thermodynamically favored ( $[(t\text{Bu})_2\text{Mes-PhAcrid}]^+\text{BF}_4^- : E_{1/2}(\text{PC}^{+*}/\text{PC}^*) = 2.15 \text{ V vs SCE (CH}_3\text{CN)}$ );<sup>294</sup> PhH:  $E_p = 2.75 \text{ V vs SCE (CH}_3\text{CN)}$ ).<sup>294</sup> As product forms under these reaction conditions, this particular set of coupling partners must react through initial amine oxidation, likely to give the aminium radical cation **433**, which can add into benzene's  $\pi$ -system, producing a resonance-stabilized, carbon-centered radical. To close the photocatalytic cycle, Nicewicz and co-workers proposed that adventitious molecular oxygen ( $\text{O}_2$ ) is reduced. Superoxide could deprotonate the aminium cation **434**, and the resultant peroxy species could again react with carbon-centered radical of **435** to give the desired product and hydrogen peroxide as a byproduct. Consistent with this hypothesis, NMR analysis of the reaction mixture immediately following reaction completion<sup>295</sup> reveals a characteristic hydrogen peroxide singlet in two different deuterated solvents.

A formally similar, yet mechanistically distinct, overall reaction has been developed by Leonori and co-workers (Scheme 98B).<sup>296</sup> They propose that their process involves access to a secondary aminium radical cation that engages in  $\text{C}(\text{sp}^2)\text{--H}$  amination. The critical aminium radical cation (i.e. **424**) is prepared via an in situ generated *N*-chloroaminium intermediate, generated by *in-situ* chlorination with NCS followed by activation with an excess of perchloric acid. Once formed, aminium radical cation **424** is readily reduced. Reduction of this cationic intermediate is expected to be thermodynamically favorable ( $E_{p/2} = +0.43 \text{ V vs SCE (CH}_3\text{CN)}$ ) and exhibits kinetically significant quenching of the excited state photocatalyst ( $K_q = 1.5 \times 10^9 \text{ M}^{-1} \text{ s}^{-1}$ ), while quenching of the photocatalyst was not observed with other components of the reaction individually or as mixtures.<sup>296</sup> Ultimately, through steps similar to those proposed with primary amines (Scheme 98A), *N*-aryl amine products such as *N*-phenylpiperidine **431h**, are accessed by C–H amination of relatively electron-dense to electron-neutral arenes and heteroarenes. Collectively, the approaches of

Nicewicz and Leonori extend the scope of viable nitrogen-centered radical precursors in arylation reactions beyond amides to include varied secondary alkyl amines.

Other stoichiometric oxidants can be used in net aryl amination reactions. Dioxxygen has been proposed to perform the same role as a stoichiometric oxidant in the eosin Y-mediated C–N cross-coupling reaction involving primary and secondary alkyl amines and 2-(1*H*)quinoxalinones (Scheme 99).<sup>297</sup> Consistent with this proposal, the reaction is dependent on the presence of molecular oxygen, with no product being produced when run under an atmosphere of nitrogen.

A complementary dehydrogenative cross-coupling reaction relies on catalytic triphenylpyrylium salt with an excess of persulfate in CH<sub>2</sub>Cl<sub>2</sub> under blue light irradiation to affect *ortho*-selective amination of electron-rich phenols by electron-rich diarylamines (Scheme 100).<sup>298</sup> The yield of the desired products decreasing directly with a decrease in electron-donating ability of the arene. Only very electron-dense arenes are viable substrates for this reaction, as phenol and 4-methylphenol do not produce any of the desired product under the reaction conditions.

Nitriles can serve as leaving groups in photo-driven C(sp<sup>2</sup>)–N bond-forming reactions, which rely on 2,4,6-tris(diphenylamino)-5-fluoroisophthalonitrile (3DPAFIPN) as a photosensitizer or photocatalyst (Scheme 101).<sup>299,300,301, 302</sup> Based on transient absorption spectroscopy and Stern-Volmer fluorescence quenching studies, *N*-methylaniline **441a** quenches the excited state photocatalyst ( $K_q = 9.8 \times 10^7 \text{ M}^{-1} \text{ s}^{-1}$ ), and oxidation of aniline **441a** is thermodynamically feasible by photoexcited catalyst ( $E_{p/2}^{\text{ox}}(\mathbf{441a}) = +0.92 \text{ V vs SCE (CH}_3\text{CN)}$ );<sup>299</sup>  $E_{1/2}(\text{PC}^*/\text{PC}^{*\cdot+}) = +1.09 \text{ V vs SCE (CH}_3\text{CN)}$ .<sup>299</sup> While 4-cyanopyridine does not exhibit fluorescence quenching of photoexcited catalyst, transient absorption spectroscopy reveals a concentration dependent quenching of reduced photocatalyst in the presence 4-cyanopyridine ( $K_q = 7.0 \times 10^7 \text{ M}^{-1} \text{ s}^{-1}$ ). Generated aminyl radical cation **443** and pyridinyl radical anion **444** are then proposed to undergo radical–radical cross-coupling to give zwitterionic species **445** which should rapidly lose cyanide to give protonated product **446**. Deprotonation furnishes aminated product **442** in 98% yield. While oxidation of DABCO ( $K_q = 5.3 \times 10^8 \text{ M}^{-1} \text{ s}^{-1}$ ) is kinetically competitive with oxidation of **441a**, this process is not critical to reaction progress as the reaction proceeds with sparingly-soluble, carbonate bases at only slightly reduced yields as well as in the complete absence of base at 21% yield. Notably, other amine sources are viable, including *N*-alkylhydroxylamines which react in DMSO absent base and, using tribasic potassium phosphate, unsymmetric *N*-alkyl and *N*-aryl hydrazines are engaged to prepare *N,N*-diaryl amine **448c** and *N*-alkyl-*N*-aryl amine **448d** in 70% yield and 45% yield respectively (Scheme 102). The process transforms secondary alkyl amines, and the procedure overall is amenable to reaction at a relatively small number of positions on heteroarenes, particularly nitriles with 1,2- or 1,4-relationship to one or more aromatic nitrogen atoms.

Further development of nascent photoredox-generated, aminium radical cation chemistry has enabled the C–H functionalization of (hetero)arenes and the amination of heteroaryl nitriles with amines. Consistent with observations from hydroamination reactions, the C–H functionalization of (hetero)arenes proceeds with preference for amination at relatively

electron-dense positions. These organophotocatalyzed reactions provide access to important *N*-(hetero)aryl products without use of transition-metal catalysis and, in several instances, without addition of stoichiometric reductants, instead engaging adventitious oxygen to close the photocatalytic cycle.

### 6.1.3. Nitrogen-Centered Aminium Radical Cations That Are Generated from Amines Are Proposed Intermediates in Amide Bond-Forming Reactions—

The construction of amide bonds is an important operation in synthetic chemistry, due in large part to their ubiquity in biological and medicinal applications. While a plethora of approaches exist for amide bond formation, the relatively mild, room-temperature, light-driven conditions are appealing for this application, particularly since this approach does not typically result in stoichiometric amounts of byproducts like many state-of-the-art processes.

Beginning in 2014, a wide variety of photocatalysts have been applied in reactions forming amides from secondary alkyl amines, such as **421c**, and aryl aldehydes, such as **449a**, using ambient oxygen as a critical component and likely oxidant (Scheme 103).<sup>21, 26, 37 38</sup> Generally, these reactions employ a visible-light excited photocatalyst and an excess of amine to generate aryl amide products, such as **450a**, in good to excellent yields. These reactions, however, rely on the presence of molecular oxygen and most of the inventors of these technologies have shown that the presence of stoichiometric hydrogen peroxide facilitates the reaction with similar efficiency. This significantly muddles the mechanistic investigation for these reactions. While each make important contributions, further discussion thereof is outside of the scope of this paper, the overall substrate scopes are limited to secondary alkyl amines and aryl aldehydes.

The most recent disclosure of a photo-driven, amide bond-forming reaction, however, has a remarkably broader scope (Scheme 104).<sup>303</sup> Utilizing a common iridium photocatalyst and two equivalents of amine **421**, aldehydes **449** are coupled to form new C–N amide bonds using CH<sub>3</sub>CN as the solvent and, in the absence of oxygen, employ bromotrichloromethane as a terminal oxidant. This manuscript provides the first examples of a photoredox-driven amide bond-forming reaction with a primary alkyl amine, furnishing amino ethyl ester product **450f**, and the synthesis of a urea product (i.e., **450g**).

In contrast to some related technologies, the proposed mechanism reaction is premised on the exclusion of oxygen from the reaction, making the mechanistic analysis and proposal of a photoredox-generated, nitrogen-centered radical more straightforward (Scheme 105).<sup>303</sup> Beginning with the photoexcited iridium complex, oxidation of pyrrolidine **421c** is thermodynamically feasible ( $E_{p/2}^{ox}(\mathbf{421c}) = +0.89$  V vs SCE in CH<sub>3</sub>CN;<sup>104</sup>  $E_{1/2}(\text{Ir}^{\text{III}*}/\text{Ir}^{\text{II}}) = +1.21$  V vs SCE in CH<sub>3</sub>CN),<sup>8</sup> while the possibility of iridium-mediated reduction of aldehyde **449b** is not thermodynamically feasible ( $E_{p/2}^{ox}(\mathbf{449b}) = -1.93$  V vs SCE in CH<sub>3</sub>CN;<sup>104</sup>  $E_{1/2}(\text{Ir}^{\text{III}}/\text{Ir}^{\text{II}}) = -1.37$  V vs SCE in CH<sub>3</sub>CN).<sup>8</sup> Oxidized aminium radical cation **451** can then add across the  $\pi$ -bond of aldehyde **449b** to give *O*-radical aminium cation **452**. Subsequent deprotonation and C–H abstraction involves bromotrichloromethane en route to desired amide **450h**.

While nitrogen-centered radicals derived from other functional groups, such as amides and sulfonamides are resonance stabilized, less stable amine-based, nitrogen-centered radicals can be powerful intermediates. Aminium radical cations engage in synthetically efficient amide bond-forming reactions, C–H functionalization processes involving (hetero)arenes, and hydroamination reactions involving of alkenes. These reactions provide indirect insight into and a richer understanding of the nature of fleeting nitrogen-centered radical intermediates.

## 6.2. Nitrogen-Centered Amidyl Radicals Can Be Generated from N–H Bonds

**6.2.1. Amidyl Radicals Form from Amides *via* Proton-Coupled Electron Transfer (PCET)**—Amidyl radicals have emerged as versatile synthetic intermediates for C–N bond construction, and as directing groups for functionalization reactions, specifically because of the invention of mild technologies to prepare amidyl radicals. Traditionally, amidyl radical intermediates have been inaccessible through direct homolytic activation of amide N–H bonds. Amidyl N–H bond homolysis is challenging because the targeted amidyl N–H bond is strong (BDFE ~100 kcal/mol).<sup>304, 305, 306</sup> Consequently, until recently, amidyl radicals were accessed from amides *indirectly via* N-functionalized precursors,<sup>79, 91, 92, 262, 307, 308, 309, 310, 311, 312, 313</sup> or *directly* with the stoichiometric use of oxidants.<sup>314, 315, 316, 317, 318, 319, 320, 321</sup> These methods limit the substrates amenable to reactions involving amidyl radicals, as many functional groups cannot tolerate the harsh conditions necessary to access such intermediates. Fortunately, Knowles and co-workers<sup>322</sup> have surmounted these challenges, to access amidyl radical intermediates that engage in productive olefin and C–H functionalization reactions (Schemes 106–109).

As a critical insight to enable these processes, Knowles and co-workers demonstrate that the strong N–H bonds of *N*-arylamides can be formally homolyzed to furnish amidyl radical intermediates directly based on Proton-Coupled Electron Transfer processes (PCET, Scheme 106A). In this PCET process, an electron from the N–H bond and the N–H proton are transferred concurrently to two independent acceptors – a one electron oxidant ( $M^{\text{II}}$ ) and a Brønsted base ( $:B^-$ ), respectively. In this system, hydrogen-bonding between the base and the amide weakens the N–H bond, and facilitates its oxidation to give an amidyl radical intermediate.

For PCET processes, a thermodynamic formalism can qualitatively predict effective bond strength for engaged bonds (Scheme 106B), which has predictive power. Specifically, a bond dissociation free energy (BDFE) is the energy required to homolytically break a bond in a particular solvent (Scheme 106B). Formally, a BDFE is the sum of the energy associated with breaking that same bond heterolytically based on deprotonation, as reflected by the acidity of that bond ( $pK_a$ ), with the energies required to oxidize the resulting anion to a neutral radical, to reduce the associated proton to a hydrogen radical.<sup>323</sup> In a PCET process, where the proton and electron travel to separate destinations, an additional term is needed.<sup>324,325,326,327</sup>

This formalism can be employed to accurately predict the reagents necessary to affect Knowles and co-workers' intramolecular carboamination reactions with synthetically useful efficiencies (Scheme 106C). Specifically, Knowles envisions that amidyl radical generation



will rely on a weakly hydrogen-bonding base, and a photocatalyst, whose excited state is capable of accepting an electron from the amide-base complex. Consequently, the optimal base/oxidant pair (entry 4) must have a calculated BDFE similar to that of the amide N–H bond. Indeed, the optimal iridium photocatalyst  $\text{Ir}(\text{dF}(\text{CF}_3)\text{ppy})_2(\text{bpy})\text{PF}_6$  and phosphate base  $(\text{NBu}_4\text{OP}(\text{O})(\text{OBu})_2)$  are predicted to engage with a bond with a BDFE of  $\sim 97$  kcal/mol, near to that of an amide N–H bond (BDFEs  $\sim 100$  kcal/mol), and furnish the desired carboamination product in 92% yield (entry 4, Scheme 106C).

Mechanistically, Knowles and co-workers envision that PCET-based oxidation of the amide to an amidyl radical involves concerted deprotonation by phosphate base ( $\text{B}^-$ ) and electron transfer to photoexcited iridium catalyst ( $^*\text{Ir}^{\text{III}}$ ) (Scheme 107). Luminescence quenching experiments demonstrate that amide oxidation is kinetically feasible, and requires the presence of base ( $k\tau = 731 \text{ M}_1$ ). Moreover, the reaction remains viable when the employed base is less acidic than the amide by 20  $\text{pK}_a$  units, an observation that is consistent with a PCET mechanism, but would not be consistent with a single electron transfer (SET) process. Furthermore, in independent rate experiments, a small kinetic isotope effect ( $k_{\text{N-H/N-D}} = 1.15$ ) suggests that hydrogen-bonding influences the rate of quenching. The formed amidyl radical undergoes 5-*exo* cyclization to form a nascent nucleophilic carbon centered radical, which further engages in an intermolecular addition with acrylate acceptor **458** to yield an electrophilic, resonance stabilized  $\alpha$ -carbonyl radical. This radical is poised for reduction by iridium(II) to regenerate the iridium(III) precatalyst, and form a resonance stabilized anion, which is poised to deprotonate the weak phosphate base and generate the desired carboamination product.

Building on this new approach to access amidyl radicals, Knowles and co-workers have used this strategy to develop efficient and practical olefin hydroamidation protocols.<sup>328, 329, 330, 331</sup> Like other amidyl radical-based functionalization reactions, traditionally, amidyl radical-based olefin hydroamidation reactions have been limited by multistep substrate syntheses, or reliance on hazardous reagents.<sup>91, 92, 162, 316, 332, 333, 334</sup> Additionally, hydroamidation processes require selective homolysis of amide N–H bond (BDFE  $\sim 99$  kcal/mol) in the presence of hydrogen atom donor that incorporates a weaker bond, such as a thiophenol S–H bond (BDFE  $\sim 79$  kcal/mol). Indeed, while empirically optimizing this reaction, Knowles and co-workers find that background reactivity does not substantially improve through the inclusion of catalytic quantities of many common hydrogen-atom donors, such as some phenols, triphenylsilane, some arylamines, and diphenyl acetonitrile (not depicted). Fortunately, reactions proceed optimally when 10 mol% of thiophenol is included as a hydrogen-atom donor (Scheme 108).

This olefin hydroamidation reaction accommodates otherwise oxidatively labile substrates due to the ability of PCET-mediated process to selectively activate amidyl N–H bonds, and can proceed with substrate-induced diastereoselectivity. For example, the reaction tolerates varied *N*-(hetero)aryl substituents to afford pyridyl **463a**, oxazolidinone-containing **463b** in excellent yields. Readily oxidizable pendant thioether **463c** and primary alcohol **463d** form efficiently, overcoming a known limitation of previous hydroamidation technologies, which do not tolerate thioethers or unmasked alcohols. Interestingly, the cyclization reactions involving carbamates derived from the isomeric polyolefins nerol and geraniol

give isoxazolidinones **463e** in 85–95% yield with 1:1 d.r., and provide evidence that substrate olefin geometry has a limited impact on reaction outcome. As expected, more rigid enantioenriched small molecules undergo hydroamidation with the high levels of diastereoselectivity to furnish products such as gibberellic acid-derived **463g** (>20:1 d.r.).

A plausible proposed mechanism for this reaction relies on one processes also critical to the disclosed carboamidation reaction: PCET-based oxidation of the amide to an amidyl radical, with concurrent reduction of the excited state catalyst to Ir(II), and subsequent reaction of the amidyl radical with a pendant olefin to form an exocyclic carbon-centered radical **459** (Scheme 109). Once exocyclic carbon-centered radical **459** forms, hydroamidation product **464** forms *via* hydrogen-atom abstraction from thiophenol, which also furnishes a thiyl radical. The resultant thiyl radical could be reduced with concurrent oxidation of the Ir(II) photocatalyst to regenerate an Ir(III) photocatalyst and a thiophenyl anion.

Of critical import, this proposal requires the stronger amidyl N–H bond (BDFE ~99 kcal/mol) to undergo direct oxidation by the photocatalyst, even in the presence of 20 kcal/mol weaker thiophenol S–H bond (BDFE ~79 kcal/mol), which is known candidate for PCET activation.<sup>335, 336, 337</sup> Although both base-coordinated amide and thiophenol engage in PCET-based activation with similar rates ( $k_{\text{PCET}} = 8.4 \times 10^9 \text{ M}^{-1} \text{ s}^{-1}$  for amide vs.  $9.5 \times 10^9 \text{ M}^{-1} \text{ s}^{-1}$  for thiophenol), chemoselective PCET-based quenching by the amide proceeds owing to the greater hydrogen-bonding ability of an amide relative to a thiophenol (hydrogen-bonding equilibrium constant,  $K_{\text{A}} = 1050 \text{ M}^{-1}$  for amide vs.  $K_{\text{A}} = 200 \text{ M}^{-1}$  for phenol; Scheme 109).<sup>329</sup> A preponderance of evidence supports this mechanistic proposal, accumulated through luminescence quenching experiments, and DFT calculations.

To improve this reaction, Nocera and co-workers investigate the reaction mechanism in gory detail, relying on computational, electrochemical, fluorescent quenching, and transient absorption spectroscopy studies (Scheme 110).<sup>338</sup> Consistent with Knowles and co-workers' analysis, after photocatalysts absorb light to produce the excited state photocatalyst, followed by the PCET between excited photocatalyst/base pair and the amide **465** form a key amidyl radical intermediate ( $k_{\text{PCET1}}$ ). The generated amidyl radical can engage in any of at least three possible reactions: (i) Nonproductive back-electron transfer (BET) between the amidyl radical **467**, and the reduced photocatalyst/conjugate base (BH) pair to regenerate the starting reagents ( $k_{\text{BET}}$ ), (ii) Nonproductive HAT between the amidyl radical and thiol to produce the starting amide **465** and thiyl radical ( $k_{\text{HAT1}}$ ), or (iii) Productive intramolecular 5-*exo* cyclization of the amidyl radical **467** with the pendant olefin form a alkyl radical **468** ( $k_{\text{c}}$ ). In the productive reaction, formed alkyl radical **468** abstracts a hydrogen atom from thiol give desired final product **466** and thiyl radical ( $k_{\text{HAT2}}$ ). Eventually, the photoredox cycle is completed by the PCET to regenerate starting reagents ( $k_{\text{PCET2}}$ ). The catalytic cycle could also be closed by the PCET between alkyl radical and reduced photocatalyst/conjugate base pair ( $k_{\text{PCET3}}$ ). In this investigation, seven rate constants ( $k_{\text{PCET1}}$ ,  $k_{\text{BET}}$ ,  $k_{\text{HAT1}}$ ,  $k_{\text{c}}$ ,  $k_{\text{HAT2}}$ ,  $k_{\text{PCET2}}$ , and  $k_{\text{PCET3}}$ ) associated with the productive and nonproductive pathways are measured using transient absorption spectroscopy.

Nocera and co-workers identify an additive, 2,4,6-trimethyldiphenyl sulfide (MesSSMes), that can decrease the incidence of nonproductive BET pathways, and increase the photon-

efficiency of the productive olefin hydroamidation. To separate the nonproductive BET pathways ( $k_{BET}$  and  $k_{HATI}$ ) from the productive transformations, the authors rely on amide **470** as a substrate, as, owing to the absence of a pendant olefin, this amide cannot cyclize. These nonproductive pathways consume 91.6% of formed amidyl radical and leave 8.4% for the intramolecular radical cyclization. Furthermore, the slow radical cyclization rate ( $k_c$ ) due to delocalization of the radical over aromatic ring also contribute to the lower quantum efficiency of the reaction. To compete with these nonproductive reaction pathways, disulfide (MesSSMes) is introduced as an additive. This additive reversibly traps the amidyl radical to form an off-cycle equilibrium product thioamide **469**, which would be released back to the catalytic cycle to effect the productive radical cyclization. Notably, thioamide **469** can be subjected to olefin hydroamination conditions in the presence of MesSH, and furnishes a mixture of amide **465** and cyclized product **466** in 87% overall yield with ratio of 1:0.2. This experiment supports the presence of reversible equilibria between amidyl radical **467** and thioamide **469** in the olefin hydroamination. Gratifyingly, the use of disulfide (MesSSMes) in place of thiol (MesSH), perturbs the nonproductive BET pathways and indeed provide four-fold increased energy efficiency, for example the quantum yield increased to 11.9% for the para-bromo analog of amide **465a** and 20% for para-cyano analog of the amide **465b**.

When Knowles' olefin hydroamidation reaction relies on thiophenol as a hydrogen-atom transfer catalyst,<sup>328</sup> *N*-aryl amides react productively. Unfortunately, the same protocol is not effective with *N*-alkyl amides, which incorporate stronger N–H bonds (N–H BDFE: *N*-aryl amides ~ 100 kcal/mol vs. *N*-alkyl amides ~ 110 kcal/mol),<sup>339</sup> and form more reactive amidyl radicals. Such highly reactive amidyl radicals engage in nonproductive pathways that compete kinetically with the desired amidyl radical addition to pendant olefins.<sup>60,340,341</sup> Thiol selection can mitigate this limitation: TRIP thiol can perform as an HAT catalyst, with TRIP disulfide as an additive in their photoredox system to effect the olefin hydroamidation of *N*-alkyl amides (Scheme 111).<sup>330</sup>

This protocol converts *N*-alkyl amides, carbamates, thiocarbamates, and ureas bearing terminal olefins to  $\gamma$ -lactams, carbamates, thiocarbamates, and cyclic *N*-acyl amine derivatives. It has been applied to functionalize the muscle relaxant, Baclofen to give Baclofen derivative **472c** in 73% yield with 1:1 dr. Notably, hydroamidation of carbamates having stereogenic centers adjacent to olefin gives product **472d** in good yield and high levels of diastereoselectivity. Predictably, substrates that incorporate multiple olefins exclusively react through a geometrically accessible pathway to furnish five-membered ring-containing product **472e**. More elaborate fine chemicals, such as a peracetylated cholic acid derivative, react in excellent yields.

In this reaction, the critical TRIP disulfide may form a stable off-cycle resting state for the amidyl radical, *N*-thioamide **475a**, as reported by Nocera and co-workers.<sup>338</sup> This hypothesis is consistent with DFT studies that indicate that the conversion of amidyl radical **473** to *N*-thioamide **475a** is energetically favorable ( $G^{\circ}_{\text{calc.}} = -4.3$  kcal/mol, DFT calculations (U $\omega$ B97XD/6–311G++(2d,3p)//UB3LYP/6–31+G(d,p))). Additionally, in parallel with Nocera's findings,<sup>338</sup> the olefin hydroamidation of presynthesized *N*-thioamide **475b** affords lactam **472h** in 86% yield. Based on these observations, Knowles hypothesizes

that the off-cycle intermediate **475b** is likely to improve the reaction efficiency by suppressing the nonproductive back electron transfer pathways.

A broader range of radical acceptors have been developed for use reactions that rely on PCET to induce amidyl radical formation. Indeed, Rueping and co-workers employ aryl alkynyl sulfones to trap the carbon centered radical formed from intramolecular 5-*exo-trig* cyclization of amidyl and carbamoyl radicals (Scheme 112).<sup>342</sup> Indeed, aryl amides, carbamates, and ureas **477a–477d** participate in the radical addition with internal and terminal alkyne, and alkene acceptors to give the functionalized alkynyl pyrrolidine-2-ones in good to excellent yields.

Premised on this approach to access amidyl radicals, arene annulation proceeds with *N*-phenylbenzamide **478** or *N*-phenylcinnamamide **480** substrates, using either iridium-based photosensitizers,<sup>343</sup> or photoactive organic complexes<sup>344</sup> (Scheme 113). In these systems, generated amidyl radicals are, or become, poised to undergo oxidative intramolecular C–H amidation to give phenanthridinones and quinolinones, respectively. With cinnamamide substrates, to achieve this outcome, (*E*)-olefins must be able to isomerize to (*Z*)-olefins under the reaction conditions. Indeed, even in the absence of base, (*E*)-cinnamamide (**482**) partially isomerizes into (*Z*)-cinnamamide, which is positioned for annulation.

Building upon this PCET-based approach to amidyl radical formation,<sup>322, 328</sup> Knowles and co-workers launched a method for a directed site-selective Hofmann-Löffler-Freytag-inspired<sup>67, 307, 345</sup> C–H functionalization reaction (Scheme 114).<sup>9</sup> By analogy to the Knowles' laboratory's olefin hydroamidation process, this pioneering transformation begins with the PCET-enabled conversion of amide **485** to amidyl radical intermediate **486**. Evidence to support the proposed PCET activation mechanism comes from luminescence quenching experiments and prior pK<sub>a</sub> measurements.<sup>346</sup> The generated nitrogen-centered radical is poised for C–H abstraction through a six-membered transition state *via* a 1,5-hydrogen-atom transfer process (1,5-HAT), which has been well-established in the context of Hofmann-Löffler-Freytag reactions.<sup>307</sup> The resultant nucleophilic alkyl radical (i.e., **487**) is trapped by intermolecular conjugate addition to olefin acceptor **489**. In the proposed reaction mechanism, reduction of this electrophilic radical with Ir<sup>II</sup>, and subsequent proton transfer afford alkylated product **491**.

**6.2.2. Amidyl Radicals Formed by PCET Engage in Giese-Type Remote Alkylation Reactions**—These Giese reactions rely on mild conditions that are compatible with a broad range of functional groups, and can be directed by aryl amides, sulfonamides and carbamates, albeit in slightly lower yields when carbamates guide the reaction (Scheme 115A). These reactions are most effective when directed at tertiary centers, and less efficient when guide to secondary centers. Furthermore, this mechanism is viable as a strategy to affect intermolecular Giese reactions, using a limiting quantity of olefin (Scheme 115B).

Following these pioneering studies,<sup>9, 322, 328</sup> and related investigations by Rovis and co-workers (*vide supra*),<sup>353, 354</sup> Meggers and co-workers have identified synergistic possibilities between their approach to chiral-Rh(III)-based, Lewis acid-mediated asymmetric catalysis<sup>347</sup> and Knowles' and Rovis' strategies for accessing amidyl radicals

to develop an enantioselective, amide-guided C–H bond alkylation reaction.<sup>348</sup> Under the optimized conditions, an *in situ*-generated amidyl radical engages in 1,5-HAT to guide the formation of an alkyl radical. Once formed, the proposed model for asymmetric induction involves radical-radical coupling between the generated alkyl radical and a persistent carbon-centered radical. The requisite persistent radical is proposed to form at the  $\beta$ -position of an  $\alpha,\beta$ -unsaturated carbonyl compound that is coordinated to an enantioenriched rhodium complex, following reduction. In this model, the rhodium complex induces asymmetry at the reactive center (Scheme 116). These reactions rely on  $\alpha,\beta$ -unsaturated 2-acyl imidazoles to generate the rhodium-coordinated complex, and benzamides as amidyl radical precursors, and are sensitive to steric encumbrance during the key bond-forming event. These reactions are ineffective for reactions at secondary centers, but with more activated centers afford products in moderate to good yields with high levels of stereoinduction.

An advantage arises from the limitations of this directed reaction – as they are sensitive to steric encumbrance during the key bond-forming event, and ineffective in directed Giese reactions at secondary centers, carbamoyl radicals that are not positioned to react efficiently in directed reactions can engage directly in asymmetric intermolecular reactions with  $\alpha,\beta$ -unsaturated  $\beta$ -aryl 2-acyl imidazoles to install C–N bonds (Scheme 117).<sup>349</sup> By analogy to the C–C bond-forming reactions, the model for asymmetric induction involves radical-radical coupling – in this instance between the generated carbamoyl radical and a persistence carbon-centered radical. Once again, the invoked persistent radical is proposed to form at the  $\beta$ -position of an  $\alpha,\beta$ -unsaturated carbonyl compound that is coordinated to an enantioenriched rhodium complex, following reduction, and the rhodium complex is expected to induce asymmetry at the reactive center (Scheme 117). The optimized conditions benefit from enantioenriched  $\text{-RhO}^{350}$ , relative to catalysts  $\text{-RhS}^{351}$  and  $\text{-IrO}^{352}$ , which do not promote efficient reactions. Interestingly, absent iridium photoredox catalyst, the reaction proceeds in high enantioselectivity and 39% yield, such that the role of iridium photocatalyst in this reaction may be less clear. Consistent with prior research, *N*-alkyl carbamate **497b**, and amide **497d** are not ideal nitrogen-centered radical precursors for this transformation, and  $\beta$ -alkyl enone **497c** does not react to furnish much product. Otherwise, this enantioselective reaction tolerates an impressive range of carbamates and  $\alpha,\beta$ -unsaturated 2-acyl imidazoles to give chiral  $\beta$ -amino acyl imidazoles in moderate to good yields as well as in high enantioselectivity.

Visible light-mediated PCET technologies are well-developed in other contexts, but have only recently emerged as direct strategies to access to amidyl radical intermediates. This PCET-mediated protocol serves as a useful alternative to the traditional strategies for generating amidyl radicals which rely on the *N*-prefunctionalization of amides or processes that involve an excess of oxidizing agents or harsh reaction conditions. As initial hydrogen bonding facilitates the PCET process, the chemoselective activation of an amide in the presence of relatively weaker H-bonding thiol can be efficient under PCET reaction conditions. The mild nature of the PCET process enables efficient reactions involving simple to complex small molecules, and even those incorporating otherwise oxidatively labile functional groups.

**6.2.3. Amidyl Radicals Form from Amides *via* Sequential Proton Transfer and Single Electron Transfer (SET) Processes**—Concurrent with Knowles and co-workers' pioneering directed Giese reactions,<sup>9</sup> the Rovis laboratory reported a similar strategy to access amidyl and carbamoyl radicals, and enter the same cascade of steps to affect C(sp<sup>3</sup>)–H bond alkylation.<sup>353,354</sup> Critically, the Rovis' and Knowles' strategies rely on complementary mechanisms to form amidyl radicals. While Knowles' protocol relies on a concerted PCET process wherein an amidyl N–H bond relies on hydrogen bonding with a weak phosphate base ( $pK_a \approx 20$ ) to activate the amide to photocatalyzed oxidation, the Rovis laboratory accesses amidyl radicals *via* sequential deprotonation of acidic amidyl N–H bond with an appropriately strong base ( $pK_a \approx 1.4$ ) with single-electron-transfer-based amidate oxidation (Scheme 118B). With acidic amide and carbamate substrates, deprotonation by K<sub>3</sub>PO<sub>4</sub> is thermodynamically favorable. Subsequent oxidation of the resultant anion with Ir-photocatalyst is kinetically and thermodynamically feasible, as demonstrated by reduction potentials and Stern-Volmer analyses.

Rovis' Giese reactions enables the functionalization of remote tertiary C–H bond of simple to sterically decorated amides/carbamates with a range of electron-deficient alkene acceptors to give products **499a–499f** with high efficiency (Scheme 118A). This protocol accommodates the methylene C–H bond of amides/carbamates **499c** in lower efficiency. These conditions enable amide alkylation with simple acrylate or acrylamide radical acceptors, which are not tolerated using Knowles and co-workers' conditions. Consistent with directed 1,5-HAT, steroid-derived acetamide **498f** is selectively functionalized at proximal position to N–H bond though multiple distinct tertiary C–H bonds as well as heteroatom activated C–H bonds present in the core.

**6.2.4. Catalytic Quantities of Photoactive Organic Compounds Can Engage Weinreb Amides in Radical-Mediated Reactions**—With the popularity of Knowles' and Rovis' technologies, techniques have emerged that employ organic photoredox catalysts in radical-mediated reactions involving Weinreb amides as substrates which is particularly remarkable as they incorporate relatively weak N–O bonds (Scheme 119,<sup>355</sup> BDE of N–H = 90 kcal/mol).<sup>304</sup> In this report, an array of methoxyacetamides or benzamides to participate in the intermolecular amidation of primary, secondary, or tertiary benzyl positions in moderate to good efficiency. In a related reaction, DDQ has been proposed as a photocatalyst to mediate the reaction between Weinreb amides and enol ethers (Scheme 120).<sup>356</sup>

Overall, photocatalyst-mediated processes surmount the use of strong oxidants, *N*-functionalized precursors, or harsh reaction conditions during the formation of key amidyl radical intermediates. These mild protocols allow oxidatively sensitive substrates to serve as precursors to amidyl radicals, which can participate in efficient intramolecular alkene carboamination/hydroamination reactions, intra- or intermolecular C–H amidation processes, and guided alkylation reactions involving remote C–H bonds.

### 6.3. Nitrogen-Centered Sulfamyl Radicals Can Be Prepared from Sulfonamides and Sulfamides

Following their success in both intermolecular hydroamination of alkenes using amines (*vide supra*, Schemes 94–95)<sup>290</sup> and intramolecular hydroamination of alkenes by PCET in amides (*vide supra*, Schemes 106–109),<sup>322, 328, 329, 330, 331</sup> Knowles and co-workers demonstrated their PCET protocols to engage sulfamyl nitrogen-centered radicals, primarily derived from sulfonamides, in both inter- and intramolecular hydroamination reactions (Scheme 121).<sup>331</sup> In the presence of catalytic amounts of strongly oxidizing iridium photocatalyst, phosphate base, and TRIP thiol under visible light irradiation, unsubstituted and mono-substituted sulfonamides **508** engage in intermolecular, anti-Markovnikov addition across unactivated alkenes. The same reaction conditions prove applicable to 5-*exo*-trig cyclization reactions with sulfonamides bearing a wide array of aryl and alkyl substituents. Of particular note, sulfamide **510** cyclizes onto pendant mono- and tri-substituted alkenes in excellent yields. Sulfamides are a less well-known directing group<sup>357</sup> but have been developed substantially over the past several years,<sup>56,358,359</sup> and structurally diverse sulfamides remain highly sought-after in synthetic targets.<sup>360</sup>

Building upon this approach to generate sulfamyl radical intermediates, Knowles and co-workers have developed an enantioselective, intramolecular hydroamination reaction that employs bulky BINOL-derived phosphate base to induce enantioselectivity (Scheme 122).<sup>361</sup> At decreased temperatures and in  $\alpha,\alpha,\alpha$ -trifluorotoluene, the reaction generates the requisite sulfamyl radical, in substrates of form **512**, through PCET with a strongly oxidizing iridium-photocatalyst and phosphate base, also including TRIP thiol as an HAT-cocatalyst (*vide supra*). Phenol-derived sulfamate ester **513a** is accessed in very good yield with 92:8 er, while a cyclobutane-containing sulfonamide **513b** is accessed in 96% yield with 95:5 er. As demonstrated by product **513c**, the procedure is somewhat sensitive to alkene isomer employed, with yield decreased by 10% when employing a *cis*-alkene rather than a *trans*-alkene and displaying a slight erosion of enantioselectivity in the same comparison. This process is relatively mild, and tolerates additional, distal olefins in the substrates, as demonstrated by unsaturated **513d** which is synthesized in very good yields with a 96:4 er and 1.5:1 dr.

While C–C bond cleavage is not a new concept in synthesis,<sup>362,363</sup> trifluoromethanesulfonamides were first reported as competent in carbon to nitrogen aryl migrations by Shi and co-workers in 2015.<sup>364</sup> While this initial disclosure employs silver reagents with an excess of strong oxidant at high temperatures, in 2017 Nevado and co-workers published a related method that relies on relatively mild, photoredox conditions (Scheme 123).<sup>365</sup> Under blue light irradiation and in the presence of a phosphate base and iridium-based photocatalyst,  $\gamma,\gamma$ -diphenyl-trifluoromethanesulfonamide **514a** reacts to produce nitrogen-centered radical **517**, likely by deprotonation and subsequent oxidation by photoexcited [Ir]. The sulfamyl radical can then proceed through spirocyclic transition state **518** which produces the new *N*-aryl bond and  $\gamma$ -disposed carbon-centered radical through concomitant radical C–N bond formation and C–C bond cleavage. Nevado and co-workers demonstrated the proposed  $\gamma$ -disposed carbon-centered radical **519** could be functionalized by several radical coupling partners, especially phenylsulfone Michael acceptor **515** to give

*N*-aryl  $\gamma$ -alkylated product **516a** in good yield. The phenylsulfonyl radical is then putatively reduced to the corresponding anion to close the photocatalytic cycle. Consistent with this mechanistic proposal, an  $\alpha,\alpha$ -dimethyl sulfonamide reacts in reduced yield but gave as a byproduct  $\gamma$ -homocoupled disulfonamide **522**, the structure of which was confirmed by crystallographic analysis; the most reasonable mechanistic explanations of this byproduct formation would proceed through carbon-centered radicals. Additionally, sulfonamide **514b**, which has electronically distinct aryl groups, is representative of Nevado and co-workers observation that more electron-rich aryl groups preferentially migrate (Scheme 124), as would be expected when mediated by electron-deficient sulfamyl radical **517**. Notably, by changing the base and replacing the acrylate coupling partner with a thiol as a proton-source or a bromine radical precursor, Nevado and co-workers are able to install a proton or a bromide at the  $\gamma$ -carbon (Scheme 125).

More recently, sulfonamide-guided heteroaryl migration reaction have been developed in conjunction with alcohol oxidation processes, which rely on silver complexes as radical trapping agents (Scheme 126).<sup>366</sup> Under strong blue light irradiation at an elevated temperature, a combination of 10-phenylphenothiazine (Ph-PTZ) as photocatalyst and excesses of silver carbonate and monobasic potassium phosphate in 1,4-dioxane enabled the ipso-migration of benzylic heteroarenes, containing two adjacent heteroatoms at tertiary benzylic alcohols to form a new C–N bond and a ketone in an arene migration/oxidation process. The reaction tolerates variation in the sulfonamide moiety and is selective for migration of the electron-dense heteroarenes over other aryl groups.

Sulfonamides are important functional groups in medicinal and agrochemical chemistry, and their application in mild, light-driven processes further bolsters their usefulness to the larger chemical industry. Though nitrogen-centered radical generation from the N–H bond of sulfonamides is less well-explored, recent research, PCET-enabled sulfonamide activation is amenable to a breadth of potential applications, from reactions involving heteroaryl migration to processes involving enantioselective cyclization. Moreover, the broader adoption of PCET-type activation of N–H bonds may enable a more straightforward application of sulfonamides as directing groups for reactions that have previously been developed using substrates with pre-functionalized nitrogen centers (*vide supra*: Sections 2-3).

#### 6.4. Sulfamate Esters Can Direct Photochemically-Mediated Giese Reactions, Likely Guided by Nitrogen-Centered Sulfamyl Radicals

Following the development of sulfamyl radical-guided halogen<sup>72, 367</sup> and group transfer reactions,<sup>110, 368, 369</sup> Roizen and co-workers,<sup>370, 371, 372</sup> Duan and co-workers,<sup>373</sup> and Shu and co-workers<sup>374</sup> each disclosed methods that, under photochemical conditions, directly engage sulfamate esters<sup>375</sup> to guide Giese reactions (Scheme 127). The position-selectivity in these reactions is noteworthy as it complements the selectivity available through other known, radical-mediated C–H functionalization processes. These reactions reliably engage otherwise unactivated secondary and tertiary  $\gamma$ -C(sp<sup>3</sup>)–H bonds in the presence of more electronically activated C(sp<sup>3</sup>)–H centers, such as the ( $\omega$ -1)-C–H bond in substrate **527**.



While there is insufficient data to elucidate a full mechanism, key aspects of the proposed mechanism are supported by the available information, in particular the sufficiency of the photocatalyst to engage in the proposed electron transfers and the intramolecular, guided proton transfer (Scheme 128). These reactions are proposed to involve initial conversion of sulfamate ester **527a** to sulfamyl radical **529**. A detailed understanding of the mechanism leading to initial generation of sulfamyl radical **529** cannot be ascertained from current data as both proton-coupled electron transfer (PCET) and serial proton transfer (PT)/single electron transfer (SET) mechanisms are plausible, and there is not yet direct experimental evidence for a nitrogen-centered radical intermediate. Evidence suggests that sequential deprotonation to form an anion and subsequent SET would be both kinetically and thermodynamically viable. Specifically, Roizen and co-workers reported that the electronically similar propyl *N*-*tert*-butyl sulfamate anion **532** has a half-peak oxidation potential ( $E_{p/2}$ ) of 0.778 V vs. SCE (in CH<sub>3</sub>CN), so its oxidation would be thermodynamically feasible if driven by photoexcited [Ir] ( $E_{1/2}^{\text{III}*/\text{II}} = +1.21$  V vs. SCE in CH<sub>3</sub>CN).<sup>370</sup> Once generated, sulfamyl radical **529** would engage in a 1,6 hydrogen-atom-transfer (1,6-HAT) process to produce a carbon-centered radical. This is proposed to be the position-selectivity-determining step and reaction outcomes are consistent with this directed process even when substrates are likely to be subject to alternative (unguided) C–H functionalization based on competitive site-selectivity (cf. Scheme 127). For example, tetrahydrogeraniol-derived substrate **527a** reacts at the  $\gamma$ -C–H bond, with no evidence of oxidation of the weaker, more electron-rich ( $\omega$ -1)-C–H bond, supporting the proposed mechanism as both selective and intramolecular. This 1,6-HAT process is likely rate-determining based on the primary kinetic isotope effect (KIE;  $k_{\text{H}}/k_{\text{D}}$ ) of 4.69 as measured in parallel experiments.<sup>374</sup> Once this carbon-centered radical is generated, nucleophilic radical addition across an electron-deficient olefin produces an ester-stabilized radical **531**, which should readily be reduced by the photocatalyst ( $E_{1/2}^{\text{III}/\text{II}} = -1.37$  V vs. SCE in CH<sub>3</sub>CN) and subsequently protonated intermolecularly<sup>374</sup> to furnish alkylated sulfamate **528a**. Notably, while sulfamates enantioenriched at the site of functionalization are converted to racemic products, sulfamates recovered from these reactions retain their initial enantioenrichment, indicating both that the carbon-centered sulfamyl radical **530** is generated irreversibly and has a radical lifetime sufficient for epimerization to occur (Scheme 129).

Though a less commonly encountered functional group, the rare  $\gamma$ -carbon selectivity demonstrated by sulfamate ester-derived nitrogen-centered radicals establishes sulfamate esters as an important to the development of C–H functionalization technologies. Furthermore, these reactions are mechanistically interesting, as the exceptionally uncommon 7-membered transition state that is requisite for 1,6-HAT processes. Further development of this  $\gamma$ -carbon selective technology is ongoing.

## 6.5. Hydrazoneyl Radicals Can Be Prepared from Hydrazones

Hydrazoneyl radicals are intermediates in organic synthesis that can be easily formed from hydrazones. Intramolecular 5-*exo*-trig or 6-*endo*-trig cyclization reactions involving hydrazoneyl radicals constitute useful synthetic strategies to prepare pyrazoline, pyrazole, 1,6-dihydropyridazine, and pyradazine analogues. Methods to access hydrazoneyl radicals have been developed that rely on the use of copper catalysis,<sup>376,377,378</sup> or stoichiometric

amounts of oxidants such as azodicarboxylates,<sup>379,380</sup> or TEMPO<sup>381,382,383</sup> or alkyl peroxides<sup>384</sup> (Scheme 130A). By avoiding high temperatures, stoichiometric oxidants, and permissive oxidants, photoredox-mediated processes can convert tosyl hydrazones to hydrazoneyl radicals that can participate in 5-*exo-trig* or 6-*endo-trig* cyclization reactions to furnish 4,5-dihydropyrazoles,<sup>340, 385</sup> or 1,6-dihydropyridazines (Scheme 130B).<sup>340</sup> Interestingly, alkene substitution dictates the type of product that forms, with  $\beta$ -unsubstituted or alkyl hydrazones **535a–b** furnishing 4,5-dihydropyrazole **536a–b**, while  $\beta$ -aryl hydrazones **535c** give 1,6-dihydropyridazines **536c** (Scheme 130B).<sup>340</sup>

A plausible mechanism for this transformation could involve initial deprotonation of the hydrazone by a strong base to afford the hydrazoneyl anion **538a–c** (Scheme 130C). A single-electron oxidation of hydrazoneyl anion (anion **538b**,  $E_{1/2} = +0.56$  V versus SCE in DMF) by the excited state of the photocatalyst ( $^*Ru^{II}$ ,  $E_{1/2}^{*III/I} = +0.77$  V vs SCE in CH<sub>3</sub>CN) could afford hydrazoneyl radical **537a–c** and reduced photocatalyst (Ru<sup>I</sup>). Luminescence quenching experiments reveal that hydrazones **538a–c** quench excited photocatalyst only in the presence of base. Subsequently, cyclization can proceed through 5-*exo-trig* over 6-*endo-trig* processes. DFT calculations provide insight into the position-selectivity of the cyclization reaction (Scheme 130D), suggesting that, with  $\beta$ -unsubstituted or alkylated intermediates, the activation free energy for 5-*exo-trig* cyclization of hydrazoneyl radicals **537a–b** is lower than that for 6-*endo-trig* cyclization. By contrast, with  $\beta$ -unsubstituted or alkylated intermediates, the activation free energy for 5-*exo-trig* cyclization of hydrazoneyl radicals **537c** is higher than that for 6-*endo-trig* cyclization, presumably because the transition state to access a relatively stable aryl radical, would itself be lower in energy, thereby favoring 6-*endo-trig* cyclization. Following cyclization, carbon-centered radicals **539a–c** could be quenched by a hydrogen atom source or TEMPO to afford products.

To complement this method, it is possible to intercept the generated alkyl radical intermediates to affect net oxyamination reactions (Scheme 131A),<sup>386</sup> or net allylation reactions (Scheme 131B).<sup>387</sup> For the oxyamination reaction, limited mechanistic investigations are consistent with TEMPO ( $E_{1/2}^{TEMPO^{\bullet}/TEMPO^+} = +0.62$  V vs Ag/AgCl) and excited state photocatalyst ( $^*PC$ ,  $E_{1/2} = +2.06$  V vs SCE in MeCN) co-operatively catalyzing hydrazoneyl radical formation. Once generated, the alkyl radical intermediate intercepts atmospheric oxygen en route to the oxyamination products, as evidenced by an <sup>18</sup>O-labeling experiment. This method transforms a series of substituted  $\beta,\gamma$ -unsaturated hydrazones into its corresponding 4,5-dihydropyrazolyl methanol or 2,3,4,5-tetrahydropyridazinol derivatives in 51–93% yields.

With these same substrates, absent an intermolecular radical trapping agent, a hydrazone can be converted to a hydrazoneyl radical intermediate, with subsequent cyclization and then undergo a productive intramolecular arylation reaction in the presence of an oxidizing cobalt complex (Scheme 132).<sup>388</sup> This research builds on visible-light photoredox/cobalt-mediated reactions disclosed by Lei<sup>389,390,391,392</sup> and Wu<sup>393,394</sup> research groups. Absent cobalt, hydrazone **535** is converted to unaromatized product **543b**. Interestingly, addition of oxidant such as 1,3-dinitrobenzene or tert-butyl perbenzoate provide aromatized product in moderate yield. Gratifyingly, ruthenium/cobalt-mediated reactions furnish aromatized product **543a**.

A plausible mechanism for this reaction involves initial conversion of hydrazone **535** to hydrazonyl radical **537** based on deprotonation, and single electron transfer to quench excited state photocatalyst (Scheme 132B). Indeed, electron transfer is a kinetically viable process given relatively rapid luminescence quenching of the excited photocatalyst ( $\text{Ru}^{\text{II}*}$ ) by hydrazone **535** in the presence of base. Following intramolecular 5-*exo-trig* radical cyclization by hydrazonyl radical, a generated alkyl radical can add intramolecularly to a pendant aromatic ring to furnish arenium radical **544**. In the presence of cobalt, arenium radical oxidation forms arenium cation **545**, which is poised for deprotonative aromatization. Under the reaction conditions, alkyl and aryl substituted hydrazones are transformed into the respective benzosultams **543a** in moderate to excellent yields. Complementary reactivity can be observed with  $\beta,\beta$ -disubstituted- $\gamma,\delta$ -unsaturated hydrazones, which engage in a 6-*exo-trig* cyclization, radical addition to tosyl group and protonation cascade to deliver tetrahydropyridazines **543b** in moderate to good yields (Scheme 132C).<sup>395</sup>

As a complement to the variety of reactions developed to transform substituted  $\beta,\gamma$ -alkenyl hydrazones based on intramolecular 5-*exo-trig* or 6-*endo-trig* cyclization of hydrazonyl radicals, 6-*exo-dig* cyclization reaction/Smiles rearrangement<sup>396</sup> cascades of hydrazonyl radical intermediates have been invented to transform substrates containing terminal alkynes (Scheme 133).<sup>397</sup> A plausible mechanism for this reaction involves base assisted formation of hydrazonyl anion **548** ( $E_{1/2} = +0.54$  V vs SCE in EtOH), which is thermochemically capable of being oxidized by excited state photocatalyst ( $^*\text{Ru}^{\text{II}}$ ,  $E_{1/2}^{\text{II}*/\text{I}} = +0.77$  V vs SCE in MeCN) to furnish hydrazonyl radical **549**. Resultant radical **549** is poised for sequential intramolecular 6-*exo-dig* cyclization and a radical Smiles rearrangement to form radical species **551**. Ultimately, the reduced state photocatalyst ( $\text{Ru}^{\text{I}}$ ) could reduce alkyl radical **551** to anion **552**, which could be protonated by the solvent to yield phthalazine. This method accommodates variety of terminal alkyl or aryl substituted alkynyl hydrazones bearing aryl or heteroaryl migrating groups. Remarkably, authors have also developed an efficient one-pot two-step protocol for the phthalazines starting directly from the corresponding aldehydes and sulfonylhydrazines.

The above described methods to prepare of dihydropyrazoles *via* hydrazonyl radical cyclization rely on  $\beta,\gamma$ -unsaturated hydrazones as substrates; however, less elaborate substrates can be viable precursor to dihydropyrazoles based on in situ access to  $\beta,\gamma$ -unsaturated hydrazones. Recently, Cai and co-workers have used  $\alpha$ -bromo hydrazones **553** and  $\beta$ -ketocarboxyls **554** as precursors to dihydropyrazoles (Scheme 134).<sup>398</sup> Mechanistically, initial deprotonation of  $\beta$ -ketocarboxyl **554** is followed by nucleophilic displacement of  $\alpha$ -bromo hydrazones to provide hydrazonyl anion. In the presence of a visible-light photosensitizer, hydrazonyl anion can be oxidized to hydrazonyl radical **556**, which undergoes intramolecular cyclization to give dihydropyrazoles. A hydrazonyl radical intermediate is implicated as, absent photocatalyst, 1,2-dihydropyridazine **557** forms. This method converts a variety of readily accessible alkyl and aryl hydrazones and 1,3-dicarbonyl analogs to furnish dihydropyrazoles.

These photocatalyst-mediated process avoid the use of high temperatures, and strong oxidants, and provide a mild protocol for the generation of the hydrazonyl radical intermediates. The intramolecular hydrazonyl radical cyclization process

offer straightforward routes functionalized benzosultams, dihydrobenzosultams, 4,5-dihydropyrazoles, and 1,6-dihydropyridazines, with substrate substitution critically influencing product-selectivity.

## 7. CONCLUSION AND OUTLOOK

With efficient access to nitrogen-centered radicals through photocatalysis, many transformations have become more broadly viable, and more efficient. Among these are C–H functionalizations involving arenes and unactivated aliphatic bonds, as well as olefin functionalization processes and transformations involving bond migration. With typically mild reaction conditions, a variety of otherwise reactive functional groups can be carried through these transformations. Nevertheless, the abundance of publications in this nascent field belies the challenges yet to be overcome that will enable broad adoption of these novel technologies by practitioners of total synthesis, or within polymer chemistry. Among reactions presented herein, stereoselective processes remain underdeveloped, with current strategies relying on exogenous, chiral transition-metal catalysts<sup>18, 270, 347, 348, 349, 350, 351, 352</sup> or chiral phosphate bases.<sup>361</sup> There are a number of stereoselective reactions that merge photocatalysis and transition-metal catalysts,<sup>246, 247, 399, 400</sup> and it is possible that some of these strategies are compatible with currently-racemic reactions, while maintaining the advantages conferred by photocatalytic reactions involving nitrogen-centered radicals. Future developments of broadly generalizable platforms for photocatalytic reactions of nitrogen-centered radicals will hinge upon and be bolstered by continuing efforts to better characterize the underlying physical and photochemical processes in this chemistry. Ultimately, technological developments to date provide a promising foundation for the future of nitrogen-centered radical chemistry.

## Funding Sources

National Institutes of Health (R35GM128741–01).

## Biographies

Kitae Kwon grew up in New York City where he received his bachelor's degree in Chemical Biology and minor in French from Baruch College. As an undergraduate, he performed theoretical organic chemistry research with Prof. Edyta M. Greer and developed insatiable curiosity for physical organic chemistry. Under the mentorship of Prof. Greer, he published research articles examining reaction mechanisms, a review article on quantum tunnelling, and a book chapter on computational methods relevant to organic chemistry. With an intent to expand his horizon, Kitae chose to pursue Ph.D. research at Duke University under the mentorship of Prof. Jennifer L. Roizen to gain training in synthetic organic chemistry. During his tenure in the Roizen laboratory, he uses principles of physical organic chemistry to invent photoredox-mediated and transition-metal catalyzed C–H functionalization reactions, and to synthesize biologically relevant small molecules.

Nandakumar Meganathan received his bachelor's degree from Pachaiyappas' College, Kanchipuram, and a master's degree from Anna University, India, before choosing to pursue a Ph.D. at the University of Madras, India with Prof. A. K. Mohanakrishnan as a CSIR-

Junior Research Fellow. Nandakumar earned his Ph.D. in 2015 for investigations to develop methods to synthesize 1,2-diaroylbenzenes, dibenzothiophene sulfones, fluorenones and vinylens. After graduation, Nandakumar moved to National Tsing Hua University, Taiwan to peruse his postdoctoral research with Prof. Yun Chi where he explored the synthesis of Ru(II) and Pt(II) complexes for optoelectronic applications. Collectively, these research experiences helped him to secure a highly prestigious Marie-Curie Postdoctoral Research Fellowship in 2017 to support research with Prof. Varinder. K. Aggarwal (University of Bristol, UK). At Bristol, he prepared and further functionalized tertiary trifluoromethyl boronic esters using lithiation-borylation chemistry. Pursuing an interest in photoredox-mediated radical chemistry, motivated Nandakumar to pursue further postdoctoral research with Prof. Jennifer L. Roizen at Duke University, where he is currently developing photoredox- and nickel-driven directed arylation strategies.

R. Thomas Simons is an alumnus of Indiana Wesleyan University and the John Wesley Honors College, where he earned a Bachelor of Science degree, with majors in Chemistry and Physics. As an undergraduate, he developed Biochemistry laboratories for undergraduates with Prof. Benjamin Linger and conducted Organic Chemistry research with Prof. Stephen Leonard. In 2018, Thomas began his graduate studies at Duke University, joining the laboratory of Prof. Roizen. His doctoral research has focused on photocatalytic reactions with sulfamides and sulfamates esters, particularly in relation to nickel catalysis and radical-mediated, C–H functionalization processes.

Jennifer Roizen first entered a synthetic chemistry research laboratory as an undergraduate at Williams College in Williamstown, MA. There, Professors J. Hodge Markgraf and Thomas E. Smith ignited her passion for total synthesis, as she pursued syntheses of benzoisocanthenones and hennoxazole A, partially sponsored as a Pfizer SURF. She followed this interest to Prof. Brian M. Stoltz's laboratory at the California Institute of Technology where she earned a Ph.D. in 2010 based on progress toward a total synthesis of ineleganolide. These efforts rely on a cyclopropanation/Cope rearrangement cascade. With emergent interests in late-stage C–H functionalization reactions, Dr. Roizen moved to Stanford University to learn with a leader in amination technologies, Prof. Justin Du Bois, as an NIH and CMAD Postdoctoral Fellow. Building on this interest, Dr. Roizen led a laboratory at Duke University, known for photo-driven, sulfamate ester and sulfamide-guided C–H functionalization processes and cross-coupling technologies. Dr. Roizen remains a curiosity-driven chemist.

## ABBREVIATIONS USED

<b>Å</b>	Ångstrom
<b>Ac</b>	acetyl
<b>Acr</b>	acridinium
<b>AIBN</b>	azobis(isobutyronitrile)
<b>API</b>	active pharmaceutical ingredient

<b>aq.</b>	Aqueous
<b>AQN</b>	anthracene-9,10-dione or anthraquinone
<b>Ar</b>	aryl
<b>B:</b>	base
<b>BET</b>	back-electron transfer
<b>BDE</b>	bond dissociation energy
<b>BDFE</b>	bond dissociation free energy
<b>BH</b>	conjugate base
<b>BHT</b>	butylhydroxytoluene
<b>BINOL</b>	1,1'-bi-2-naphthol
<b>Bn</b>	benzyl
<b>BNAH</b>	1-benzyl-1,4-dihydronicotinamide
<b>Boc</b>	<i>tert</i> -butoxycarbonyl
<b>BODIPY</b>	4,4-Difluoro-4-bora-3a,4a-diaza- <i>s</i> -indacene
<b>Bpy</b>	2,2'-bipyridine
<b>Bs</b>	benzenesulfonyl
<b>Bu</b>	butyl
<b>Bz</b>	benzoyl
<b>C</b>	Celsius
<b>cat</b>	catalytic or catalyst
<b>calcd</b>	calculated
<b>Cbz</b>	carboxybenzyl
<b>CFL</b>	compact fluorescent lamp
<b>cod</b>	1,5-cyclooctadiene
<b>4CzIPN</b>	2,4,5,6-tetrakis(9 <i>H</i> -carbazol-9-yl)isophthalonitrile
<b>DABCO</b>	1,4-diazabicyclo[2.2.2]octane
<b>DCA</b>	9,10-dicyanoanthracene
<b>DCE</b>	1,2-dichloroethane
<b>DDQ</b>	2,3-dichloro-5,6-dicyano-1,4-benzoquinone

<b>dF</b>	difluoro (in reference to photocatalysts)
<b>dF(CF<sub>3</sub>)ppy</b>	2-(2,4-difluorophenyl)-5-trifluoromethylpyridine
<b>dFppy</b>	2-(2,4-difluorophenyl)pyridine
<b>DFT</b>	density functional theory
<b>DIPA</b>	diisopropylamine
<b>DIPEA</b>	<i>N,N</i> -diisopropylethylamine
<b>DMF</b>	<i>N,N</i> -dimethylformamide
<b>dmgH</b>	conjugate base of dimethylglyoxime (dmgH <sub>2</sub> )
<b>dmgH<sub>2</sub></b>	dimethylglyoxime
<b>DMN</b>	1,5-dimethoxynaphthalene
<b>DMPU</b>	<i>N,N'</i> -dimethylpropyleneurea
<b>DMSO</b>	dimethylsulfoxide
<b>dmTroc</b>	dimethyltrichloroethyl chloroformate
<b>3DPAFIPN</b>	2,4,6-tris(diphenylamino)-5-fluoroisophthalonitrile
<b>dr</b>	diastereomeric ratio
<b>dtbbpy</b>	4,4'-di-tert-butyl-2,2'-bipyridine
<b><i>E</i><sub>1/2</sub></b>	half-wave potential
<b><i>E</i><sub>p</sub></b>	peak potential
<b><i>E</i><sub>p/2</sub></b>	half-peak potential
<b>ee</b>	enantiomeric excess
<b>E.A.S</b>	
<b>EDG</b>	electron donating group
<b>EnT</b>	energy transfer
<b>equiv</b>	equivalent
<b>Et</b>	ethyl
<b>ET</b>	electron transfer
<b>EWG</b>	electron withdrawing group
<b>EY</b>	eosin Y or 2',4',5',7'-tetrabromofluorescein
<b>Fc</b>	ferrocene

<b>FMO</b>	frontier molecular orbital
<b>g</b>	gram
<b>GC-MS</b>	gas chromatography–mass spectrometry
<b>h</b>	hour(s)
<b>H-Bonding</b>	hydrogen bonding
<b>HAT</b>	hydrogen atom transfer
<b>HATU</b>	1-[bis(dimethylamino)methylene]-1H-1,2,3-triazolo[4,5-b]pyridinium-3-oxidehexafluorophosphate
<b>HFIP</b>	1,1,1,3,3,3-hexafluoroisopropanol
<b>HLF</b>	Hofmann-Löffler-Freytag
<b>HRMS</b>	High-resolution mass spectrometry
<b>ISC</b>	intersystem crossing
<b>k</b>	kilo
<b>kcal</b>	kilocalorie
<b>L</b>	ligand
<b>LED</b>	light-emitting diode
<b>M</b>	molar
<b><i>m</i></b>	meta
<b>m</b>	milli
<b>Me</b>	methyl
<b>MeCN</b>	acetonitrile
<b>Mes</b>	mesityl
<b>MesSH</b>	2,4,6-trimethylbenzenethiol or mesitylthiol
<b>mol</b>	mole
<b>mol %</b>	mole percentage
<b>MS</b>	molecular sieve
<b>Ms</b>	methanesulfonyl
<b>MTBE</b>	methyl <i>tert</i> -butyl ether
<b><i>n</i></b>	normal



<b>NCR</b>	nitrogen centered radical
<b>NCS</b>	<i>N</i> -chlorosuccinimide
<b>NFSI</b>	<i>N</i> -fluorobenzenesulfonimide
<b>NIS</b>	<i>N</i> -iodosuccinimide
<b>NMM</b>	<i>N</i> -methylmorpholine
<b>NMP</b>	<i>N</i> -methyl-2-pyrrolidinone
<b>NMR</b>	nuclear magnetic resonance
<i>o</i>	ortho
<b>ox</b>	oxidation
<i>p</i>	para
<b>PC</b>	photocatalyst
<b>PCET</b>	proton-coupled electron transfer
<b>Ph</b>	phenyl
<b>Phth</b>	phthalimido
<b>Ph-PTZ</b>	10-phenylphenothiazine
<b>pin</b>	pinacolato
<b>PMP</b>	<i>para</i> -methoxyphenyl
<b>ppy</b>	2-phenylpyridinato
<b>Pr</b>	propyl
<b>Py</b>	pyridine
$\phi$	quantum yield
<b>R</b>	undefined group
<b>red</b>	reduction
<b>rt</b>	room temperature
<b>SCE</b>	saturated calomel electrode
<b>SET</b>	single electron transfer
$\tau$	excited state lifetime
<i>t</i>	tert
<b>TAS</b>	transient absorption spectroscopy

<b>TBAI</b>	tetra-n-butylammonium iodide
<b>TEMPO</b>	(2,2,6,6-tetramethyl-piperidin-1-yl)oxyl
<b>Tf</b>	trifluoromethanesulfonyl
<b>TFE</b>	2,2,2-trifluoroethanol
<b>THF</b>	tetrahydrofuran
<b>TMS</b>	trimethylsilyl
<b>TMB</b>	1,3,5-trimethoxybenzene
<b>TRIP</b>	1,3,5-triisopropylbenzene
<b>Trisyl</b>	2,4,6-triisopropylbenzenesulfonyl
<b>Ts</b>	<i>para</i> -toluenesulfonyl or tosyl
<b>TTET</b>	triplet-triplet energy transfer
<b>UV</b>	ultraviolet
<b>V</b>	volt

## REFERENCES

1. Zard SZ Recent Progress in the Generation and Use of Nitrogen-Centered Radicals. *Chem. Soc. Rev.* 2008, 37, 1603–1618. [PubMed: 18648685]
2. Shaw MH; Twilton J; MacMillan DWC Photoredox Catalysis in Organic Chemistry. *J. Org. Chem.* 2016, 81, 6898–6926. [PubMed: 27477076]
3. Cismesia MA; Yoon TP Characterizing Chain Processes in Visible Light Photoredox Catalysis. *Chem. Sci.* 2015, 6, 5426–5434. [PubMed: 26668708]
4. Majek M; Filace F; von Wangelin AJ On the Mechanism of Photocatalytic Reactions with Eosin Y. *Beilstein J. Org. Chem.* 2014, 10, 981–989. [PubMed: 24991248]
5. Julliard M; Chanon M Photoelectron-Transfer Catalysis: Its Connections with Thermal and Electrochemical Analogues. *Chem. Rev.* 1983, 83, 425–506.
6. Fraij LK; Hayes DM; Werner TC Static and Dynamic Fluorescence Quenching Experiments for the Physical Chemistry Laboratory. *J. Chem. Ed.* 1992, 69, 424–428.
7. Arias-Rotondo DM; McCusker JK The Photophysics of Photoredox Catalysis: A Roadmap for Catalyst Design. *Chem. Soc. Rev.* 2016, 45, 5803–5820. [PubMed: 27711624]
8. Lowry MS; Goldsmith JI; Slinker JD; Rohl R; Pascal RA Jr.; Malliaras GG; Bernhard S Single-Layer Electroluminescent Devices and Photoinduced Hydrogen Production from an Ionic Iridium(III) Complex. *Chem. Mater.* 2005, 17, 5712–5719.
9. Choi GJ; Zhu Q; Miller DC; Gu CJ; Knowles RR Catalytic Alkylation of Remote C–H Bonds Enabled by Proton-coupled Electron Transfer. *Nature* 2016, 539, 268–271. [PubMed: 27732585]
10. Hanss D; Freys JC; Bernardinelli G; Wenger OS Cyclometalated Iridium(III) Complexes as Photosensitizers for Long-Range Electron Transfer: Occurrence of a Coulomb Barrier. *Eur. J. Inorg. Chem.* 2009, 4850–4859.
11. Excited potential calculated from E00 (In MeCN) from: Ochola JR; Wolf MO The Effect of Photocatalyst Excited State Lifetime On the Rate of Photoredox Catalysis. *Org. Biomol. Chem.* 2016, 14, 9088–9092. [PubMed: 27714220]

12. Ladouceur S; Fortin D; Zysman-Colman E Enhanced Luminescent Iridium(III) Complexes Bearing Aryltriazole Cyclometallated Ligands. *Inorg. Chem.* 2011, 50, 11514–11526. [PubMed: 21961698]
13. Slinker JD; Gorodetsky AA; Lowry MS; Wang J; Parker S; Rohl R; Bernhard S; Malliaras GG Efficient Yellow Electroluminescence from a Single Layer of a Iridium Complex. *J. Am. Chem. Soc.* 2004, 126, 2763–2767. [PubMed: 14995193]
14. Kalyanasundaram K Photophysics, Photochemistry and Solar Energy Conversion with Tris(bipyridyl)ruthenium(II) and Its Analogues. *Coord. Chem. Rev.* 1982, 46, 159–244.
15. Juris A; Balzani V; Belser P; von Zelewsky A Characterization of the Excited State Properties of Some New Photosensitizers of the Ruthenium (Polypyridine) Family. *Helv. Chim. Acta* 1981, 64, 2175–2182.
16. Flamigni L; Barbieri A; Sabatini C; Ventura B; Barigelletti F Photochemistry and Photophysics of Coordination Compounds: Iridium. *Top. Curr. Chem.* 2007, 281, 143–203.
17. Singh A; Teegardin K; Kelly M; Prasad KS; Krishnan S; Weaver JD Facile Synthesis and Complete Characterization of Homoleptic and Heteroleptic Cyclometalated Iridium(III) Complexes for Photocatalysis. *J. Organomet. Chem.* 2015, 776, 51–59.
18. Soni VK; Lee S; Kang J; Moon YK; Hwang HS; You Y; Cho EJ Reactivity Tuning for Radical-Radical Cross-Coupling via Selective Photocatalytic Energy Transfer: Access to Amine Building Blocks. *ACS Catal.* 2019, 9, 10454–10463.
19. Tucker JW; Stephenson CRJ Shining Light on Photoredox Catalysis: Theory and Synthetic Applications. *J. Org. Chem.* 2012, 77, 1617–1622 [PubMed: 22283525]
20. Shen X; Harms K; Marsch M; Meggers E A Rhodium Catalyst Superior to Iridium Congeners for Enantioselective Radical Amination Activated by Visible Light. *Chem. Eur. J.* 2016, 22, 9102–9105. [PubMed: 27145893]
21. Hsu Y-C; Wang VC-C; Au-Yeung K-C; Tsai C-Y; Chang C-C; Lin B-C; Chan Y-T; Hsu C-P; Yap GPA; Jurca T; Ong T-G One-pot Tandem Photoredox and Cross-coupling Catalysis with a Single Palladium Carbodicarbene Complex. *Angew. Chem. Int. Ed.* 2018, 57, 4622–4626.
22. The potential reported here was determined in MeOH: Shen T; Zhao Z-G; Yu Q; Xu H-J Photosensitized Reduction of Benzil by Heteroatom-Containing Anthracene Dyes. *J. Photochem. Photobiol. A* 1989, 47, 203–212.
23. Gini A; Uygur M; Rigotti T; Alemán J; Mancheño OG Novel Oxidative Ugi Reaction for the Synthesis of Highly Active, Visible-Light, Imide-Acrinium Organophotocatalysts. *Chem. Eur. J.* 2018, 24, 12509–12514. [PubMed: 29882609]
24. Wang Y; Haze O; Dinnocenzo JP; Farid S; Farid RS; Gould IR Bonded Exciplexes. A New Concept in Photochemical Reactions. *J. Org. Chem.* 2007, 72, 6970–6981. [PubMed: 17676917]
25. Treat NJ; Sprafke H; Kramer JW; Clark PG; Barton BE; Read de Alaniz J; Fors BP; Hawker CJ Metal-Free Atom Transfer Radical Polymerization. *J. Am. Chem. Soc.* 2014, 136, 16096–16101. [PubMed: 25360628]
26. Leow D Phenazinium Salt-catalyzed Aerobic Oxidative Amidation of Aromatic Aldehydes. *Org. Lett.* 2014, 16, 5812–5815. [PubMed: 25350690]
27. Reduction potential for the ground-state of 9-mesityl-10- methylacridinium cation: Benniston AC; Harriman A; Li P; Rostron JP; van Ramesdonk HJ; Groeneveld MM; Zhang H; Verhoeven JW Charge Shift and Triplet State Formation in the 9-Mesityl-10- Methylacridinium Cation. *J. Am. Chem. Soc.* 2005, 127, 16054–16064. [PubMed: 16287292]
28. Reduction potential for the excited-state of 9-mesityl-10- methylacridinium cation: Ohkubo K; Fukuzumi S 100 Selective Oxygenation of *p*-Xylene to *p*-Tolualdehyde via Photoinduced Electron Transfer. *Org. Lett.* 2000, 2, 3647–3650. [PubMed: 11073666]
29. Romero NA; Margrey KA; Tay NE; Nicewicz DA Site-selective arene C-H amination via photoredox catalysis. *Science*, 2015, 349, 1326. [PubMed: 26383949]
30. Reduction potential for the ground-state of 1,5-DMN: Zweig A; Maurer AH; Roberts BG Oxidation, Reduction, and Electrochemiluminescence of Donor-substituted Polycyclic Aromatic Hydrocarbons. *J. Org. Chem.* 1967, 32, 1322–1329.
31. Reduction potential (in MeCN) for the excited state of 1,5-DMN calc. from E00 from: Hamada T; Nishida A; Yonemitsu O Selective Removal of Electron-accepting *p*-Toluene- and

- Naphthalenesulfonyl Protecting Groups for Amino Function via Photoinduced Donor Acceptor Ion Pairs with Electron-donating Aromatics. *J. Am. Chem. Soc.* 1986, 108, 140–145.
32. Kim I; Park B; Kang G; Kim J; Jung H; Lee H; Baik M-H; Hong S Visible-Light-Induced Pyridylation of Remote C(sp<sup>3</sup>)-H Bonds by Radical Translocation of *N*-Alkoxyppyridinium Salts. *Angew. Chem. Int. Ed.* 2018, 57, 15517–15522.
33. Timpe H-J; Kronfeld K-P Light-Induced Polymer and Polymerization Reactions XXXIII: Direct Photoinitiation of Methyl Methacrylate Polymerization by Excited States of Ketones. *J. Photochem. Photobiol. A* 1989, 46, 253–267.
34. Usami K; Yamaguchi E; Tada N; Itoh A Visible-Light-Mediated Iminyl Radical Generation from Benzyl Oxime Ether: Synthesis of Pyrroline via Hydroimination Cyclization. *Org. Lett.* 2018, 20, 5714–5717. [PubMed: 30188723]
35. Reduction potential for the ground-state of DDQ: Yamago S; Miyazoe H; Iida K; Yoshida J-I Highly Efficient and Chemoselective Reductive Bis-silylation of Quinones by Silyltellurides. *Org. Lett.* 2000, 2, 3671–3673. [PubMed: 11073672]
36. Reduction potential (in MeCN) for the excited state of DDQ: Ohkubo K; Fujimoto A; Fukuzumi S Visible-Light-Induced Oxygenation of Benzene by the Triplet Excited State of 2,3-Dichloro-5,6-Dicyano-*p*-Benzoquinone. *J. Am. Chem. Soc.* 2013, 135, 5368–5371. [PubMed: 23534829]
37. Deol H; Kumar M; Bhalla V Exploring Organic Photosensitizers Based on Hemicyanine Derivatives: a Sustainable Approach for Preparation of Amide Linkages. *RSC Adv.* 2018, 8, 31237–31245.
38. Wang X-F; Yu S-S; Wang C; Xue D; Xiao J BODIPY Catalyzed Amide Synthesis Promoted by BHT and Air Under Visible Light. *Org. Biomol. Chem.* 2016, 14, 7028–7037. [PubMed: 27363514]
39. Zhang J; Luo J Donor–Acceptor Fluorophores for Visible-Light-Promoted Organic Synthesis: Photoredox/Ni Dual Catalytic C(sp<sup>2</sup>)-C(sp<sup>3</sup>) Cross-Coupling. *ACS Catal.* 2016, 6, 873–877.
40. Le Vaillant F; Garreau M; Nicolai S; Gryn'ova G; Corminbouef C; Waser J Fine-Tuned Organic Photoredox Catalysts for Fragmentation-Alkynylation Cascades of Cyclic Oxime Ethers. *Chem. Sci.* 2018, 9, 5883–5889 [PubMed: 30079201]
41. Speckmeier E; Fischer TG; Zeitler K A Toolbox Approach To Construct Broadly Applicable Metal-Free Catalysts for Photoredox Chemistry: Deliberate Tuning of Redox Potentials and Importance of Halogens in Donor–Acceptor Cyanoarenes. *J. Am. Chem. Soc.* 2018, 140, 15353–15365. [PubMed: 30277767]
42. Reduction potential (in MeCN) for the excited state of 2,4,6-triphenylpyrylium calc. from *E*<sub>00</sub> from: Searle R; Williams JLR; DeMeyer DE; Doty JC The Sensitization of Stilbene Isomerization. *Chem. Commun.* 1967, 1165–1165.
43. Cambié D; Bottecchia C; Straathof NJW; Hessel V; Noël T Applications of Continuous-Flow Photochemistry in Organic Synthesis, Material Science, and Water Treatment. *Chem. Rev.* 2016, 116, 10276–10341. [PubMed: 26935706]
44. Halperin SD; Kwon D; Holmes M; Regalado EL; Campeau L-C; DiRocco DA; Britton R Development of a Direct Photocatalytic C–H Fluorination for the Preparative Synthesis of Odanacatib. *Org. Lett.* 2015, 17, 5200–5203. [PubMed: 26484983]
45. Cline ED; Bernhard S The Transformation and Storage of Solar Energy: Progress Towards Visible-Light Induced Water Splitting. *Chimia* 2009, 63, 709–713.
46. Romero A; Nicewicz DA Organic Photoredox Catalysis. *Chem. Rev.* 2016, 116, 10075–10166. [PubMed: 27285582]
47. Strieth-Kalthoff F; James MJ; Teders M; Pitzer L; Glorius F Energy Transfer Catalysis Mediated by Visible Light: Principles, Applications, Directionis. *Chem. Soc. Rev.* 2018, 47, 7190–7202. [PubMed: 30088504]
48. Michelin C; Hoffmann N Photosensitization and Photocatalysis—Perspectives in Organic Synthesis. *ACS Catal.* 2018, 8, 12046–12055.
49. For pioneering examples of this class of transformation, see: Zuo Z; Ahneman DT; Chu L; Terret JA; Doyle AG; MacMillan DWC Merging Photoredox with Nickel Catalysis: Coupling of  $\alpha$ -Carboxyl sp<sup>3</sup>-Carbons with Aryl Halides. *Science* 2014, 345, 437–440. [PubMed: 24903563]

50. For an early review on this topic, see: Twilton J; Le C; Zhang P; Shaw MH; Evans RW; MacMillan DWC The Merger of Transition Metal and Photocatalysis. *Nature Reviews Chemistry* 2017, 1, 52.
51. For a recent example of a trifluoroacetamide-directed remote C(sp<sup>3</sup>)-H allylation, see: Xu B; Tambar UK Remote Allylation of Unactivated C(sp<sup>3</sup>)-H Bonds Triggered by Photogenerated Amidyl Radicals. *ACS Catal.* 2019, 9, 4627–4631. [PubMed: 34109055]
52. For a recent example of an intramolecular olefin amidoarylation involving amides, carbamates and ureas as substrates, see: Zheng S; Gutiérrez-Boent Á; Molander GA Merging Photoredox PCET with Ni-Catalyzed Cross-Coupling: Cascade Amidoarylation of Unactivated Olefins. *Chem* 2019, 5, 339–352. [PubMed: 31080910]
53. For a recent example of an intramolecular diastereoselective olefin amidoacylation of amides and carbamates as substrates, see: Zheng S; Zhang S-Q; Saednia B; Zhou J; Anna JM; Hong X; Molander GA Diastereoselective Olefin Amidoacylation via Photoredox PCET/Nickel-dual Catalysis: Reaction Scope and Mechanistic Insights. *Chem. Sci.* 2020, 11, 4131–4137.
54. For an amide-directed alkylative cross-coupling reaction, see: Thullen SM; Treacy SM; Rovis T Regioselective Alkylative Cross-Coupling of Remote Unactivated C(sp<sup>3</sup>)-H Bonds. *J. Am. Chem. Soc.* 2019, 141, 14062–14067. [PubMed: 31478370]
55. Blackburn JM; Kanegusuku ALG; Scott GE; Roizen JL Photochemically-Mediated, Nickel-Catalyzed Synthesis of *N*-(Hetero)aryl Sulfamate Esters. *Org. Lett.* 2019, 21, 7049–7054. [PubMed: 31436104]
56. Simons RT; Scott GE; Kanegusuku AG; Roizen JL Photochemically Mediated Nickel-Catalyzed Synthesis of *N*-(Hetero)aryl Sulfamides. *J. Org. Chem.* 2020, 85, 6380–6391. [PubMed: 32312047]
57. Till NA; Tian L; Dong Z; Scholes GD; MacMillan DWC Mechanistic Analysis of Metallaphotoredox C–N Coupling: Photocatalysis Initiates and Perpetuates Ni(I)/Ni(III) Coupling Activity. *J. Am. Chem. Soc.* 2020, 142, 15830–15841. [PubMed: 32786779]
58. Beatty JW; Stephenson CRJ Amine Functionalization via Oxidative Photoredox Catalysis: Methodology Development and Complex Molecule Synthesis. *Acc. Chem. Res.* 2015, 48, 1474–1484. [PubMed: 25951291]
59. For review on this topic, see: Hu J; Wang J; Nguyen TH; Zheng N The Chemistry of Amine Radical Cations Produced by Visible Light Photoredox. *Beilstein J. Org. Chem.* 2013, 9, 1977–2001. [PubMed: 24204409]
60. For brief tutorial review on photoredox-mediated generations and reactions of nitrogen-centered radicals and radical ions from N–Cl, N–Br, N–O, N–S, N–N, and N–H bonds, see: Chen J-R; Hu X-Q; Lu L-Q; Xiao W-J Visible Light Photoredox-Controlled Reactions of *N*-Radicals and Radical Ions. *Chem. Soc. Rev.* 2016, 45, 2044–2056. [PubMed: 26839142]
61. For mini review on oxidatively generated nitrogen-centered radicals from photoredox catalysis, see: Jiang H; Studer A Chemistry With *N*-Centered Radicals Generated by Single-Electron Transfer-Oxidation Using Photoredox Catalysis. *CCS Chem.* 2019, 1, 38–49.
62. For focus review on photochemically generated amidyl, hydrazoneyl and imidyl radicals, see: Kärkäs MD Photochemical Generation of Nitrogen-Centered Amidyl, Hydrazoneyl, and Imidyl Radicals: Methodology Developments and Catalytic Applications. *ACS Catal.* 2017, 7, 4999–5022.
63. For perspective on photocatalytically generated aminium radical cations for C–N bond forming reactions, see: Ganley JM; Murray PRD; Knowles RR Photocatalytic Generation of Aminium Radical Cations for C–N Bond Formation. *ACS Catal.* 2020, 10, 11712–11738. [PubMed: 33163257]
64. For an account summarizing reactions involving photocatalytically generated nitrogen-centered radical research led by Chen and co-workers, see: Yu X-Y; Zhao Q-Q; Chen J; Xiao W-J; Chen J-R When Light Meets Nitrogen-Centered Radicals: From Reagents to Catalysts. *Acc. Chem. Res.* 2020, 53, 1066–1083. [PubMed: 32286794]
65. For focus review summarizing photocatalyst-mediated nitrogen-radical cyclization reactions, see: Wang P; Zhao Q; Xiao W; Chen J Recent Advances in Visible-Light Photoredox-Catalyzed Nitrogen Radical Cyclization. *Green Synth. Catal.* 2020, 1, 42–51.
66. Hofmann AW Zur Kenntniss des Piperidins und Pyridins. *Ber. Dtsch. Chem. Ges.* 1879, 12, 984–990.

67. Löffler K; Freytag C Über eine neue Bildungsweise von *N*-alkylierten Pyrrolidinen. Ber. Dtsch. Chem. Ges. 1909, 42, 3427–3431.
68. Wawzonek S; Thelen PJ Preparation of *N*-methylgranatanine. J. Am. Chem. Soc. 1950, 72, 5, 2118–2120.
69. Corey EJ; Hertler WR A Study of the Formation of Haloamines and Cyclic Amines by the Free Radical Chain Decomposition of *N*-Haloammonium Ions (Hofmann-Löffler Reaction). J. Am. Chem. Soc. 1960, 82, 1657–1668.
70. Neale RS Nitrogen Radicals as Synthesis Intermediates. *N*-Halamide Rearrangements and Additions to Unsaturated Hydrocarbons. Synthesis, 1971, 1, 1–15.
71. Baldwin SW; Doll RJ Synthesis of the 2-aza-7-oxatricyclo[4.3.2.0<sup>4,8</sup>]undecane Nucleus of some Gelsemium Alkaloids. Tetrahedron Letters, 1979, 35, 3275–3278.
72. Short MA; Blackburn JM; Roizen JL Sulfamate Esters Guide Selective Radical-mediated Chlorination of Aliphatic C–H Bonds. Angew. Chem. Int. Ed. 2018, 57, 296–299.
73. Okahara M; Ohashi T; Komori S Synthesis of  $\gamma$ - and  $\delta$ -Chloroalkanesulfonamides via the Photorearrangement of *N*-Chlorosulfonamides. J. Org. Chem. 1968, 33, 3066–3070. [PubMed: 5742858]
74. Neale RS; Marcus NL The Chemistry of Nitrogen Radicals. IX. Reactions of *N*-Halocyanamides and *N*-Halosulfonamides. J. Org. Chem. 1969, 34, 1808–1816.
75. Qin Q; Yu S Visible-Light-Promoted Remote C(sp<sup>3</sup>)–H Amidation and Chlorination. Org. Lett. 2015, 17, 1894–1897. [PubMed: 25853884]
76. Wayner DDM; McPhee DJ; Griller D Oxidation and Reduction Potentials of Transient Free Radicals. J. Am. Chem. Soc. 1988, 110, 132–137.
77. Zhu Y; Wang J-J; Wu D; Yu W Visible-Light-Driven Remote C–H Chlorination of Aliphatic Sulfonamides with Sodium Hypochlorite. Asian J. Org. Chem. 2020, 9, 1650–1654.
78. Qin Q; Ren D; Yu S Visible-light-promoted Chloramination of Olefins with *N*-chlorosulfonamide as both Nitrogen and Chlorine Sources. Org. Biomol. Chem. 2015, 13, 10295–10298. [PubMed: 26416235]
79. Esker JL; Newcomb M Chemistry of Amidyl Radicals Produced from *N*-Hydroxypyridine-2-thione Imidate Esters. J. Org. Chem. 1993, 58, 4933–4940.
80. Horner JH; Musa OM; Bouvier A; Newcomb M Absolute Kinetics of Amidyl Radical Reactions. J. Am. Chem. Soc. 1998, 120, 7738–7748.
81. Akasaka T; Furukawa N; Oae S Sulfoximidoyl Radical. Homolytic Addition of *N*-halosulfoximides to Olefins. Tetrahedron Letters, 1979, 22, 2035–2038.
82. Prieto A; Diter P; Toffano M; Hannedouche J; Magnier E Photoredox-initiated 1,2-difunctionalization of Alkenes with *N*-chloro, *S*-fluoroalkyl Sulfoximines. Adv. Synth. Catal. 2019, 361, 436–440.
83. Wang J-D; Liu Y-X; Xue D; Wang C; Xiao J Amination of Benzoxazoles by Visible-Light Photoredox Catalysis. Synlett 2014, 25, 2013–2018.
84. Kim H; Kim T; Lee DG; Roh SW; Lee C Nitrogen-centered Radical-mediated C–H Imidation of Arenes and Heteroarenes via Visible Light Induced Photocatalysis. Chem. Commun. 2014, 50, 9273–9276.
85. Allen LJ; Cabrera PJ; Lee M; Sanford MS *N*-Acyloxyphthalimides as Nitrogen Radical Precursors in the Visible Light Photocatalyzed Room Temperature C–H Amination of Arenes and Heteroarenes. J. Am. Chem. Soc. 2014, 136, 5607–5610. [PubMed: 24702705]
86. Foo K; Sella E; Thomé I; Eastgate MD; Baran PS A Mild Ferrocene-Catalyzed C–H Imidation of (Hetero)Arenes. J. Am. Chem. Soc. 2014, 136, 5279–5282. [PubMed: 24654983]
87. Pluta R; Nikolaienko P; Rueping M Direct Catalytic Trifluoromethylthiolation of Boronic Acids and Alkynes Employing Electrophilic Shelf-Stable *N*-(trifluoro-methylthio)phthalimide. Angew. Chem. Int. Ed. 2014, 53, 1650–1653.
88. Minisci F Novel Applications of Free-Radical Reactions in Preparative Organic Chemistry. Synthesis, 1973, 1, 1–24.
89. This manuscript does not summarize publications with dates after February 1, 2021. Nevertheless, pertinent manuscripts have been published since this date, see as an example: Lee W; Jung S; Kim

- M; Hong S Site-Selective Direct C–H Pyridylation of Unactivated Alkanes by Triplet Excited Anthraquinone. *J. Am. Chem. Soc.* 2021, 143, 3003–3012. [PubMed: 33557526]
90. This manuscript does not summarize publications with dates after February 1, 2021. Nevertheless, pertinent manuscripts have been published since this date, see as an example: Shin S; Lee S; Choi W; Kim N; Hong S Visible-Light-Induced 1,3-Aminopyridylation of [1.1.1]Propellane with *N*-Aminopyridinium Salts. *Angew. Chem. Int. Ed.* 2021, 60, 7873–7879.
91. Kemper J; Studer A Stable Reagents for the Generation of *N*-Centered Radicals: Hydroamination of Norbornene. *Angew. Chem. Int. Ed.* 2005, 44, 4914–4917.
92. Guin J; Fröhlich R; Studer A Thiol-catalyzed Stereoselective Transfer Hydroamination of Olefins with *N*-Aminated Dihydropyridines. *Angew. Chem. Int. Ed.* 2008, 47, 779–782.
93. Greulich TW; Daniliuc CG; Studer A *N*-Aminopyridinium Salts as Precursors for *N*-Centered Radicals – Direct Amidation of Arenes and Heteroarenes. *Org. Lett.* 2015, 17, 254–257. [PubMed: 25541887]
94. Bock CR; Connor JA; Gutierrez AR; Meyer JT; Whitten DG; Sullivan BP; Nagle JK Estimation of Excited-state Redox Potentials by Electron-transfer Quenching. Application of Electron-transfer Theory to Excited-state Redox Processes. *J. Am. Chem. Soc.* 1979, 101, 4815–4824.
95. Okada K; Okamoto K; Morita N; Okubo K; Oda M Photosensitized Decarboxylative Michael Addition through *N*-(Acylloxy)phthalimides via an Electron-Transfer Mechanism. *J. Am. Chem. Soc.* 1991, 113, 9401–9402.
96. Miyazawa K; Koike T; Akita M Regiospecific Intermolecular Aminohydroxylation of Olefins by Photoredox Catalysis. *Chem. Eur. J.* 2015, 21, 11677–11680. [PubMed: 26179746]
97. Miyazawa K; Koike T; Akita M Aminohydroxylation of Olefins with Iminopyridinium Ylides by Dual Ir Photocatalysis and Sc(OTf)<sub>3</sub> catalysis. *Tetrahedron* 2016, 72, 7813–7820.
98. Yu W-L; Chen J-Q; Wei Y-L; Wang Z-Y; Xu P-F Alkene Functionalization for the Stereospecific Synthesis of Substituted Aziridines by Visible-light Photoredox Catalysis. *Chem. Commun.* 2018, 54, 1948–1951.
99. Goliszewska K; Rybicka-Jasinska K; Szurmak J Gryko, D. Visible-Light-Mediated Amination of  $\pi$ -Nucleophiles with *N*-aminopyridinium Salts. *J. Org. Chem.* 2019, 84, 15834–15844. [PubMed: 31594308]
100. Moon Y; Park B; Kim I; Kang G; Shin S; Kang D; Baik M-H; Hong S Visible Light Induced Alkene Aminopyridylation using *N*-aminopyridinium Salts as Bifunctional Reagents. *Nat. Commun* 2019, 10, 4117. [PubMed: 31511595]
101. Lazarides T; McCormick T; Du P; Luo G; Lindley B; Eisenberg R Making Hydrogen from Water Using a Homogeneous System without Noble Metals. *J. Am. Chem. Soc.* 2009, 131, 9192–9194. [PubMed: 19566094]
102. Distortion-interaction energies were calculated in the Jaguar 9.1 suite with the PW6B95-D3/def2-QZVP level of theory and the atomic charges from electrostatic potential were examined using the CHELPG program as implemented in ORCA.
103. Moon Y; Lee W; Hong S Visible-Light-Enabled *Ortho*-selective Aminopyridylation of Alkenes with *N*-Aminopyridinium Ylides. *J. Am. Chem. Soc.* 2020, 142, 12420–12429. [PubMed: 32614175]
104. Roth HG; Romero NA; Nicewicz DA Experimental and Calculated Electrochemical Potentials of Common Organic Molecules for Applications to Single-Electron Redox Chemistry. *Synlett* 2016, 27, 714–723.
105. Geometry optimization and energies were calculated in the Jaguar 9.1 suite with the B3LYP-D3 level of theory using the LACVP\*\* basis set.
106. Kim N; Lee C; Kim T; Hong S Visible-Light-Induced Remote C(sp<sup>3</sup>)-H Pyridylation of Sulfonamides and Carboxamides. *Org. Lett.* 2019, 21, 9719–9723. [PubMed: 31736318]
107. Zhang D; Wang H; Bolm C Photocatalytic Difunctionalisations of Alkenes with *N*-SCN Sulfoximines. *Chem. Commun.* 2018, 54, 5772–5775.
108. Soto A; Yorimitsu H; Oshima K *O*-Alkyl *S*-3,3-Dimethyl-2-oxobutyl Dithiocarbonates as Versatile Sulfur-Transfer Agents in Radical C(sp<sup>3</sup>)-H Functionalization. *Chem. Asian J.* 2007, 2, 1568–1573. [PubMed: 17929230]

109. Czaplowski WL; Na CG; Alexanian EJ C–H Xanthylation: A Synthetic Platform for Alkane Functionalization. *J. Am. Chem. Soc.* 2016, 138, 13854–13857. [PubMed: 27739673]
110. Ayer SK; Roizen JL Sulfamate Esters Guide C(3)-selective Xanthylation of Alkanes. *J. Org. Chem.* 2019, 84, 3508–3523. [PubMed: 30779561]
111. Xuan J; Li B-J; Feng Z-J; Sun G-D; Ma H-H; Yuan Z-W, Chen J-R Lu L-Q Xiao W-J Desulfonylation of Tosyl Amides Through Catalytic Photoredox Cleavage of N–S Bond Under Visible-Light Irradiation. *Chem. Asian J.* 2013, 8, 1090–1094. [PubMed: 23554359]
112. MacKenzie IA; Wang L; Onuska NPR; Williams OF; Begam K; Moran AM; Dunietz BD; Nicewicz DA Discovery and Characterization of an Acridine Radical Photoreductant. *Nature* 2020, 580, 76–80. [PubMed: 32238940]
113. For an example, see: Rössler SL; Jelier BJ; Triplet PF; Shemet A; Jeschke G; Togni A; Carreira EM Pyridyl Radical Cation for C–H Amination of Arenes. *Angew. Chem. Int. Ed.* 2019, 58, 526–531.
114. For an example, see: Ham WS; Hillenbrand J; Jacq J; Genicot C; Ritter T Divergent Late-Stage (Hetero)aryl C–H Amination by the Pyridinium Radical Cation. *Angew. Chem. Int. Ed.* 2019, 58, 532–536.
115. Yin W; Wang X Recent Advances in Iminyl Radical-Mediated Catalytic Cyclizations and Ring-Opening Reactions. *New J. Chem.* 2019, 43, 3254–3264.
116. For review that summarizes early research into *O*-aryloximes as precursors to 1-pyrrolines, see: Kitamura M; Narasaka K Catalytic Radical Cyclization of Oximes Induced by One-Electron Transfer. *Bull. Chem. Soc. Jpn.* 2008, 81, 539–547.
117. For review that highlights 1-pyrrolines in medicinal chemistry, see: Dannhardt G; Kiefer W 1-Pyrrolines (3,4-Dihydro-2*H*-pyrroles) as a Template for New Drugs. *Arch. Pharm. Pharm. Med. Chem.* 2001, 334, 183–188.
118. Blake JA; Pratt DA; Lin S; Walton JC; Mulder P; Ingold KU Thermolyses of *O*-Phenyl Oxime Ethers. A New Source of Iminyl Radicals and a New Source of Aryloxyl Radicals. *J. Org. Chem.* 2004, 69, 3112–3120. [PubMed: 15104450]
119. Krylov IB; Segida OO; Budnikov AS; Terent'ev AO Oxime-Derived Iminyl Radicals in Selective Processes of Hydrogen Atom Transfer and Addition to Carbon–Carbon  $\pi$ -Bonds. *Adv. Synth. Catal.* 2021, 363, 2502–2528.
120. Uchiyama K; Hayashi Y; Narasaka K Synthesis of 8-Hydroxyquinolines by the Cyclization of *m*-Hydroxyphenethyl Ketone *O*-2,4-Dinitrophenyloximes. *Synlett* 1997, 445–446.
121. Katsuya U; Ayako O; Yujiro H; Koichi Narasaka. Regioselective Synthesis of Quinolin-8-ols and 1,2,3,4-Tetrahydroquinolin-8-ols by the Cyclization of 2-(3-Hydroxyphenyl)ethyl Ketone *O*-2,4-Dinitrophenyloximes. *Bull. Chem. Soc. Jpn.* 1998, 71, 2945–2955.
122. Uchiyama K; Hayashi Y; Narasaka K Synthesis of Dihydropyrroles by the Intramolecular Addition of Alkylideneaminyll Radicals Generated from *O*-2,4-Dinitrophenyloximes of  $\gamma,\delta$ -Unsaturated Ketones. *Chem. Lett.* 1998, 27, 1261–1262.
123. Tetsuhiro M; Narasaka K Photochemical Transformation of  $\gamma,\delta$ -Unsaturated Ketone *O*-(*p*-Cyanophenyl)oximes to 3,4-Dihydro-2*H*-pyrrole Derivatives. *Chem. Lett.* 2000, 29, 338–339.
124. Mikami T; Narasaka K Photochemical Transformation of  $\gamma,\delta$ -Unsaturated Ketone *O*-(*p*-cyanophenyl)oximes to 3,4-Dihydro-2*H*-Pyrrole Derivatives. *C. R. Acad. Sci. Paris, Chimie / Chemistry* 2001, 4, 477–485.
125. In 2005, Narasaka and co-workers published their research on UV-light-mediated and 1,5-DMN-catalyzed iminyl radical 5-*exo-trig* hydroamination reactions in *Tetrahedron Letter*. Kitamura M; Mori Y; Narasaka K Photochemical Radical Cyclization of  $\gamma,\delta$ -Unsaturated Ketone Oximes to 3,4-Dihydro-2*H*-pyrroles. *Tetrahedron Lett.* 2005, 46, 2373–2376.
126. Davies J; Booth SG; Essafi S; Dryfe RAW; Leonori D Visible-Light-Mediated Generation of Nitrogen-Centered Radicals: Metal-Free Hydroamination and Iminohydroxylation Cyclization Reactions. *Angew. Chem. Int. Ed.* 2015, 54, 14017–14021.
127. Srivastava V; Singh PP Eosin Y Catalyzed Photoredox Synthesis: A Review. *RSC Adv.* 2017, 7, 31377–31392.



128. Cai S-H; Xie J-H; Song S; Ye L; Feng C; Loh T-P Visible-Light-Promoted Carboimination of Unactivated Alkenes for the Synthesis of Densely Functionalized Pyrroline Derivatives. *ACS Catal.* 2016, 6, 5571–5574.
129. Nakafuku KM; Fosu SC; Nagib DA Catalytic Alkene Difunctionalization via Imidate Radicals. *J. Am. Chem. Soc.* 2018, 140, 11202–11205. [PubMed: 30156404]
130. For review on employing oximes as precursors to access the *N*-heterocycles, see: Walton J The Oxime Portmanteau Motif: Released Heteroradicals Undergo Incisive EPR Interrogation and Deliver Diverse Heterocycles. *Acc. Chem. Res.* 2014, 47, 1406–1416. [PubMed: 24654991]
131. Jiang H; An X; Tong K; Zheng T; Zhang Y; Yu S Visible-Light-Promoted Iminyl-Radical Formation from Acyl Oximes: A Unified Approach to Pyridines, Quinolines, and Phenanthridines. *Angew. Chem. Int. Ed.* 2015, 54, 4055–4059.
132. Alonso R; Campos PJ; Rodríguez MA; Sampedro D Photocyclization of Iminyl Radicals: Theoretical Study and Photochemical Aspects. *J. Org. Chem.* 2008, 73, 2234–2239. [PubMed: 18290662]
133. Ishihara Y; Azuma S; Choshi T; Kohno K; Ono K; Tsutsumi H; Ishizu T; Hibino S Total Synthesis of Benzo[*c*]phenanthridine Alkaloids Based on a Microwave-Assisted Electrocyclic Reaction of the Aza  $6\pi$ -Electron System and Structural revision of Broussonpapyrine. *Tetrahedron* 2011, 67, 1320–1333.
134. An X -D.; Yu, S. Visible-Light-Promoted and One-Pot Synthesis of Phenanthridines and Quinolines from Aldehydes and *O*-Acyl Hydroxylamine. *Org. Lett.* 2015, 17, 2692–2695. [PubMed: 25964987]
135. Istvan Z; Rethy B; Hohmann J; Molnar J; Imre O; Falkay G Antitumor Activity of Alkaloids Derived from Amaryllidaceae Species. *In Vivo* 2009, 23, 41–48. [PubMed: 19368123]
136. Caballero A; Campos PJ; Rodríguez MA Fluorescence sensing of Cu(II) based on triphaeridine derivatives. *Tetrahedron* 2013, 69, 4631–4635.
137. Szlávik L; Gyuris A; Minárovits J; Forgo P; Molnár J; Hohmann J Alkaloids from *Leucojum vernum* and Antiretroviral Activity of Amaryllidaceae Alkaloids. *Planta Med.* 2004, 70, 871–873. [PubMed: 15386196]
138. Chen W-L; Chen C-Y; Chen Y-F; Hsieh J-C Hydride-Induced Anionic Cyclization: An Efficient Method for the Synthesis of 6-*H*-Phenanthridines *via* a Transition-Metal-Free Process. *Org. Lett.* 2015, 17, 1613–1616. [PubMed: 25763919]
139. Forrester AR; Gill M; Napier RJ; Thomson RH Iminyls. Part 5. Intramolecular Hydrogen Atom Abstraction by Alkyl(aryl)-iminyls. A New Tetralone Synthesis. *J. Chem. Soc. Perkin 1* 1978, 632–636.
140. Forrester AR; Napier RJ; Thomson RH Iminyls. Part 7. Intramolecular Hydrogen Atom Abstraction; Synthesis of Heterocyclic Analogues of  $\alpha$ -Tetralone. *J. Chem. Soc. Perkin 1* 1981, 984–987.
141. For representative reference, see: Legoabe LJ; Peltzer A; Petzer JP  $\alpha$ -Tetralone derivatives as inhibitors of monoamine oxidase. *Bioorg. Med. Chem. Lett.* 2014, 24, 2758–2763. [PubMed: 24794105]
142. Shu W; Nevado C Visible-Light-Mediated Remote Aliphatic C–H Functionalizations through a 1,5-Hydrogen Transfer Cascade. *Angew. Chem. Int. Ed.* 2017, 56, 1881–1884.
143. Forrester AR; Gill M; Sadd JS; Thomson RH New Chemistry of Iminyl Radicals. *J. Chem. Soc. Chem. Comm* 1975, 291–291.
144. Forrester AR; Gill M; Meyer CJ; Sadd JS; Thomson RH Iminyls. Part 1. Generations of Iminyls. *J. Chem. Soc. Perkin 1* 1979, 601–611.
145. Boivin J; Fouquet E; Zard SZ; A New and Synthetically Useful Source of Iminyl Radicals. *Tetrahedron Lett.* 1991, 32, 4299–4302.
146. For a review summarizing the development of photomediated Giese reactions, see: Prier CK; Rankic DA; MacMillan DWC Visible Light Photoredox Catalysis with Transition Metal Complexes: Applications in Organic Synthesis. *Chem. Rev.* 2013, 113, 5322–5363. [PubMed: 23509883]

147. For an updated review of photomediated Giese reactions, see: Kanegusuku ALG; Roizen JL Recent Advances in Photoredox-Mediated Radical Conjugate Addition Reactions: An Expanding Toolkit for the Giese Reaction. *Angew. Chem. Int. Ed.* 10.1002/anie.202016666.
148. Jiang H; Studer A Iminyl-Radicals by Oxidation of  $\alpha$ -Imino-oxy Acids: Photoredox-Neutral Alkene Carboimination for the Synthesis of Pyrrolines. *Angew. Chem. Int. Ed.* 2017, 56, 12273–12276.
149. Davies J; Sheikh NS; Leonori D Photoredox Imino Functionalizations of Olefins. *Angew. Chem. Int. Ed.* 2017, 56, 13361–13365.
150. For pioneering research that employs  $\alpha,\alpha$ -dimethylated carboxylate as iminyl radical precursor, see: Forrester AR; Gill M; Meyer CJ; Sadd JS; Thomson RH Iminyls. Part 1. Generation of Iminyls. *J. Chem. Soc. Perkin 1* 1979, 606–611 *J. Chem. Soc. Perkin 1* 1978, 632–636.
151. Rueda-Becerril M; Sazepin CC; Leung JCT; Okbinoglu T; Kennepohl P; Paquin J-F; Sammis GM Fluorine Transfer to Alkyl Radicals. *J. Am. Chem. Soc.* 2012, 134, 4026–4029. [PubMed: 22320293]
152. Goł biewski WM; Gucma M Applications of *N*-Chlorosuccinimide in Organic Synthesis. *Synthesis*, 2007, 3599–3619.
153. Gleicher GJ; Mahiou B; Aretakis AJ Selectivities in the Addition of Radicals Generated from Derivatives of 2-Bromomalonate to Alkene Pairs. *J. Org. Chem.* 1989, 54, 308–311.
154. Kulbitski K; Nisnevich G; Gandelman M Metal-Free Efficient, General and Facile Iododecarboxylation Method with Biodegradable Co-Products. *Adv. Synth. Catal.* 2011, 353, 1438–1442
155. For seminal report on *N*(SCF<sub>3</sub>)-benzosuccinimide as electrophilic SCF<sub>3</sub> transfer reagent, see: Haas A; Möller G Preparation and Reactivity of Tris(trifluoromethylselenyl)carbenium [(CF<sub>3</sub>Se)<sub>3</sub>C<sup>+</sup>] and Trifluoromethylsulfanylacetic Acid Derivatives [(CF<sub>3</sub>S)<sub>3-n</sub>C<sub>2n</sub>(O)R]. *Chem. Ber.* 1996, 129, 1383–1388.
156. For seminal report on *N*(SePh)-benzosuccinimide as electrophilic SePh transfer reagent, see: Nicolau KC; Claremon DA; Barnette WE; Seitz SP *N*-Phenylselenophthalimide (N-PSP) and *N*-Phenylselenosuccinimide (N-PSS). Two Versatile Carriers of the Phenylseleno Group. Oxyselenation of Olefins and a Selenium-Based Macrolide Synthesis. *J. Am. Chem. Soc.* 1979, 101, 3704–3706.
157. Ollivier C; Renaud P A Novel Approach for the Formation of Carbon–Nitrogen Bonds: Azidation of Alkyl Radicals with Sulfonyl Azides. *J. Am. Chem. Soc.* 2001, 123, 4717–4727. [PubMed: 11457281]
158. Griffin JD; Zeller MA; Nicewicz DA Hydrodecarboxylation of Carboxylic and Malonic Acid Derivatives via Organic Photoredox Catalysis: Substrate Scope and Mechanistic Insight. *J. Am. Chem. Soc.* 2015, 137, 11340–11348. [PubMed: 26291730]
159. For seminal report on vinylbenziodoxolones as electrophilic vinylating transfer agent, see: Stridfeldt E; Seemann A; Bouma MJ; Dey C; Ertan A; Olofsson B Synthesis, Characterization and Unusual Reactivity of Vinylbenziodoxolones—Novel Hypervalent Iodine Reagents. *Chem. Eur. J.* 2016, 22, 16066–16070. [PubMed: 27629653]
160. For seminal report on alkynylbenziodoxolones as electrophilic alkynylating transfer agent, see: Frei R; Wodrich MD; Hari DP; Broin P-A; Chauvier C; Waser J Fast and Highly Chemoselective Alkynylation of Thiols with Hypervalent Iodine Reagents Enabled through a Low Energy Barrier Concerted Mechanism. *J. Am. Chem. Soc.* 2014, 136, 16563–16573. [PubMed: 25365776]
161. For seminal report on cyanobenziodoxolones as electrophilic cyano transfer agent, see: Le Vaillant F; Wodrich M; Waser J Room temperature decarboxylative cyanation of carboxylic acids using photoredox catalysis and cyanobenziodoxolones: a divergent mechanism compared to alkynylation. *Chem. Sci.* 2017, 8, 1790–1800. [PubMed: 28451301]
162. Boivin J; Callier-Dublanche A-C; Quiclet-Sire B; Schiano A-M; Zard SZ Iminyl, Amidyl, and Carbamyl Radicals from *O*-Benzoyl Oximes and *O*-Benzoyl Hydroxamic Acid Derivatives. *Tetrahedron* 1995, 51, 6517–6528.

163. Tu J-L; Liu J-L; Tang W; Su M; Liu F Radical Aza-Cyclization of  $\alpha$ -Imino-oxy Acids for Synthesis of Alkene-Containing *N*-Heterocycles via Dual Cobaloxime and Photoredox Catalysis. *Org. Lett.* 2020, 22, 1222–1226. [PubMed: 31984754]
164. For seminal report on Narasaka-Heck reaction, see: Tsutsui H; Narasaka K Synthesis of Pyrrole Derivatives by the Heck-Type Cyclization of  $\gamma,\delta$ -Unsaturated Ketone *O*-Pentafluorobenzoyloximes. *Chem. Lett.* 1999, 28, 45–46.
165. For review on the Narasaka-Heck reaction, see: Race NJ; Hazelden IR; Faulkner A; Bower JF Recent Developments in the Use of Aza-Heck Cyclizations for the Synthesis of Chiral *N*-Heterocycles. *Chem. Sci.* 2017, 8, 5248–5260. [PubMed: 28959424]
166. Cabrera-Afonso MJ; Cembellín S; Halima-Salem A; Berton M; Marzo L; Miloudi A; Maestro MC; Alemán J Metal-Free Visible Light-Promoted Synthesis of Isothiazoles: A Catalytic Approach for N–S Bond Formation from Iminyl Radicals Under Batch and Flow Conditions. *Green Chem.* 2020, 22, 6792–6797.
167. Patra T; Satobhisha M; Ma J; Strieth-Kalthoff F; Glorius F Visible-Light-Photosensitized Aryl and Alkyl Decarboxylative Functionalization Reactions. *Angew. Chem. Int. Ed.* 2019, 58, 10514–10520.
168. Patra T; Bellotti P; Strieth-Kalthoff F; Glorius F Photosensitized Intermolecular Carboimination of Alkenes through the Persistent Radical Effect. *Angew. Chem. Int. Ed.* 2020, 59, 3172–3177.
169. Leifert D; Studer A The Persistent Radical Effect in Organic Synthesis. *Angew. Chem. Int. Ed.* 2020, 59, 74–108.
170. Zhang Y; Liu H; Tang L; Tang H-J; Wang L; Zhu C; Feng C Intermolecular Carboamination of Unactivated Alkenes. *J. Am. Chem. Soc.* 2018, 140, 10695–10699. [PubMed: 30102522]
171. Patra T; Das M; Daniliuc CG; Glorius F; Metal-Free Photosensitized Oxyimination of Unactivated Alkenes with Bifunctional Oxime Carbonates. *Nat. Catal.* 2021, 4, 54–61.
172. Nicastrì MC; Lehnher D; Lam Y-H; DiRocco DA; Rovis T Synthesis of Sterically Hindered Primary Amines by Concurrent Tandem Photoredox Catalysis. *J. Am. Chem. Soc.* 2020, 142, 987–998. [PubMed: 31904228]
173. Talele TT The “Cyclopropyl Fragment” is a Versatile Player that Frequently Appears in Preclinical/Clinical Drug Molecules. *J. Med. Chem.* 2016, 59, 8712–8756. [PubMed: 27299736]
174. Meanwell NA Fluorine and Fluorinated Motifs in the Design and Application of Bioisosteres for Drug Design. *J. Med. Chem.* 2018, 61, 5822–5880. [PubMed: 29400967]
175. The lifetime ( $\tau_0$ ), the rate of radiative decay ( $k_r$ ) and the rate of non-radiative decay ( $k_{nr}$ ) of excited-state of  $[\text{Ir}(\text{dMeppy})_2(\text{dtbbpy})]\text{PF}_6$  were obtained from: Ladouceur S; Swanick KN; Gallagher-Duval S; Ding Z; Zysman-Colman E Strongly Blue Luminescent Cationic Iridium(III) Complexes with an Electron-Rich Ancillary Ligand: Evaluation of Their Optoelectronic and Electrochemiluminescence Properties. *Eur. J. Inorg. Chem.* 2013, 5329–5343.
176. Zhang M; Duan Y; Li W; Xu P; Cheng J; Yu S; Zhu C A Single Electron Transfer (SET) Approach to C–H Amidation of Hydrazones via Visible-Light Photoredox Catalysis. *Org. Lett.* 2016, 18, 5356–5359. [PubMed: 27689817]
177. For discussion on electronic structures of three-electron bonds, see: Danovich D; Foroutan-Nejad C; Hiberty PC; Shaik S Nature of the Three-Electron Bond. *J. Phys. Chem. A* 2018, 122, 1873–1885. [PubMed: 29338261]
178. Boivin J; Fouquet E; Schiano A-M; Zard SZ Iminyl Radicals: Part III. Further Synthetically Useful Sources of Iminyl Radicals. *Tetrahedron* 1994, 50, 1769–1776.
179. Anslyn EV; Dougherty DA *Modern Physical Organic Chemistry*, 1st ed.; University Science Books: Sausalito, 2006.
180. Dauncey EM; Morcillo SP; Douglas JJ; Sheikh NS; Leonori D Photoinduced Remote Functionalizations by Iminyl Radical Promoted C–C and C–H Bond Cleavage Cascades. *Angew. Chem. Int. Ed.* 2018, 57, 744–748.
181. Yan H; Zhu C SelectFluor Radical Fluorination for Preparing Alkyl Fluorides. In *Synthetic Organofluorine Chemistry* [Online]; Hu J, Umemoto T, Series Eds.; Fluorination. Springer: Singapore, 2018; 3, pp 1–9. 10.1007/978-981-10-1855-8 (accessed December 10, 2020).

182. Wang P-Z; He B-Q; Cheng Y; Chen J-R; Xiao W-J Radical C–C Bond Cleavage/Addition Cascade of Benzyl Cycloketone Oxime Ethers Enabled by Photogenerated Cyclic Iminyl Radicals. *Org. Lett.* 2019, 21, 6924–6929. [PubMed: 31436103]
183. For related mechanism on excited 2-Cl-AQN engaging in hydrogen-atom abstraction, see: Matsui K; Ishigami T; Yamaguchi T; Yamaguchi E; Tada N; Miura T; Itoh A Aerobic Photooxidative Synthesis of Phenols from Arylboronic Acids Using 2-Propanol as Solvent. *Synlett* 2014, 25, 2613–2616.
184. Bortolamei N; Isse AA; Gennaro A Estimation of Standard Reduction Potentials of Alkyl Radicals Involved in Atom Transfer Radical Polymerization. *Electrochim. Acta* 2010, 55, 8312–8318.
185. He Y; Anand D; Sun Z; Zhou L Visible-Light-Promoted Redox Neutral  $\gamma,\gamma$ -Difluoroallylation of Cycloketone Oxime Ethers with Trifluoromethyl Alkenes via C–C and C–F Bond Cleavage. *Org. Lett.* 2019, 21, 3769–3773. [PubMed: 31063391]
186. For seminal report on the Hudson reaction, see: Brown C; Hudson RF; Record KAF The Reaction Between Oximes and Sulphinyl Chlorides: A Ready, Low-Temperature Radical Rearrangement Process. *J. Chem. Soc., Perkin Trans. 2* 1978, 822–828.
187. Lin X-C; Stien D; Weinreb SM A New Method for the Generation and Cyclization of Iminyl Radicals via the Hudson Reaction. *Org. Lett.* 1999, 1, 637–639. [PubMed: 10823192]
188. Pratt DA; Blake JA; Mulder P; Walton JC; Korth H-G; Ingold KU O–H Bond Dissociation Enthalpies in Oximes: Order Restored. *J. Am. Chem. Soc.* 2004, 126, 10667–10675. [PubMed: 15327325]
189. Xia P-J; Ye Z-P; Hu Y-Z; Song D; Xiang H-Y; Chen X-Q Yang H Photocatalytic, Phosphoranyl Radical-Mediated N–O Cleavage of Strained Cycloketone Oximes. *Org. Lett.* 2019, 21, 2658–2662. [PubMed: 30942601]
190. For an electron spin resonance spectroscopy investigation of phosphoranyl radicals from phosphines, see: Kochi JK; Krusic PJ Displacement of Alkyl Groups from Organophosphorus Compounds Studied by Electron Spin Resonance. *J. Am. Chem. Soc.* 1969, 91, 3944–3946.
191. For the pioneering literature in this area, see: Zhang M-L; Xie J; Zhu C-J A General Deoxygenation Approach For Synthesis Of Ketones From Aromatic Carboxylic Acids And Alkenes. *Nat. Commun.* 2018, 9, 3517. [PubMed: 30158628]
192. Zhang M; Yuan X-A; Zhu C; Xie J Deoxygenative Deuteration of Carboxylic Acids with D<sub>2</sub>O. *Angew. Chem. Int. Ed.* 2019, 58, 312–316.
193. Stache EE; Ertel AB; Rovis T; Doyle AG Generation of Phosphoranyl Radicals via Photoredox Catalysis Enables Voltage-Independent Activation of Strong C–O Bonds. *ACS Catal.* 2018, 8, 11134–11139. [PubMed: 31367474]
194. Single-crystal X-ray diffraction structure of triarylphosphine radicals have been characterized. See: Pan X; Chen X; Li T; Li Y; Wang X Isolation and X-ray Crystal Structures of Triarylphosphine Radical Cations. *J. Am. Chem. Soc.* 2013, 135, 3414–3417. [PubMed: 23425226]
195. Padney G; Pooranchand D; Bhalerao UT Photoinduced single electron transfer activation of organophosphines: Nucleophilic trapping of phosphine radical cation. *Tetrahedron* 1991, 47, 1745–1752.
196. Phosphoranyl radicals have emerged as popular synthetic intermediates in the photoredox community. For general review on this topic, see: Ashton-Rossi JA; Clarke AK; Unsworth WP; Taylor RJK Phosphoranyl Radical Fragmentation Reactions Driven by Photoredox Catalysis. *ACS Catal.* 2020, 10, 7250–7261. [PubMed: 32905246]
197. For pioneering literature on  $\beta$ -scission of phosphoranyl-radical, see: Bentrude WG; Hansen ER; Khan WA; Rogers PE  $\alpha$  vs.  $\beta$  Scission in Reactions of Alkoxy and Thiyl Radicals with Diethyl Alkylphosphonites. *J. Am. Chem. Soc.* 1972, 94, 2867–2868.
198. For the first reported use of trifluoromethyl alkene as an electrophile in an S<sub>N</sub>2' reaction with carbon-nucleophile, see: Kendrick DA; Kolb M A New, Short, Synthetic Route to  $\alpha$ -Substituted 5,5-Difluoro-4-Pentenoic Acid Esters. *J. Fluorine Chem.* 1989, 45, 265–272.
199. For the pioneering literature that discloses photoredox-mediated strategy to employs trifluoromethyl alkene to install gem-difluoroalkene moiety, see: Xiao T; Li L; Zhou L Synthesis

- of Functionalized *gem*-Difluoroalkenes via a Photocatalytic Decarboxylative/Defluorinative Reaction. *J. Org. Chem.* 2016, 81, 7908–7916. [PubMed: 27467781]
200. Dauncey EM; Dighe SU; Douglas JJ; Leonori D A dual photoredox-nickel strategy for remote functionalization via iminyl radicals: radical ring-opening-arylation, -vinylation and -alkylation cascades. *Chem. Sci.*, 2019, 10, 7728–7733. [PubMed: 32180920]
201. Tu J-L; Tang W; Xu W; Liu F Iminyl-Radical-Promoted C–C Bond Cleavage/Heck-Like Coupling via Dual Cobaloxime and Photoredox Catalysis. *J. Org. Chem.* 2021, 86, 2929–2940. [PubMed: 33481602]
202. Nishimura T; Yoshinaka T; Nishiguchi Y; Maeda Y; Uemura S Iridium-Catalyzed Ring Cleavage Reaction of Cyclobutanone O-Benzoyloximes Providing Nitriles. *Org. Lett.* 2005, 7, 2425–2427. [PubMed: 15932214]
203. Li L; Chen H; Mei M; Zhou L Visible-light promoted  $\gamma$ -cyanoalkyl radical generation: three-component cyanopropylation/etherification of unactivated alkenes. *Chem. Commun.*, 2017, 53, 11544–11547.
204. Wayner DDM; McPhee DJ; Griller D Oxidation and Reduction Potentials of Transient Free Radicals. *J. Am. Chem. Soc.* 1988, 110, 132–137.
205. Shen X; Zhao J-J; Yu S Photoredox-Catalyzed Intermolecular Remote C–H and C–C Vinylation via Iminyl Radicals. *Org. Lett.* 2018, 20, 5523–3327. [PubMed: 30136853]
206. Källström S; Leino R Synthesis of pharmaceutically active compounds containing a disubstituted piperidine framework. *Bioorg. Med. Chem.* 2008, 16, 601–635. [PubMed: 17980609]
207. Yu X-Y; Chen J-R; Wang P-Z; Yang M-N; Lian D; Xiao W-J A Visible-Light-Driven Iminyl Radical-Mediated C–C Single Bond Cleavage/Radical Addition Cascade of Oxime Esters. *Angew. Chem. Int. Ed.* 2018, 57, 738–743.
208. Yao S; Zhang K; Zhou Q-Q; Zhao Y; Shi D-Q; Xiao W-J Photoredox-Promoted Alkyl Radical Addition/Semipinacol Rearrangement Sequences of Alkenylcyclobutanols: Rapid Access to Cyclic Ketones. *Chem. Commun.*, 2018, 54, 8096–8099.
209. He B-Q; Yu X-Y; Wang P-Z; Chen J-R; Xiao W-J A photoredox catalyzed iminyl radical-triggered C–C bond cleavage/addition/Kornblum oxidation cascade of oxime esters and styrenes: synthesis of ketonitriles. *Chem. Commun.*, 2018, 54, 12262–12265.
210. Zhao B; Tan H; Chen C; Jiao N; Shi Z Photoinduced C–C Bond Cleavage and Oxidation of Cycloketoxime Esters. *Chin. J. Chem.* 2018, 36, 995–999.
211. Tomita R; Yasu Y; Koike T; Akita M Combining Photoredox-Catalyzed Trifluoromethylation and Oxidation with DMSO: Facile Synthesis of  $\alpha$ -Trifluoromethylated Ketones from Aromatic Alkenes. *Angew. Chem. Int. Ed.* 2014, 53, 7144–7148.
212. Notably, radical-mediated formal Kornblum oxidation reactions relied primarily on peroxide substrates in Kornblum–LaMer reactions. For a pioneering example, see: Kornblum N; DeLaMare HE The Base Catalyzed Decomposition of a Dialkyl Peroxide. *J. Am. Chem. Soc.* 1951, 73, 880–881.
213. Mao R; Yuan Z; Li Y; Wu J *N*-Radical-Initiated Cyclization through Insertion of Sulfur Dioxide under Photoinduced Catalyst-Free Conditions. *Chem. Eur. J.* 2017, 23, 8176–8179. [PubMed: 28485893]
214. Li Y; Mao R; Wu J *N*-Radical Initiated Aminosulfonylation of Unactivated C(sp<sup>3</sup>)-H Bond through Insertion of Sulfur Dioxide. *Org. Lett.* 2017, 19, 4472–4475. [PubMed: 28809576]
215. Ye S; Wu J A Palladium-Catalyzed Reaction of Aryl Halides, Potassium Metabisulfite, and Hydrazines. *Chem. Commun.*, 2012, 48, 10037–10039.
216. Zhang J; Li X; Xie W; Ye S; Wu J Photoredox-Catalyzed Sulfonylation of *O*-Acyl Oximes via Iminyl Radicals with the Insertion of Sulfur Dioxide. *Org. Lett.* 2019, 21, 4950–4954. [PubMed: 31179704]
217. Bowry VW; Luszyk J; Ingold KU Calibration of a New Horology of Fast Radical “Clocks”. Ring-Opening Rates for Ring- and  $\alpha$ -Alkyl-Substituted Cyclopropylcarbinyl Radicals and for the Bicyclo[2.1.0]pent-2-yl Radical. *J. Am. Chem. Soc.* 1991, 113, 5687–5698.
218. Liu Y; Wang Q-L; Chen Z; Li H; Xiong B-Q; Zhang P-L; Tang K-W Visible-Light Photoredox-Catalyzed Dual C–C Bond Cleavage: Synthesis of 2-Cyanoalkylsulfonylated 3,4-

- Dihydronaphthalenes Through the Insertion of Sulfur Dioxide. *Chem. Commun.* 2020, 56, 3011–3014.
219. Zheng M; Li G; Lu H Photoredox- or Metal-Catalyzed in Situ SO<sub>2</sub>-Capture Reactions: Synthesis of β-Ketosulfones and Allylsulfones. *Org. Lett.* 2019, 21, 1216–1220. [PubMed: 30698440]
220. Huang W; Hu L The Chemistry of Perfluoroalkanesulfonyl Iodides. *J. Fluorine Chem.* 1989, 44, 25–44.
221. Sulfone byproduct from radical addition to SO<sub>2</sub> generated from organic triflate fragmentation has been documented. See: Uenoyama Y; Fukuyama T; Morimoto K; Nobuta O; Nagai H; Ryu I Trifluoromethyl-Radical-Mediated Carbonylation of Alkanes Leading to Ethynyl Ketones. *Helv. Chim. Acta* 2006, 89, 2483–2494.
222. Liu S; Jie J; Yu J; Yang X Visible light induced Trifluoromethyl Migration: Easy Access to α-Trifluoromethylated Ketones from Enol Triflates. *Adv. Synth. Catal.* 2018, 360, 267–271.
223. For pioneering literature on the Minisci reaction, see: Minisci F; Galli R; Cecere M; Malatesta V; Caronna MT Nucleophilic character of alkyl radicals: new syntheses by alkyl radicals generated in redox processes. *Tetrahedron* 1968, 8, 5609–5612.
224. For review on Minisci reactions in organic synthesis, see: Proctor RSJ; Phipps RJ Recent Advances in Minisci-Type Reactions. *Angew. Chem. Int. Ed.* 2019, 58, 13666–13699.
225. Gu Y-R; Duan X-H; Yang L; Guo L-N Direct C–H Cyanoalkylation of Heteroaromatic N-Oxides and Quinones via C–C Bond Cleavage of Cyclobutanone Oximes. *Org. Lett.* 2017, 19, 5908–5911. [PubMed: 29072466]
226. Zhao B; Kong X; Xu B Visible-light-driven cyanoalkylation of quinoxalinones using cyclobutanone oxime esters as the radical precursors. *Tetrahedron Lett.* 2019, 60, 2063–2066.
227. Zhang -W; Pan Y-L; Yang C; Li X; Wang B Ring-opening C(sp<sup>3</sup>)–C coupling of cyclobutanone oxime esters for the preparation of cyanoalkyl containing heterocycles enabled by photocatalyst. *Org. Chem. Front.* 2019, 6, 2765–2770.
228. Xia P-J; Hu Y-Z; Ye Z-P; Li X-J; Xiang H-Y; Yang H O-Perfluoropyridin-4-yl Oximes: Iminyl Radical Precursors for Photo- or Thermal-Induced N–O Cleavage in C(sp<sup>2</sup>)–C(sp<sup>3</sup>) Bond Formation. *J. Org. Chem.* 2020, 85, 3538–3547. [PubMed: 31971800]
229. Jian Y; Chen M; Yang C; Xia W-J Minisci-Type C–H Cyanoalkylation of Heteroarenes Through N–O/C–C Bonds Cleavage. *Eur. J. Org. Chem.* 2020, 1439–1442.
230. Li X; Yan X; Wang Z; He X; Dai Y; Yan X; Zhao D; Xu X Complementary Oxidative Generation of Iminyl Radicals from α-Imino-oxy Acids: Silver-Catalyzed C–H Cyanoalkylation of Heterocycles and Quinones. *J. Org. Chem.* 2020, 85, 2504–2511. [PubMed: 31910620]
231. Wang P-Z; Yu X-Y; Li C-Y; He B-Q; Chen J-R; Xiao W-J A Photocatalytic Iminyl Radical-Mediated C–C Bond Cleavage/Addition/Cyclization Cascade for the Synthesis of 1,2,3,4-Tetrahydrophenanthrenes. *Chem. Commun.* 2018, 54, 9925–9928.
232. Yuan Y; Dong W-H; Gao X-S; Xie X-M; Zhang Z-G Visible-light-induced radical cascade cyclization of oxime esters and aryl isonitriles: synthesis of cyclopenta[*b*]quinoxalines. *Chem. Commun.* 2019, 55, 11900–11903.
233. Lenoir I; Smith ML Vinyl isonitriles in radical cascade reactions: formation of cyclopenta-fused pyridines and pyrazines. *J. Chem. Soc., Perkin Trans. 1* 2000, 641–643.
234. Camaggi CM; Leardini R; Nanni D; Zanardi G Radical Annulations with Nitriles: Novel Cascade Reactions of Cyano-Substituted Alkyl and Sulfonyl Radicals with Isonitriles. *Tetrahedron*, 1998, 54, 5587–5598.
235. Anand D; He Y; Li L; Zhou L A Photocatalytic sp<sub>3</sub> C–S, C–Se and C–B Bond Formation Through C–C Bond Cleavage of Cycloketone Oxime Esters. *Org. Biomol. Chem.* 2019, 17, 533–540. [PubMed: 30569940]
236. Zhang Z; Ye J-H; Ju T; Liao L-L; Huang H; Gui Y-Y; Zhou W-J; Yu D-G Visible-Light-Driven Catalytic Reductive Carboxylation with CO<sub>2</sub>. *ACS Catal.* 2020, 10, 10871–10885.
237. Jiang Y-X; Chen L; Ran C-K; Song L; Zhang W; Liao L-L; Yu D-G Visible-Light Photoredox-Catalyzed Ring-Opening Carboxylation of Cyclic Oxime Esters with CO<sub>2</sub>. *ChemSusChem* 2020, 13, 6312–6317. [PubMed: 33017513]

238. Pischel U; Zhang X; Hellrung B; Haselbach E; Muller P-A; Nau WM Fluorescence Quenching of  $n,\pi^*$ -Excited Azoalkanes by Amines: What Is a Sterically Hindered Amine? *J. Am. Chem. Soc.* 2000, 122, 2027–2034.
239. Li Z; Torres-Ochoa RO; Wang Q; Zhu J Functionalization of Remote  $C(sp^3)$ -H Bonds Enabled by Copper-Catalyzed Coupling of *O*-acyloximes with Terminal Alkynes. *Nat. Commun.* 2020, 11, 403. [PubMed: 31964870]
240. Hossain A; Bhattacharyya A; Reiser O Copper's Rapid Ascent in Visible-Light Photoredox Catalysis. *Science* 2019, 364, 450.
241. Pintauer T; Matyjaszewski K Atom Transfer Radical Addition and Polymerization Reactions Catalyzed by ppm Amounts of Copper Complexes. *Chem. Soc. Rev.* 2008, 37, 1087–1097. [PubMed: 18497922]
242. Yu X-Y; Zhao Q-Q; Chen J; Chen J-R Xiao W-J Copper-Catalyzed Radical Cross-Coupling of Redox-Active Oxime Esters, Styrenes, and Boronic Acids. *Angew. Chem. Int. Ed.* 2018, 57, 15505–15509.
243. Chen J; He B-Q; Wang P-Z; Yu X-Y; Zhao Q-Q; Chen J-R; Xiao W-J Photoinduced, Copper-Catalyzed Radical Cross-Coupling of Cycloketone Oxime Esters, Alkenes, and Terminal Alkynes. *Org. Lett.* 2019, 21, 4359–4364. [PubMed: 31141377]
244. Huang H; Ji X; Wu W; Jiang H Transition Metal-Catalyzed C–H Functionalization of N-Oxyenamine Internal Oxidants. *Chem. Soc. Rev.* 2015, 44, 1155–1171. [PubMed: 25417560]
245. Zhao B; Wu Y; Yuan Y; Shi Z Copper-catalysed  $Csp^3$ -Csp cross-couplings between cyclobutanone oxime esters and terminal alkynes induced by visible light. *Chem. Commun.* 2020, 56, 4676–4679.
246. Wang T; Wang Y-N; Wang R; Zhang B-C; Yang C; Li Y-L; Wang X-S Enantioselective Cyanation via Radical-Mediated C–C Single Bond Cleavage For Synthesis of Chiral Dinitriles. *Nat. Commun.* 2019, 10, 5373. [PubMed: 31772198]
247. Chen J; Wang P-Z; Lu B; Liang D; Yu X-Y; Xiao W-J Chen J-R Enantioselective Radical Ring-Opening Cyanation of Oxime Esters by Dual Photoredox and Copper Catalysis. *Org. Lett.* 2019, 21, 9763–9768. [PubMed: 31746212]
248. Davies IA; Gerena L; Castonguay L; Senanayake CH; Larsen RD; Verhoeven TR; Reider PJ The Influence of Ligand Bite Angle On the Enantioselectivity of Copper(II)-Catalysed Diels-Alder Reactions. *Chem. Commun.* 1996, 1753–1754.
249. Holzer W; Penzkofer A; Tsuboi T Absorption And Emission Spectroscopic Characterization of  $Ir(ppy)_3$ . *Chem. Phys.* 2005, 308, 93–102.
250. Yu X-Y; Wang P-Z; Yan D-M; Lu B; Chen J-R; Xiao W-J Photocatalytic Neophyl Rearrangement and Reduction of Distal Carbon Radicals by Iminyl Radical-Mediated C–C Bond Cleavage. *Adv. Synth. Catal.* 2018, 360, 3601–3606.
251. Zhao B; Chen C; Lu J; Li Z; Yuan Y; Shi Z Photoinduced Fragmentation-Rearrangement Sequence of Cycloketoxime Esters. *Org. Chem. Front.* 2018, 5, 2719–2722.
252. It is reported that aminium radical cations are more electrophilic than their neutral aminyl radical counterparts and can rapidly engage in HAT events. For a physical-organic investigation on this matter, see: Hioe J; Šaki D; Vr ek V; Zipse H The stability of nitrogen-centered radicals. *Org. Biomol. Chem.* 2015, 13, 157–169. [PubMed: 25351112]
253. Xuan J; Zhang Z-G; Xiao W-J Visible-Light-Induced Decarboxylative Functionalization of Carboxylic Acids and Their Derivatives. *Angew. Chem. Int. Ed.* 2015, 54, 15632–15641.
254. Liang T; Neumann CN; Ritter T Introduction of Fluorine and Fluorine-Containing Functional Groups. *Angew. Chem. Int. Ed.* 2013, 52, 8214–8264.
255. Jiang H; Studer A  $\alpha$ -Aminoxy-Acid-Auxillary-Enabled Intermolecular Radical  $\gamma$ - $C(sp^3)$ -H Functionalization of Ketones. *Angew. Chem. Int. Ed.* 2018, 57, 1692–1696.
256. Xie J; Jin H; Hashmi ASK The recent achievements of redox-neutral radical C–C cross-coupling enabled by visible-light. *Chem. Soc. Rev.* 2017, 46, 5193–5203. [PubMed: 28762417]
257. Chen L; Guo L-N; Ma Z-Y; Gu Y-R; Zhang J; Duan X-H Iminyl Radical-Triggered 1,5-Hydrogen-Atom Transfer/Heck-Type Coupling by Visible-Light Photoredox Catalysis. *J. Org. Chem.* 2019, 84, 6475–6482. [PubMed: 31050432]

258. Ma Z-Y; Guo L-N; Gu Y-R; Chen L; Duan X-H Iminyl Radical-Mediated Controlled Hydroxyalkylation of Remote C(sp<sup>3</sup>)-H Bond via Tandem 1,5-HAT and Difunctionalization of Aryl Alkenes. *Adv. Synth. Catal.* 2018, 360, 4341–4347.
259. For mechanistic discussions about radical enantioselective C(sp<sup>3</sup>)-H reactions, see: Zhang C; Li Z-L; Gu Q-S; Liu X-Y Catalytic Enantioselective C(sp<sup>3</sup>)-H Functionalization Involving Radical Intermediates. *Nat. Commun* 2021, 12, 475. [PubMed: 33473126]
260. Nakafuku KM; Zhang Z; Wappes EA; Stateman LM; Chen AD; Nagib DA Enantioselective Radical C-H Amination for the Synthesis of β-Amino Alcohols. *Nat. Chem* 2020, 12, 697–704. [PubMed: 32572164]
261. Qin Q; Yu S; Visible-Light-Promoted Redox Neutral C-H Amidation of Heteroarenes with Hydroxylamine Derivatives. *Org. Lett.* 2014, 16, 3504–3507. [PubMed: 24964153]
262. Davies J; Svejstrup TD; Reina DF; Sheikh NS; Leonori D Visible-Light-Mediated Synthesis of Amidyl Radicals: Transition-Metal-Free Hydroamination and *N*-Arylation Reactions. *J. Am. Chem. Soc.* 2016, 138, 8092–8095. [PubMed: 27327358]
263. Pertinent manuscripts were published contemporaneously with the submission of this review, see as an example: Zhang Z; Ngo DT; Nagib DA Regioselective Radical Amino-Functionalizations of Allyl Alcohols via Dual Catalytic Cross-Coupling. *ACS Catal.* 2021, 11, 3473–3477. [PubMed: 34745713]
264. Wu K; Du Y; Wang T Visible-Light-Mediated Construction of Pyrroloindolines via an Amidyl Radical Cyclization/Carbon Radical Addition Cascade: Rapid Synthesis of (±)-Flustramide B. *Org. Lett.* 2017, 19, 5669–5672. [PubMed: 28972766]
265. Wu K; Du Y; Wei Z; Wang T Synthesis of Functionalized Pyrroloindolines via a Visible-Light-Induced Radical Cascade Reaction: Rapid Synthesis of (±)-Flustraminol B. *Chem. Commun.* 2018, 54, 7443–7446.
266. Qin Q; Han Y-Y; Jiao Y-Y; He Y; Yu S Photoredox-Catalyzed Diamidation and Oxidative Amidation Alkenes: Solvent-Enabled Synthesis of 1,2-Diamides and α-Amino Ketones. *Org. Lett.* 2017, 19, 2909–2912. [PubMed: 28508648]
267. Sim BA; Milne PH; Griller D; Wayner DDM Thermodynamic Significance of ρ<sup>+</sup> and ρ<sup>-</sup> from Substituent Effects on the Redox Potentials of Arylmethyl Radicals. *J. Am. Chem. Soc.* 1990, 112, 6635–6638.
268. Jiang H; Studer A Amidyl Radicals by Oxidation of α-Amido-oxy acids: Transition-Metal-Free Amidofluorination of Unactivated Alkenes. *Angew. Chem. Int. Ed.* 2018, 57, 10707–10711.
269. Jiang H; Studer A Anti-Markovnikov Radical Hydro- and Deuteroamidation of Unactivated Alkenes. *Chem. Eur. J.* 2019, 25, 7105–7109. [PubMed: 30957905]
270. Huo H; Shen X; Wang C; Zhang L; Röse P; Chen L-A; Harms K; Marsch M; Hilt G; Meggers E Asymmetric Photoredox Transition-Metal Catalysis Activated by Visible Light. *Nature*, 2014, 515, 100–103. [PubMed: 25373679]
271. For review on the concept of “smart initiator”, see: Studer A; Curran DP Catalysis of Radical Reactions: A Radical Chemistry Perspective. *Angew. Chem. Int. Ed.* 2016, 55, 58–102.
272. Kim JH; Ruffoni A; Al-Faiyz YSS; Sheikh NS; Leonori D Divergent Strain-Release Amino-Functionalization of [1.1.1]Propellane with Electrophilic Nitrogen-Radicals. *Angew. Chem. Int. Ed.* 2020, 59, 8225–8231.
273. Morcillo SP; Dauncey EM; Kim JH; Douglas JJ; Sheikh NS; Leonori D Photoinduced Remote Functionalization of Amides and Amines Using Electrophilic Nitrogen Radicals. *Angew. Chem. Int. Ed.* 2018, 57, 12945–12949.
274. Gennet D; Zard SZ; Zhang HW Amidinyl radicals: new and useful intermediates for the synthesis of imidazolines and imidazoles. *Chem. Commun.* 2003, 15, 1870–1871.
275. Yang HB; Selander N Divergent iron-catalyzed coupling of *O*-acyloximes with silyl enol ethers. *Chem. Eur. J.* 2017, 23, 1779–1783. [PubMed: 27995682]
276. Yang HB; Pathipati SR; Selander N Nickel-Catalyzed 1,2-Aminoarylation of Oxime Ester-Tethered Alkenes with Boronic Acids. *ACS Catal.* 2017, 7, 8441–8445.
277. Huang J; He Y; Wang Y; Zhu Q Synthesis of Benzimidazoles by PIDA-Promoted Direct C(sp<sup>2</sup>)-H Imidation of *N*-Arylamidines. *Chem. Eur. J.* 2012, 18, 13964–13967. [PubMed: 22996950]



278. Alla SK; Kumar RK; Sadhu P; Punniyamurthy T Iodobenzene Catalyzed C–H Amination of *N*-Substituted Amidines Using *m*-Chloroperbenzoic Acid. *Org. Lett.* 2013, 15, 1334–1337. [PubMed: 23444897]
279. Zhao HB; Hou ZW; Liu ZJ; Zhou ZF; Song JS; Xu HT Amidinyl Radical Formation Through Anodic N–H Bond Cleavage And Its Application in Aromatic C–H Bond Functionalization. *Angew. Chem. Int. Ed.* 2017, 56, 587–590.
280. Li G; He R; Liu Q; Wang Z; Liu Y; Wang Q Formation of Amidinyl Radicals via Visible-Light-Promoted Reduction of *N*-Phenyl Amidoxime Esters and Application to the Synthesis of 2-Substituted Benzimidazoles. *J. Org. Chem.* 2019, 84, 8646–8660. [PubMed: 31198038]
281. Neale RS; Hinman RL The Chemistry of Ion Radicals. The Free Radical Addition of *N*-Chlorodialkylamines to Butadiene. *J. Am. Chem. Soc.* 1963, 85, 2666–2667.
282. Neale RS The Chemistry of Ion Radicals. The Free-Radical Addition of *N*-Chloramines to Olefinic and Acetylenic Hydrocarbons. *J. Am. Chem. Soc.* 1964, 86, 5340–5342.
283. *N*-nitrosylated analogues have been employed. See: Chow L Nitrosamine Photochemistry. Reactions of Aminium Radicals. *Acc. Chem. Res.* 1973, 6, 354–360.
284. Chow YC; Danen WC; Nelsen SF; Rosenblatt D Nonaromatic Aminium Radicals. *Chem. Rev.* 1978, 78, 243–274.
285. Musacchio AJ; Nguyen LQ; Beard GH; Knowles RR Catalytic Olefin Hydroamination with Aminium Radical Cations: A Photoredox Method for Direct C–N Bond Formation. *J. Am. Chem. Soc.* 2014, 136, 12217–12220. [PubMed: 25127420]
286. For the first known, photocatalytic, aminium radical process for C–N bond formation, see: Maity S; Zheng N A Visible-Light-Mediated Oxidative C–N Bond Formation/Aromatization Cascade: Photocatalytic Preparation of *N*-Arylindoles. *Angew. Chem. Int. Ed.* 2012, 51, 9562–9566.
287. Michejda CJ; Campbell DH Addition of Complexed Amino Radicals to Conjugated Alkenes. *J. Am. Chem. Soc.* 1979, 101, 7687–7693.
288. Wayner DDM; Griller D Oxidation and Reduction Potentials of Transient Free Radicals. *J. Am. Chem. Soc.* 1985, 107, 7764–7765.
289. Nguyen TM; Nicewicz DA Anti-Markovnikov Hydroamination of Alkenes Catalyzed by an Organic Photoredox System. *J. Am. Chem. Soc.* 2013, 135, 9588–9591. [PubMed: 23768239]
290. Musacchio AJ; Lainhart BC; Zhang X; Naguib SG; Sherwood TC; Knowles RR Catalytic Intermolecular Hydroaminations of Unactivated Olefins with Secondary Alkyl Amines. *Science* 2017, 355, 727–730. [PubMed: 28209894]
291. Wagner BD; Ruel G; Luszyk J Absolute Kinetics of Aminium Radical Reactions with Olefins in Acetonitrile Solution. *J. Am. Chem. Soc.* 1996, 118, 13–19.
292. Miller DC; Ganley JM; Musacchio AJ; Sherwood TC; Ewing WR; Knowles RR Anti-Markovnikov Hydroamination of Unactivated Alkenes with Primary Alkyl Amines. *J. Am. Chem. Soc.* 2019, 141, 16590–16594. [PubMed: 31603324]
293. Romero NA; Margrey KA; Tay NE; Nicewicz DA Site-Selective Arene C–H Amination via Photoredox Catalysis. *Science* 2015, 349, 1326–1330. [PubMed: 26383949]
294. Margrey KA; Levens A; Nicewicz DA Direct C–H Amination with Primary Amines Using Organic Photoredox Catalysis. *Angew. Chemie. Int. Ed.* 2017, 129, 15850–15854.
295. Ohkubo K; Mizushima K; Iwata R; Fukuzumi S Selective Photocatalytic Aerobic Bromination with Hydrogen Bromide via an Electron-transfer State of 9-mesityl-10-methylacridinium Ion. *Chem. Sci.* 2011, 2, 715–722.
296. Ruffoni A; Juliá F; Svejstrup TD; McMillan AJ; Douglas JJ; Leonori D Practical and Regioselective Amination of Arenes Using Alkyl Amines. *Nature Chemistry* 2019, 11, 426–433.
297. Wei W; Wang L; Bao P; Shao Y; Yue H; Yang D; Yang X; Zhao X; Wang H Metal-free C(sp<sup>2</sup>)-H/N–H Cross-dehydrogenative Coupling of Quinoxalinones with Aliphatic Amines under Visible-light Photoredox Catalysis. *Org. Lett.* 2018, 20, 7125–7130. [PubMed: 30372088]
298. Zhao Y; Huang B; Yang C; Li B; Gou B; Xia W Photocatalytic Cross-dehydrogenative Amination Reactions Between Phenols and Diarylamines. *ACS Catal.* 2017, 7, 2446–2451.
299. Zhou C; Lei T; Wei X-Z; Ye C; Liu Z; Chen B; Tung C-H; Wu L-Z Metal-Free, Redox-Neutral, Site-Selective Access to Heteroarylamines via Direct Radical–Radical Cross-Coupling

- Powered by Visible Light Photocatalysis. *J. Am. Chem. Soc.* 2020, 142, 16805–16813. [PubMed: 32897073]
300. For an early example of transition metal-catalyzed aryl amination employing nitrile groups as a pseudo-halide leaving-group, see: Miller JA; Dankwardt JW; Penney JM Nickel-Catalyzed Cross-Coupling and Amination Reactions of Aryl Nitriles. *Synthesis* 2003, 11, 1643–1648.
301. Carbon–carbon cross-coupling via loss of nitrile from a (hetero)arene has been previously demonstrated, see: Zuo Z; MacMillan DWC Decarboxylative Arylation of  $\alpha$ -Amino Acids via Photoredox Catalysis: A One-step Conversion of Biomass to Drug Pharmacophore. *J. Am. Chem. Soc.* 2014, 136, 5257–5260. [PubMed: 24712922]
302. For a recent review of metal-mediated C–CN bond activation, see: Nakao Y Metal-mediated C–CN Bond Activation in Organic Synthesis. *Chem. Rev.* 2021, 121, 327–344. [PubMed: 33047951]
303. Pandey G; Koley S; Talukdar R; Sahani PK Cross-dehydrogenating Coupling of Aldehydes with Amines/R-OTBS Ethers by Visible-light Photoredox Catalysis: Synthesis of Amides, Esters, and Ureas. *Org. Lett.* 2018, 20, 5861–5865. [PubMed: 30192550]
304. Bordwell FG; Harrelson JA; Lynch TY Homolytic Bond Dissociation Energies for the Cleavage of Alpha-nitrogen-hydrogen Bonds in Carboxamides, Sulfonamides, and Their Derivatives. The Question of Synergism in Nitrogen-centered Radicals. *J. Org. Chem.* 1990, 55, 3337–3341.
305. Bordwell FG; Ji G-Z Effects of Structural Changes on Acidities and Homolytic Bond Dissociation Energies of the H–N bonds in Amidines, Carboxamides, and Thiocarboxamides. *J. Am. Chem. Soc.* 1991, 113, 8398–8401.
306. Bordwell FG; Zhang S; Zhang X-M; Liu W-Z Homolytic Bond Dissociation Enthalpies of the Acidic H–A Bonds Caused by Proximate Substituents in Sets of Methyl Ketones, Carboxylic Esters, and Carboxamides Related to Changes in Ground State Energies. *J. Am. Chem. Soc.* 1995, 117, 7092–7096.
307. Wolff ME Cyclization of *N*-Halogenated Amines (The Hofmann-Löffler Reaction). *Chem. Rev.* 1963, 63, 55–64.
308. Lin X; Stien D; Weinreb SM A Mild New Procedure for Production, Cyclization and Trapping of Amidyl Radicals: Application to a Formal Total Synthesis of Peduncularine. *Tetrahedron Lett.* 2000, 41, 2333–2337.
309. Gagosz F; Moutrille C; Zard SZ A New Tin-Free Source of Amidyl Radicals. *Org. Lett.* 2002, 4, 2707–2709. [PubMed: 12153215]
310. Fuentes N; Kong W; Fernandez-Sanchez L; Merino E; Nevado C Cyclization Cascades via *N*-Amidyl Radicals Toward Highly Functionalized Heterocyclic Scaffolds. *J. Am. Chem. Soc.* 2015, 137, 964–973. [PubMed: 25561161]
311. Fallis AG; Brinza IM Free Radical Cyclizations Involving Nitrogen. *Tetrahedron* 1997, 53, 17543–17594.
312. Esker JL; Newcomb M Amidyl Radicals from *N*-(Phenylthio)amides. *Tetrahedron Lett.* 1993, 34, 6877–6880.
313. Chen K; Richter JM; Baran PS 1,3-Diol Synthesis via Controlled, Radical-Mediated C–H Functionalization. *J. Am. Chem. Soc.* 2008, 130, 7247–7249. [PubMed: 18481847]
314. Zhou L; Tang S; Qi X; Lin C; Liu K; Liu C; Lan Y; Lei A Transition-metal-assisted Radical/radical Cross-coupling: A New Strategy to the Oxidative C(sp<sup>3</sup>)-H/N-H Cross-coupling. *Org. Lett.* 2014, 16, 3404–3407. [PubMed: 24921665]
315. Nicolaou KC; Baran PS; Zhong YL; Sugita K Iodine(V) Reagents in Organic Synthesis. Part 1. Synthesis of Polycyclic Heterocycles via Dess–Martin Periodinane-Mediated Cascade Cyclization: Generality, Scope, and Mechanism of the Reaction. *J. Am. Chem. Soc.* 2002, 124, 2212–2220. [PubMed: 11878975]
316. Nicolaou KC; Baran PS; Zhong YL; Barluenga S; Hunt KW; Kranich R; Vega JA Iodine(V) Reagents in Organic Synthesis. Part 3. New Routes to Heterocyclic Compounds via *o*-Iodoxybenzoic Acid-Mediated Cyclizations: Generality, Scope, and Mechanism. *J. Am. Chem. Soc.* 2002, 124, 2233–2244. [PubMed: 11878977]

317. Nicolaou KC; Baran PS; Kranich R; Zhong Y-L; Sugita K; Zou N Mechanistic Studies of Periodinane-Mediated Reactions of Anilides and Related Systems. *Angew. Chem. Int. Ed.* 2001, 40, 202–206.
318. Martín A; Pérez-Martín I; Suárez E Intramolecular Hydrogen Abstraction Promoted by Amidyl Radicals. Evidence for Electronic Factors in the Nucleophilic Cyclization of Ambident Amides to Oxocarbenium Ions. *Org. Lett.* 2005, 7, 2027–2030. [PubMed: 15876046]
319. Janza B; Studer A Stereoselective Cyclization Reactions of IBX-Generated Alkoxyamidyl Radicals. *J. Org. Chem.* 2005, 70, 6991–6994. [PubMed: 16095334]
320. Hernández R; Medina MC; Salazar JA; Suárez E; Prangé T Intramolecular Functionalization of Amides Leading to Lactams. *Tetrahedron Lett.* 1987, 28, 2533–2536.
321. Freire R; Martín A; Pérez-Martín I; Suárez E Synthesis of Oxa-aza Spirobicycles by Intramolecular Hydrogen Abstraction Promoted by *N*-Radicals in Carbohydrate Systems. *Tetrahedron Lett.* 2002, 43, 5113–5116.
322. Choi GJ; Knowles RR Catalytic Alkene Carboaminations Enabled by Oxidative Proton-Coupled Electron Transfer. *J. Am. Chem. Soc.* 2015, 137, 9226–9229. [PubMed: 26166022]
323. Bordwell FG; Cheng J-P; Harrelson JA Homolytic bond dissociation energies in solution from equilibrium acidity and electrochemical data. *J. Am. Chem. Soc.* 1988, 110, 1229–1231.
324. Mayer JM Proton-coupled Electron Transfer: A Reaction Chemist's View. *Annu. Rev. Phys. Chem.* 2004, 55, 363–390. [PubMed: 15117257]
325. Warren JJ; Tronic TA; Mayer JM Thermochemistry of Proton-Coupled Electron Transfer Reagents and Its Implications. *Chem. Rev.* 2010, 110, 6961–7001. [PubMed: 20925411]
326. Waidmann CR; Miller AJM; Ng C-WA; Scheuermann ML; Porter TR; Tronic TA; Mayer JM Using Combinations of Oxidants and Bases as PCET Reactants: Thermochemical and Practical Considerations. *Energy Environ. Sci.* 2012, 5, 7771–7780.
327. Miller DC; Tarantino KT; Knowles RR Proton-Coupled Electron Transfer in Organic Synthesis: Fundamentals, Applications, and Opportunities. *Top. Curr. Chem.* 2016, 374, 30, DOI: 10.1007/s41061-016-0030-6.
328. Miller DC; Choi GJ; Orbe HS; Knowles RR Catalytic Olefin Hydroamidation Enabled by Proton-Coupled Electron Transfer. *J. Am. Chem. Soc.* 2015, 137, 13492–13495. [PubMed: 26439818]
329. Qiu G; Knowles RR Understanding Chemoselectivity in Proton-Coupled Electron Transfer: A Kinetic Study of Amide and Thiol Activation. *J. Am. Chem. Soc.* 2019, 141, 16574–16578. [PubMed: 31573194]
330. Nguyen ST; Zhu Q; Knowles RR PCET-Enabled Olefin Hydroamidation Reactions with *N*-Alkyl Amides. *ACS Catal.* 2019, 9, 4502–4507. [PubMed: 32292642]
331. Zhu Q; Graff DE; Knowles RR Intermolecular Anti-Markovnikov Hydroamination of Unactivated Alkenes with Sulfonamides Enabled by Proton-Coupled Electron Transfer. *J. Am. Chem. Soc.* 2018, 140, 741–747. [PubMed: 29268020]
332. Newcomb M; Esker JL Facile Production and Cyclizations of Amidyl Radicals. *Tetrahedron Lett.* 1991, 32, 1035–1038.
333. Chou CM; Guin J; Muck-Lichtenfeld C; Grimme A; Studer A Radical-Transfer Hydroamination of Olefins with *N*-Aminated Dihydropyridines. *Chem. - Asian J* 2011, 6, 1197–1209. [PubMed: 21384557]
334. Tang Y; Li C Facile 5-Endo Amidyl Radical Cyclization Promoted by Vinylic Iodine Substitution. *Org. Lett.* 2004, 6, 3229–3231. [PubMed: 15355019]
335. Medina-Ramos J; Oyesanya O; Alvarez JC Buffer Effects in the Kinetics of Concerted Proton-Coupled Electron Transfer: The Electrochemical Oxidation of Glutathione Mediated by  $[\text{IrCl}_6]^{2-}$  at Variable Buffer *pK*<sub>a</sub> and Concentration. *J. Phys. Chem. C* 2013, 117, 902–912.
336. Kuss-Petermann M; Wenger OS Mechanistic Diversity in Proton-Coupled Electron Transfer between Thiophenols and Photoexcited  $[\text{Ru}(2,2'\text{-Bipyrazine})_3]^{2+}$ . *J. Phys. Chem. Lett* 2013, 4, 2535–2539.
337. Gagliardi CJ; Murphy CF; Binstead RA; Thorp HH; Meyer TJ Concerted Electron–Proton Transfer (EPT) in the Oxidation of Cysteine. *J. Phys. Chem. C* 2015, 119, 7028–7038.

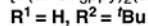
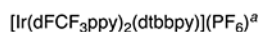
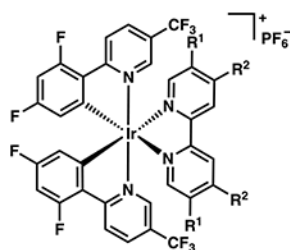
338. Rucolo S; Qin Y; Schnedermann C; Nocera DG General Strategy for Improving the Quantum Efficiency of Photoredox Hydroamidation Catalysis. *J. Am. Chem. Soc.* 2018, 140, 14926–14937. [PubMed: 30372046]
339. Zhao Y; Bordwell FG; Cheng J-P; Wang D Equilibrium Acidities and Homolytic Bond Dissociation Energies (BDEs) of the Acidic H–N Bonds in Hydrazines and Hydrazides. *J. Am. Chem. Soc.* 1997, 119, 9125–9129.
340. Hu X-Q; Qi X; Chen J-R; Zhao Q-Q; Wei Q; Lan Y; Xiao W-J Catalytic N-Radical Cascade Reaction of Hydrazones by Oxidative Deprotonation Electron Transfer and TEMPO Mediation. *Nat. Commun.* 2016, 7, 11188–11200. [PubMed: 27048886]
341. Rand AW; Yin H; Xu L; Giacoboni J; Martin-Montero R; Romano C; Montgomery J; Martin R Dual Catalytic Platform for Enabling  $sp^3$   $\alpha$ -C–H Arylation and Alkylation of Benzamides. *ACS Catal.* 2020, 10, 4671–4676.
342. Jia J; Ho YA; Bülow RF; Rueping M Brønsted Base Assisted Photoredox Catalysis: Proton Coupled Electron Transfer for Remote C–C Bond Formation Via Amidyl Radicals. *Chem. Eur. J.* 2018, 24, 14054–14058. [PubMed: 29939456]
343. Moon Y; Jang E; Choi S; Hong S Visible-Light-Photocatalyzed Synthesis of Phenanthridinones and Quinolinones Via Direct Oxidative C–H Amidation. *Org. Lett.* 2018, 20, 240–243. [PubMed: 29239619]
344. Usami K; Yamaguchi E; Tada N; Itoh A Transition-Metal-Free Synthesis of Phenanthridinones Through Visible-Light-Driven Oxidative C–H Amidation. *Eur. J. Org. Chem.* 2020, 1496–1504.
345. Hofmann AW *Chem. Ber.* 1883, 16, 558–560.
346. Kumler WD; Eiler JJ The Acid Strength of Mono and Diesters of Phosphoric Acid. The n-Alkyl Esters from Methyl to Butyl, the Esters of Biological Importance, and the Natural Guanidine Phosphoric Acids. *J. Am. Chem. Soc.* 1943, 65, 2355–2361.
347. Zhang L; Meggers E Steering Asymmetric Lewis Acid Catalysis Exclusively with Octahedral Metal-Centered Chirality. *Acc. Chem. Res.* 2017, 50, 320–330. [PubMed: 28128920]
348. Yuan W; Zhou Z; Gong L; Meggers E Asymmetric Alkylation of Remote C( $sp^3$ )–H Bonds by Combining Proton-coupled Electron Transfer with Chiral Lewis Acid Catalysis. *Chem. Commun.* 2017, 53, 8964–8967.
349. Zhou Z; Li Y; Han B; Gong L; Meggers E Enantioselective Catalytic  $\beta$ -Amination Through Proton-coupled Electron Transfer Followed by Stereocontrolled Radical–Radical Coupling. *Chem. Sci* 2017, 8, 5757–5763. [PubMed: 28989615]
350. Wang C; Chen L-A; Huo H; Shen X; Harms K; Gong L; Meggers E Asymmetric Lewis Acid Catalysis Directed by Octahedral Rhodium Centrochirality. *Chem. Sci.* 2015, 6, 1094–1100. [PubMed: 29560197]
351. Ma J; Shen X; Harms K; Meggers E Expanding the Family of Bis-cyclometalated Chiral-at-metal Rhodium(III) Catalysts with a Benzothiazole Derivative. *Dalton Trans.* 2016, 45, 8320–8323. [PubMed: 27143346]
352. Huo H, Fu C, Harms K and Meggers E, Asymmetric Catalysis with Substitutionally Labile yet Stereochemically Stable Chiral-at-Metal Iridium(III) Complex. *J. Am. Chem. Soc.* 2014, 136, 2990–2993. [PubMed: 24754748]
353. Chu JCK; Rovis T Amide-directed photoredox-catalysed C–C bond formation at unactivated  $sp^3$  C–H bonds. *Nature* 2016, 539, 272–275. [PubMed: 27732580]
354. Chen D-F; Chu JCK; Rovis T Directed  $\gamma$ -C( $sp^3$ )–H Alkylation of Carboxylic Acid Derivatives through Visible Light Photoredox Catalysis. *J. Am. Chem. Soc.* 2017, 139, 14897–14900. [PubMed: 29022709]
355. Pandey G; Laha R Visible-Light-Catalyzed Direct Benzylic C( $sp^3$ )–H Amination Reaction by Cross-Dehydrogenative Coupling. *Angew. Chem. Int. Ed.* 2015, 54, 14875–14879.
356. Zhang Y; Chen W; Wang L; Li P Visible-light-induced Selective Amination of Enol Ethers with N-Alkoxyamides by Using DDQ as a Photoredox Catalyst. *Org. Chem. Front.* 2018, 5, 3562–3566.
357. Short MA; Shehata MF; Sanders MA; Roizen JL Sulfamides Direct Radical-mediated Chlorination of Aliphatic C–H Bonds. *Chem. Sci.* 2020, 11, 217–223.

358. Shehata MF; Short MA; Sanders MA; Roizen JL Efficient Synthesis of Unsymmetrical Sulfamides with Sulfamic Acid Salts by Activation with Triphenylphosphine Ditriflate. *Tetrahedron* 2019, 75, 3186–3194.
359. Bafaluy D; Georgieva Z; Muniz K Iodine Catalysis for C(sp<sup>3</sup>)-H Fluorination with a Nucleophilic Fluorine Source. *Angew. Chem. Int. Ed.* 2020, 59, 14241–14245.
360. For a recent review of sulfamide-related chemistry, see: Spillane W; Malaubier J-B Sulfamic Acid and Its N- and O-Substituted Derivatives. *Chem. Rev.* 2014, 114, 2507–2586. [PubMed: 24341435]
361. Roos CB; Demaerel J; Graff DE; Knowles RR Enantioselective Hydroamination of Alkenes with Sulfonamides Enabled by Proton-Coupled Electron Transfer. *J. Am. Chem. Soc.* 2020, 142, 5974. [PubMed: 32182054]
362. Nairoukh Z; Cormier M; Marek I Merging C–H and C–C bond Cleavage in Organic Synthesis. *Nature Reviews. Chemistry* 2017, 1, 35.
363. Chen Z-M; Zhang X-M; Tu Y-Q Radical Aryl Migration Reactions and Synthetic Applications. *Chem. Soc. Rev.* 2015, 44, 5220–5245. [PubMed: 25954772]
364. Zhou T; Luo F-X; Yang M-Y; Shi Z-J Silver-Catalyzed Long-Distance Aryl Migration from Carbon Center to Nitrogen Center. *J. Am. Chem. Soc.* 2015, 137, 14586–14589. [PubMed: 26523735]
365. Shu W; Genoux A; Li Z; Nevado C  $\gamma$ -Functionalizations of Amines through Visible-Light-Mediated, Redox-Neutral C–C Bond Cleavage. *Angew. Chem. Int. Ed.* 2017, 56, 10521–10524.
366. Liu C; Cai C; Yuan C; Jiang Q; Fang Z; Guo K Visible-light-promoted *N*-centered Radical Generation for Remote Heteroaryl Migration. *Org. Biomol. Chem.* 2020, 18, 7663–7670. [PubMed: 32966504]
367. Sathyamoorthi S; Banerjee S; Du Bois J; Burns N; Zare RN Site-selective bromination of sp<sup>3</sup> C–H bonds. *Chem. Sci.* 2018, 9, 100–104. [PubMed: 29629078]
368. These investigations have been reviewed: Short MA, Blackburn J. Miles, Roizen JL Modifying Positional Selectivity in C–H Functionalization Reactions with Nitrogen-Centered Radicals: Generalizable Approaches to 1,6-Hydrogen-Atom Transfer Processes. *Synlett* 2020, 31, 102–116. [PubMed: 33986583]
369. For related studies of sulfamides as directing groups for exogenous atom-transfer, see: Short MA, Shehata MF, Sanders MA, Roizen JL Sulfamides Direct Radical-Mediated Chlorination of Aliphatic C–H Bonds. *Chem. Sci.* 2020, 11, 217–223.
370. Kanegusuku ALG; Castanheiro T; Ayer SK; Roizen JL Sulfamyl Radicals Direct Photoredox-Mediated Giese Reactions at Unactivated C(3)-H Bonds. *Org. Lett.* 2019, 21, 6089–6095. [PubMed: 31313933]
371. A preprint of this manuscript was published on May 31, 2019: Kanegusuku ALG; Castanheiro T; Ayer SK; Roizen JL Sulfamyl Radicals Direct Photoredox-Mediated Giese Reactions at Unactivated C(3)-H Bonds. *ChemRxiv* 2019, Preprint.
372. The bulk of this research was initially disclosed in August 19, 2018: Kanegusuku ALG; Castanheiro T; Roizen JL Sulfamate esters guide selective alkylation at traditionally non-reactive gamma-C(sp<sup>3</sup>)-H bonds. *ABSTRACTS OF PAPERS OF THE AMERICAN CHEMICAL SOCIETY* 256.
373. Ma Z-Y; Guo L-N; You Y; Yang F; Hu M; Duan X-H Visible Light Driven Alkylation of C(sp<sup>3</sup>)-H Bonds Enabled by 1,6-Hydrogen Atom Transfer/Radical Relay Addition. *Org. Lett.* 2019, 21, 5500–5504. [PubMed: 31246029]
374. Shu W; Zhang H; Huang Y  $\gamma$ -Alkylation of Alcohols Enabled by Visible-Light Induced 1,6-Hydrogen Atom Transfer. *Org. Lett.* 2019, 21, 6107–6111. [PubMed: 31339735]
375. Publications describing these Giese reactions rely, at least in part, on sulfamate ester preparation methods disclosed in Blackburn JM, Short MA, Castanheiro T, Ayer SK, Muellers TD, Roizen JL Synthesis of *N*-Substituted Sulfamate Esters from Sulfamic Acid Salts by Activation with Triphenylphosphine Ditriflate. *Org. Lett.* 2017, 19, 6012–6015. [PubMed: 29048913]
376. These copper-mediated reactions oxidize 1,6-dihydropyridazine intermediates to afford pyrazole products.

377. Pünner F; Sohtome Y; Sodeoka M Solvent-dependent Copper-catalyzed Synthesis of Pyrazoles under Aerobic Conditions. *Chem. Commun.* 2016, 52, 14093–14096.
378. Fan Z; Feng J; Hou Y; Rao Min.; Cheng J Copper-Catalyzed Aerobic Cyclization of  $\beta,\gamma$ -Unsaturated Hydrazones with Concomitant C=C Bond Cleavage. *Org. Lett.* 2020, 22, 7981–7985. [PubMed: 33021381]
379. Zhu MK; Chen YC; Loh TP Radical-Mediated Diamination of Alkenes with Phenylhydrazine and Azodicarboxylates: Highly Diastereoselective Synthesis of *trans*-Diamines from Cycloalkenes. *Chem. Eur. J.* 2013, 19, 5250–5254. [PubMed: 23471689]
380. Duan X-Y; Yang XL; Fang R; Peng XX; Yu W; Han B Hydrazone Radical Promoted Vicinal Difunctionalization of Alkenes and Trifunctionalization of Allyls: Synthesis of Pyrazolines and Tetrahydropyridazines. *J. Org. Chem.* 2013, 78, 10692–10704. [PubMed: 24063683]
381. Zhu X; Wang Y; Ren W; Zhang F-L; Chiba S TEMPO-Mediated Aliphatic C–H Oxidation with Oximes and Hydrazones. *Org. Lett.* 2013, 15, 3214–3217. [PubMed: 23767852]
382. Zhu X; Chiba S TEMPO-mediated allylic C–H amination with hydrazones. *Org. Biomol. Chem.* 2014, 12, 4567–4570. [PubMed: 24854457]
383. Duan X-Y; Zhou N-N; Fang R; Yang X-L; Yu W; Han B Transition from  $\pi$  Radicals to  $\sigma$  Radicals: Substituent-Tuned Cyclization of Hydrazone Radicals. *Angew. Chem., Int. Ed.* 2014, 53, 3158–3162.
384. Duan X-Y; Yang X-L; Jia P-P; Zhang M; Han B Hydrazone Radical-Participated Tandem Reaction: A Strategy for the Synthesis of Pyrazoline-Functionalized Oxindoles. *Org. Lett.* 2015, 17, 6022–6025. [PubMed: 26641278]
385. Hu X-Q; Chen J-R; Wei Q; Liu F-L; Deng Q-H; Beauchemin AM; Xiao W-J Photocatalytic Generation of N-Centered Hydrazone Radicals: A Strategy for Hydroamination of  $\beta,\gamma$ -Unsaturated Hydrazones. *Angew. Chem., Int. Ed.* 2014, 53, 12163–12167.
386. Hu X-Q; Chen J; Chen J-R; Yan D-M; Xiao W-J Organophotocatalytic Generation of *N*- and *O*-Centred Radicals Enables Aerobic Oxyamination and Dioxygenation of Alkenes. *Chem. Eur. J.* 2016, 22, 14141–14146. [PubMed: 27258972]
387. Zhao Q-Q; Chen J; Yan D-M; Chen J-R; Xiao W-J Photocatalytic Hydrazone Radical-Mediated Radical Cyclization/ Allylation Cascade: Synthesis of Dihydropyrazoles and Tetrahydropyridazines. *Org. Lett.* 2017, 19, 3620–3623. [PubMed: 28640626]
388. Zhao Q-Q; Hu XQ; Yang M-N; Chen J-R; Xiao W-J A Visible-light Photocatalytic *N*-Radical Cascade of Hydrazones for the Synthesis of Dihydropyrazole-fused Benzosultams. *Chem. Commun.* 2016, 52, 12749–12752.
389. Zhang G; Liu C; Yi H; Meng Q; Bian C; Chen H; Jian J-X; Wu L-Z; Lei A External Oxidant-Free Oxidative Cross-Coupling: A Photoredox Cobalt-Catalyzed Aromatic C–H Thiolation for Constructing C–S Bonds. *J. Am. Chem. Soc.* 2015, 137, 9273–9280. [PubMed: 26158688]
390. Zhang G; Zhang L; Yi H; Luo Y; Qi X; Tung C-H; Wu L-Z; Lei A Visible-light Induced Oxidant-free Oxidative Cross-Coupling for Constructing Allylic Sulfones from Olefins and Sulfinic Acids. *Chem. Commun.* 2016, 52, 10407–10410.
391. Niu L; Yi H; Wang S; Liu T; Liu J; Lei A Photo-induced Oxidant-free Oxidative C–H/N–H Cross-coupling between Arenes and Azoles. *Nat. Commun* 2017, 8, 14226. [PubMed: 28145410]
392. Yi H; Niu L; Song C; Li Y; Dou B; Singh AK; Lei A Photocatalytic Dehydrogenative Cross-Coupling of Alkenes with Alcohols or Azoles without External Oxidant. *Angew. Chem. Int. Ed.* 2017, 56, 1120–1124.
393. Gao X-W; Meng Q-Y; Li J-X; Zhong J-J; Lei T; Li X-B; Tung C-H; Wu L-Z Visible Light Catalysis Assisted Site-Specific Functionalization of Amino Acid Derivatives by C–H Bond Activation without Oxidant: Cross-Coupling Hydrogen Evolution Reaction. *ACS Catal.* 2015, 5, 2391–2396.
394. Xiang M; Meng Q-Y; Li J-X; Zheng Y-W; Ye C; Li Z-J; Chen B; Tung CH; Wu L-Z Activation of C–H Bonds through Oxidant-Free Photoredox Catalysis: Cross-Coupling Hydrogen-Evolution Transformation of Isochromans and  $\beta$ -Keto Esters. *Chem. Eur. J.* 2015, 21, 18080–18084. [PubMed: 26515479]
395. Azzi E; Ghigo G; Parisatto S; Pellegrino F; Priola E; Renzi P; Deagostino A Visible Light Mediated Photocatalytic *N*-Radical Cascade Reactivity of  $\gamma,\delta$ -Unsaturated *N*-

- Arylsulfonylhydrazones: A General Approach to Structurally Diverse Tetrahydropyridazines. *J. Org. Chem.* 2021, 86, 3300–3323. [PubMed: 33523670]
396. Allart-Simon I; Gérard S; Sapi J Radical Smiles Rearrangement: An Update. *Molecules*, 2016, 21, 878–889.
397. Brachet E; Marzo L; Selkti M; König B; Belmont P Visible Light Amination/Smiles Cascade: Access to Phthalazine Derivatives. *Chem. Sci.* 2016, 7, 5002–5006. [PubMed: 30155150]
398. Yu J-M; Lu G-P; Cai C; Photocatalytic Radical Cyclization of  $\alpha$ -Halo Hydrazones with  $\beta$ -Ketocarboxyls: Facile Access to Substituted Dihydropyrazoles. *Chem. Commun.* 2017, 53, 5342–5345.
399. For review on stereoselective reactions that merge photocatalysis and cobalt-catalysis, see: Kojima M; Matsunaga S The Merger of Photoredox and Cobalt Catalysis. *Trends Chem.* 2020, 2, 410–426.
400. For review on stereoselective reactions that merge photocatalysis and palladium- or nickel-catalysis, see: Zhang H-H; Chen H; Zhu C; Yu S A Review of Enantioselective Dual Transition Metal/Photoredox Catalysis. *Sci. China: Chem* 2020, 63, 637–647.
401. Simons RT Photo-Enabled Synthesis of Carbon–Nitrogen and Remote Carbon–Carbon Bonds. Master's Thesis, Duke University, Durham, NC, 2021.

## (A) Iridium photosensitizers

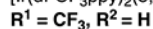
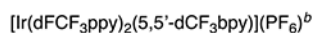


$E_{1/2}(*PC/PC^-) = +1.21 \text{ V vs SCE}$

$E_{1/2}(PC/PC^-) = -1.37 \text{ V vs SCE}$

$E_{1/2}(PC^+/*PC) = -0.89 \text{ V vs SCE}$

$E_{1/2}(PC^+/PC) = +1.69 \text{ V vs SCE}$

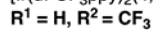
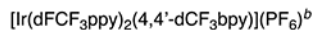


$E_{1/2}(*PC/PC^-) = +1.68 \text{ V vs SCE}$

$E_{1/2}(PC/PC^-) = -0.69 \text{ V vs SCE}$

$E_{1/2}(PC^+/*PC) = -0.43 \text{ V vs SCE}$

$E_{1/2}(PC^+/PC) = +1.94 \text{ V vs SCE}$

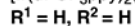
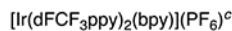


$E_{1/2}(*PC/PC^-) = +1.65 \text{ V vs SCE}$

$E_{1/2}(PC/PC^-) = -0.79 \text{ V vs SCE}$

$E_{1/2}(PC^+/*PC) = -0.51 \text{ V vs SCE}$

$E_{1/2}(PC^+/PC) = +1.93 \text{ V vs SCE}$

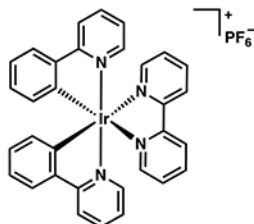


$E_{1/2}(*PC/PC^-) = +1.32 \text{ V vs SCE}$

$E_{1/2}(PC/PC^-) = -1.37 \text{ V vs SCE}$

$E_{1/2}(PC^+/*PC) = -1.00 \text{ V vs SCE}$

$E_{1/2}(PC^+/PC) = +1.69 \text{ V vs SCE}$

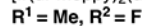
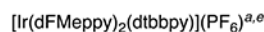
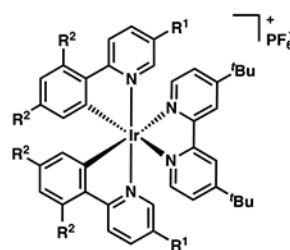


$E_{1/2}(*PC/PC^-) = +1.22 \text{ V vs SCE}$

$E_{1/2}(PC/PC^-) = -1.44 \text{ V vs SCE}$

$E_{1/2}(PC^+/*PC) = -1.17 \text{ V vs SCE}$

$E_{1/2}(PC^+/PC) = +1.49 \text{ V vs SCE}$

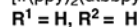


$E_{1/2}(*PC/PC^-) = +0.97 \text{ V vs SCE}$

$E_{1/2}(PC/PC^-) = -1.44 \text{ V vs SCE}$

$E_{1/2}(PC^+/*PC) = -0.92 \text{ V vs SCE}$

$E_{1/2}(PC^+/PC) = +1.49 \text{ V vs SCE}$

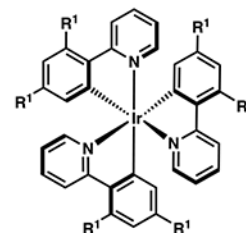


$E_{1/2}(*PC/PC^-) = +0.66 \text{ V vs SCE}$

$E_{1/2}(PC/PC^-) = -1.51 \text{ V vs SCE}$

$E_{1/2}(PC^+/*PC) = -0.96 \text{ V vs SCE}$

$E_{1/2}(PC^+/PC) = +1.21 \text{ V vs SCE}$



$E_{1/2}(*PC/PC^-) = +0.31 \text{ V vs SCE}$

$E_{1/2}(PC/PC^-) = -2.19 \text{ V vs SCE}$

$E_{1/2}(PC^+/*PC) = -1.73 \text{ V vs SCE}$

$E_{1/2}(PC^+/PC) = +0.77 \text{ V vs SCE}$



$E_{1/2}(*PC/PC^-) = +0.64 \text{ V vs SCE}$

$E_{1/2}(PC/PC^-) = -1.57 \text{ V vs SCE}$

$E_{1/2}(PC^+/*PC) = -0.98 \text{ V vs SCE}$

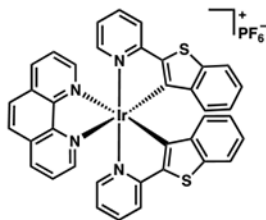
$E_{1/2}(PC^+/PC) = +1.23 \text{ V vs SCE}$

**Figure 1.**

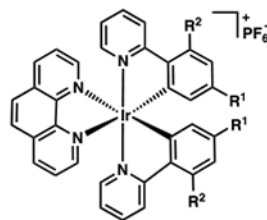
Iridium-Based Photocatalysts and Their Associated Photochemical and Electrochemical Data (All potentials are measured in acetonitrile). <sup>a</sup>See ref 8.<sup>8</sup> <sup>b</sup>See ref 9.<sup>9</sup> <sup>c</sup>See ref 10.<sup>10</sup> <sup>d</sup>See ref 11<sup>11</sup>. <sup>e</sup>See ref 12.<sup>12</sup> <sup>f</sup>See ref 13.<sup>13</sup> <sup>g</sup>See ref 14.<sup>14</sup> <sup>h</sup>See ref 15.<sup>15</sup> <sup>i</sup>See ref 16.<sup>16</sup> <sup>j</sup>See ref 17.<sup>17</sup>



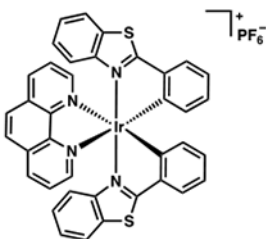
## (A) Iridium photosensitizers



[Ir(btp)<sub>2</sub>(phen)](PF<sub>6</sub>)<sup>a</sup>  
 $E_{1/2}(*PC/PC^-) = +0.94$  V vs SCE  
 $E_{1/2}(PC/PC^-) = -1.04$  V vs SCE  
 $E_{1/2}(PC^+/*PC) = -1.21$  V vs SCE  
 $E_{1/2}(PC^+/PC) = +0.77$  V vs SCE



[Ir(Fppy)<sub>2</sub>(phen)](PF<sub>6</sub>)<sup>a</sup>  
 $R^1 = F, R^2 = H$   
 $E_{1/2}(*PC/PC^-) = +1.35$  V vs SCE  
 $E_{1/2}(PC/PC^-) = -1.11$  V vs SCE  
 $E_{1/2}(PC^+/*PC) = -1.32$  V vs SCE  
 $E_{1/2}(PC^+/PC) = +1.14$  V vs SCE

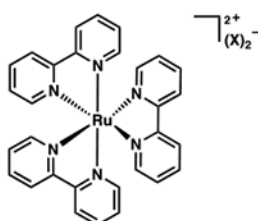


[Ir(dFppy)<sub>2</sub>(phen)](PF<sub>6</sub>)<sup>a</sup>  
 $R^1, R^2 = F$   
 $E_{1/2}(*PC/PC^-) = +1.42$  V vs SCE  
 $E_{1/2}(PC/PC^-) = -1.15$  V vs SCE  
 $E_{1/2}(PC^+/*PC) = -1.22$  V vs SCE  
 $E_{1/2}(PC^+/PC) = +1.35$  V vs SCE

[Ir(pbt)<sub>2</sub>(phen)](PF<sub>6</sub>)<sup>a</sup>  
 $E_{1/2}(*PC/PC^-) = +1.16$  V vs SCE  
 $E_{1/2}(PC/PC^-) = -1.39$  V vs SCE  
 $E_{1/2}(PC^+/*PC) = -1.17$  V vs SCE  
 $E_{1/2}(PC^+/PC) = +1.38$  V vs SCE

[Ir(dFCF<sub>3</sub>ppy)<sub>2</sub>(phen)](PF<sub>6</sub>)<sup>a</sup>  
 $R^1, R^2 = CF_3$   
 $E_{1/2}(*PC/PC^-) = +1.33$  V vs SCE  
 $E_{1/2}(PC/PC^-) = -1.22$  V vs SCE  
 $E_{1/2}(PC^+/*PC) = -0.99$  V vs SCE  
 $E_{1/2}(PC^+/PC) = +1.56$  V vs SCE

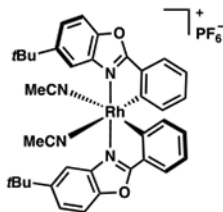
## (B) Ruthenium photosensitizer



[Ru(bpy)<sub>3</sub>](X)<sub>2</sub><sup>b, c</sup>,  $X = Cl$   
 $E_{1/2}(*PC/PC^-) = +0.78$  V vs SCE  
 $E_{1/2}(PC/PC^-) = -1.35$  V vs SCE  
 $E_{1/2}(PC^+/*PC) = -0.87$  V vs SCE  
 $E_{1/2}(PC^+/PC) = +1.26$  V vs SCE

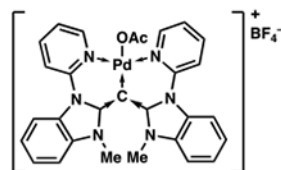
[Ru(bpy)<sub>3</sub>](PF<sub>6</sub>)<sub>2</sub><sup>c, d, e</sup>,  $X = PF_6$   
 $E_{1/2}(*PC/PC^-) = +0.77$  V vs SCE  
 $E_{1/2}(PC/PC^-) = -1.33$  V vs SCE  
 $E_{1/2}(PC^+/*PC) = -0.81$  V vs SCE  
 $E_{1/2}(PC^+/PC) = +1.29$  V vs SCE

## (C) Rhodium photosensitizers



Δ-RhO<sup>f</sup>

## (D) Palladium photosensitizer



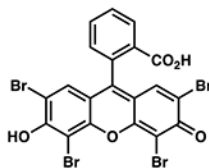
palladium dicarbene PC<sup>g</sup>  
 $E_{1/2}(PC^+/*PC) = +0.87$  V vs SCE (DMF)  
 $E_{1/2}(*PC/PC^-) = -1.31$  V vs SCE (DMF)

**Figure 2.**

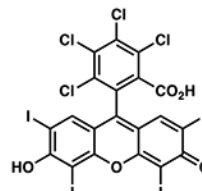
Transition-Metal-Based Photocatalysts and Their Associated Photochemical and Electrochemical Data (All potentials are measured in acetonitrile unless otherwise noted.).

<sup>a</sup>See ref 18.<sup>18</sup> <sup>b</sup>See ref 19.<sup>19</sup> <sup>c</sup>See ref 14.<sup>14</sup> <sup>d</sup>See ref 15.<sup>15</sup> <sup>e</sup>See ref 16.<sup>16</sup> <sup>f</sup>See ref 20.<sup>20</sup> <sup>g</sup>See ref 21.<sup>21</sup>

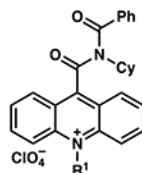
## (A) Organic photosensitizers

**eosin Y<sup>a</sup>**

$E_{1/2}(*PC/PC^-) = +0.83$  V vs SCE  
 $E_{1/2}(PC/PC^-) = -1.08$  V vs SCE  
 $E_{1/2}(PC^+/^*PC) = -1.15$  V vs SCE  
 $E_{1/2}(PC^+/PC) = +1.23$  V vs SCE

**rose bengal<sup>a</sup>**

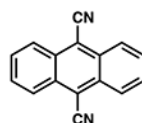
$E_{1/2}(*PC/PC^-) = +0.81$  V vs SCE  
 $E_{1/2}(PC/PC^-) = -0.99$  V vs SCE  
 $E_{1/2}(PC^+/^*PC) = -0.96$  V vs SCE  
 $E_{1/2}(PC^+/PC) = +0.84$  V vs SCE

**[Imi-PhAc]ClO<sub>4</sub><sup>b</sup>****R<sup>1</sup> = Ph**

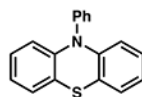
$E_{1/2}(*PC/PC^-) = +2.36$  V vs SCE  
 $E_{1/2}(PC/PC^-) = -0.33$  V vs SCE

**[Imi-MeAc]ClO<sub>4</sub><sup>b</sup>****R<sup>1</sup> = Me**

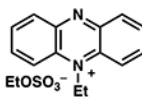
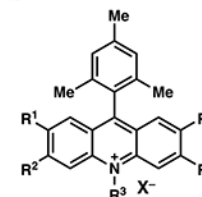
$E_{1/2}(*PC/PC^-) = +2.40$  V vs SCE  
 $E_{1/2}(PC/PC^-) = -0.28$  V vs SCE

**DCA, 9,10-dicyanoanthracene<sup>c</sup>**

$E_{1/2}(*PC/PC^-) = +1.99$  V vs SCE  
 $E_{1/2}(PC/PC^-) = -0.91$  V vs SCE

**Ph-PTZ, 10-phenylphenothiazine<sup>d</sup>**

$E_{1/2}(PC^+/^*PC) = -2.10$  V vs SCE  
 $E_{1/2}(PC^+/PC) = +0.68$  V vs SCE

**phenazinium photocatalyst<sup>e</sup>****[Mes-Acr]BF<sub>4</sub><sup>f,g</sup>****R<sup>1</sup>, R<sup>2</sup> = H, R<sup>3</sup> = Me, X = BF<sub>4</sub>****[Mes-Acr]ClO<sub>4</sub><sup>f,g</sup>****R<sup>1</sup>, R<sup>2</sup> = H, R<sup>3</sup> = Me, X = ClO<sub>4</sub>**

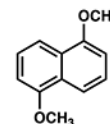
$E_{1/2}(*PC/PC^-) = +2.08$  V vs SCE  
 $E_{1/2}(PC/PC^-) = -0.57$  V vs SCE

**[2,7-dMe-Mes-PhAc]BF<sub>4</sub><sup>h</sup>****R<sup>1</sup> = Me, R<sup>2</sup> = H, R<sup>3</sup> = Ph, X = BF<sub>4</sub>**

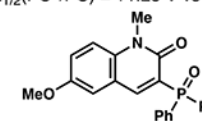
$E_{1/2}(*PC/PC^-) = +2.09$  V vs SCE  
 $E_{1/2}(PC/PC^-) = -0.58$  V vs SCE

**[(<sup>t</sup>Bu)<sub>2</sub>Mes-PhAc]BF<sub>4</sub><sup>h</sup>****R<sup>1</sup> = H, R<sup>2</sup> = <sup>t</sup>Bu, R<sup>3</sup> = Ph, X = BF<sub>4</sub>**

$E_{1/2}(*PC/PC^-) = +2.15$  V vs SCE  
 $E_{1/2}(PC/PC^-) = -0.52$  V vs SCE

**1,5-DMN<sup>i,j</sup>**

$E_{1/2}(PC^+/^*PC) = -2.50$  V vs SCE  
 $E_{1/2}(PC^+/PC) = +1.28$  V vs SCE

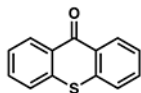
**3-phosphonate quinolinone<sup>k</sup>**

$E_{p/2}(PC^+/^*PC) = -1.29$  V vs SCE  
 $E_{p/2}(PC^+/PC) = +1.63$  V vs SCE

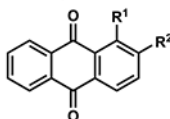
**Figure 3.**

Organic Photocatalysts and Their Associated Photochemical and Electrochemical Data (All potentials are measured in acetonitrile). <sup>a</sup>See ref 22.<sup>22</sup> <sup>b</sup>See ref 23.<sup>23</sup> <sup>c</sup>See ref 24.<sup>24</sup> <sup>d</sup>See ref 25.<sup>25</sup> <sup>e</sup>See ref 26.<sup>26</sup> <sup>f</sup>See ref 27.<sup>27</sup> <sup>g</sup>See ref 28.<sup>28</sup> <sup>h</sup>See ref 29.<sup>29</sup> <sup>i</sup>See ref 30.<sup>30</sup> <sup>j</sup>See ref 31.<sup>31</sup> <sup>k</sup>See ref 32.<sup>32</sup>

## (A) Organic photosensitizers

**thioxanthone<sup>a</sup>**

$E_{1/2}(*PC/PC^-) = +1.18$  V vs SCE  
 $E_{1/2}(PC/PC^-) = -1.65$  V vs SCE  
 $E_{1/2}(PC^+/PC) = -1.11$  V vs SCE  
 $E_{1/2}(PC^+/PC) = +1.69$  V vs SCE

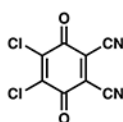
**1-CI-AQN<sup>b</sup>**

$R^1 = Cl, R^2 = H$

$E_{1/2}(*PC/PC^-) = +2.30$  V vs SCE

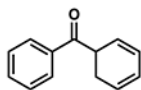
**2-CI-AQN**

$R^1 = H, R^2 = Cl$

**DDQ<sup>c,d</sup>**

$E_{1/2}(*PC/PC^-) = +3.18$  V vs SCE

$E_{1/2}(PC/PC^-) = +0.49$  V vs SCE

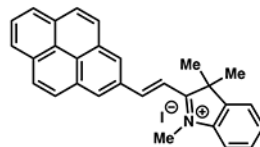
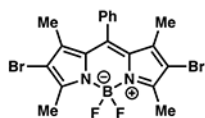
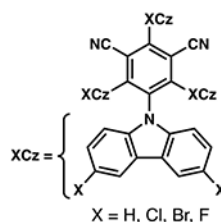
**benzophenone<sup>a</sup>**

$E_{1/2}(*PC/PC^-) = +1.28$  V vs SCE

$E_{1/2}(PC/PC^-) = -1.72$  V vs SCE

$E_{1/2}(PC^+/PC) = -0.61$  V vs SCE

$E_{1/2}(PC^+/PC) = +2.39$  V vs SCE

**hemicyanine photocatalyst<sup>e</sup>****BODIPY photocatalyst<sup>f</sup>****4-CziIPN<sup>g</sup>**

$X = H$

$E_{1/2}(*PC/PC^-) = +1.35$  V vs SCE

$E_{1/2}(PC/PC^-) = -1.21$  V vs SCE

$E_{1/2}(PC^+/PC) = -1.04$  V vs SCE

$E_{1/2}(PC^+/PC) = +1.52$  V vs SCE

**4-CICziIPN<sup>h</sup>**

$X = Cl$

$E_{1/2}(*PC/PC^-) = +1.49$  V vs SCE (DCM)

$E_{1/2}(PC/PC^-) = -1.10$  V vs SCE (DCM)

$E_{1/2}(PC^+/PC) = -0.72$  V vs SCE (DCM)

$E_{1/2}(PC^+/PC) = +1.87$  V vs SCE (DCM)

**4-BrCziIPN<sup>h</sup>**

$X = Br$

$E_{1/2}(*PC/PC^-) = +1.73$  V vs SCE (DCM)

$E_{1/2}(PC/PC^-) = -0.85$  V vs SCE (DCM)

$E_{1/2}(PC^+/PC) = -0.60$  V vs SCE (DCM)

$E_{1/2}(PC^+/PC) = +1.98$  V vs SCE (DCM)

**4-FCziIPN<sup>h</sup>**

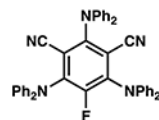
$X = F$

$E_{1/2}(*PC/PC^-) = +1.42$  V vs SCE (DCM)

$E_{1/2}(PC/PC^-) = -1.18$  V vs SCE (DCM)

$E_{1/2}(PC^+/PC) = -0.81$  V vs SCE (DCM)

$E_{1/2}(PC^+/PC) = +1.79$  V vs SCE (DCM)

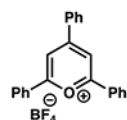
**3DPAFIPN<sup>i</sup>**

$E_{1/2}(*PC/PC^-) = +1.09$  V vs SCE

$E_{1/2}(PC/PC^-) = -1.59$  V vs SCE

$E_{1/2}(PC^+/PC) = -1.38$  V vs SCE

$E_{1/2}(PC^+/PC) = +1.31$  V vs SCE

**2,4,6-triphenylpyrylium<sup>j,k</sup>**

$E_{1/2}(*PC/PC^-) = +2.02$  V vs SCE

$E_{1/2}(PC/PC^-) = -0.32$  V vs SCE

**Figure 4.**

Organic Photocatalysts and Their Associated Photochemical and Electrochemical Data (All potentials are measured in acetonitrile unless otherwise noted.). <sup>a</sup>See ref 33. <sup>b</sup>See ref 34. <sup>c</sup>See ref 35. <sup>d</sup>See ref 36. <sup>e</sup>See ref 37. <sup>f</sup>See ref 38. <sup>g</sup>See ref 39. <sup>h</sup>See ref 40. <sup>i</sup>See ref 41. <sup>j</sup>See ref 24. <sup>k</sup>See ref 42.

## Examples of pro-aromatic, N-radical precursors

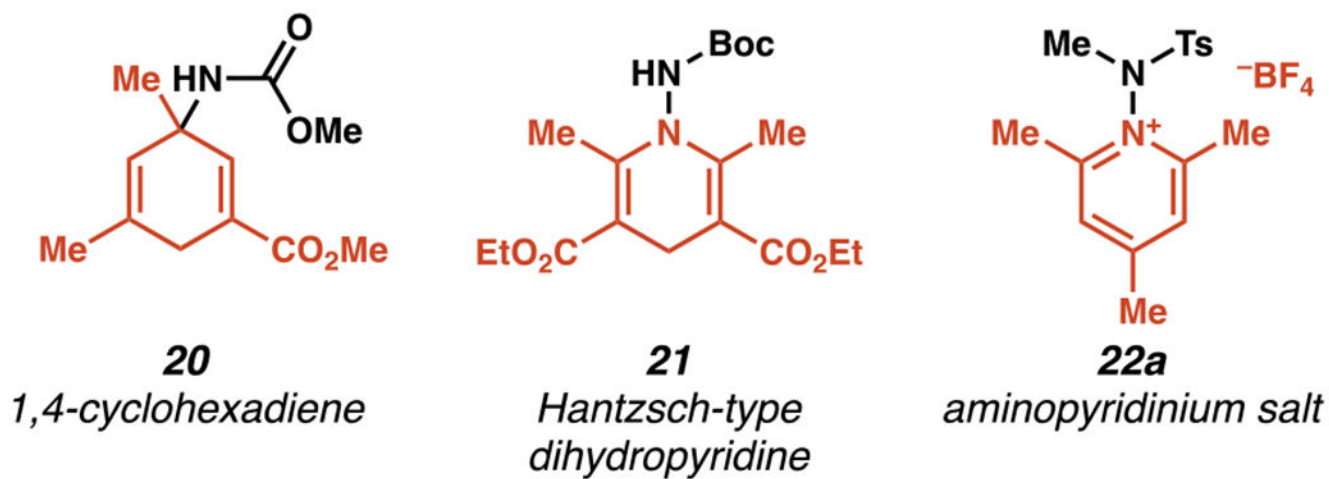
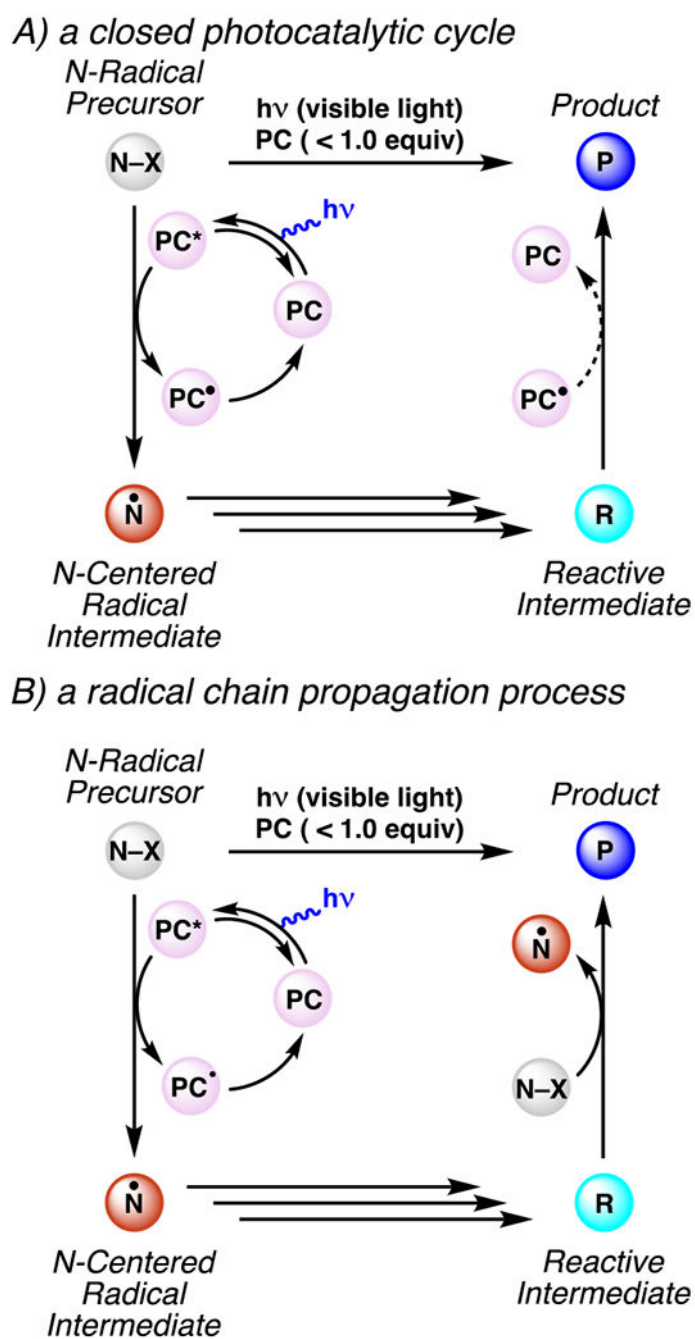
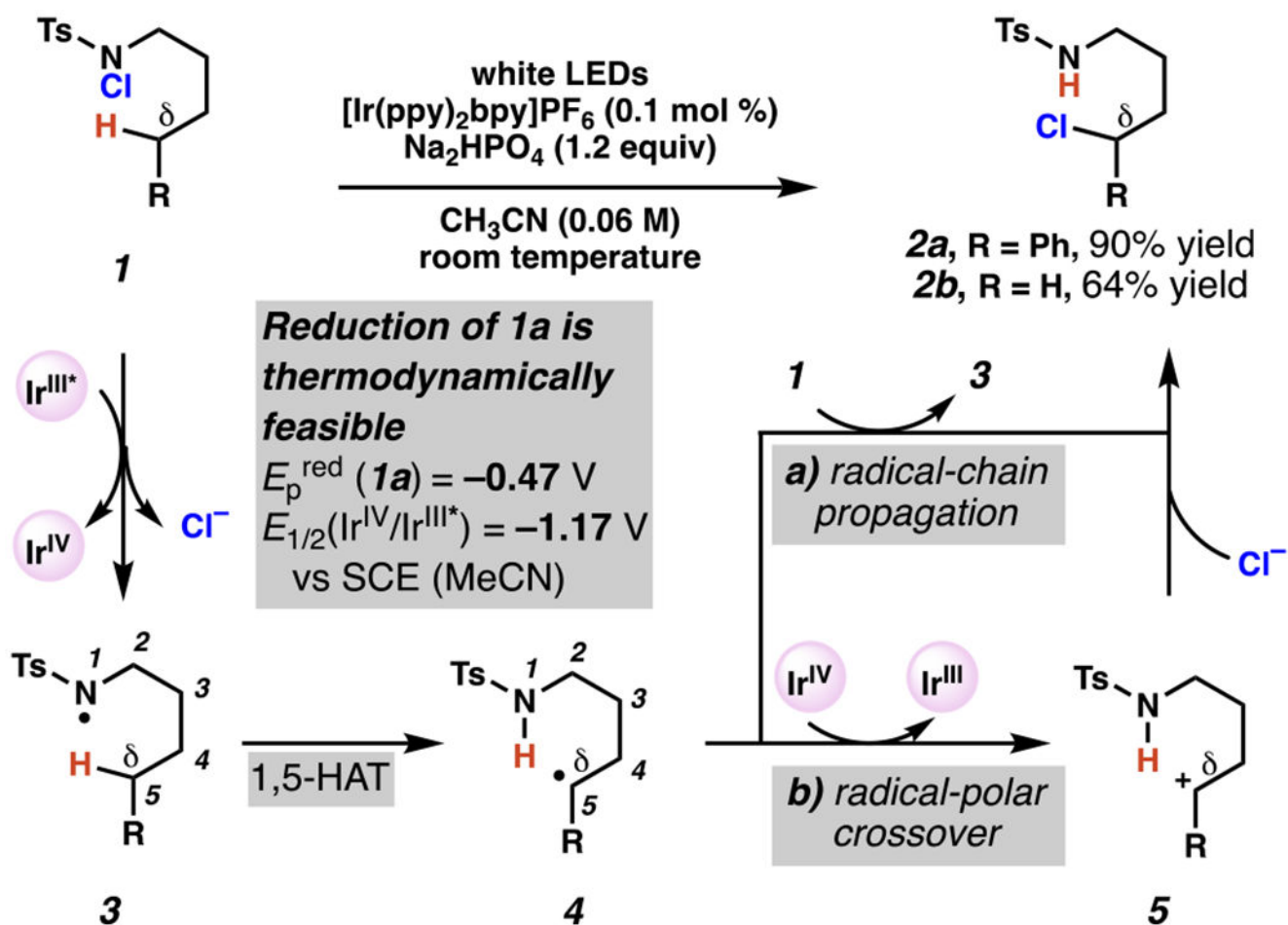


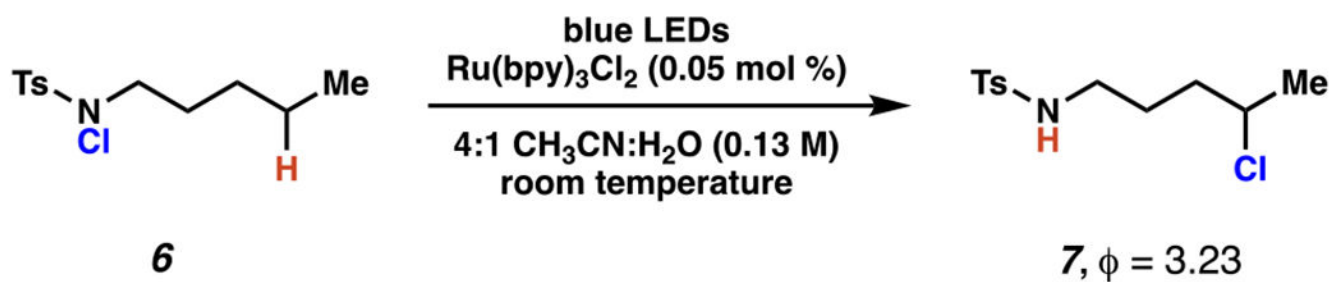
**Figure 5.** Nitrogen-Centered Radicals Derived from Pro-aromatic Compounds Inspired a Photo-mediated Strategy to Access Nitrogen-Centered Radicals Based on Nitrogen–Nitrogen Bond Cleavage



**Scheme 1.**  
Comparison of Mechanisms That Proceed by Radical Chain Propagation Versus Closed Reaction Cycle

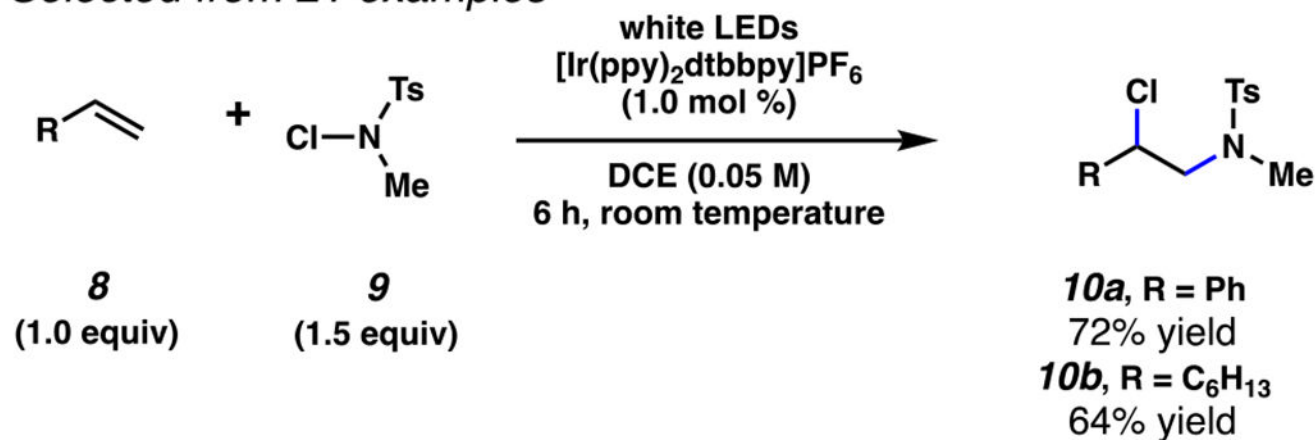


Scheme 2.  
 N-Chlorosulfonamides Undergo C(sp<sup>3</sup>)-H Chlorination in the Presence of Photoredox Catalysts

**Scheme 3.**

W. Yu and Co-workers' Quantum Yield Calculation Supports a Radical Chain Propagation Mechanism in Sulfonamide-Guided Chlorination Reactions

*Selected from 21 examples*



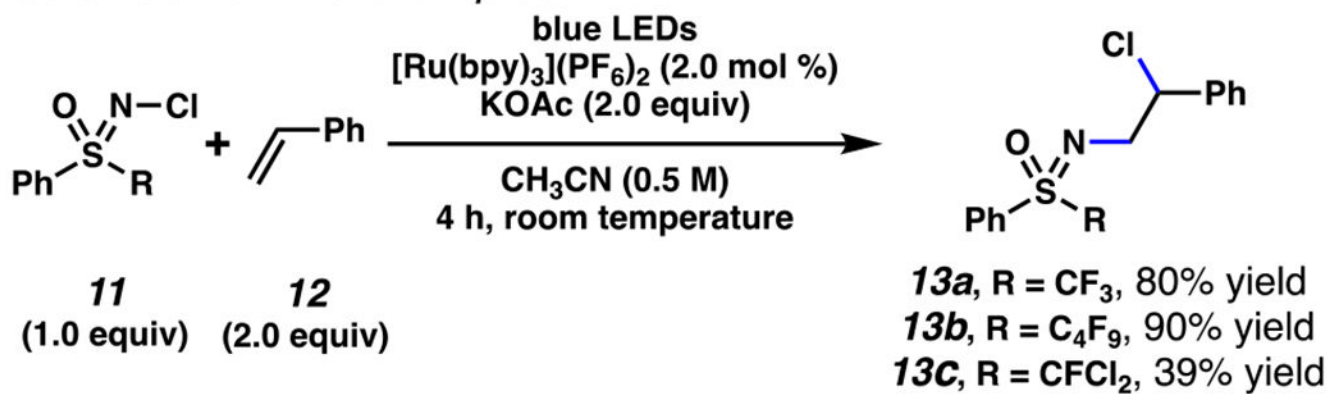
no reaction was observed in the absence of a photocatalyst

**Scheme 4.**

S. Yu and Co-workers Protocol to Access Chlorosulfonamidation of Olefins with *N*-Chlorosulfonamides by Photoredox Catalysis



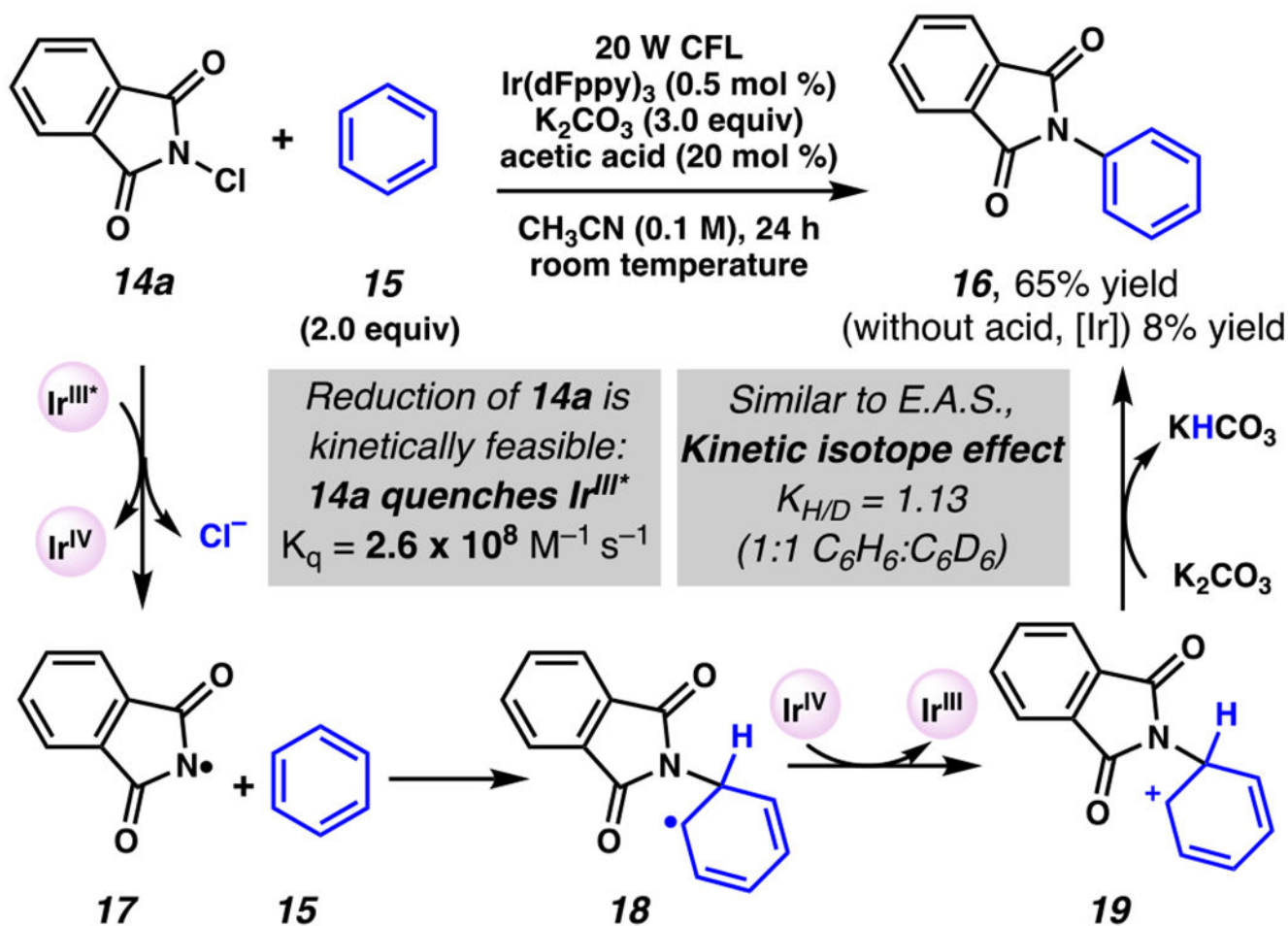
Selected from 20 examples



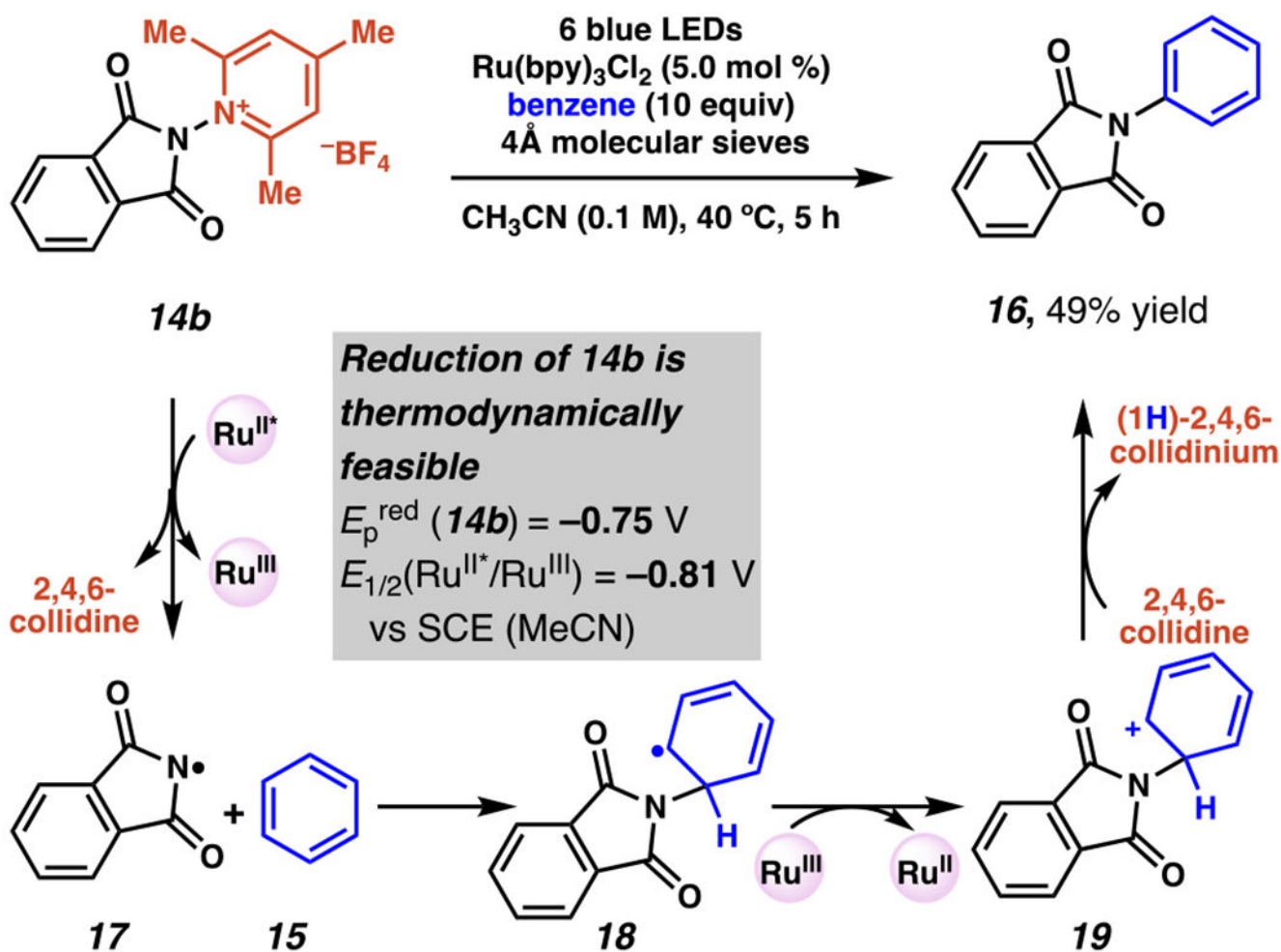
no reaction was observed in the absence of a photocatalyst

**Scheme 5.**

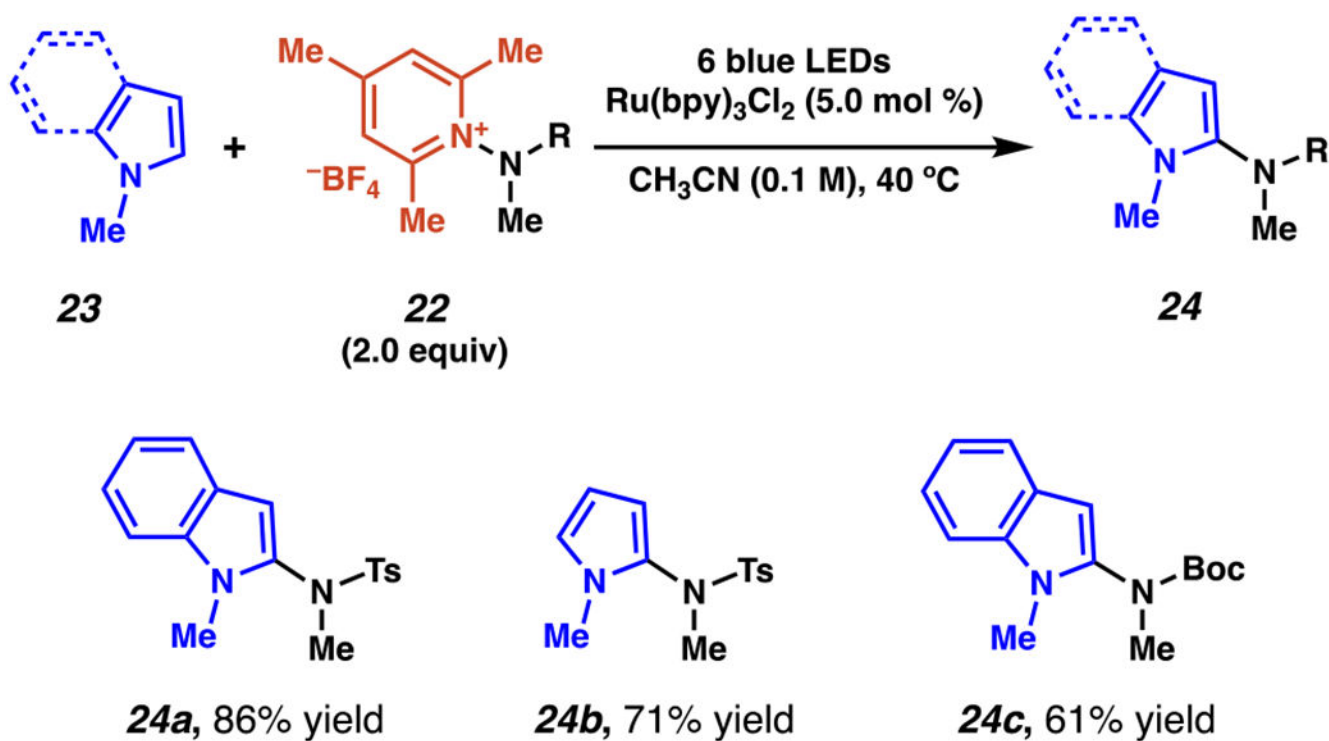
Photoredox-Catalysis Enables 1,2-Difunctionalization of Electron-Rich Olefins by *N*-Chlorosulfoximines Bearing *S*-Fluoroalkyl Substituents



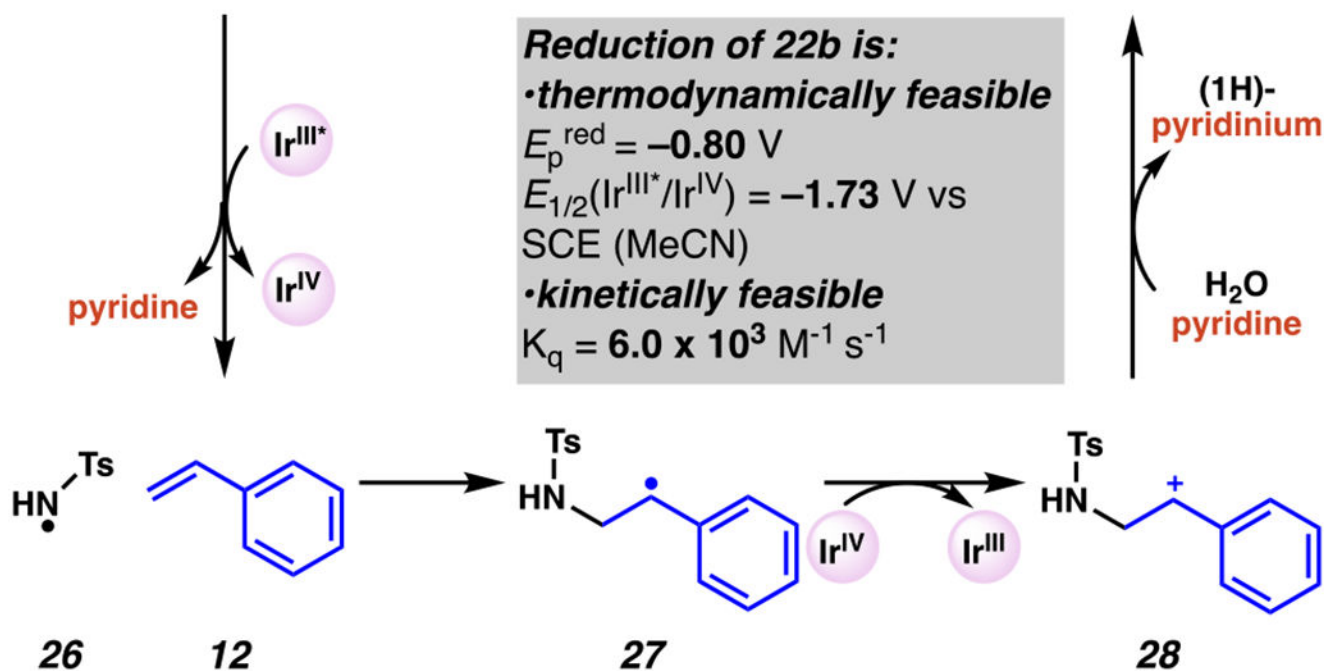
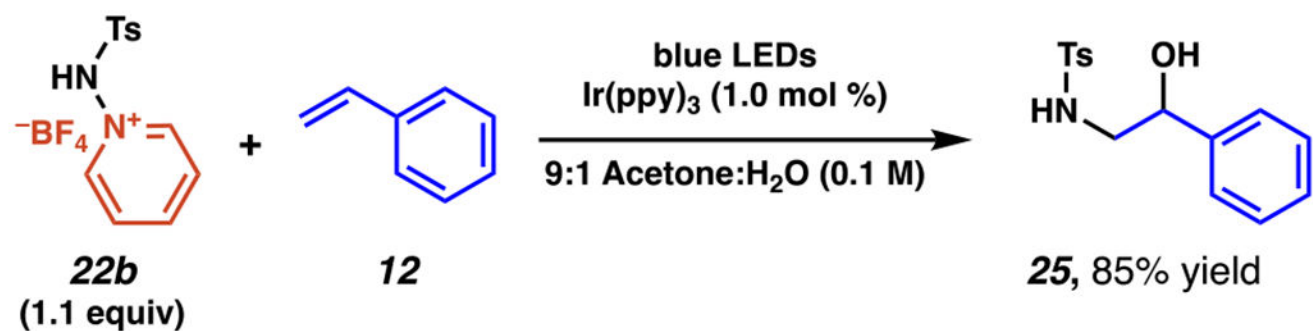
**Scheme 6.**  
 A Plausible Mechanism By Which Photoredox Catalysis Enables Efficient C–H Imidation of Arenes



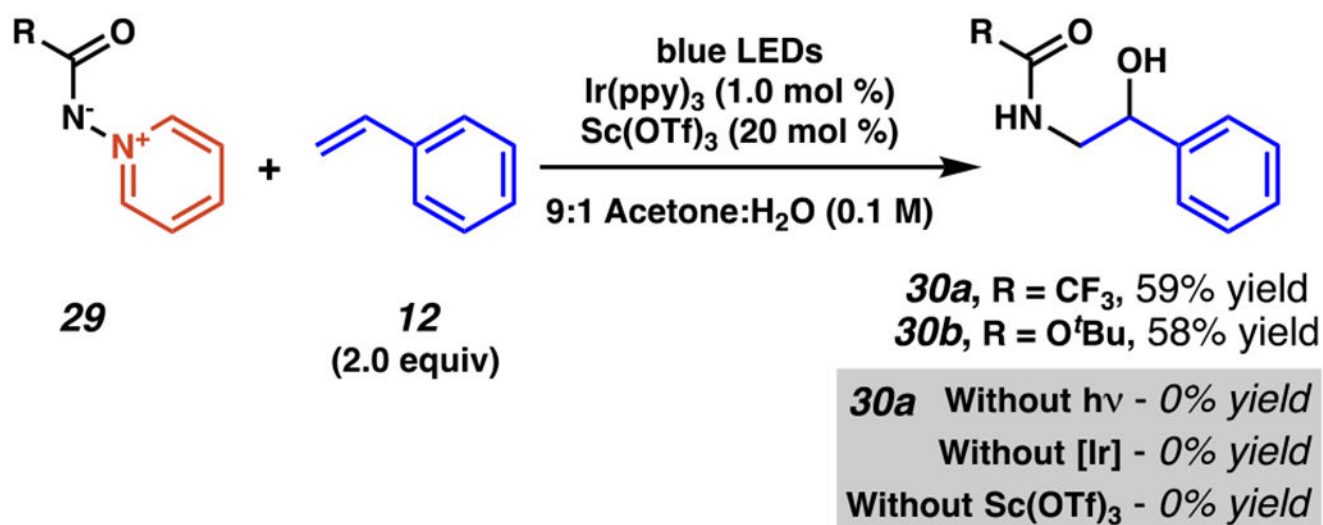
Scheme 7.  
 Light Enables Nitrogen-Centered Radical Generation from Pyridinium Salts in the Course of C–H Amination of Arenes



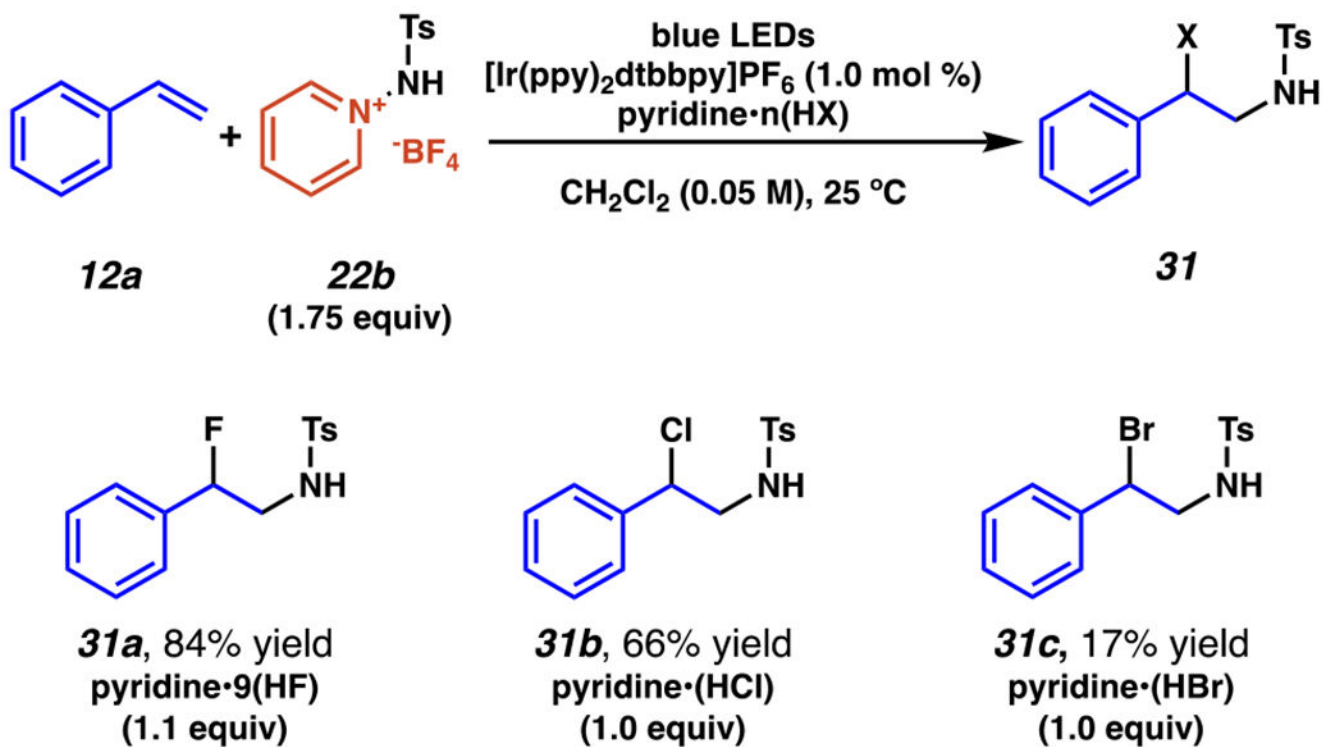
**Scheme 8.**  
Radical C(2)-Amidation of *N*-Methyl Indoles and Pyrroles Can Engage *N*-Aminopyridinium Salts as Nitrogen-Centered Radical Precursors



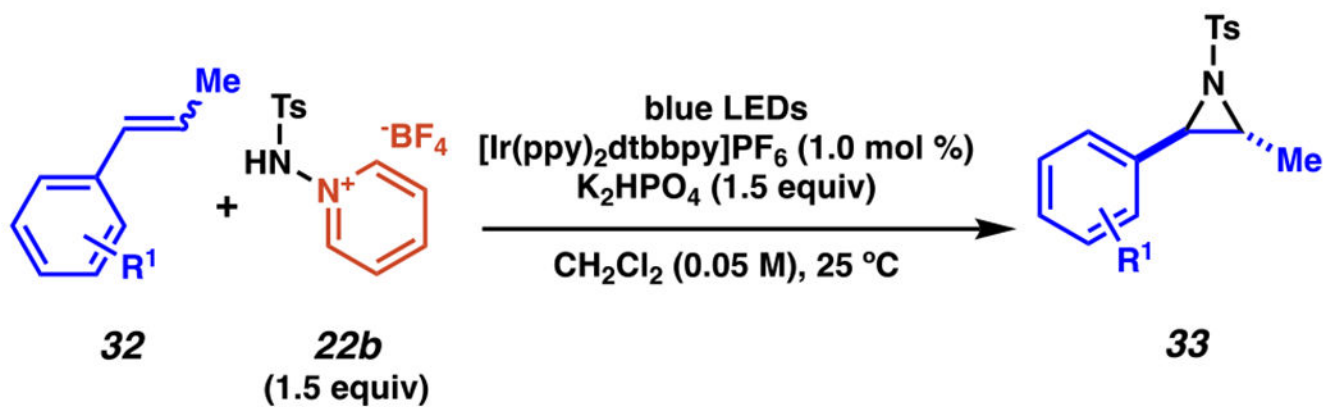
**Scheme 9.**  
 Sulfonamide-Based Aminopyridinium Salts Engage in Photoredox-Mediated Aminohydroxylation of Olefins

**Scheme 10.**

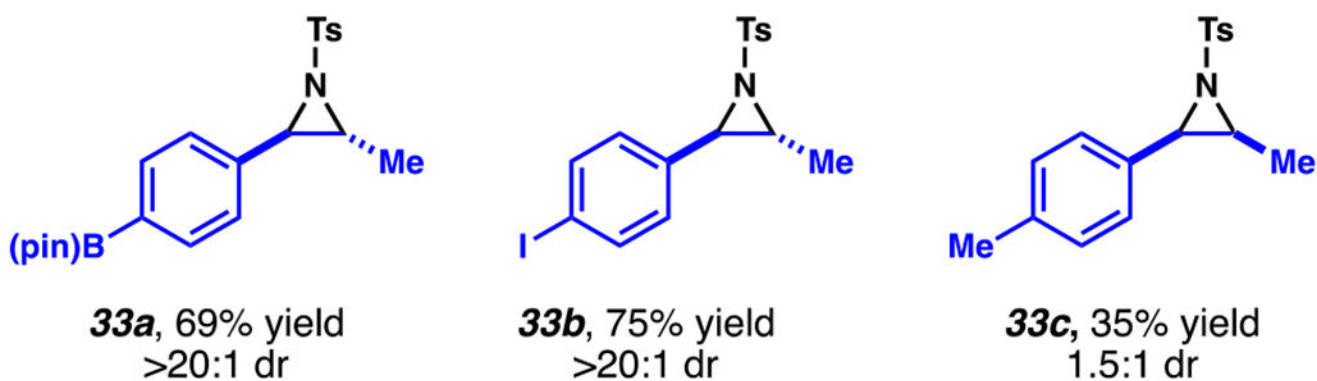
Amidopyridinium Salts Engage in Photo-driven Amidohydroxylation of Olefins



**Scheme 11.**  
Aminopyridinium Salt-Derived Sulfamyl Radicals Enable Regiospecific Aminohalogenation of Styrenes in the Presence of Pyridinium Halides

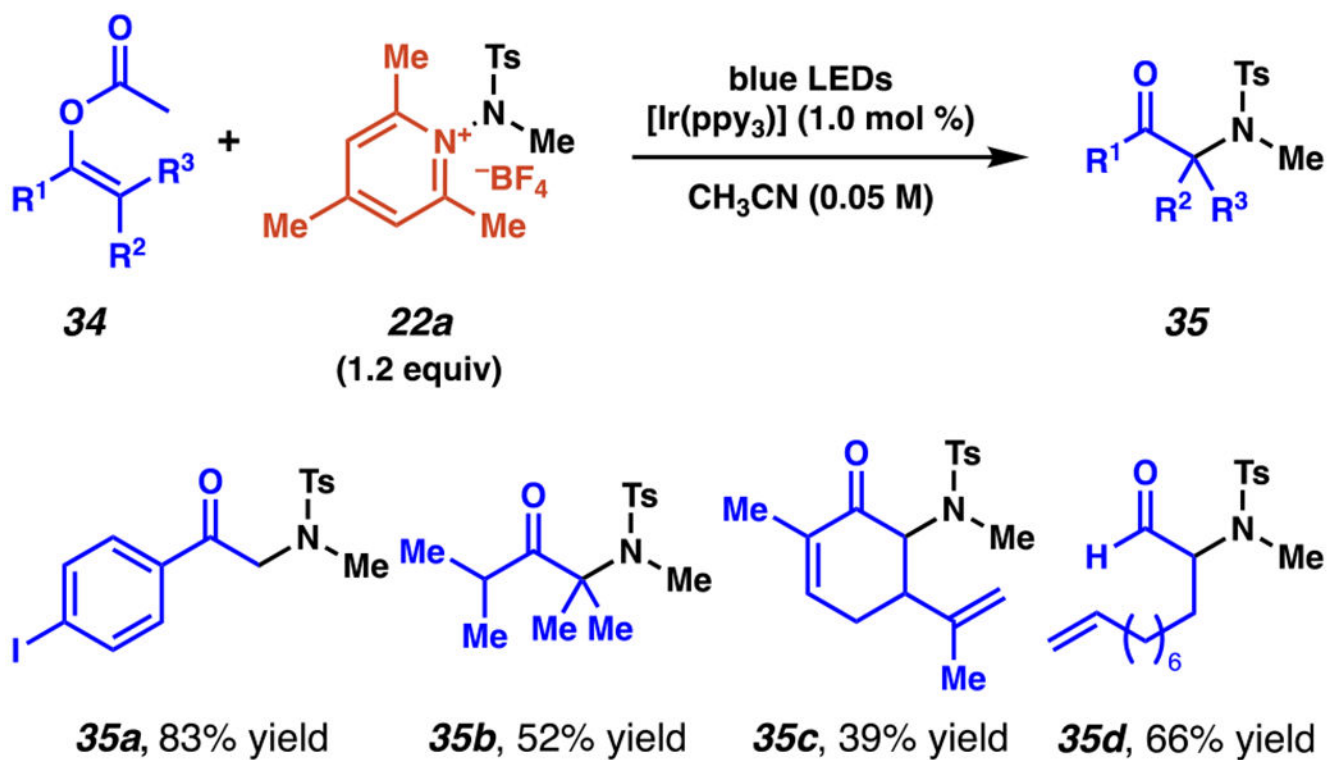


Selected from 34 Examples

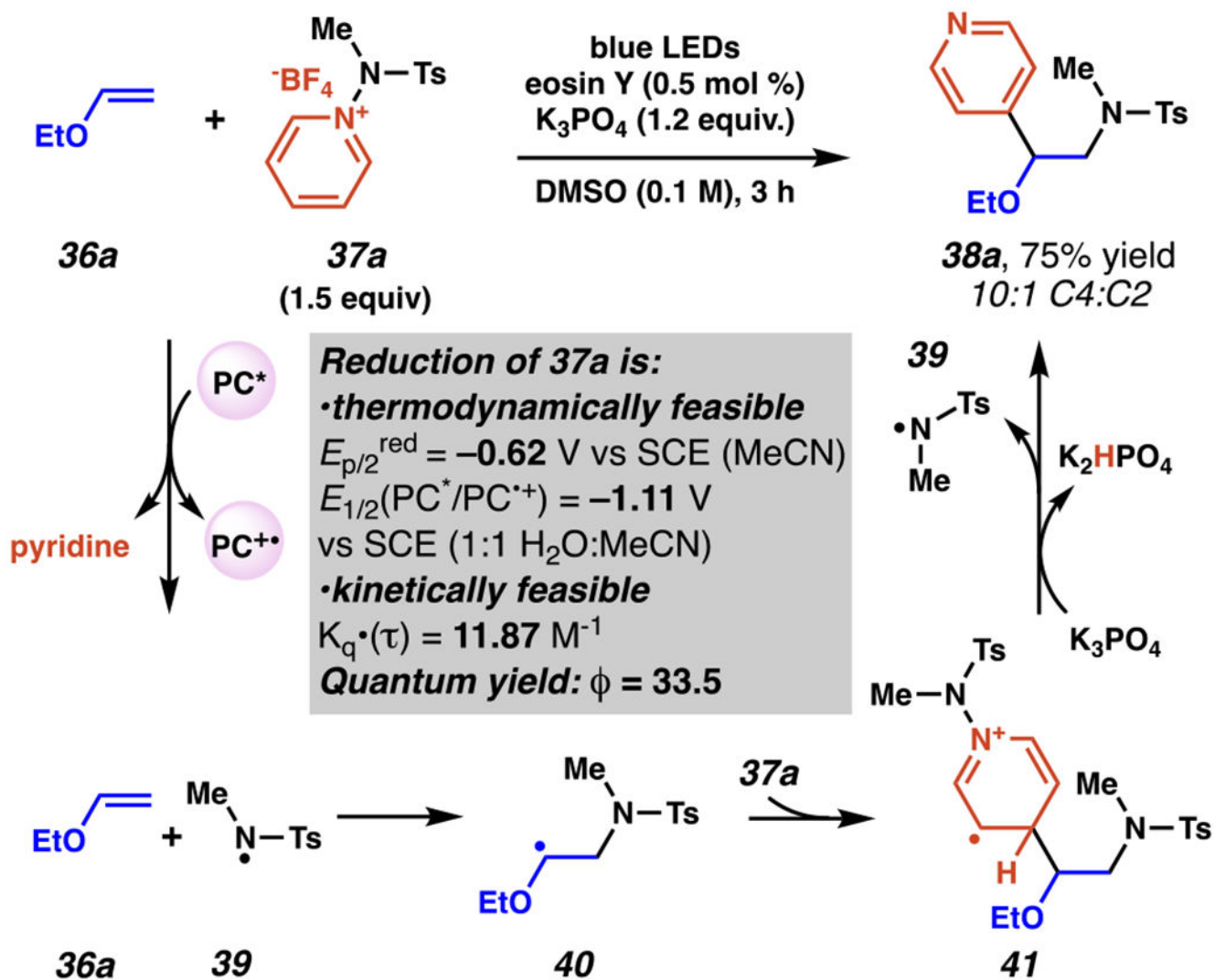


Scheme 12.  
 Sulfamyl Radicals Engage in Diastereoselective Aziridination of Substituted Styrenes

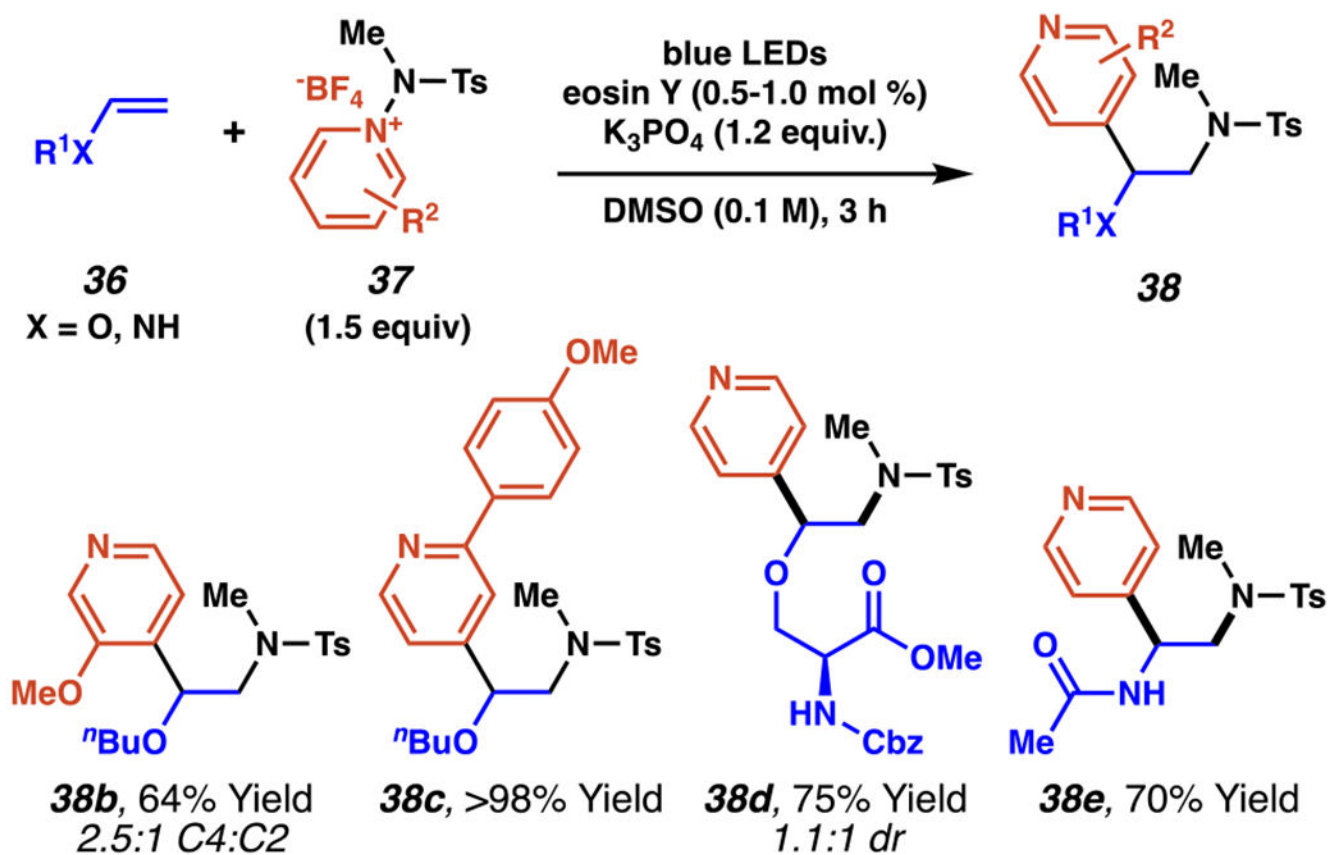




**Scheme 13.**  
Regioselective Amination of *O*-Protected Enolates Furnishes  $\alpha$ -Sulfamyl-Containing Carbonyl Compounds

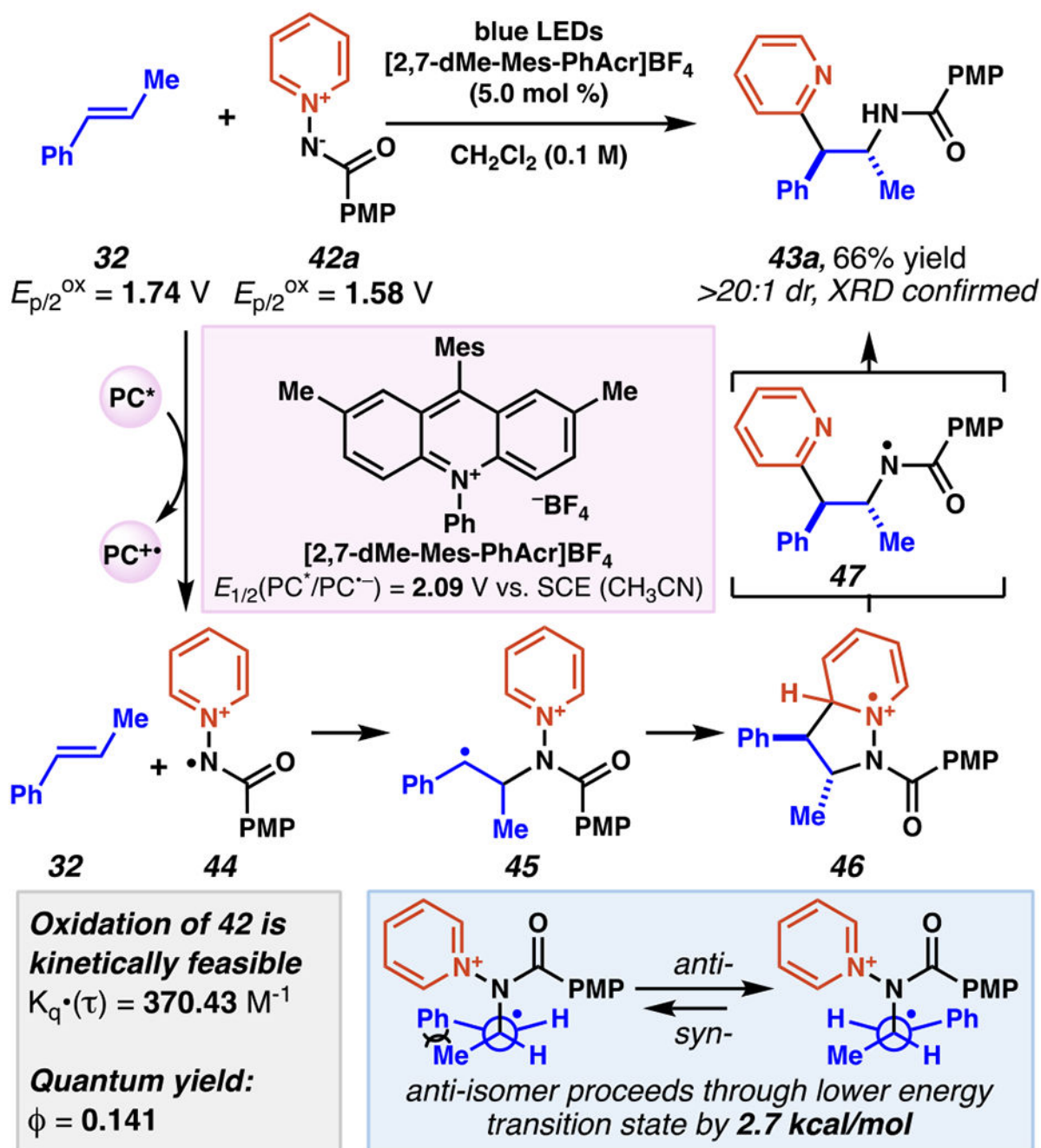


**Scheme 14.**  
 Aminopyridinium Salts Engage in Aminopyridylation of Vinyl Ethers with a Preference for Pyridyl C(4)-Selectivity Likely *via* Radical Chain Mechanism

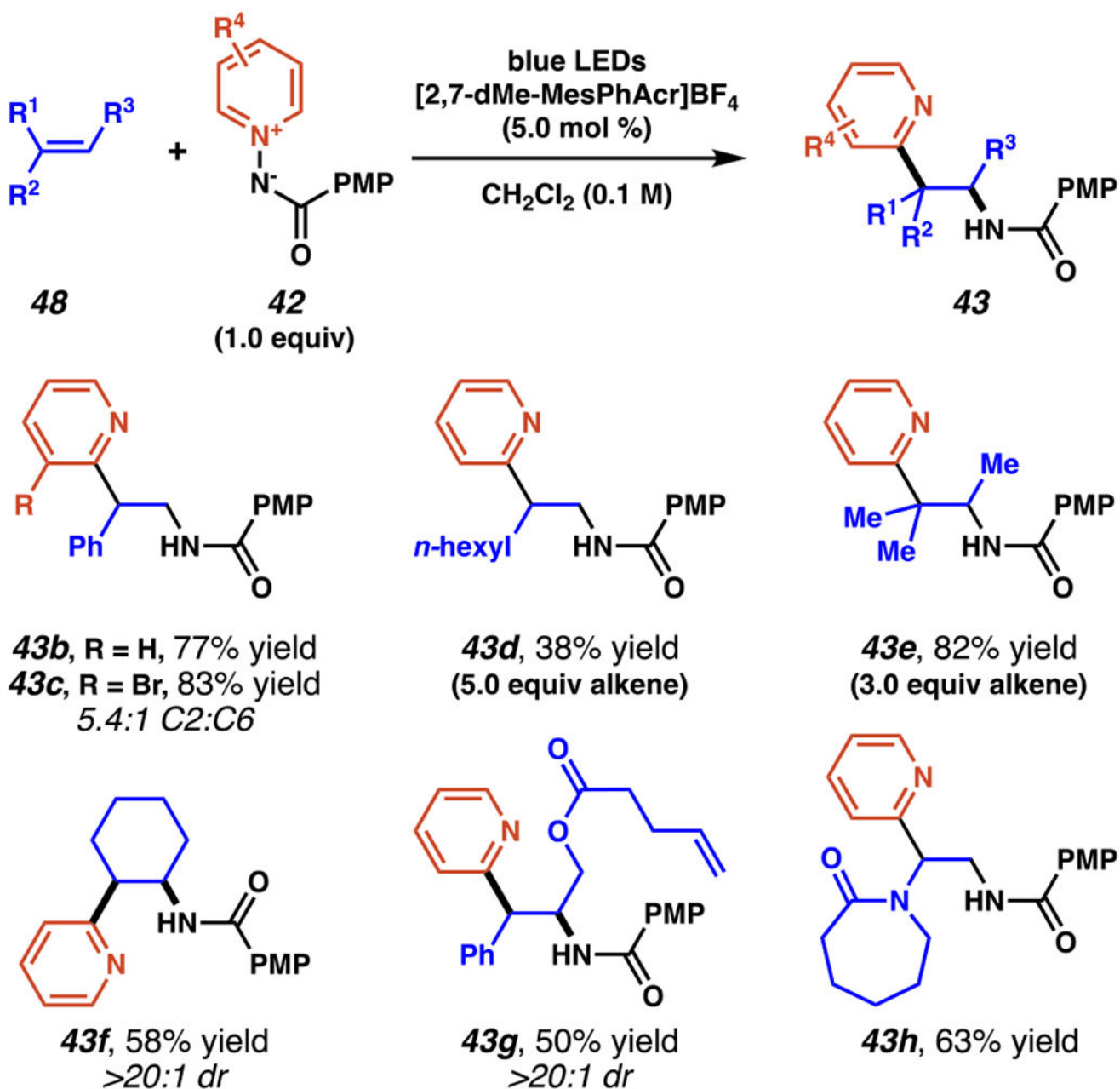


Scheme 15.

Vinyl Aminopyridylation Tolerates Variations in Vinyl and Pyridyl Substitution

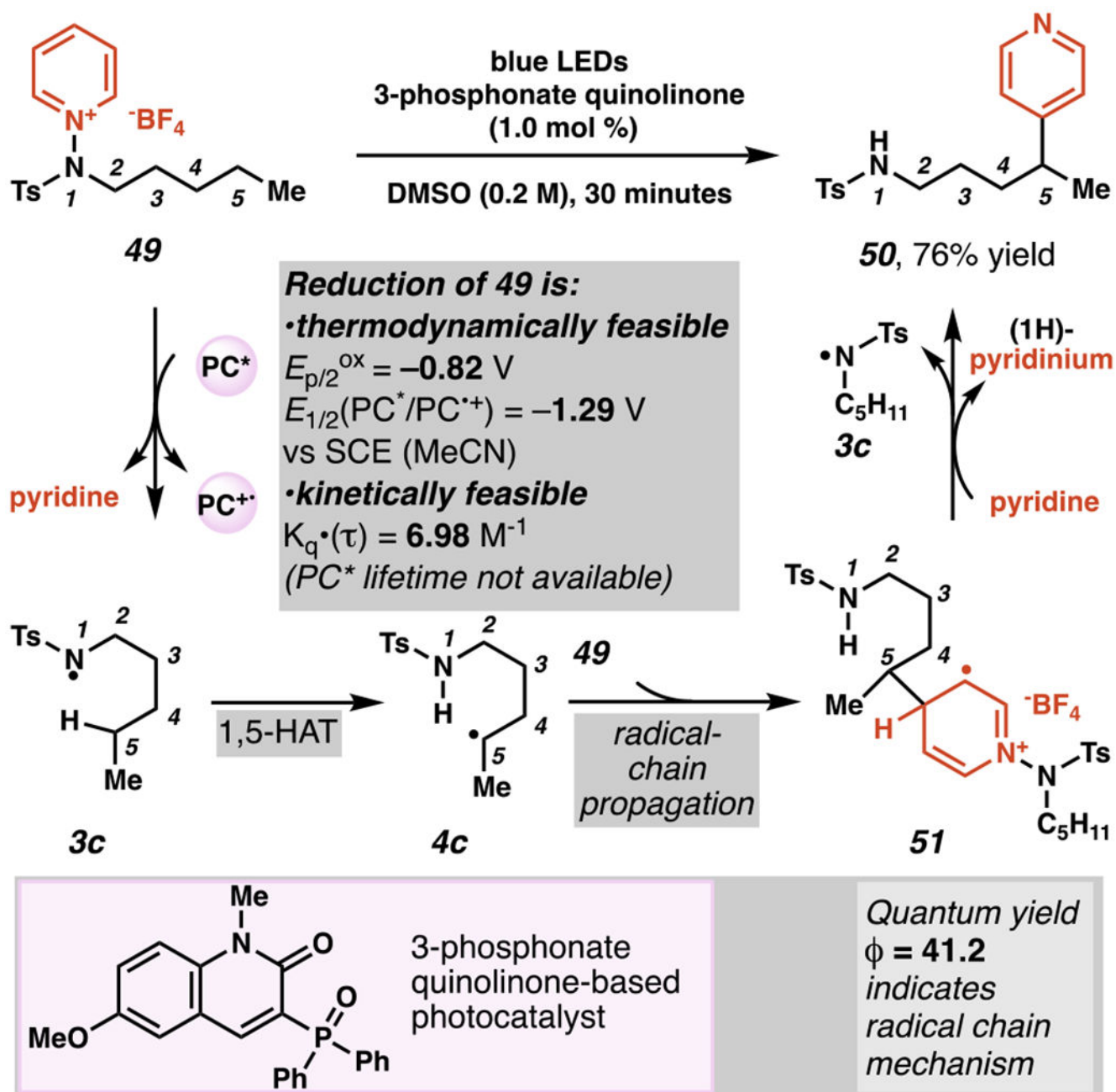


Scheme 16.  
 Aminopyridylation Proceeds Selectively at the Pyridyl-C(2) *via* Radical Formal 1,3-Dipolar Cycloaddition Process

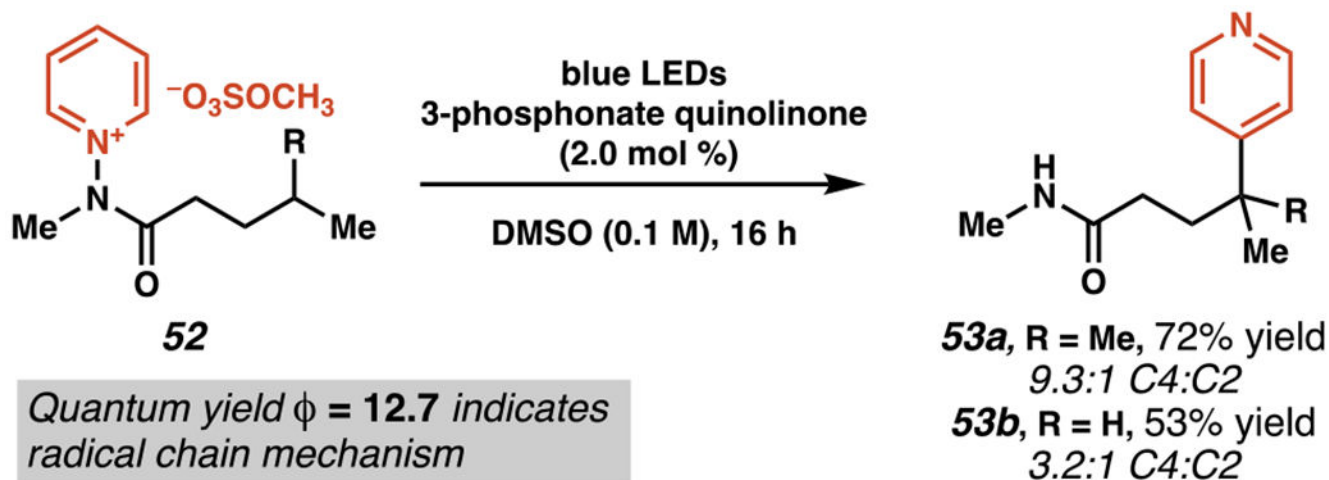


Scheme 17.

Amidopyridylation Products Are Readily Produced from Both Activated and Unactivated Alkenes

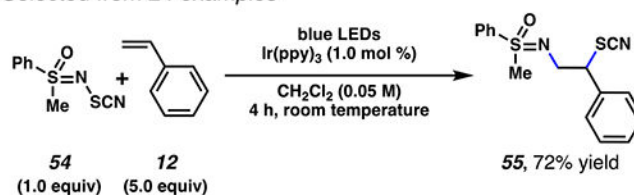


Scheme 18.  
Aminopyridinium Salts are Appropriate Substrates for Directed Pyridylation Reactions

**Scheme 19.**

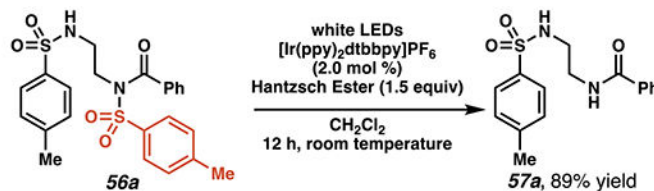
*N,N*-Dialkylamidopyridinium Salts Engage in 1,5-HAT-Mediated C–H Pyridylation

(A) 1,2-Difunctionalization Engages Sulfoximines and Thiocyanates  
Selected from 24 examples

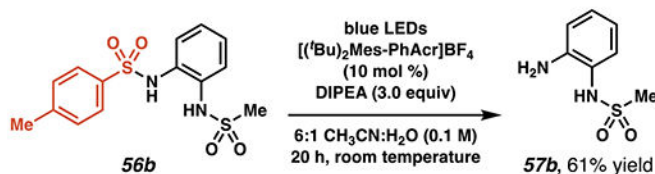


no reaction was observed in the absence of a photocatalyst

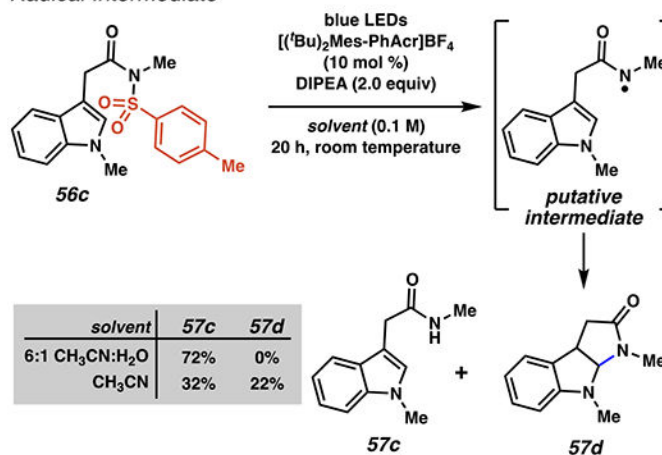
(B) Lu, Xiao, and co-workers (2013) Detosylate Tosyl Aryl Amides  
Selected from 20 examples



(C) Nicewicz and co-workers (2020) Detosylate Amines  
Selected from 38 examples



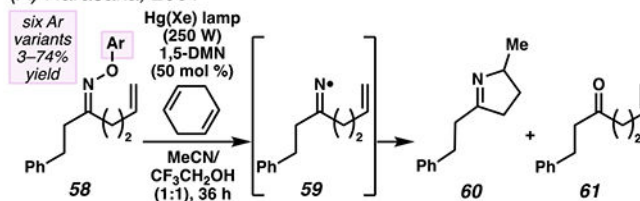
(D) Cyclization Product Suggestive of Putative N-Centered Radical Intermediate



**Scheme 20.**  
Photo-driven Nitrogen–Sulfur Bond Cleavage



## (A) Narasaka, 2001

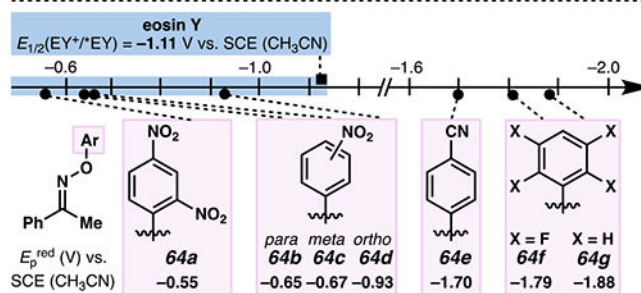
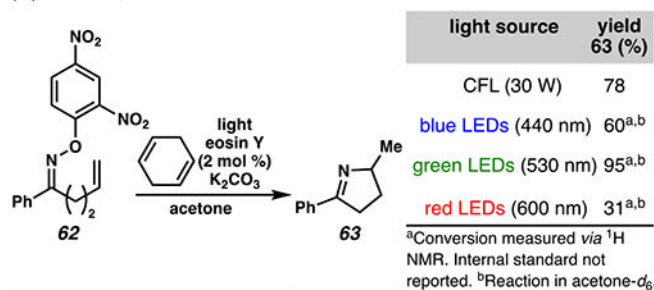


entry	-Ar	range (nm)	variation	yield 60 (%)	yield 61 (%)
1		300–2000 <sup>a</sup>	–	23	6
2		300–2000 <sup>a</sup>	no 1,5-DMN	23	38
3		320–2000 <sup>b</sup>	–	35	5
4		320–2000 <sup>b</sup>	–	70	9
5		320–2000 <sup>b</sup>	24 h, no CF <sub>3</sub> CH <sub>2</sub> OH	74	7
6		320–2000 <sup>b</sup>	500 W, no CF <sub>3</sub> CH <sub>2</sub> OH	75	6
7		320–2000 <sup>b</sup>	500 W, 1,5-DMN (15 mol %), no CF <sub>3</sub> CH <sub>2</sub> OH	75	7

<sup>a</sup>A Kenko UV-30 filter was employed to exclude light of lower wavelengths.

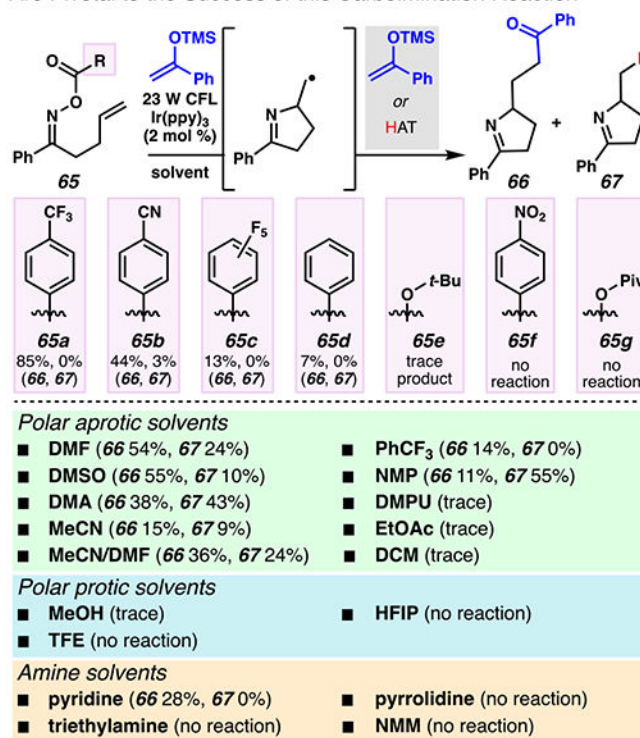
<sup>b</sup>A Kenko UV-32 filter was employed to exclude light of lower wavelengths.

## (B) Leonori, 2015

**Scheme 21.**

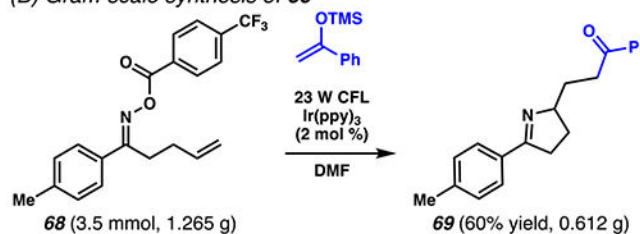
Photoredox Catalysis Transforms *O*-Aryl Oximes to Iminyl Radicals, Which Participate in 5-*exo*-trig-Hydroiminium Reactions to Afford Pyrrolines

(A) Electron-Deficient Acyl Handles and Polar Aprotic Solvents Are Pivotal to the Success of this Carboimination Reaction

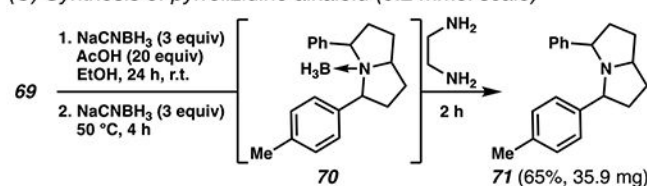


<sup>a</sup>The acyl group screening was performed in DMF as solvent. <sup>b</sup>The yields were calculated from <sup>1</sup>H NMR analysis with mesitylene as an internal standard.

(B) Gram-scale synthesis of **69**



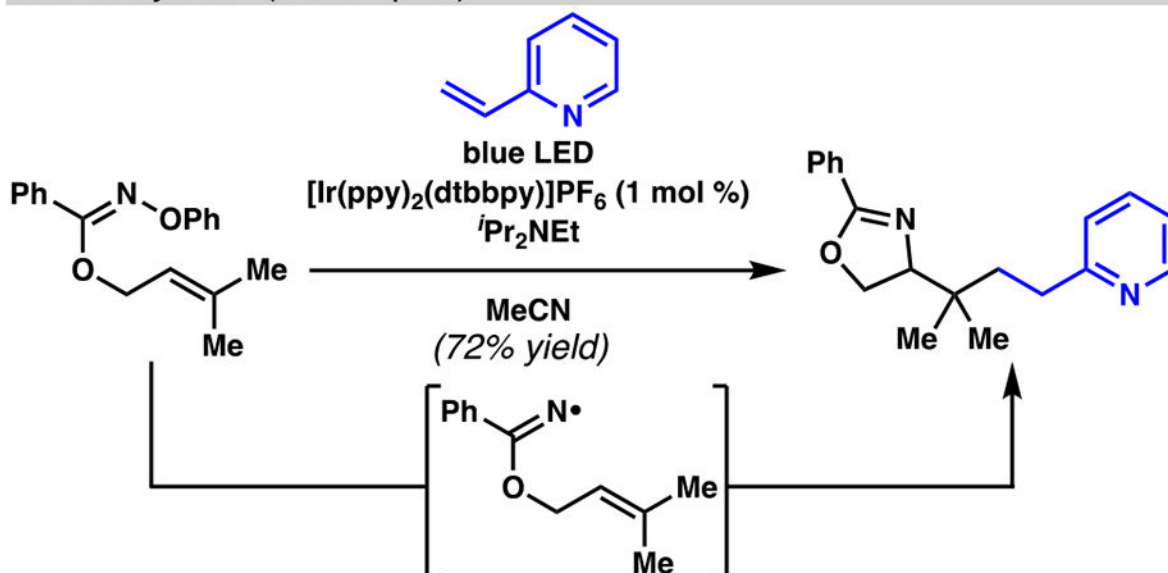
(C) Synthesis of pyrrolizidine alkaloid (0.2 mmol scale)



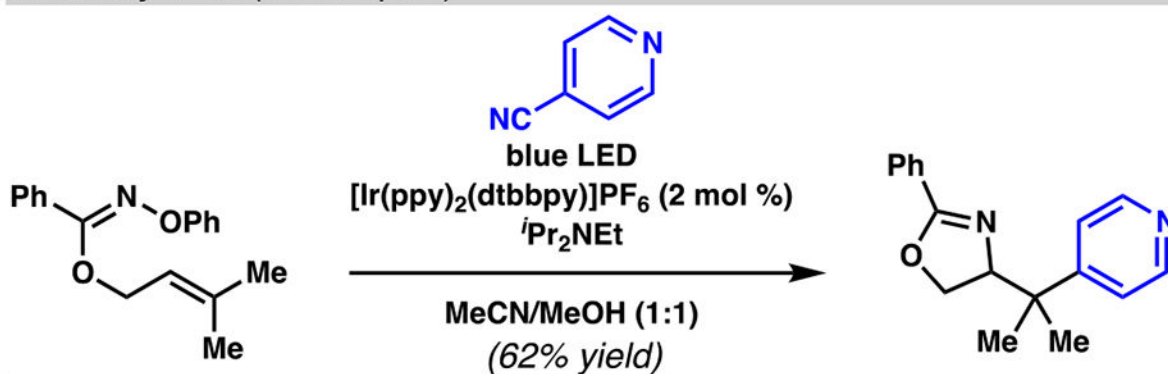
**Scheme 22.**

Effective Carboimination Reaction Relies on *O*-Acyl Oxime in Scalable Reaction That Provides Rapid Entry to Pyrrolizidine Alkaloid Derivative

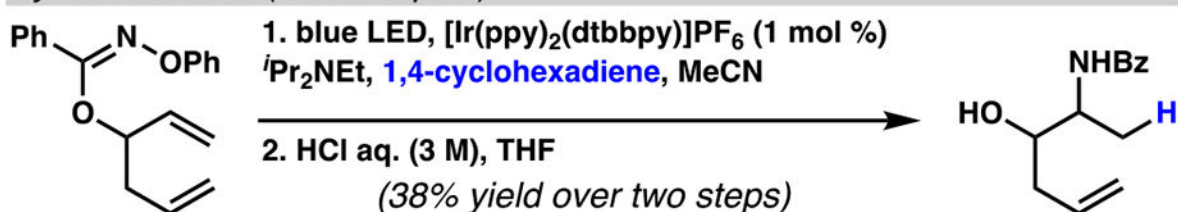
### Aminoalkylation (8 examples)



### Aminoarylation (4 examples)



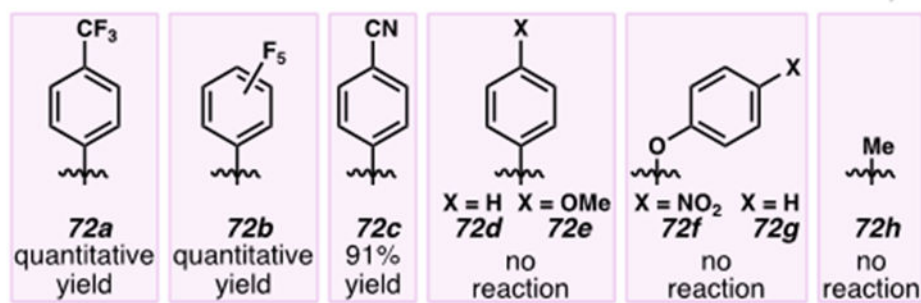
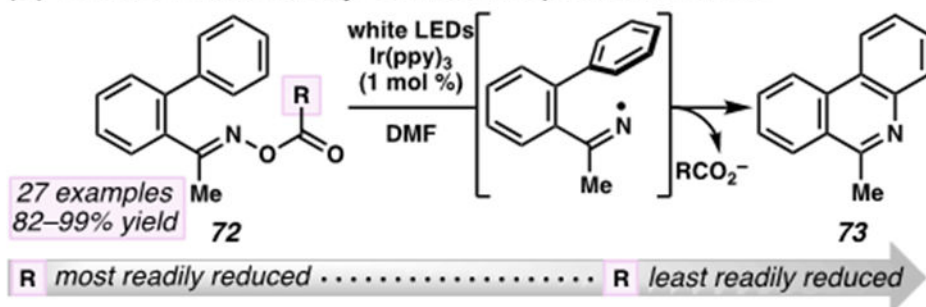
### Hydroamination (14 examples)



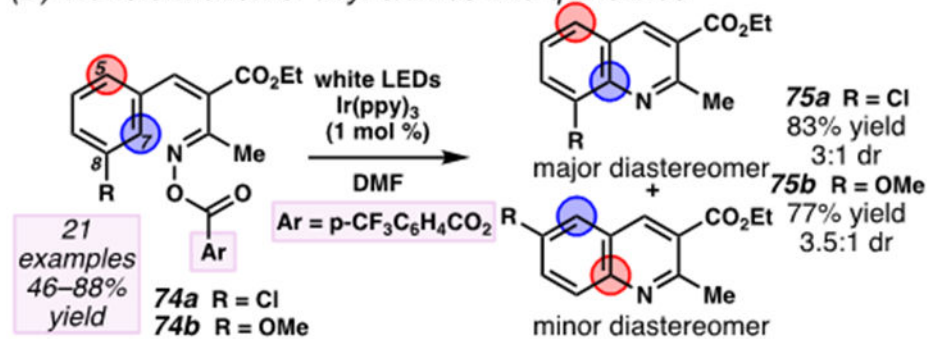
Scheme 23.

*O*-Aryl Oximes Can Serve as Imidate Radical Precursors Sequences to Access Masked 1,2-Aminoalcohols

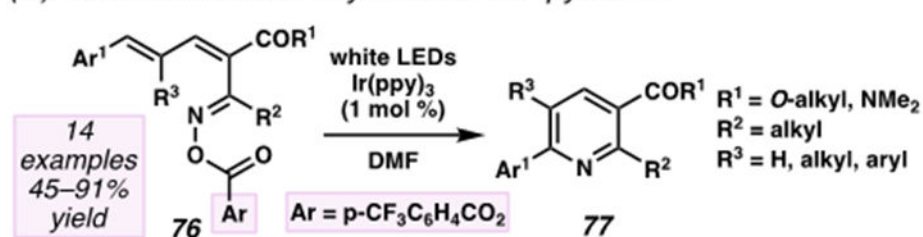
## (A) Transformation of acyl oximes into phenanthridines



## (B) Transformation of acyl oximes into quinolines

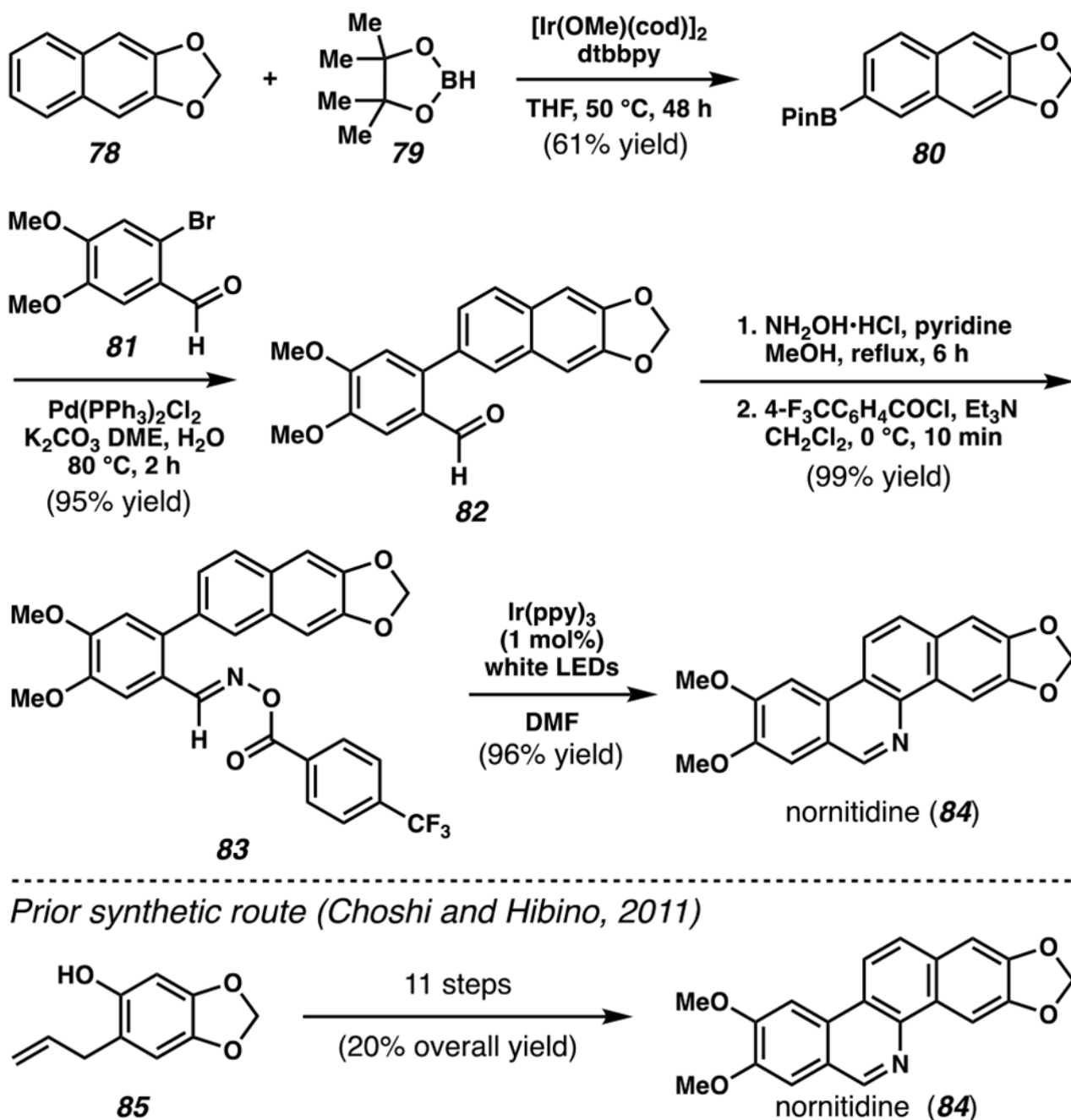


## (C) Transformation of acyl oximes into pyridines



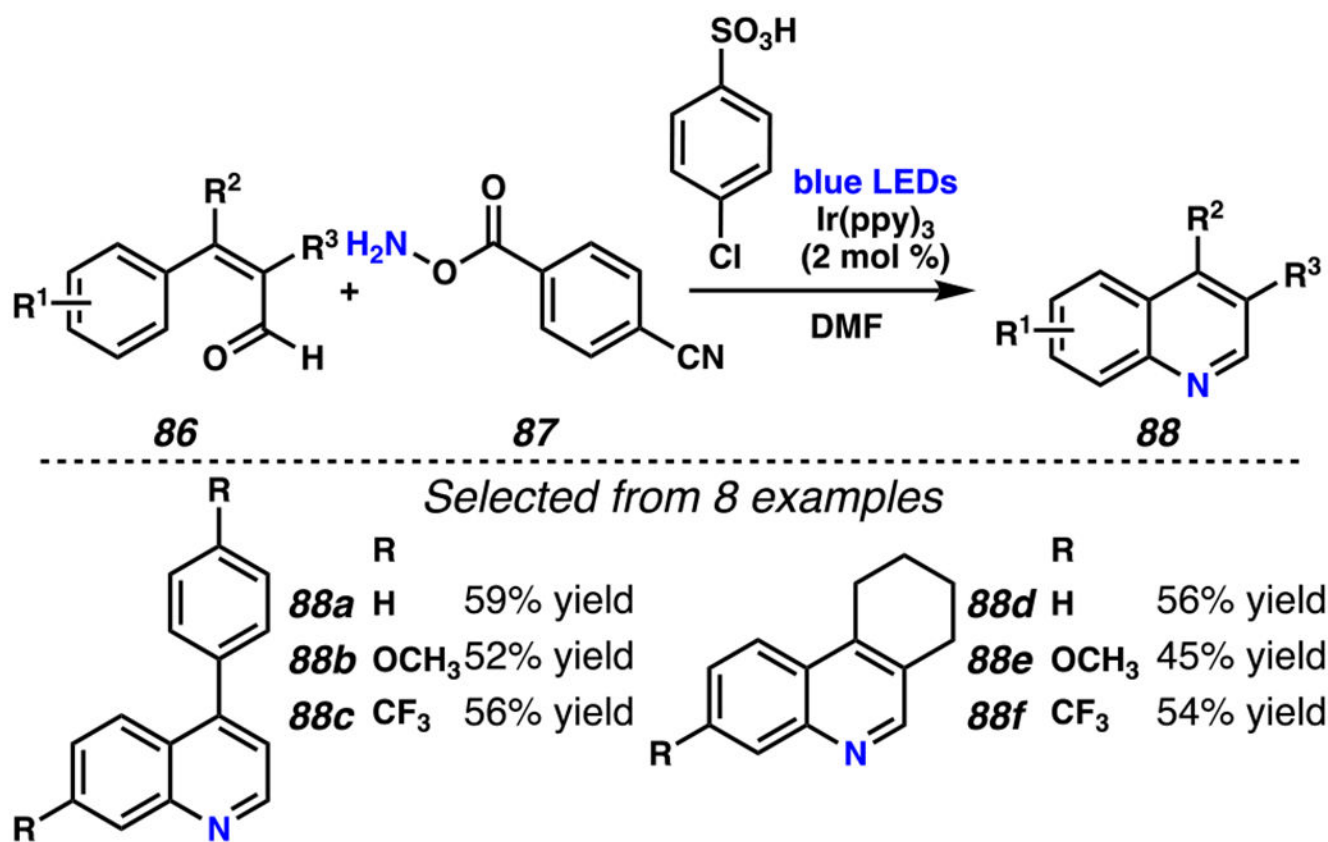
Scheme 24.

Iminyl Radical with Conjugated  $\pi$ -System Participates in 6-*endo-trig* Cyclization to Assemble *N*-Heteroarenes



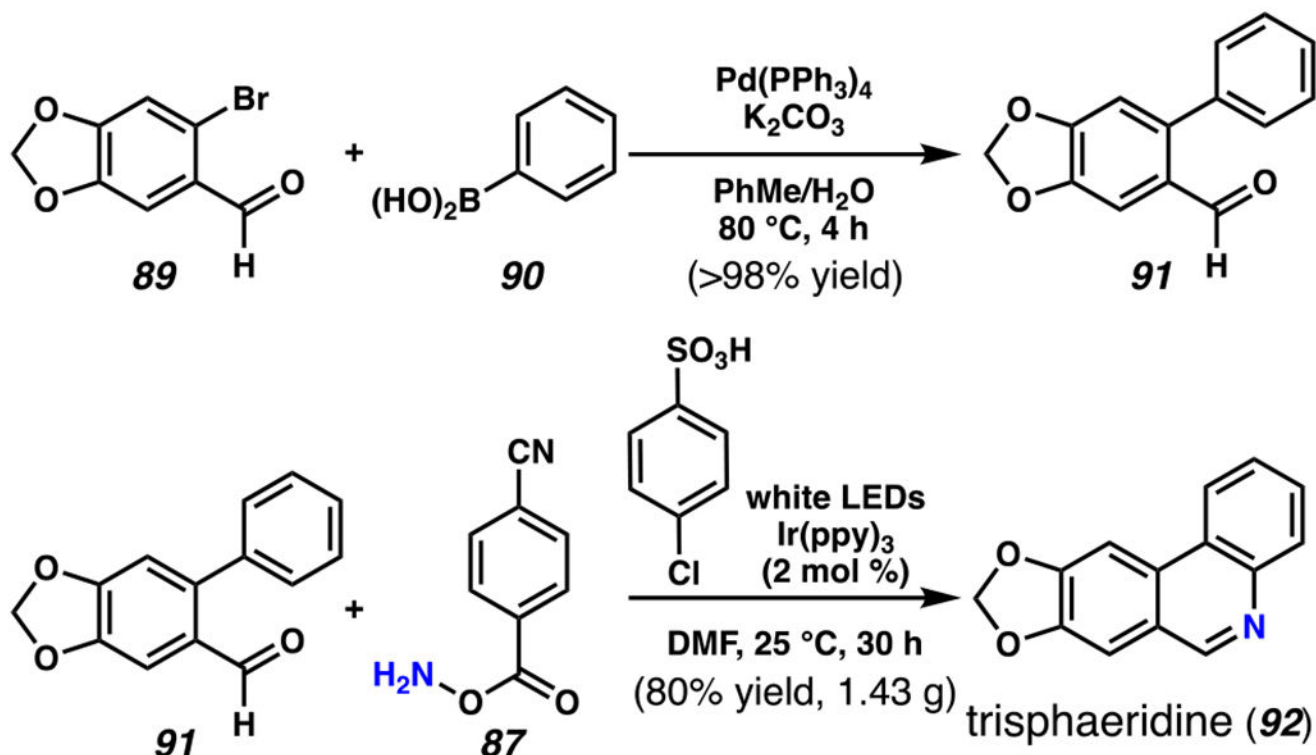
Scheme 25.

Yu and Zhao Use This Technology to Accelerate Access to Nornitidine



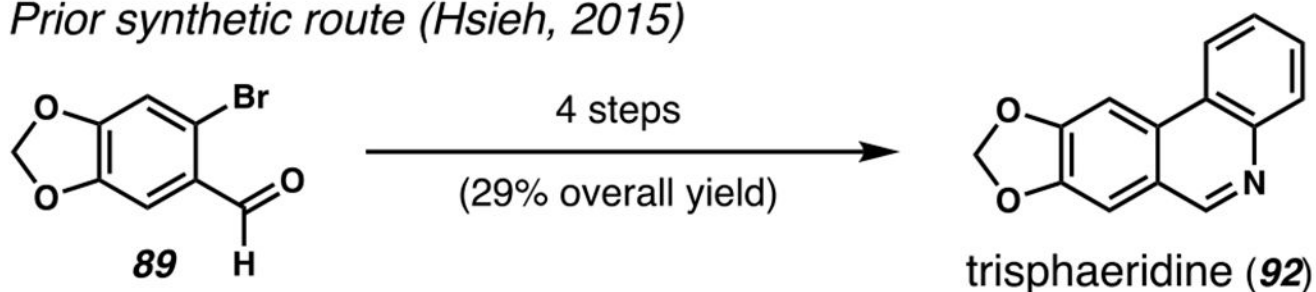
Scheme 26.

*O*-Acyl Hydroxylamines React with Aryl Aldehydes in a One-Pot Quinoline Syntheses



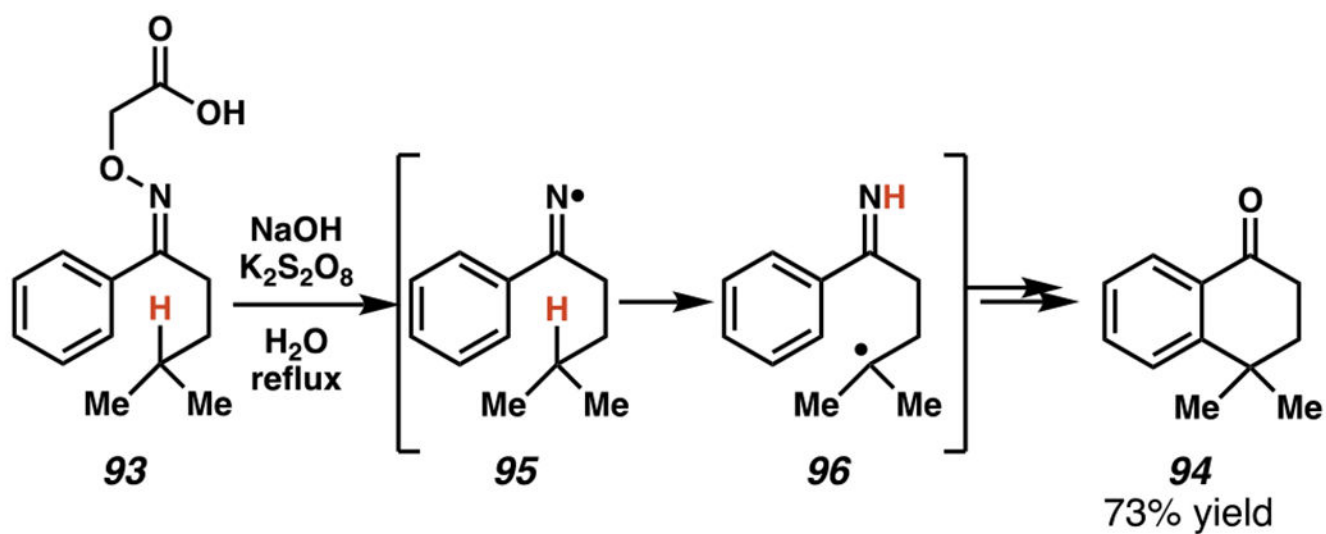
*19 examples of phenanthridines produced using this protocol*

Prior synthetic route (Hsieh, 2015)



Scheme 27.

*O*-Acyl Hydroxylamines React with Biaryl Aldehydes to Afford a One-Pot Syntheses of Phenanthridines, Which Is Used in a Two-Step Synthesis of Trisphaeridine

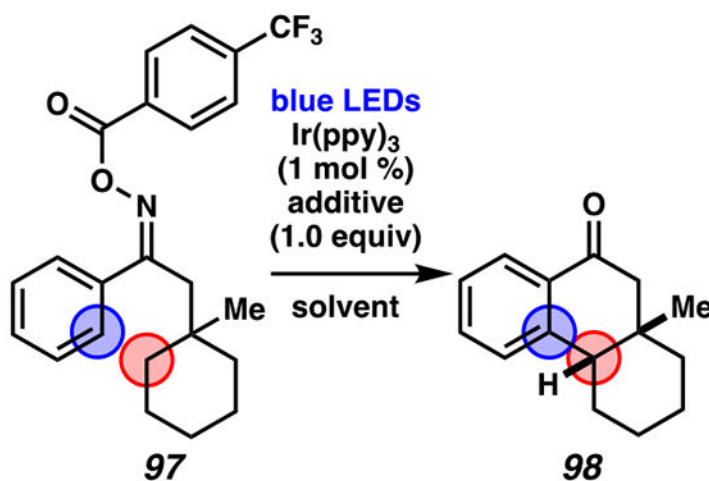


**Scheme 28.**

Forrester and Co-workers Pioneer Cascade Sequence to Convert Oxime through Iminyl Radical Intermediate, Which Engages Sequentially in a HAT Process and Addition Across an Arene Prior to Hydrolysis



(A) Efficient  $C(sp^3)-C(sp^2)$  bond formation relies on aqueous media and acidic additive

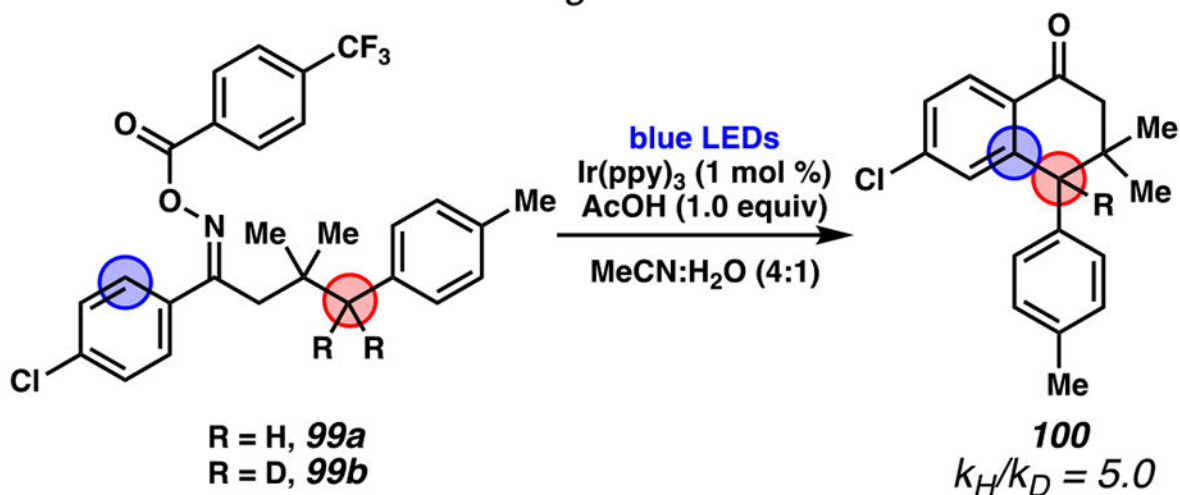


solvent	additive	yield [%]
MeCN	—	0
MeCN:H <sub>2</sub> O (1:1)	—	31
MeCN:H <sub>2</sub> O (4:1)	—	75
MeCN:H <sub>2</sub> O (4:1)	Et <sub>3</sub> N	31
MeCN:H <sub>2</sub> O (4:1)	AcOH	83

<sup>1</sup>H NMR yield using an internal standard of 1,3,5-trimethoxybenzene.

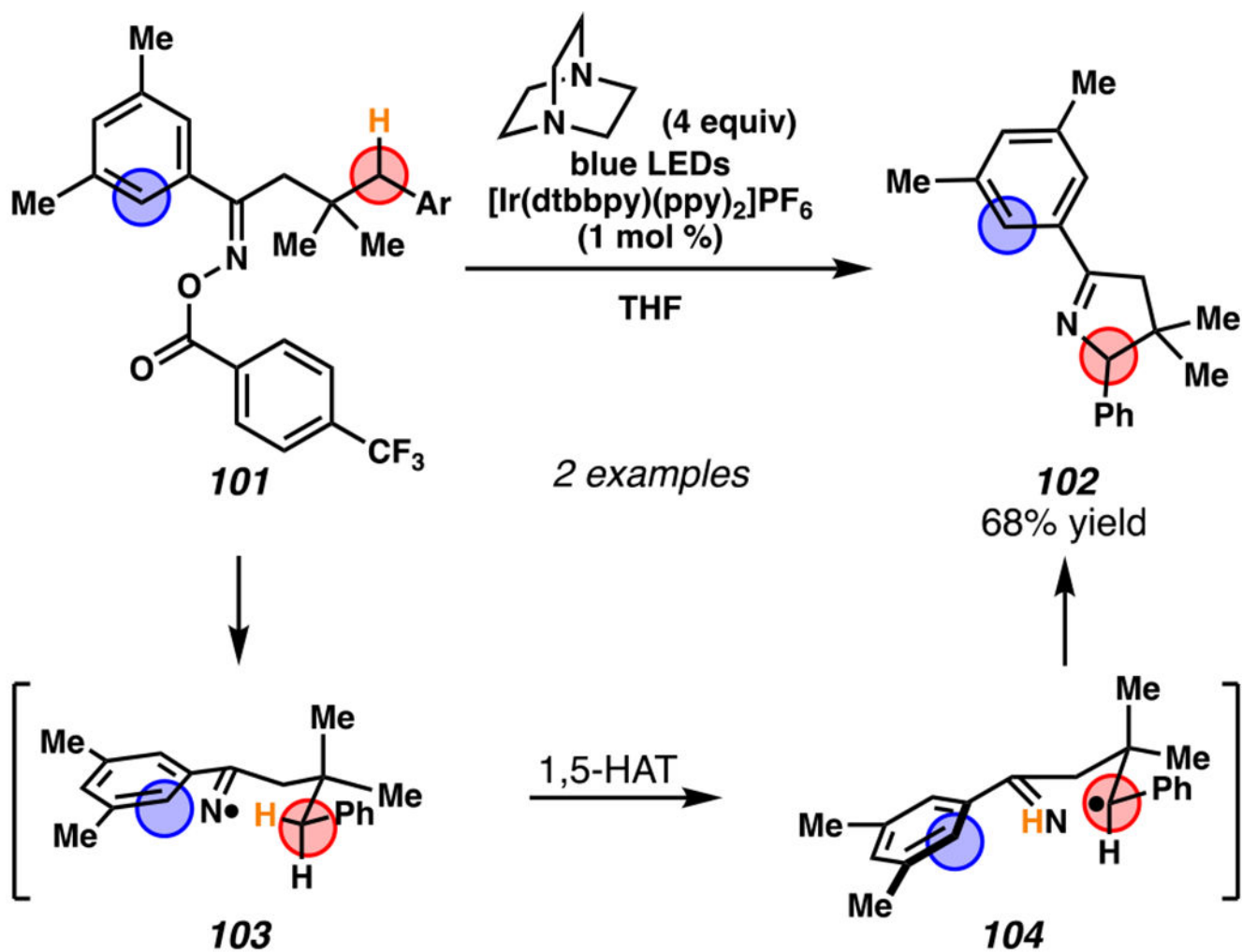
15 examples

(B) Rate measurements with individual substrates are consistent with rate-determining C–H abstraction

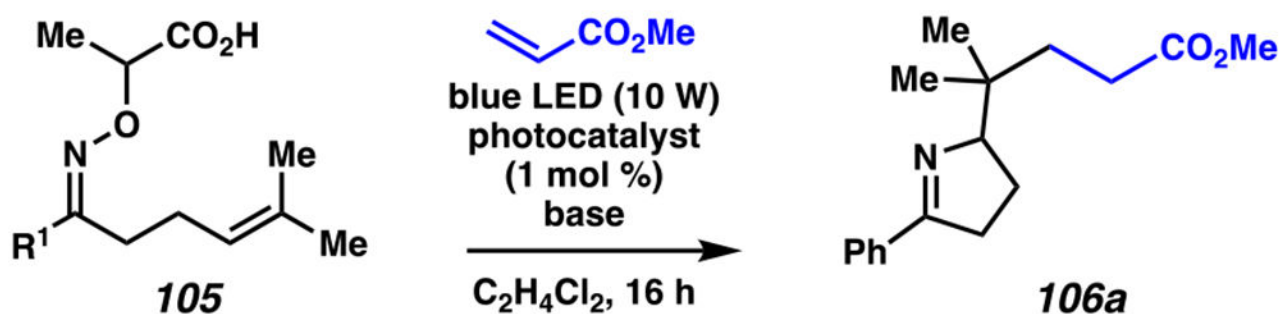


Scheme 29.

Cyclization Reaction Relies on Aqueous Media and Acidic Additive, and Involves Rate-Determining C–H Abstraction



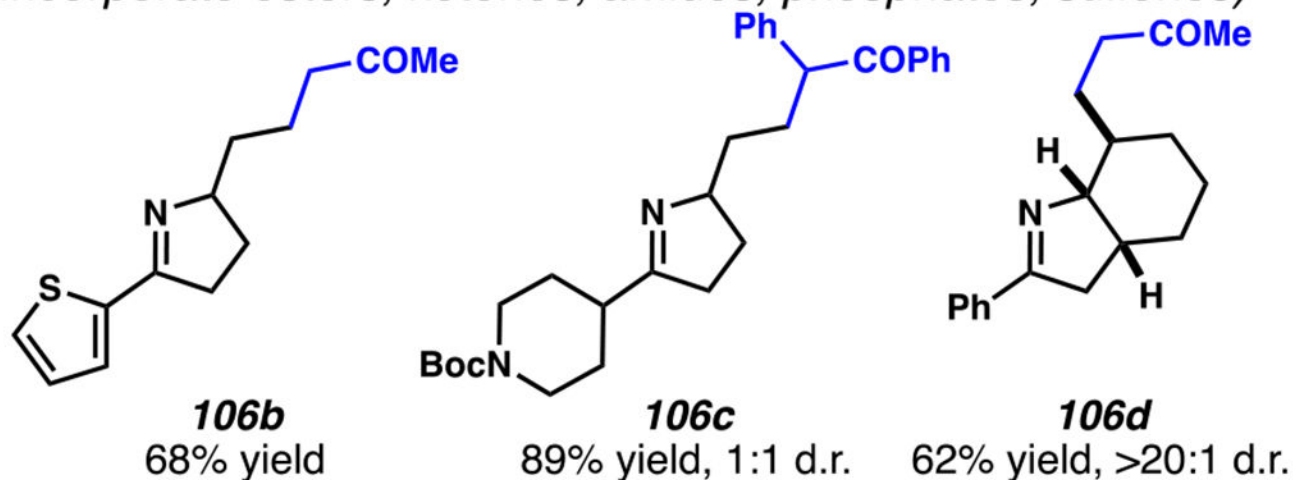
**Scheme 30.**  
 Complementary Reaction Conditions Trigger Chemodivergent C(sp<sup>3</sup>)-N Bond Formation to Provide 1-Pyrrolines



entry	photocatalyst	base	yield (%) <sup>a</sup>
1	$[\text{Ir}(\text{dF}(\text{CF}_3)\text{ppy})_2(\text{dtbbpy})]\text{PF}_6$	CsF	79
2	$[\text{Ir}(\text{dF}(\text{CF}_3)\text{ppy})_2(\text{dtbbpy})]\text{PF}_6$	$\text{Cs}_2\text{CO}_3$	49
3	$[\text{Mes-Acr}]\text{BF}_4$	CsF	n.d. <sup>b</sup>

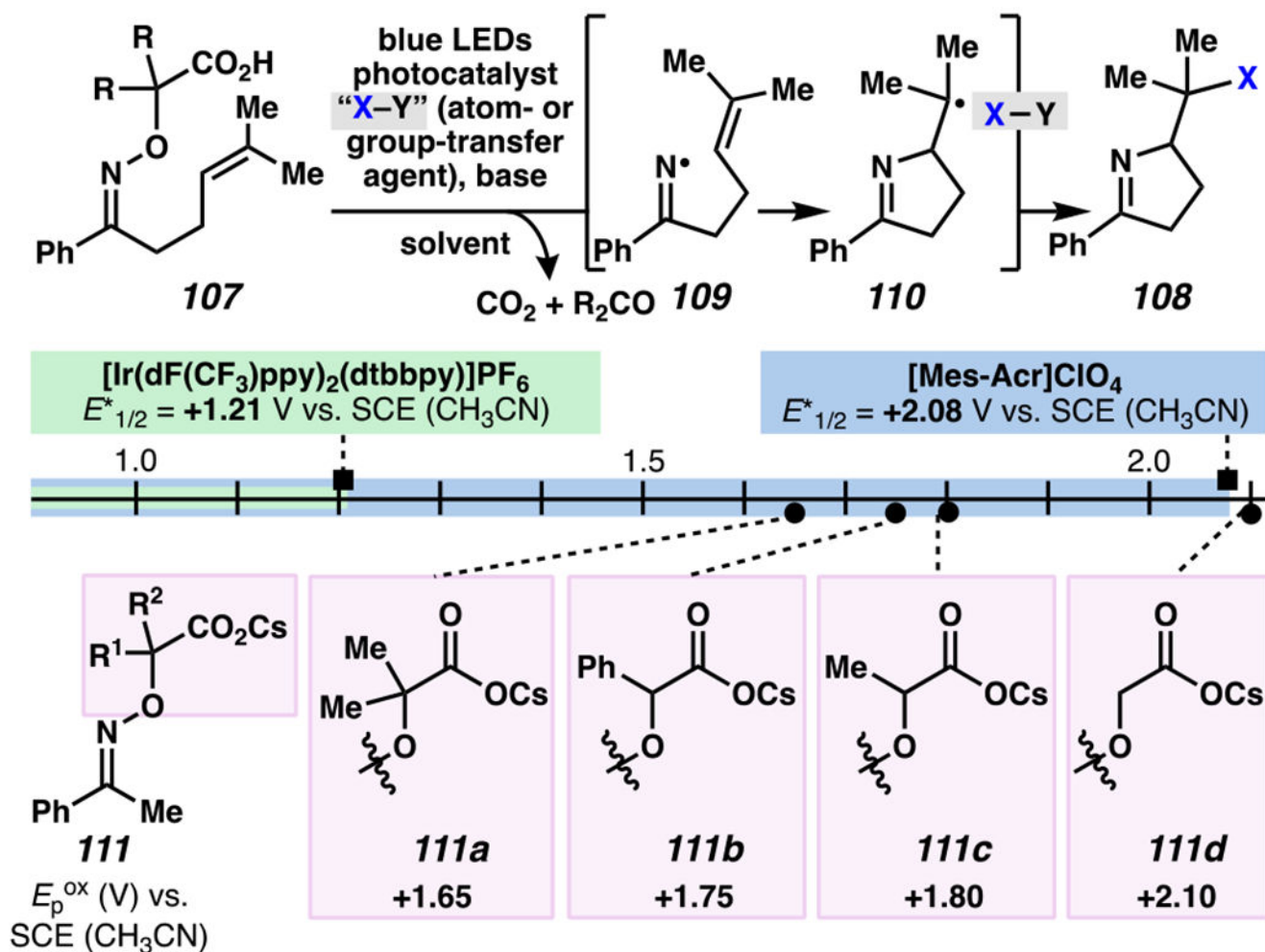
<sup>a</sup>  $^1\text{H}$  NMR yield using an internal standard of  $\text{CH}_2\text{Br}_2$ . <sup>b</sup> Not detected by  $^1\text{H}$  NMR of a crude reaction mixture.

Selected from 28 examples (*radical trapping agents incorporate esters, ketones, amides, phosphates, sulfones*)



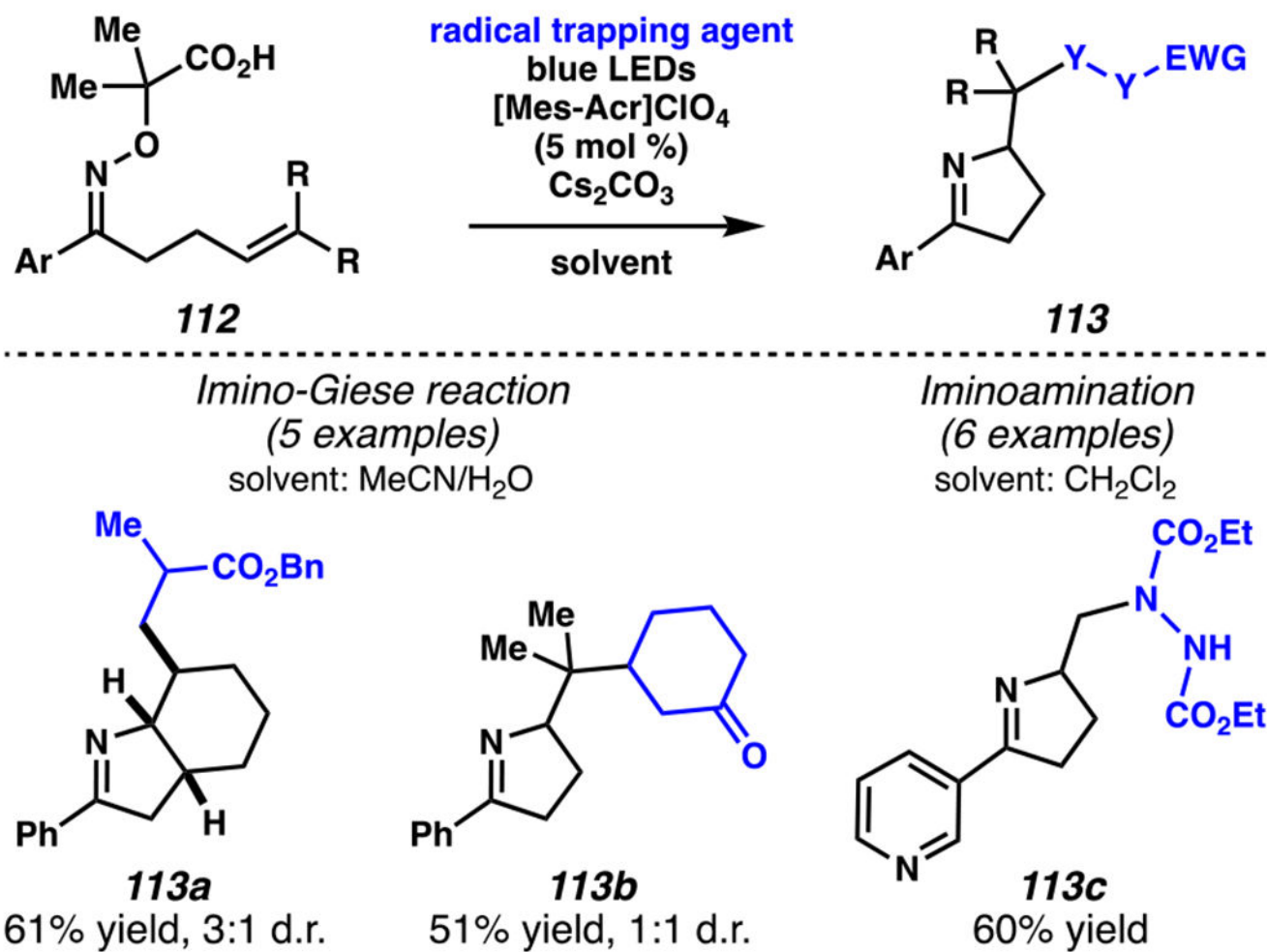
**Scheme 31.**

Jiang and Studer Demonstrate That Hydroxyacid-Derived  $\gamma,\delta$ -Unsaturated Ketoximes Engage in the Giese Reactions



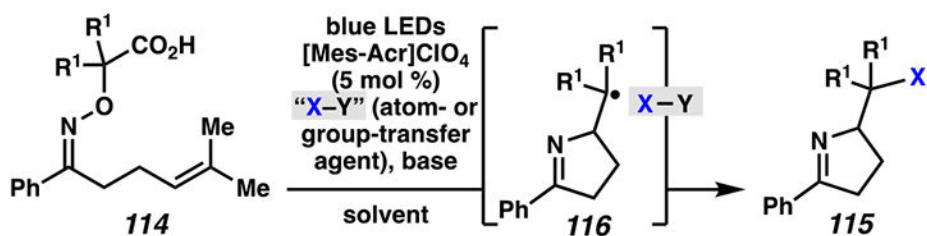
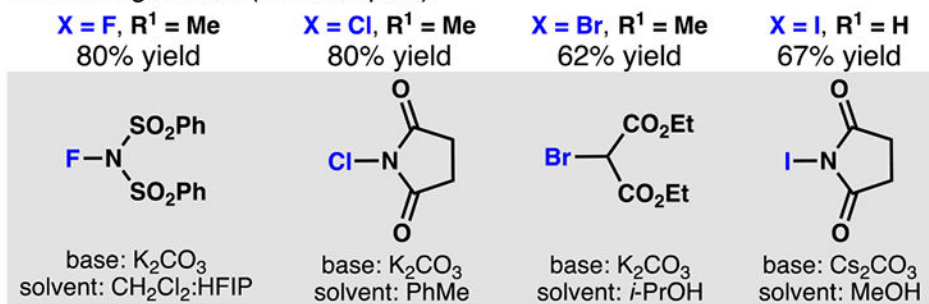
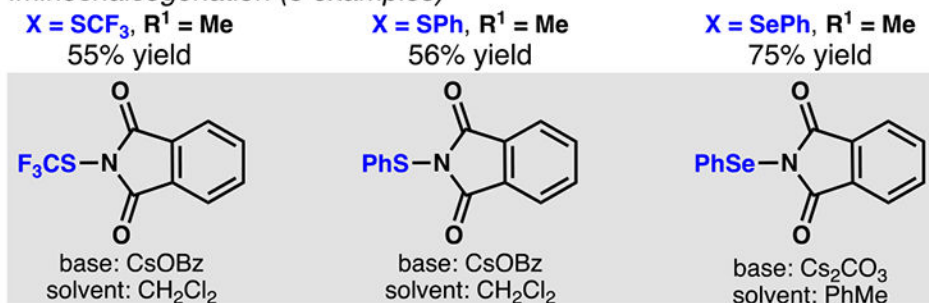
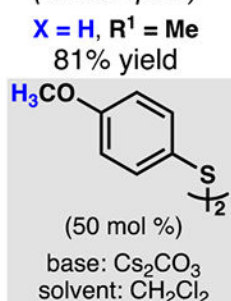
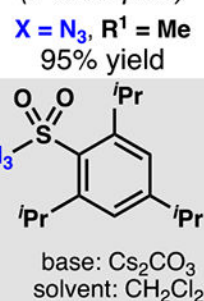
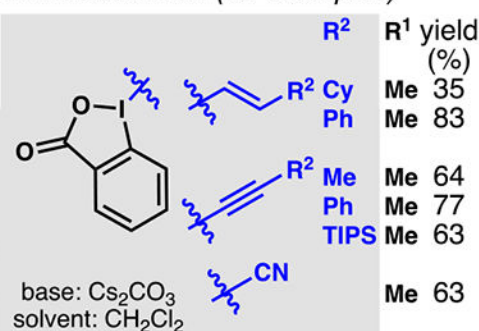
Scheme 32.

A Photocatalyst That Readily Oxidizes the Hydroxyacid Handle Is Critical in the Success of the Iminyl Radical-Initiated Giese-Type Reactions



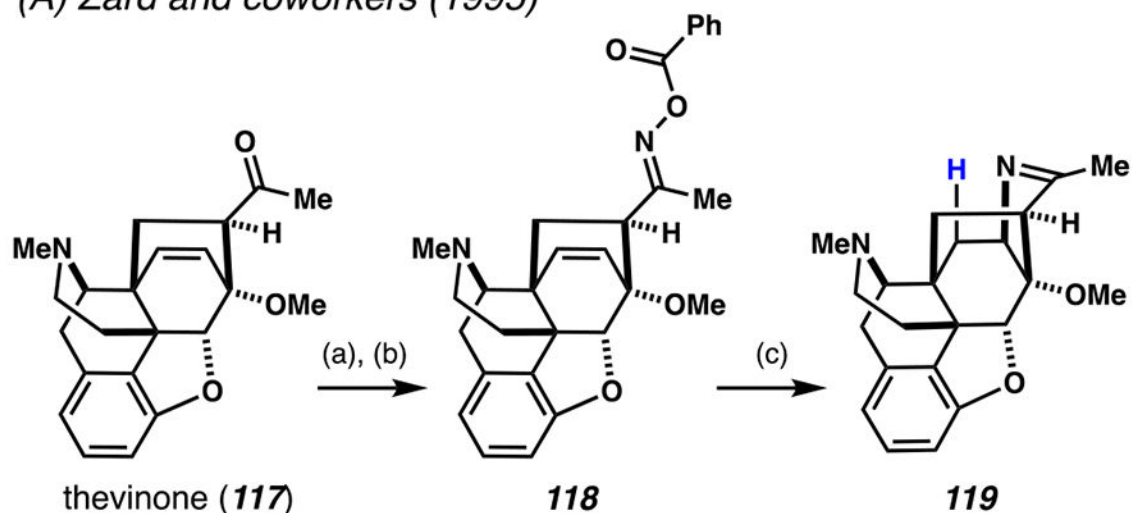
Scheme 33.

Concurrently, Leonori and Co-workers Demonstrate That Hydroxyacid-Derived  $\gamma,\delta$ -Unsaturated Ketoximes Engage in the Giese Reactions

*Iminohalogenation (13 examples)**Imino-chalcogenation (8 examples)**Hydroimination (4 examples)**Iminoazidation (4 examples)**Iminoolefination (15 examples)***Scheme 34.**

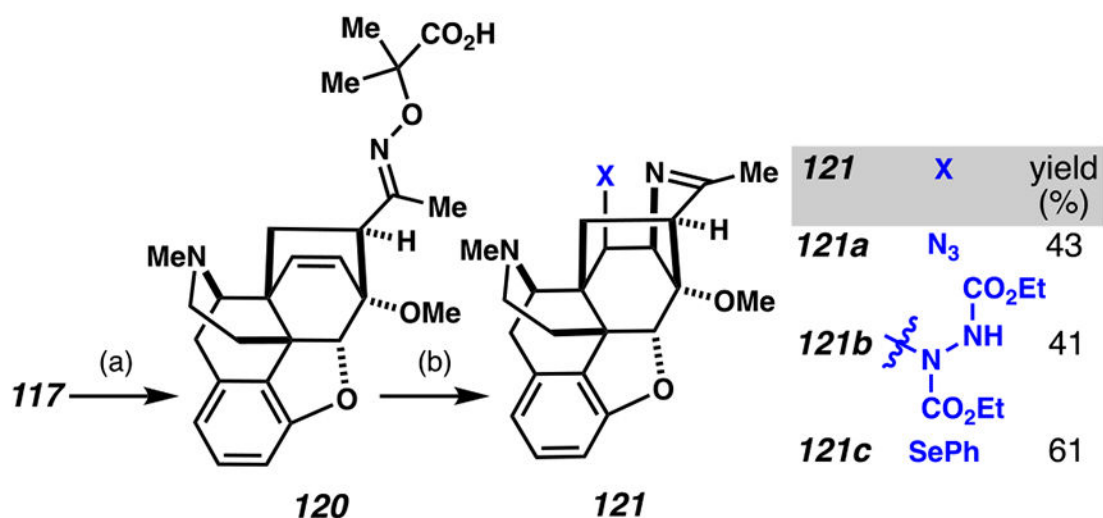
Hydroxyacid-Derived Oximes Are Appropriate Substrates for Iminofunctionalization Reactions

## (A) Zard and coworkers (1995)



(a)  $\text{NH}_2\text{OH}\cdot\text{HCl}$ , AcONa, MeOH; (b)  $\text{PhCOCl}$ , pyridine (98% yield over two steps);  
 (c)  $\text{Bu}_3\text{SnH}$ , AIBN, CyH (82% yield)

## (B) Leonori and coworkers (2017)

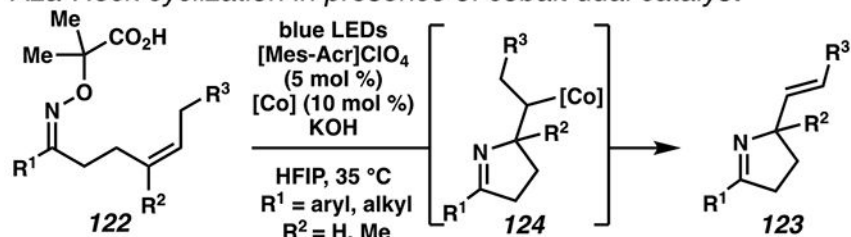


(a) 1-carboxy-1-methylethoxyammonium chloride, pyridine, MeOH (69% yield);  
 (b) blue LEDs,  $[\text{Mes-Acr}]\text{ClO}_4$  (5 mol %), with group-transfer agent, base, and solvent as specified in Scheme 34.

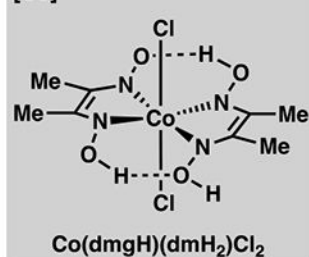
**Scheme 35.**

Late-Stage Iminofunctionalization Reactions Highlight the Potential of Radical Intermediates

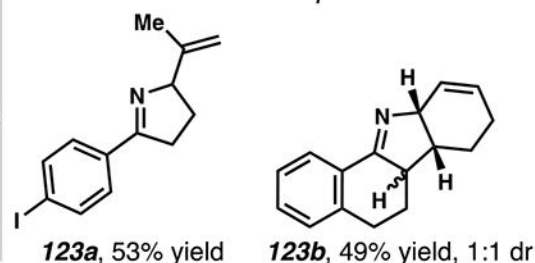
(A)  $\gamma,\delta$ -Unsaturated oxime ester undergoes radical Aza-Heck cyclization in presence of cobalt dual catalyst



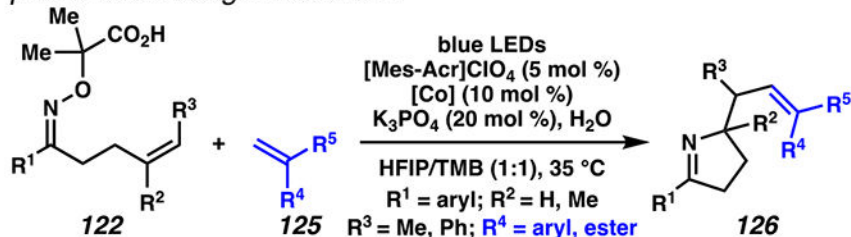
[Co] =



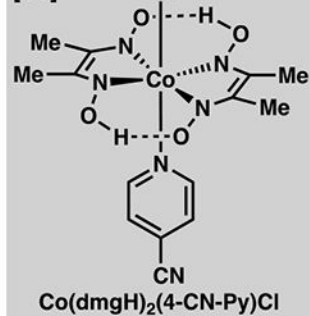
Selected from 32 examples



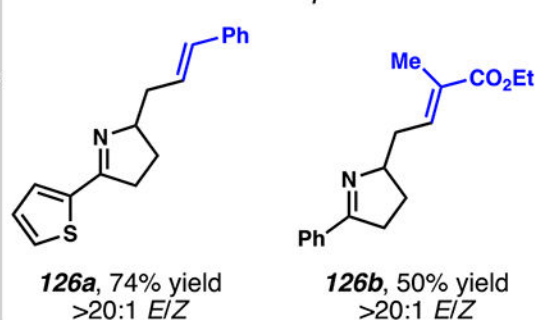
(B)  $\gamma,\delta$ -Unsaturated oxime ester undergoes radical Aza-cyclization / intermolecular Heck-type reaction cascade in presence of exogenous olefin



[Co] =



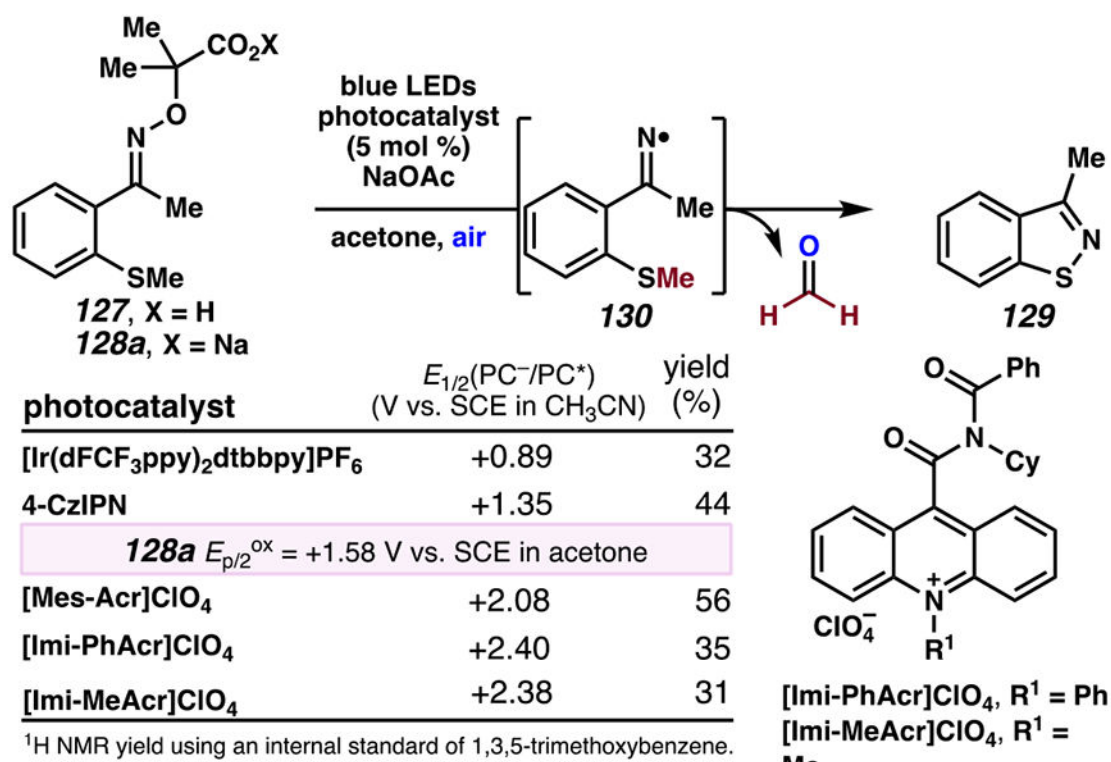
Selected from 29 examples



Scheme 36.

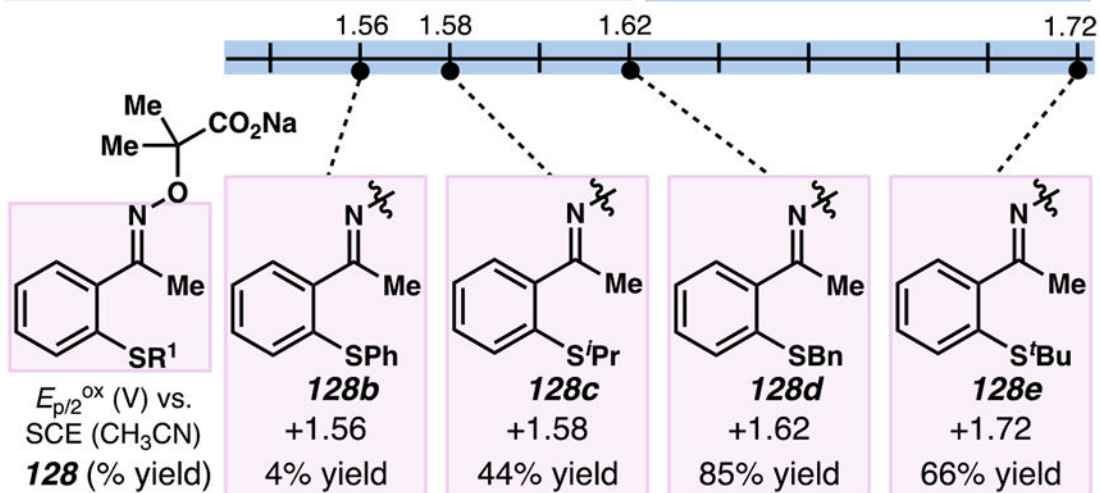
A Photocatalyst and Cobalt Complex Mediate Aza-Heck Cyclization Cascade Sequences





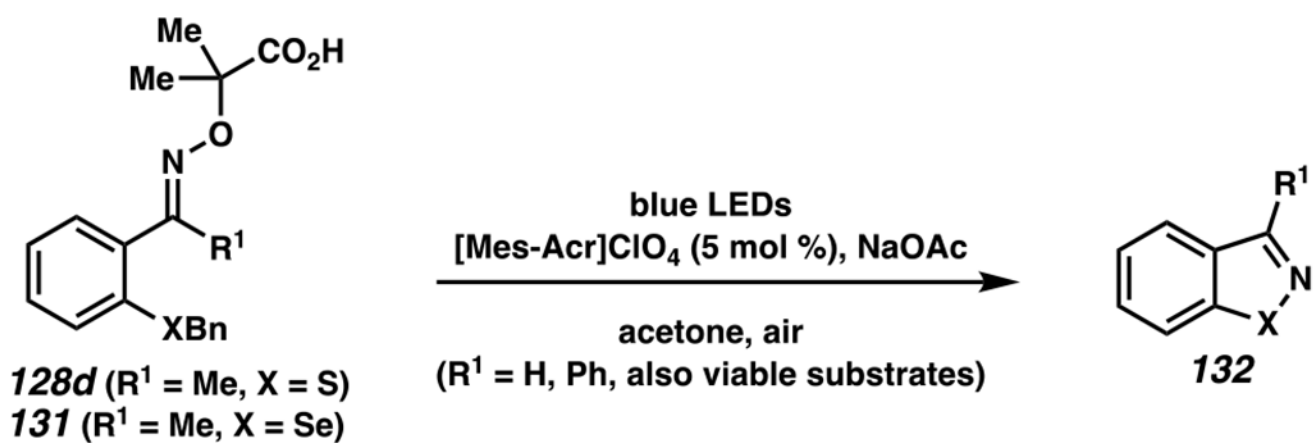
Thioether affects substrate  $E_{p/2}^{\text{ox}}$  values.

$[\text{Mes-Acr}]\text{ClO}_4$   
 $E_{1/2}^* = +2.08$  V vs. SCE ( $\text{CH}_3\text{CN}$ )

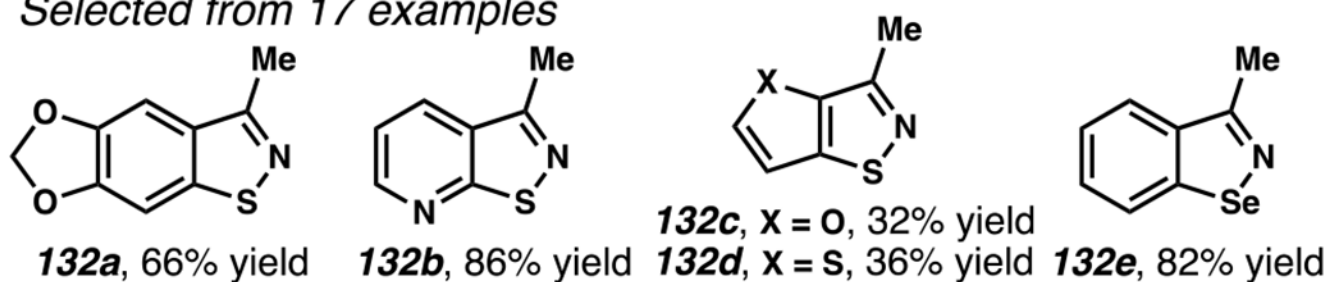


**Scheme 37.**

Intramolecular Reactions Between Iminyl Radicals and Thioethers Provide Isothiazoles



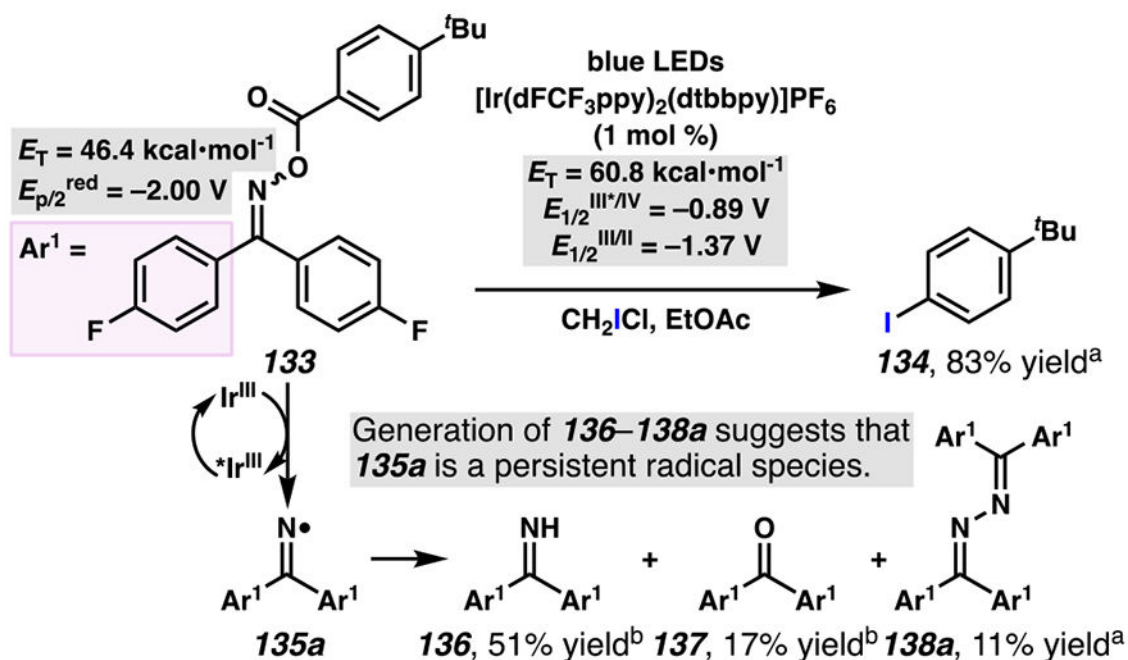
Selected from 17 examples



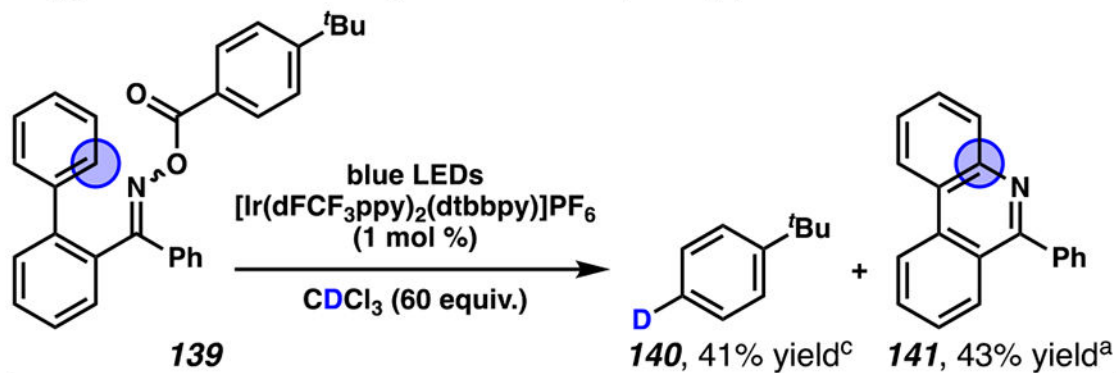
Scheme 38.

Heterocyclic Isothiazoles Are Constructed from  $\alpha$ -Imino Oxy Acids

(A) Benzophenone-derived oximes generate N-centered iminyl radical through energy-transfer process with photosensitizer rather than single-electron transfer process



(B) Iminyl radical generated from energy transfer process can be trapped intramolecularly to access 6-phenylphenanthridine

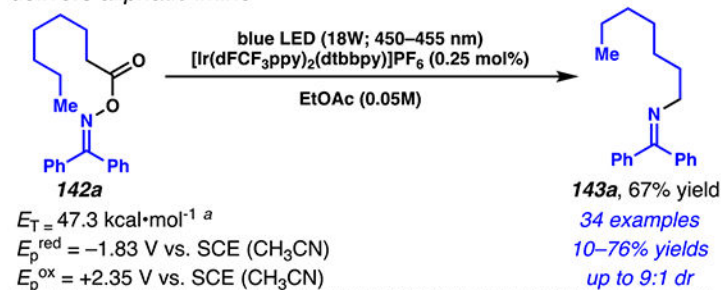


<sup>a</sup>Isolated yields. <sup>b</sup>GC yields without internal standard. <sup>c</sup>GC yield with anisole as internal standard.

**Scheme 39.**

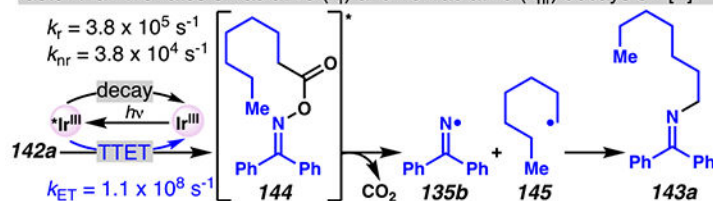
Oxime Analogues of Benzophenone Generate Nitrogen-Centered Iminyl Radicals *via* an Energy-Transfer Process

(A) Productive reaction between oxime ester and photosensitizer delivers aliphatic imine



(B) Dexter triplet–triplet energy transfer (TTET) process is kinetically feasible

The rate of triplet-triplet energy transfer ( $k_{ET}$ ) between **142a** and  $^*[\text{Ir}]$  is faster than the rates of radiative ( $k_r$ ) and nonradiative ( $k_{nr}$ ) decays of  $^*[\text{Ir}]$ .



(C) Förster-type resonant energy transfer is excluded, as there is negligible spectral overlap between the absorption spectrum of oxime **142a** and phosphorescence of Ir(III) complex

(D) Electrochemical potentials indicate that single electron transfer (SET) between substrate and catalysts is not thermodynamically favorable

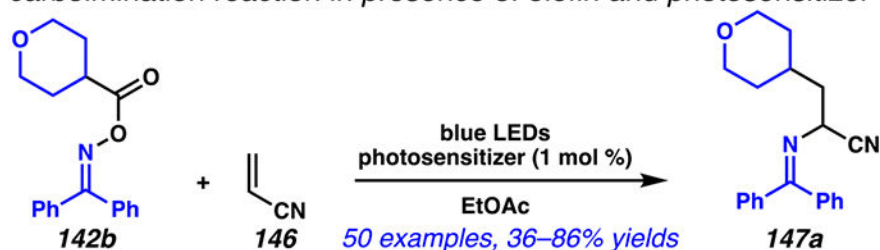
photosensitizer	$E_T^a$ (kcal·mol <sup>-1</sup> )	$E_{1/2}[\text{PC}^{+}/^*\text{PC}]$ (V) vs. SCE	$E_{1/2}[^*\text{PC}/\text{PC}^-]$ (V) vs. SCE	yield (%) <sup>b</sup>
[Ir(btp) <sub>2</sub> (phen)]PF <sub>6</sub>	45.7	-1.21	+0.94	7 (65)
[Ru(bpy) <sub>3</sub> ](PF <sub>6</sub> ) <sub>2</sub>	46.4	-0.81	+0.77	0 (98)
[Ir(pbt) <sub>2</sub> (phen)]PF <sub>6</sub>	54.9	-1.17	+1.16	7 (65)
Ir(fppy) <sub>2</sub> (phen)]PF <sub>6</sub>	56.7	-1.32	+1.35	20 (24)
Ir(dFppy) <sub>2</sub> (phen)]PF <sub>6</sub>	58.8	-1.22	+1.42	30 (10)
[Ir(dFCF <sub>3</sub> ppy) <sub>2</sub> (phen)]PF <sub>6</sub>	59.3	-0.99	+1.33	23 (30)
[Ir(dFCF <sub>3</sub> ppy) <sub>2</sub> (dtbbpy)]PF <sub>6</sub>	63.6	-1.04 <sup>c</sup>	+1.39 <sup>c</sup>	40 (18)
no photosensitizer, $h\nu$ ( $\lambda = 365 \text{ nm}$ )	—	—	—	0 (98)
Ph <sub>2</sub> CO, $h\nu$ ( $\lambda = 300 \text{ nm}$ )	~ 69	—	—	0 (97)

<sup>a</sup> $E_T$  values were estimated from DFT calculations using optimized geometry at the uB3LYP/6-31G(d,p)/LANL2DZ level of theory and single-point energy calculation at the uB3LYP/6-311++G(d,p) level of theory in EtOAc by PCM method. <sup>b</sup><sup>1</sup>H NMR yields of imine **143a** using CHBr<sub>3</sub> as internal standard; the remaining yield of recovered **142a** is in parentheses. Reactions with photosensitizer (1 mol%), in C<sub>2</sub>H<sub>4</sub>Cl<sub>2</sub> (0.2 M) unless otherwise noted. <sup>c</sup>The excited-state potentials were calculated based on measured ground-state potentials of [Ir(dFCF<sub>3</sub>ppy)<sub>2</sub>(dtbbpy)]PF<sub>6</sub>. <sup>d</sup>Trace benzophenone imine and benzophenone detected.

#### Scheme 40.

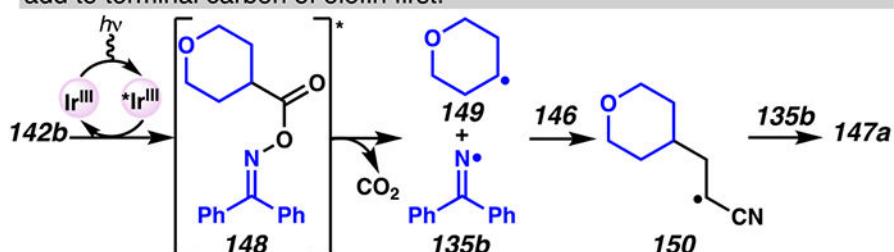
Benzophenone Oxime Esters Engage in Photosensitized Reaction to Deliver Aliphatic Imine

(A) Benzophenone-derived oximes ester undergoes carboimination reaction in presence of olefin and photosensitizer

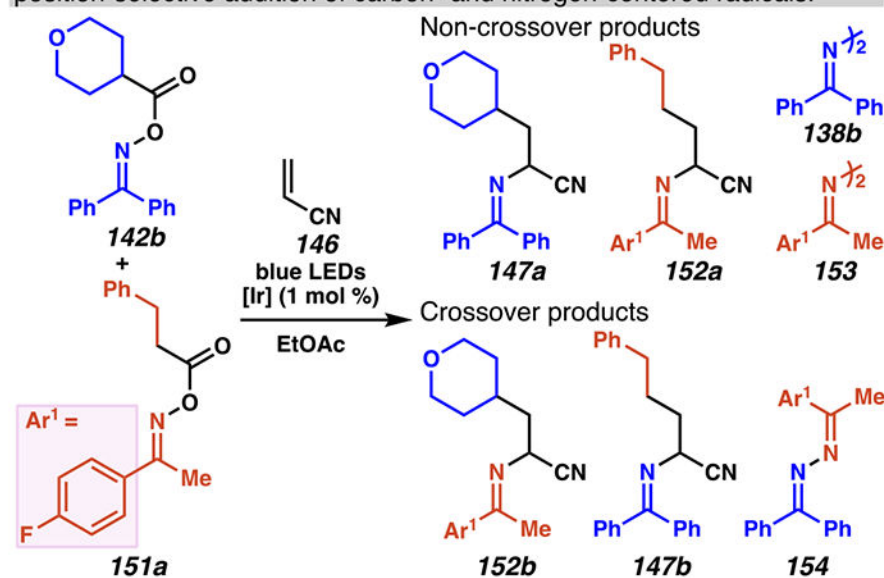


(B) Position-selective addition of carbon- and nitrogen-centered radical species to olefin hinges on persistent radical effect

The long lifetime of **135b** enables **149** to escape the solvent cage and add to terminal carbon of olefin first.



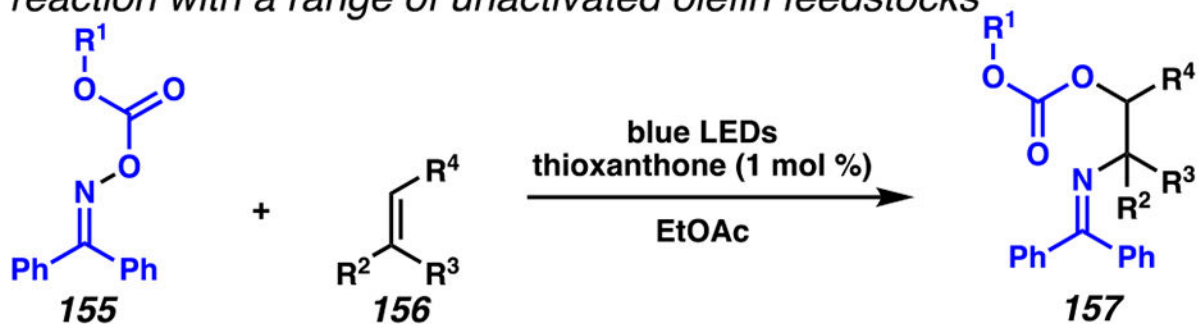
Radical crossover experiments corroborate the persistent radical effect in position-selective addition of carbon- and nitrogen-centered radicals.



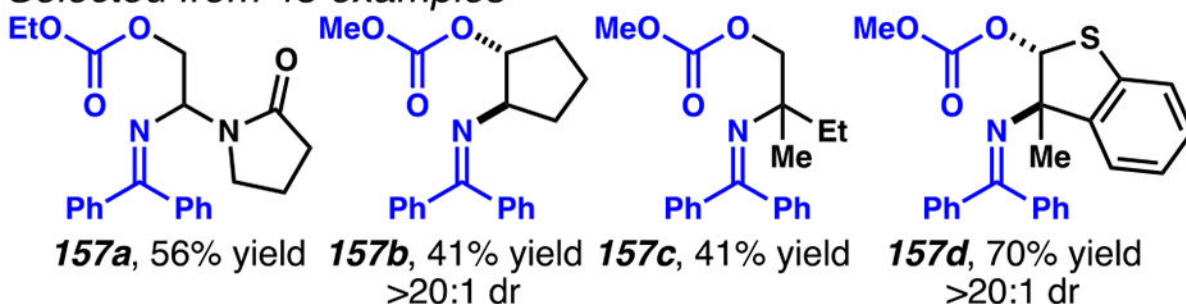
**Scheme 41.**

Aliphatic *O*-Acyl Benzophenone-Derived Oxime and Electron-Deficient Olefin Participate in Photosensitized Three-Component Carboimination Reaction

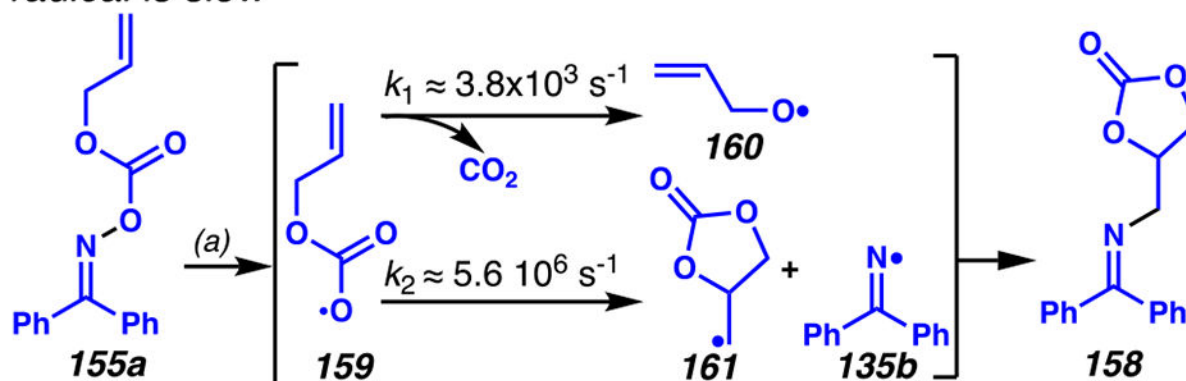
(A) Oxime carbonate undergoes position-selective oxyimination reaction with a range of unactivated olefin feedstocks



Selected from 48 examples



(B) Intramolecular alkoxy-carbonyloxy radical trap suggests that radical-radical coupling of alkyl radical and benzophenone iminyl radical is slow

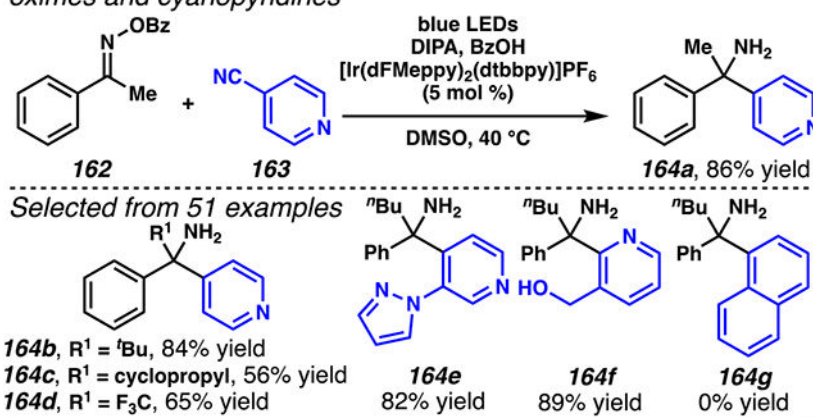


(a) Blue LEDs, thioxanthone (1 mol %), EtOAc

**Scheme 42.**

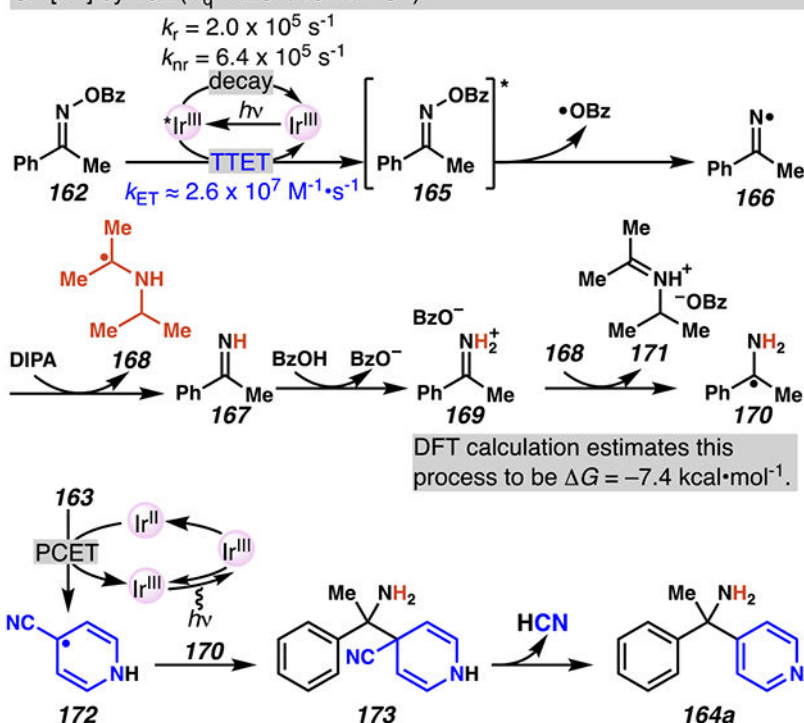
In Oxyimination Reaction, Chemoselectivity May Arise Due to the Low Rate of Radical Recombination Between Alkoxy-carbonyloxy and Iminyl Radicals

(A) Sterically congested 1° amines are synthesized from benzylic oximes and cyanopyridines



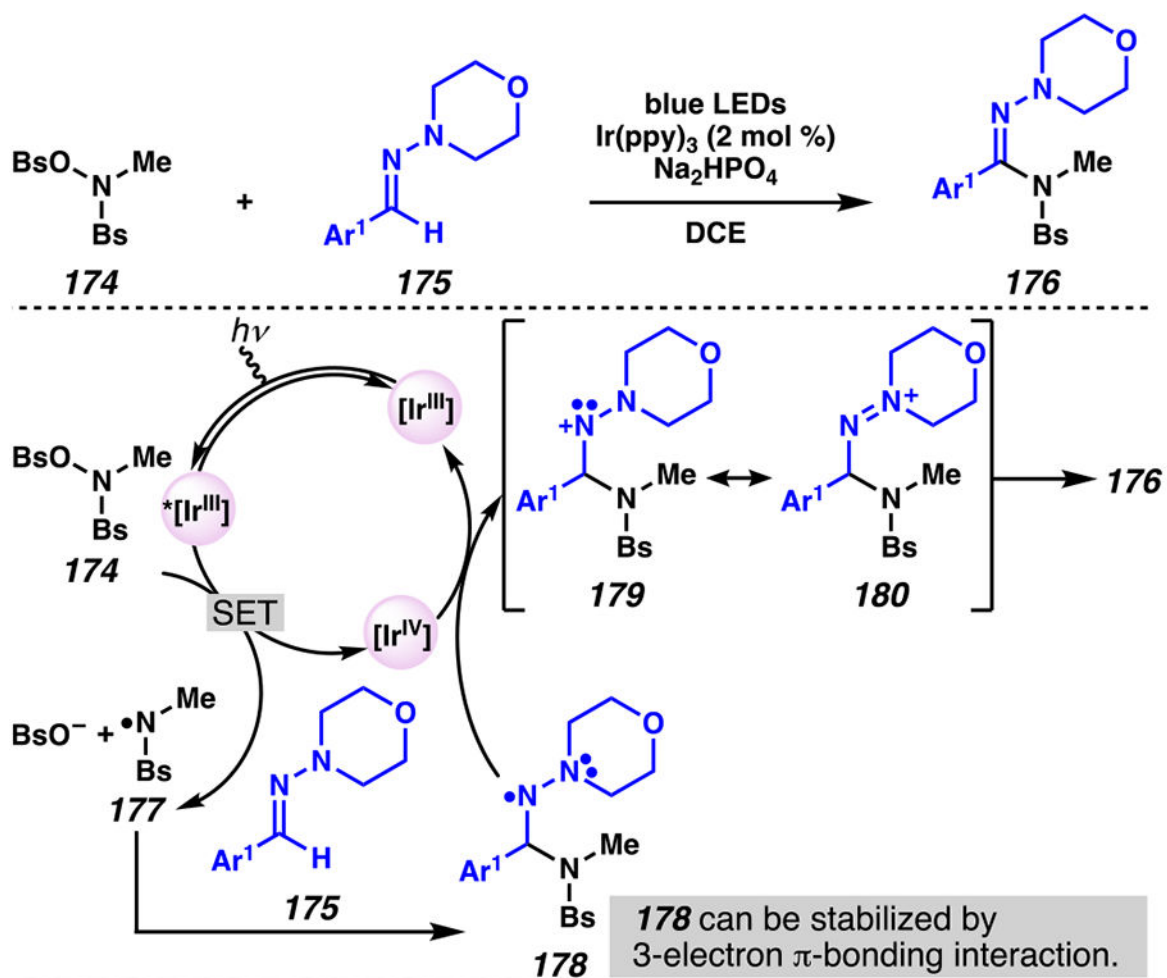
(B) Benzylic oxime undergoes energy-transfer process with photosensitizer to reveal iminyl radical

Stern-Volmer analysis provides evidence for kinetically feasible quenching of  $^*[\text{Ir}^{\text{III}}]$  by **162** ( $K_q \approx 2.6 \times 10^7 \text{ M}^{-1} \cdot \text{s}^{-1}$ ).

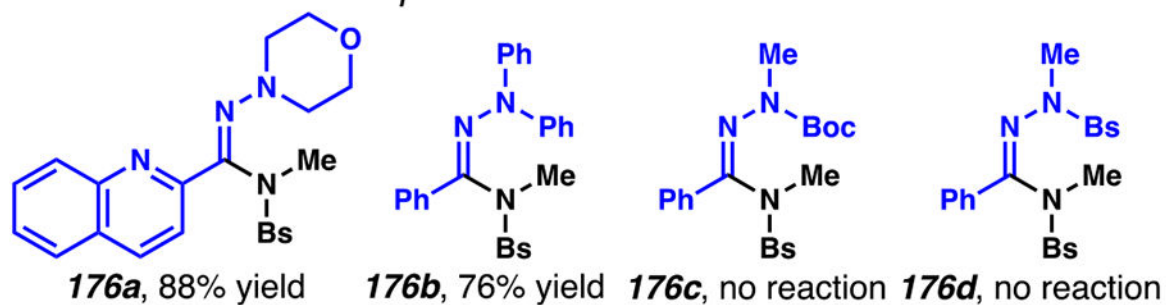


**Scheme 43.**

Acetophenone-Derived *O*-Acyl Oxime and Cyanopyridines Undergo Photosensitized Two-Component Coupling Reaction to Afford Sterically Congested Primary Amines



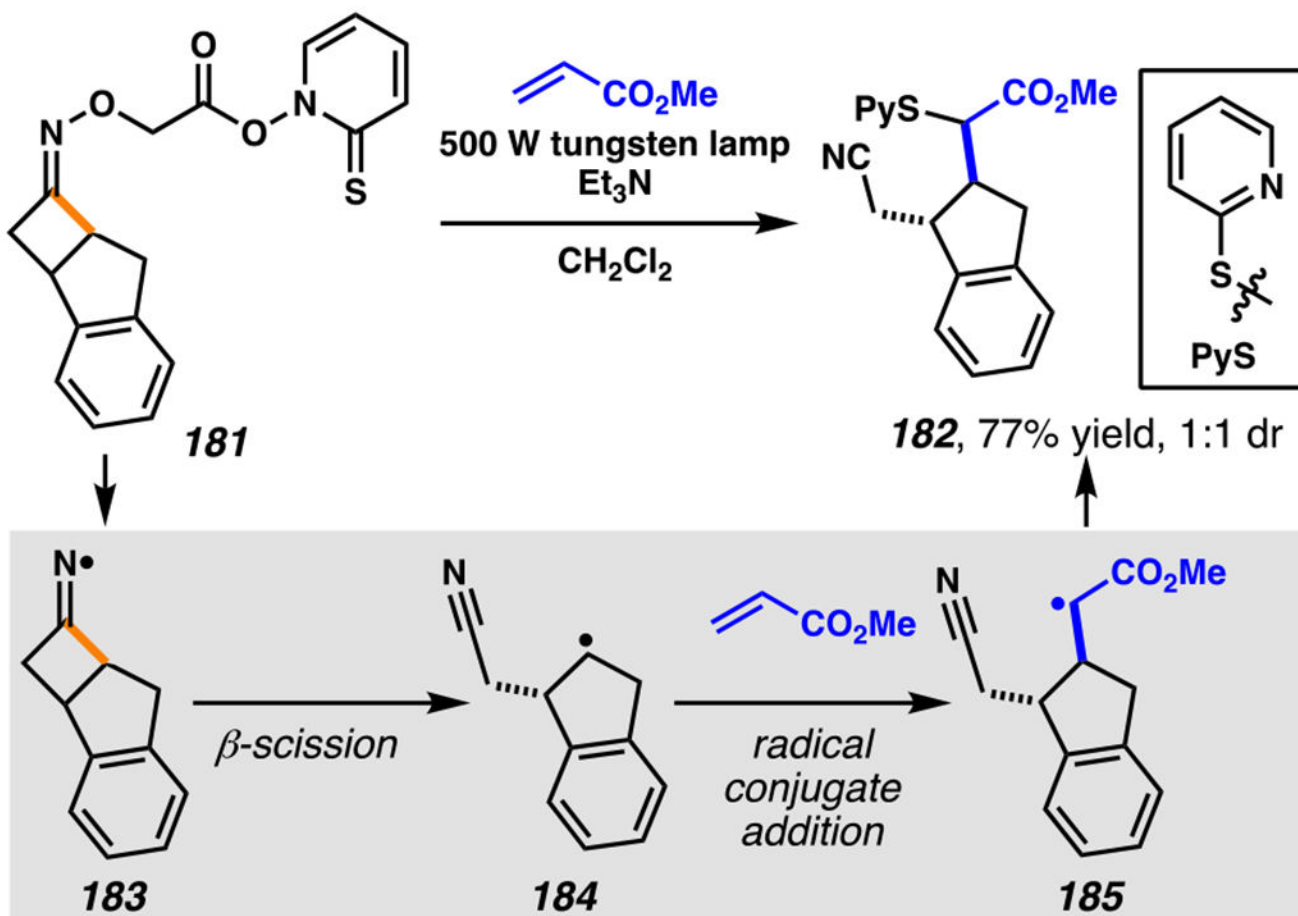
Selected from 31 examples



Scheme 44.

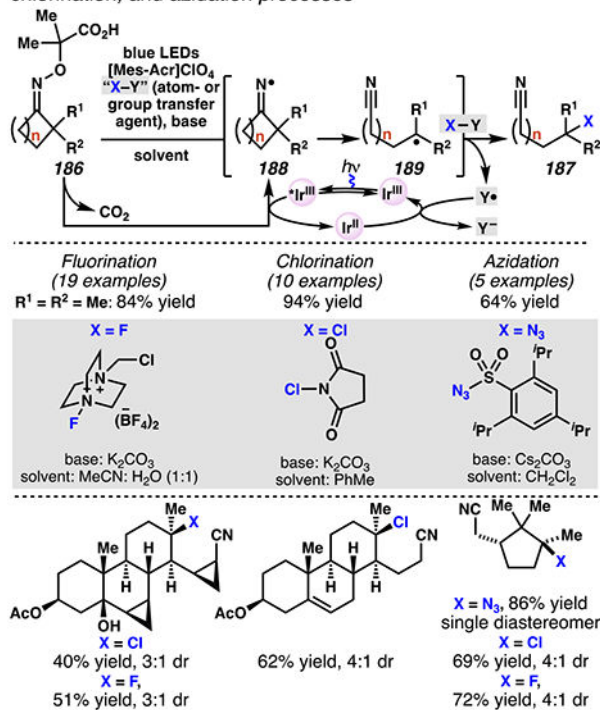
*O*-Aryloxy Amide and Hydrazones React in a C–H Amidation Process



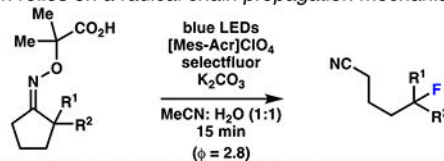


**Scheme 45.**  
Cyclobutanone-Derived Oxime Triggers  $\beta$ -Scission / Radical Conjugate Addition /  
Chalcogenation Cascade

(A) Leonori and co-workers develop ring-opening fluorination, chlorination, and azidation processes



(B) A quantum yield ( $\phi$ ) of 2.8 indicates that this fluorination reaction relies on a radical chain propagation mechanism



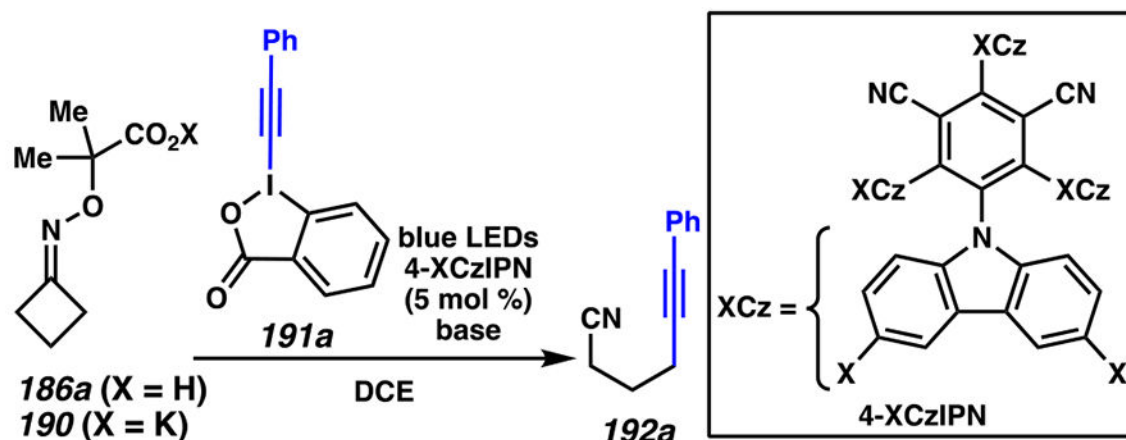
(C) "Experimentally successful" fluorination reactions appear to benefit from ring-strain release, and the radical stabilizing effects of substituents

R <sup>1</sup>	R <sup>2</sup>	radicaloid center in 189	ring size in 186:							
			four (n = 1)	five (n = 2)	six (n = 3)	seven (n = 4)				
			$\Delta G^{\circ a}$	yield <sup>b</sup>	$\Delta G^{\circ}$	yield	$\Delta G^{\circ}$	yield		
H	H	primary	-10.2	76	7.9	— <sup>d</sup>	13.8	— <sup>d</sup>	9.4	— <sup>d</sup>
H	Me	secondary	-11.8	e.s. <sup>c</sup>	5.4	— <sup>d</sup>	9.1	— <sup>d</sup>	4.4	— <sup>d</sup>
H	Ph	benzylic <sup>e</sup>	-22.8	63	-5.7	68	-1.8	61	-7.3	72
Me	Me	tertiary	-14.4	e.s. <sup>c</sup>	2.4	84	5.9	— <sup>d</sup>	0.8	— <sup>d</sup>

<sup>a</sup> $\Delta G^{\circ}$  (kcal/mol) for the conversion of iminyl radical **186** to alkyl radical **189** [UB3LYP/6-31+G(d,p)] <sup>b</sup>isolated yield (%; X = F). <sup>c</sup>Reaction described as "experimentally successful". Specific reaction (i.e. X = F, Cl, N<sub>3</sub>) and yield not reported. <sup>d</sup>Reaction not "experimentally successful". Specific reaction and yield not reported. <sup>e</sup>Chlorination and azidation reactions involving secondary benzylic centers are not documented.

### Scheme 46.

Cascade C–C Cleavage and Functionalization Reactions Afford Aliphatic Nitriles with Fluorine, Chlorine and Azide Functional Handles

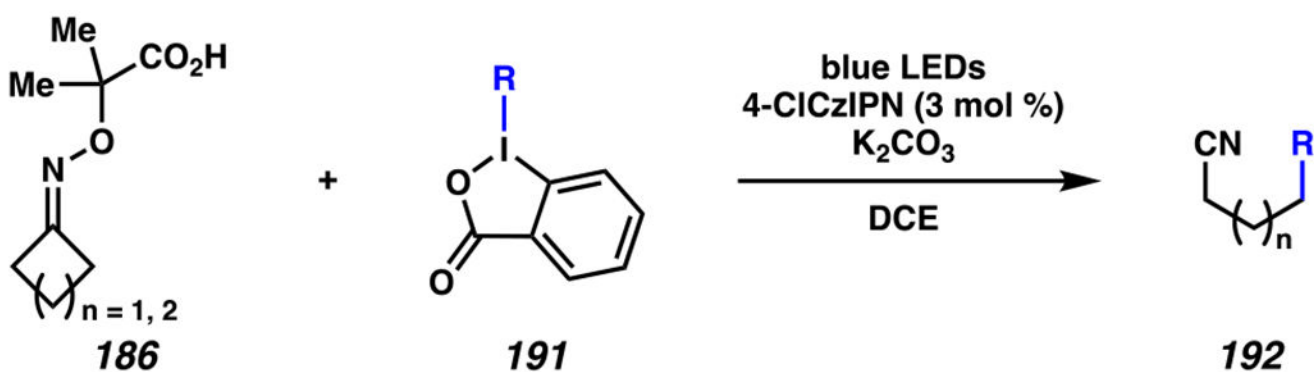


PC	$E_{1/2}(\text{PC}^*/\text{PC}^-)$ (V) vs. SCE	base	conversion (%)	yield (%)
[Ir(dFCF <sub>3</sub> ppy) <sub>2</sub> dtbbpy]PF <sub>6</sub>	+1.21	Cs <sub>2</sub> CO <sub>3</sub>	>95	55
4-CzIPN (X = H)	+1.35	Cs <sub>2</sub> CO <sub>3</sub>	60	50
4-FCzIPN (X = F)	+1.42	K <sub>2</sub> CO <sub>3</sub>	>95	75
<b>190 <math>E_p^{\text{ox}} = +1.48</math> V vs. SCE (DMF)</b>				
4-ClCzIPN (X = Cl)	+1.49	Cs <sub>2</sub> CO <sub>3</sub>	>95	70
4-ClCzIPN (X = Cl)	+1.49	K <sub>2</sub> CO <sub>3</sub>	>95	80
4-BrCzIPN (X = Br)	+1.73	K <sub>2</sub> CO <sub>3</sub>	>95	75
[Mes-Acr]ClO <sub>4</sub>	+2.06	Cs <sub>2</sub> CO <sub>3</sub>	50	20
9,10-dicyanoanthracene	+2.06	Cs <sub>2</sub> CO <sub>3</sub>	90	5

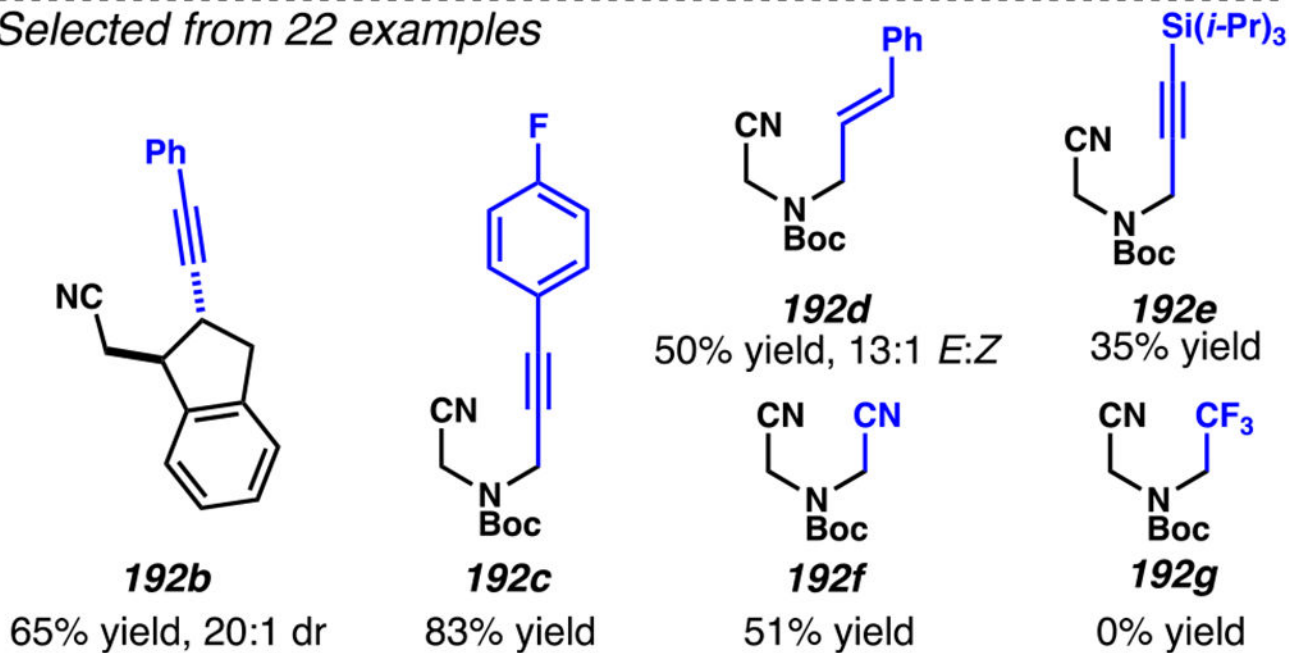
<sup>a</sup> $E_{1/2}(\text{PC}^*/\text{PC}^-)$  for [Ir(dFCF<sub>3</sub>ppy)<sub>2</sub>dtbbpy]PF<sub>6</sub>, 4-CzIPN, [Mes-Acr]ClO<sub>4</sub> and 9,10-dicyanoanthracene are in CH<sub>3</sub>CN, and  $E_{1/2}(\text{PC}^*/\text{PC}^-)$  for 4-FCzIPN, 4-ClCzIPN and 4-BrCzIPN are in DCM.

**Scheme 47.**

Ethynyl Benziodoxolone-Based Alkyne-Transfer Reagents Facilitates C(sp<sup>3</sup>)-C(sp) Cross-Coupling Reactions to Furnish Aliphatic Nitriles with Internal Alkyne

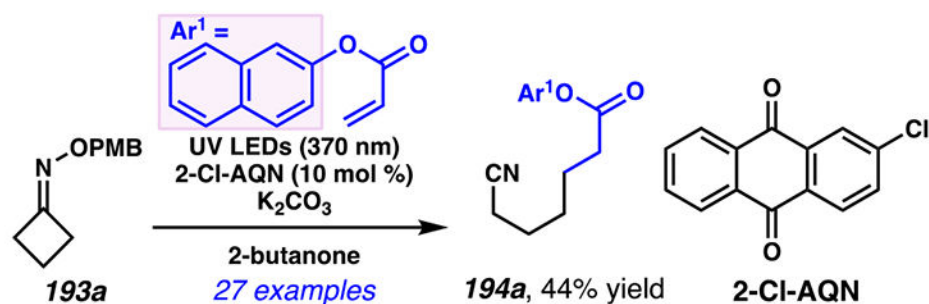


*Selected from 22 examples*

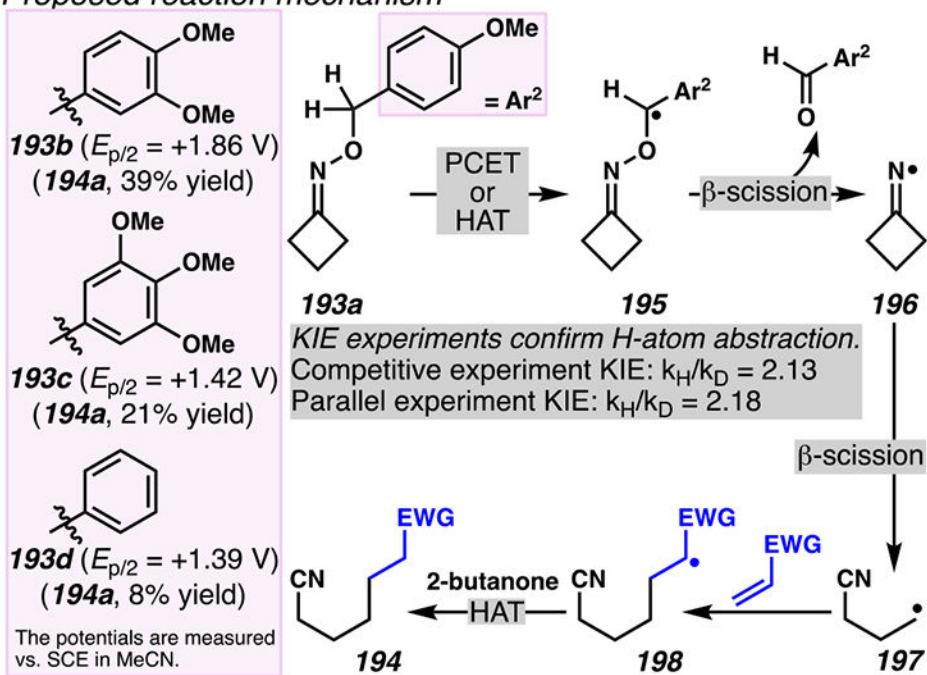


**Scheme 48.**

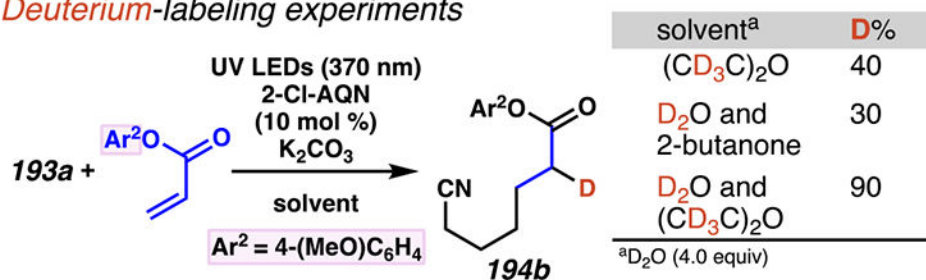
An Iminyl Radical Formation/  $\beta$ -Scission Cascade Can Be Used to Induce Vinylation, Alkynylation, or Alkylation



*Proposed reaction mechanism*

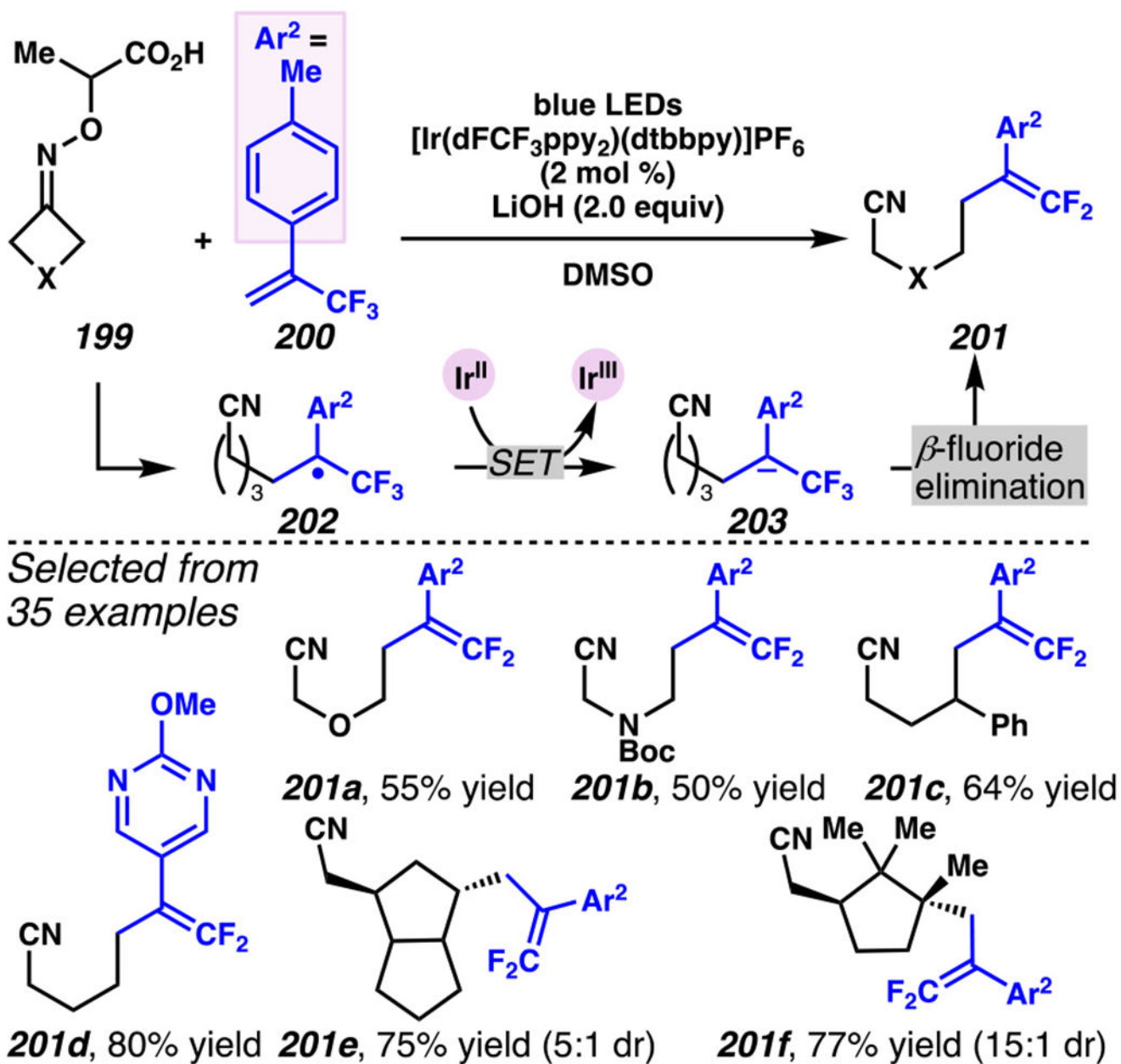


*Deuterium-labeling experiments*



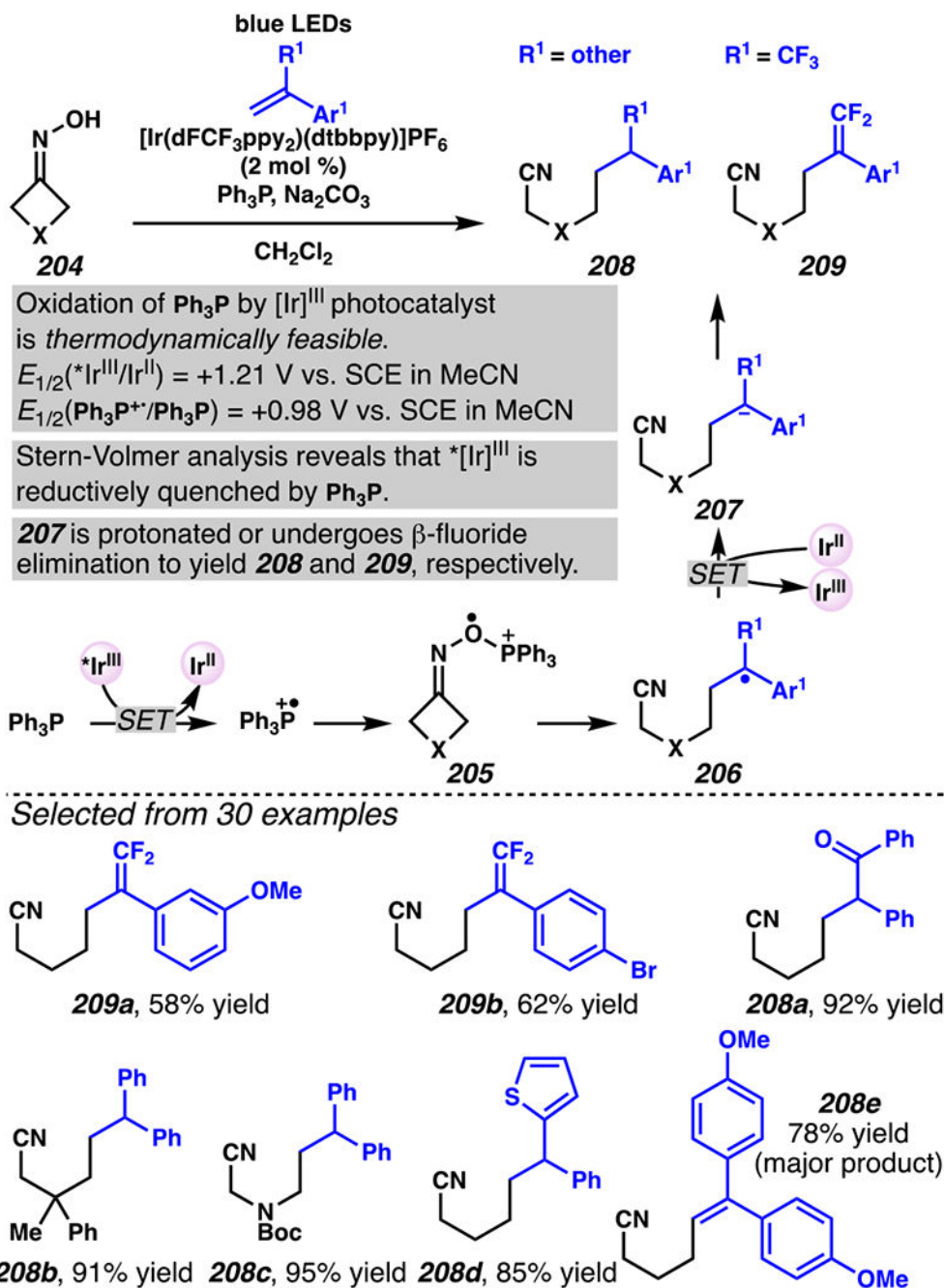
**Scheme 49.**

PMB-Substituents Make Oximes Labile to Oxidation, Which Can Facilitate a Photoinitiated Cascade Sequence

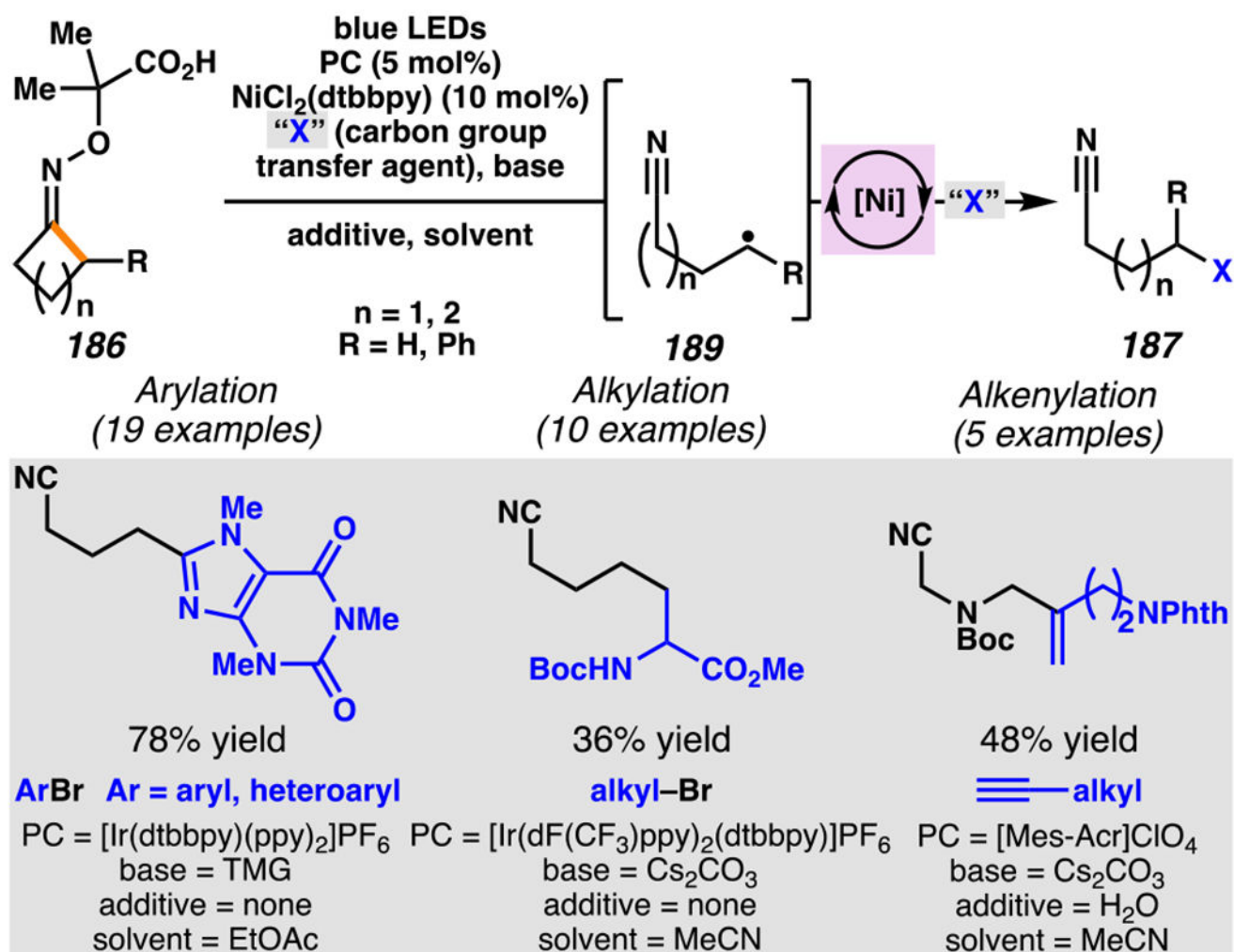


Scheme 50.

Hydroxy Acid-Derived Oximes Engage in Two-Component Coupling Reactions with  $\alpha$ -Trifluoromethyl Alkenes to Furnish *gem*-Difluoroalkenes



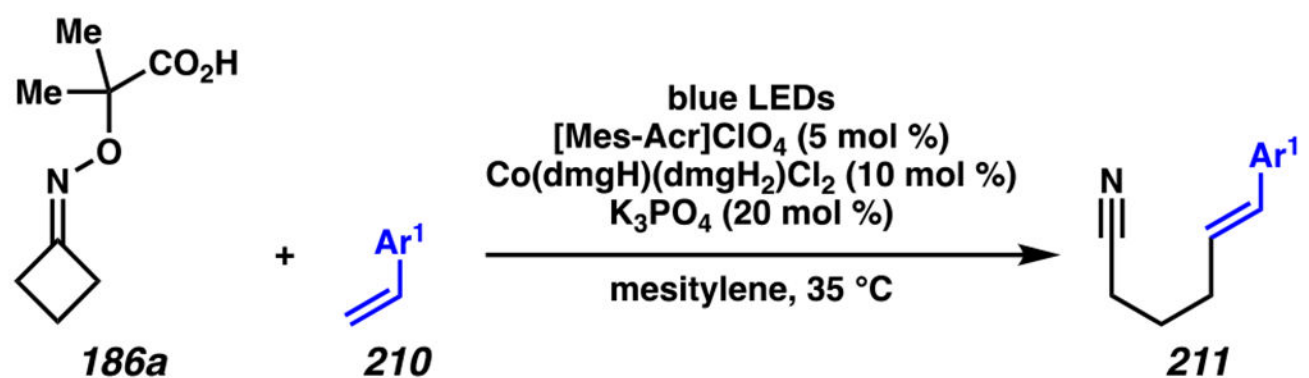
**Scheme 51.**  
 Triphenylphosphine Can Enable Hydroximes to Serve as Direct Precursors to Iminyl Radicals



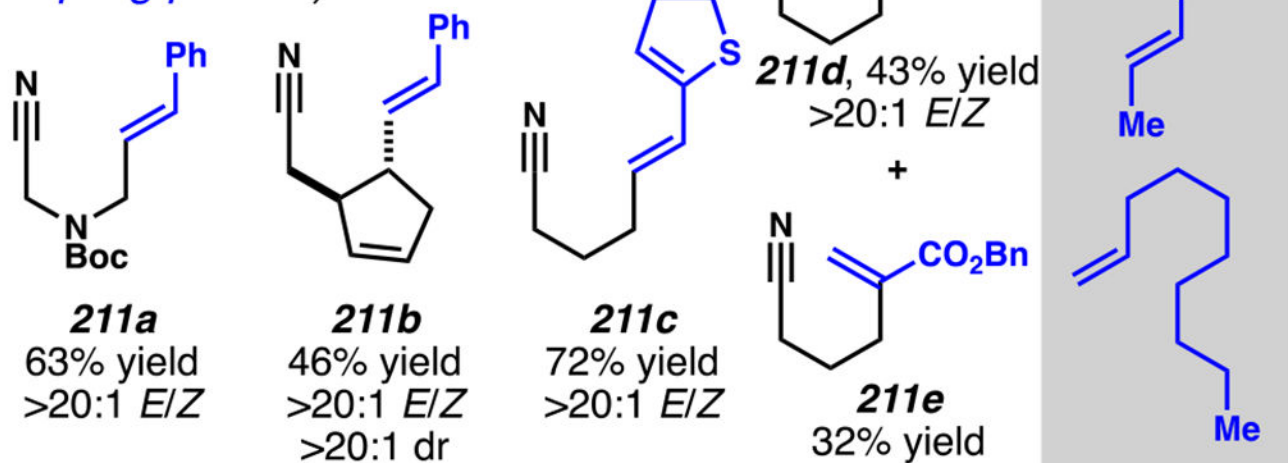
Scheme 52.

Dual Photoredox and Nickel Catalysts-Mediated Strategy Confers Synthetic Capabilities to Access Nitriles with New C–C Bonds

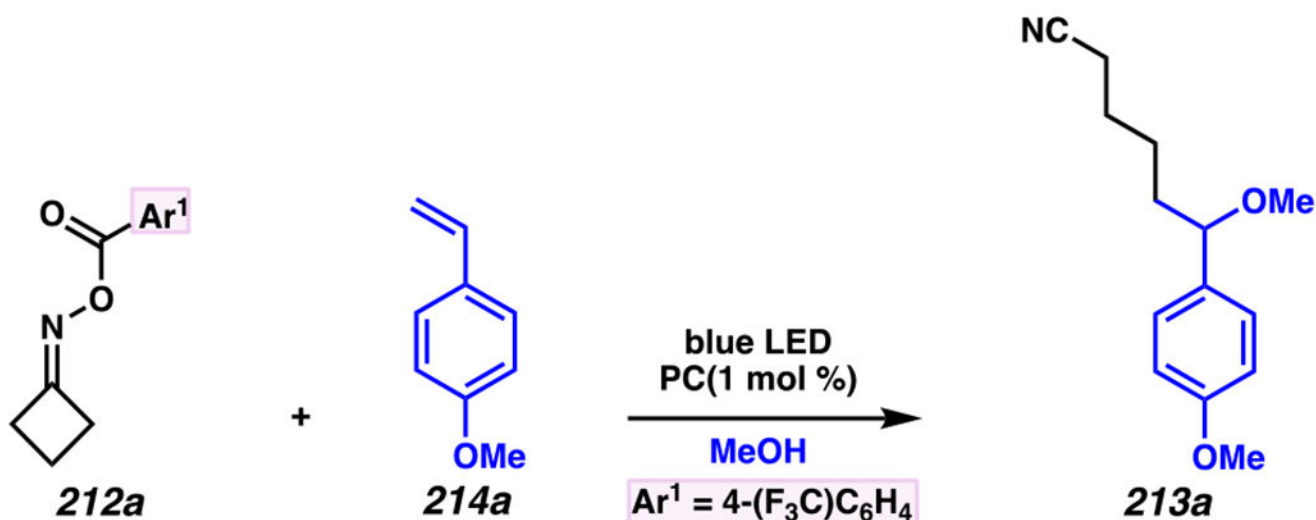




Selected from 31 examples  
(including 1,3-enyne as olefin  
coupling partner)



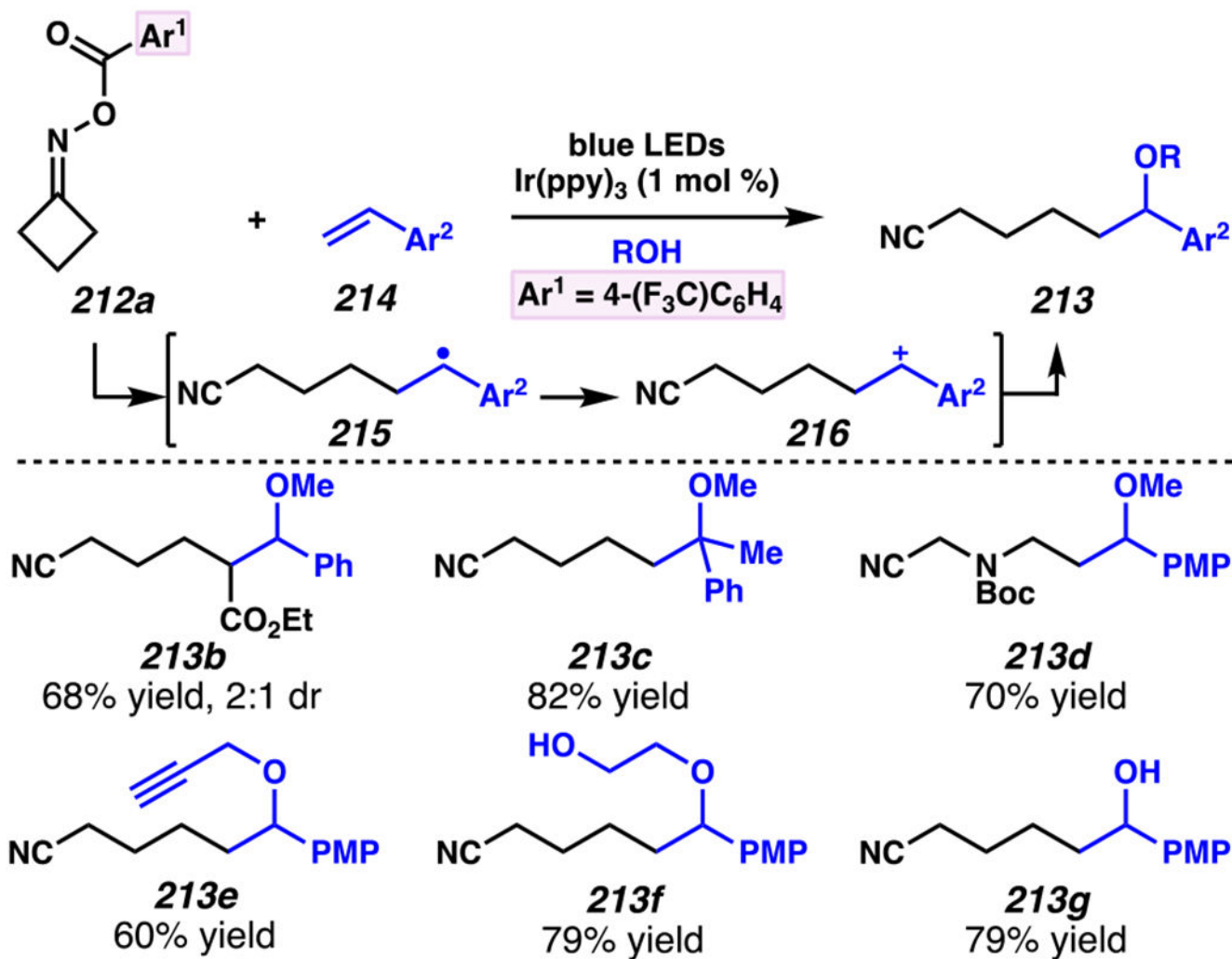
**Scheme 53.**  
Photoredox-Mediated and Cobalt-Catalyzed Intermolecular Heck-type Coupling Reaction Is Amenable with Cyclic Oxime and Styrenes



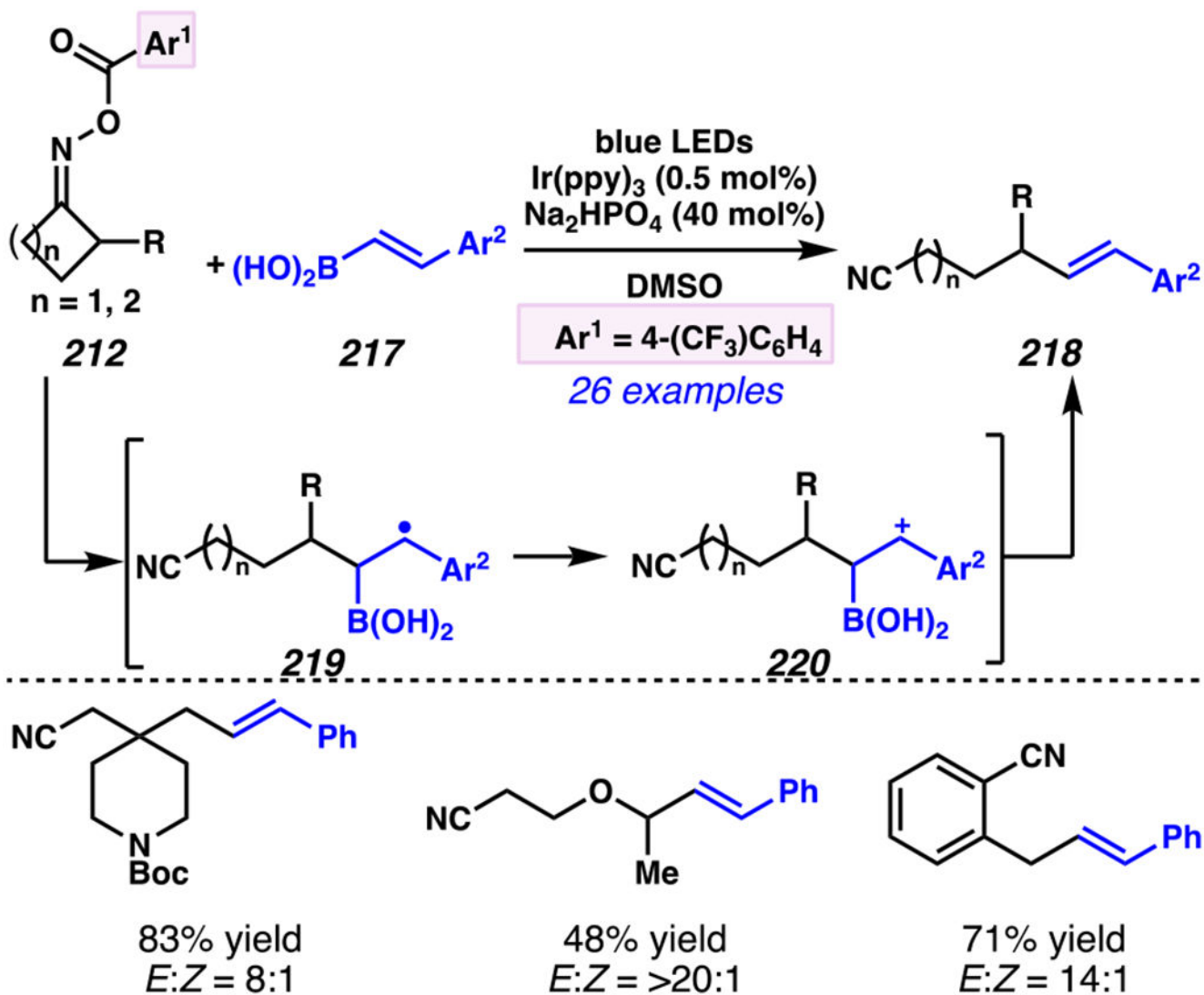
PC	$E_{1/2}(\text{PC}^+/\text{PC}^*)$ (V vs. SCE)	yield (%) <sup>a</sup>
Ir(ppy) <sub>3</sub>	-1.73	96
eosin Y	-1.11	62
<b>212a</b> $E_p^{\text{red}} = -0.99$ V vs. SCE in CH <sub>2</sub> Cl <sub>2</sub>		
rose bengal	-0.96	< 5
[Ir(ppy) <sub>2</sub> dtbbpy]PF <sub>6</sub>	-0.96	0
[Ir(dFCF <sub>3</sub> ppy) <sub>2</sub> dtbbpy]PF <sub>6</sub>	-0.89	0
Ru(bpy) <sub>3</sub> Cl <sub>2</sub>	-0.81	0

<sup>a</sup> <sup>1</sup>H NMR yield using an internal standard of CH<sub>2</sub>Br<sub>2</sub>.

**Scheme 54.**  
Strongly Reducing Photocatalyst Confers Optimal Reaction Efficiency in Three-Component Coupling Reactions

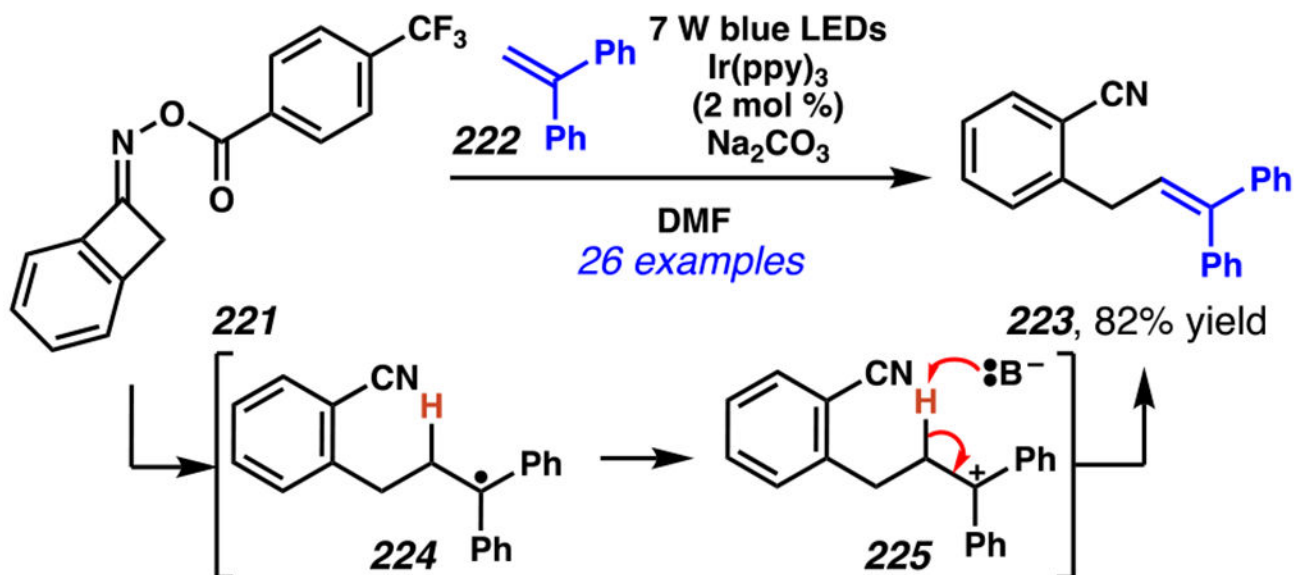


Scheme 55.  
 Three-Component Coupling Reactions Furnish Highly Decorated Aliphatic Nitriles

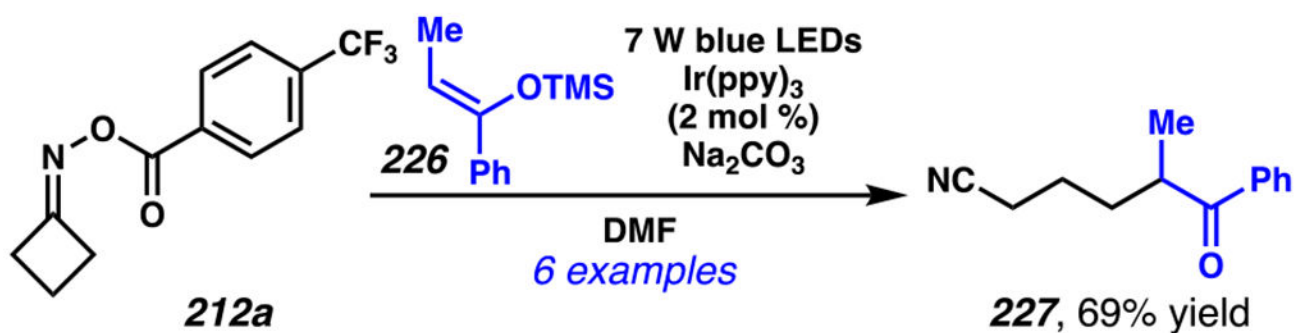


Scheme 56.  
 C–C Cleavage and Radical Addition Cascade Proceeds when *O*-Acyloximes React with Styrylboronic Acids to Affect a Net Vinylation Reaction

(A) Cascade C–C cleavage and radical addition between *O*-acyloximes and alkenes

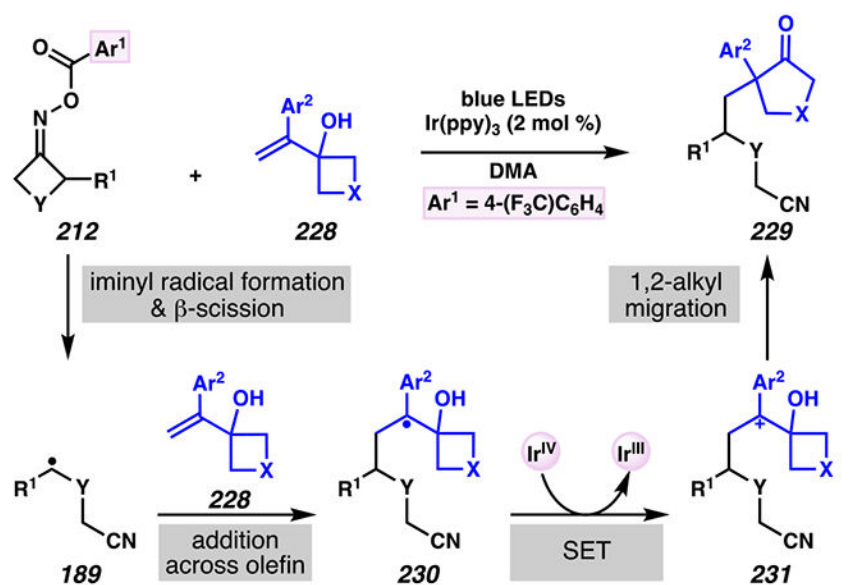


(B) Cascade C–C cleavage and radical addition between *O*-acyloximes and silyl enol ethers

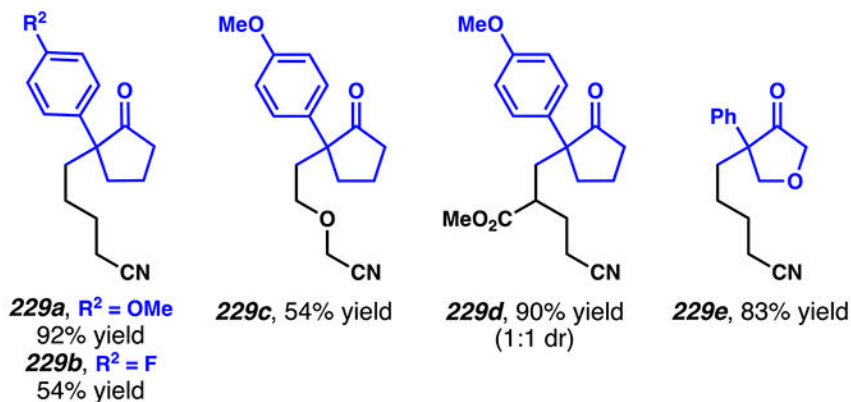


Scheme 57.

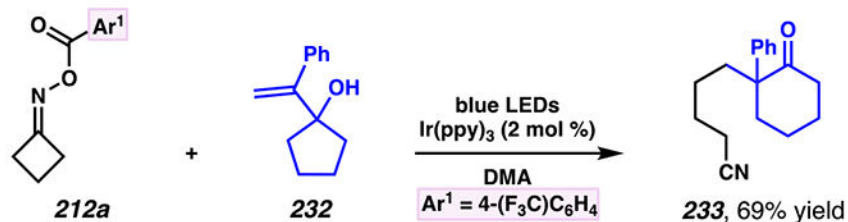
Cascade C–C Cleavage and Radical Addition Between *O*-Acylloximes and Olefin Radical Acceptors Provide Nitriles with  $\pi$ -Systems



Selected from 16 examples



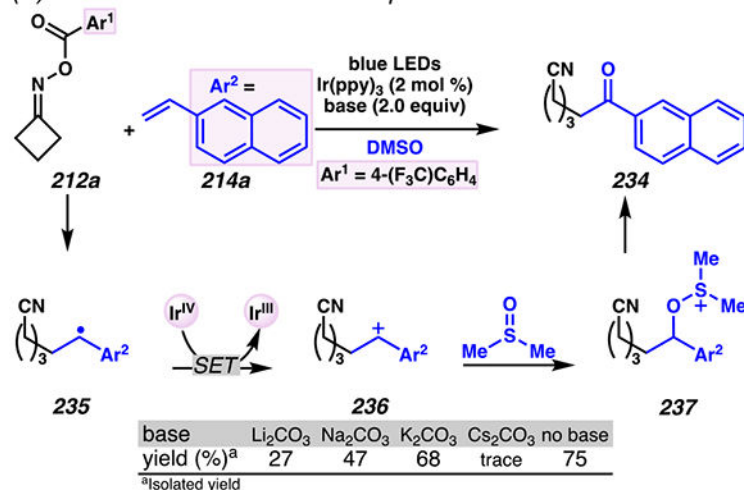
Cyclopentanol derivative engages in semi-pinacol rearrangement to provide cyclohexanone scaffold



#### Scheme 58.

When Terminal Alkenyl Cyclobutanols Are Radical Trapping Agents, They Ring Expand to Furnish Cyclopentanone Scaffolds

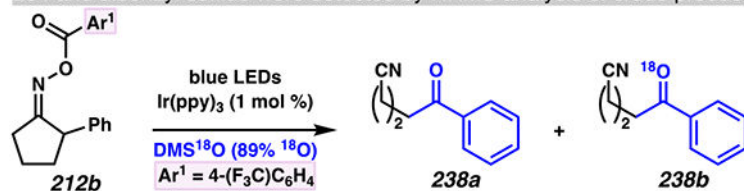
(A) The reaction manifold is most productive in absence of base



(B) HRMS experiment corroborates the dual role of DMSO as a reaction solvent and an oxidant

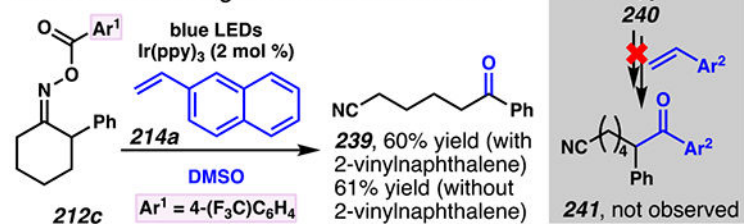


234 and dibenzyl sulfide were detected by HRMS analysis of crude product.



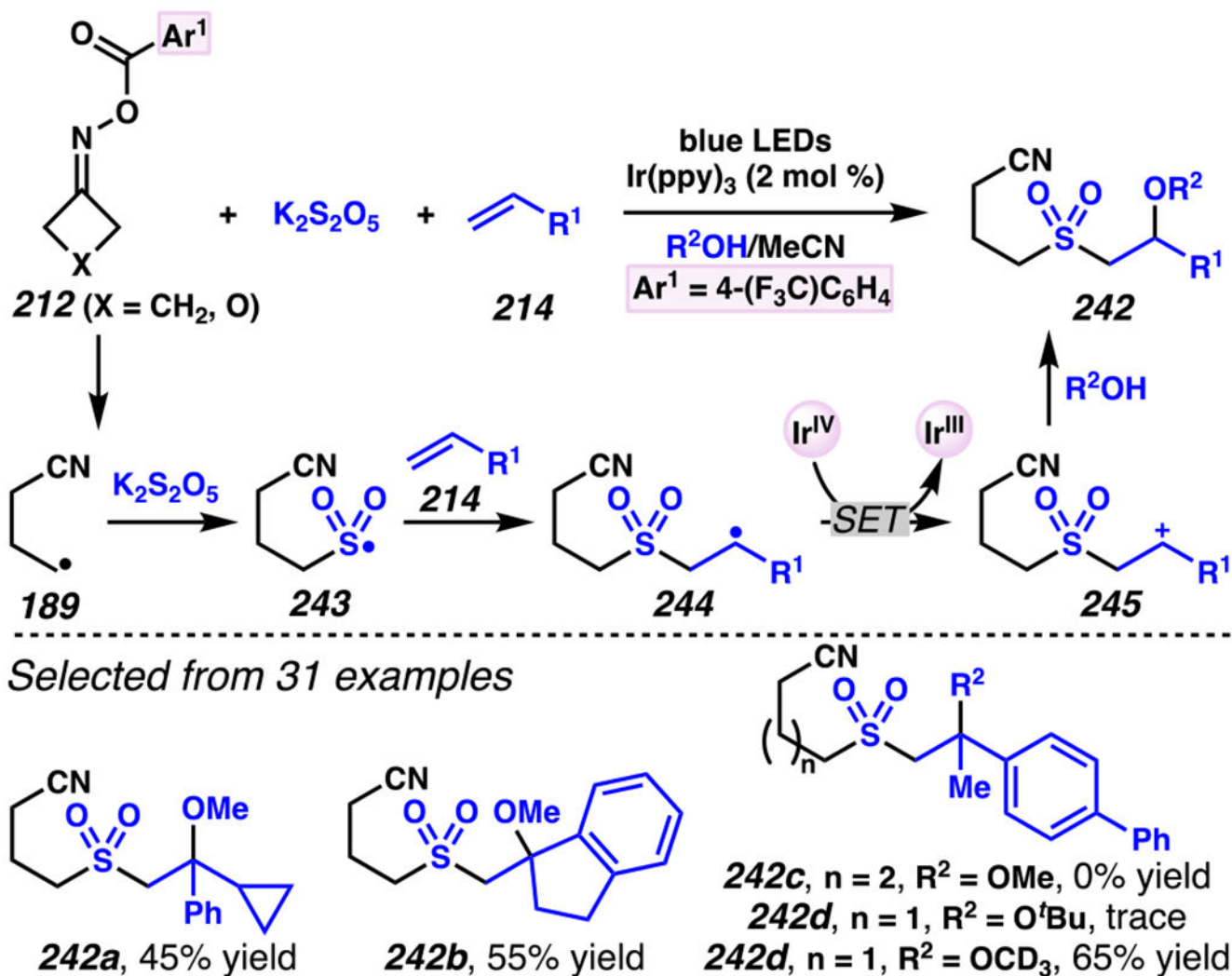
27:73 of 238a:238b detected by HRMS analysis of reaction mixture.

(C) Benzyl radical bypasses radical addition to olefin and undergoes Kornblum oxidation



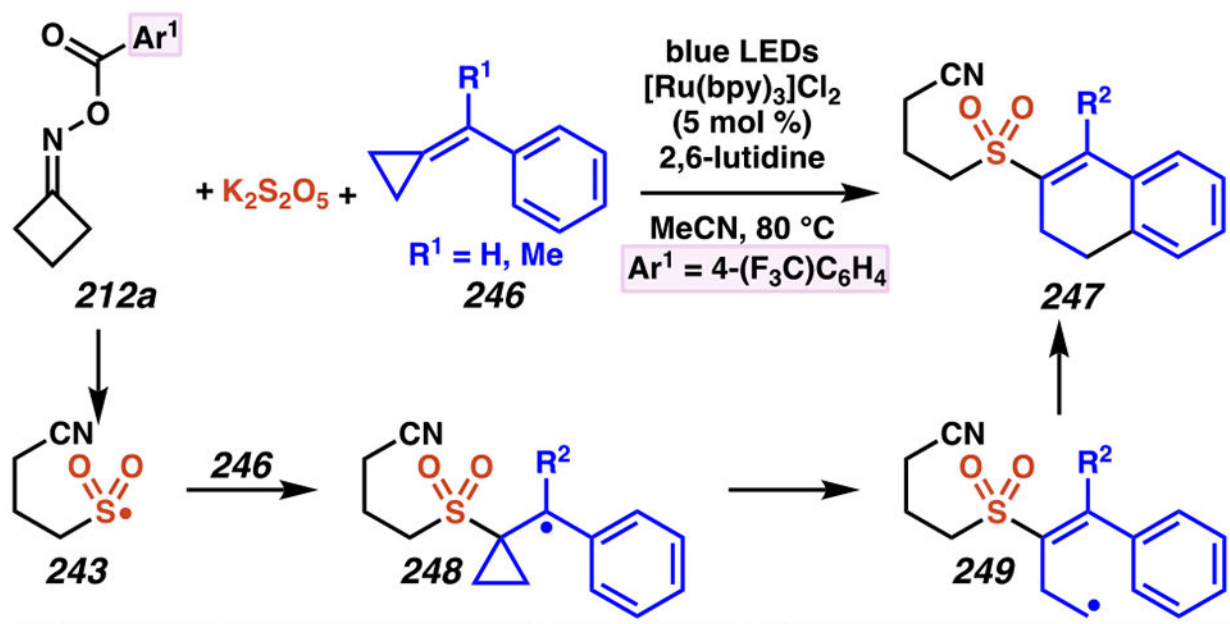
### Scheme 59.

Base-Free C–C Cleavage / Radical Addition / Kornblum Oxidation Cascade Reactions Are Triggered by Photoredox Catalysts in the Presence of Vinylarenes and DMSO

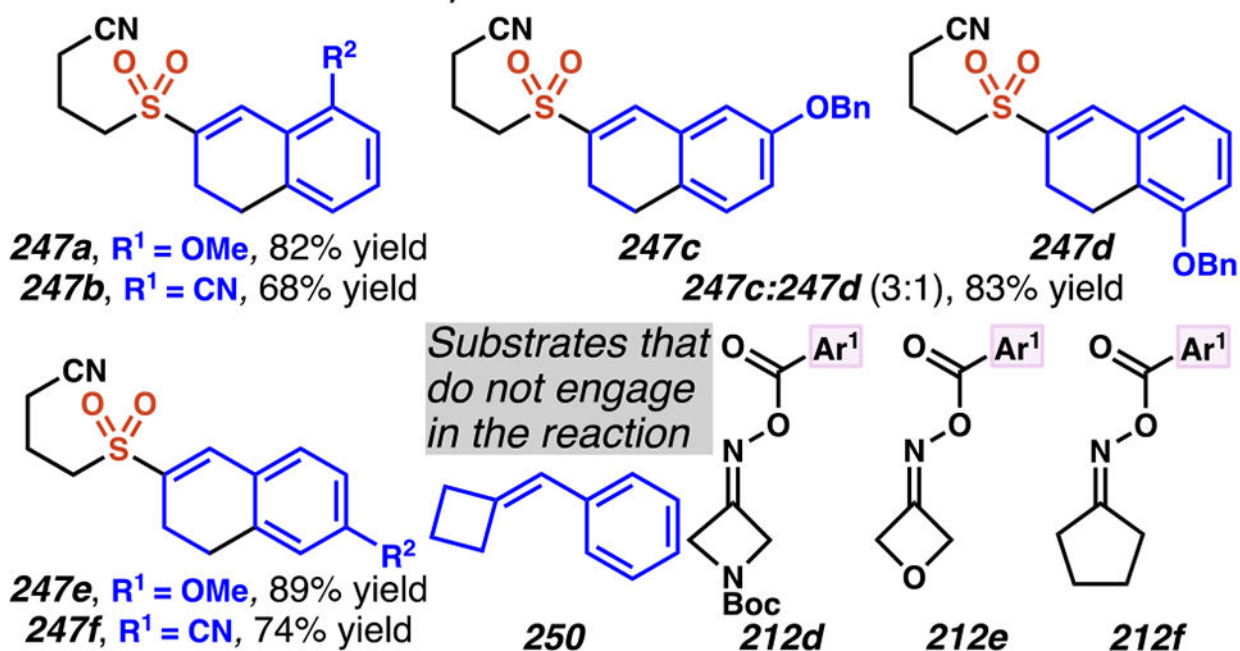


Scheme 60.  
 Potassium Metabisulfite Is an Effective SO<sub>2</sub> Source to Assemble Benzylic Sulfones



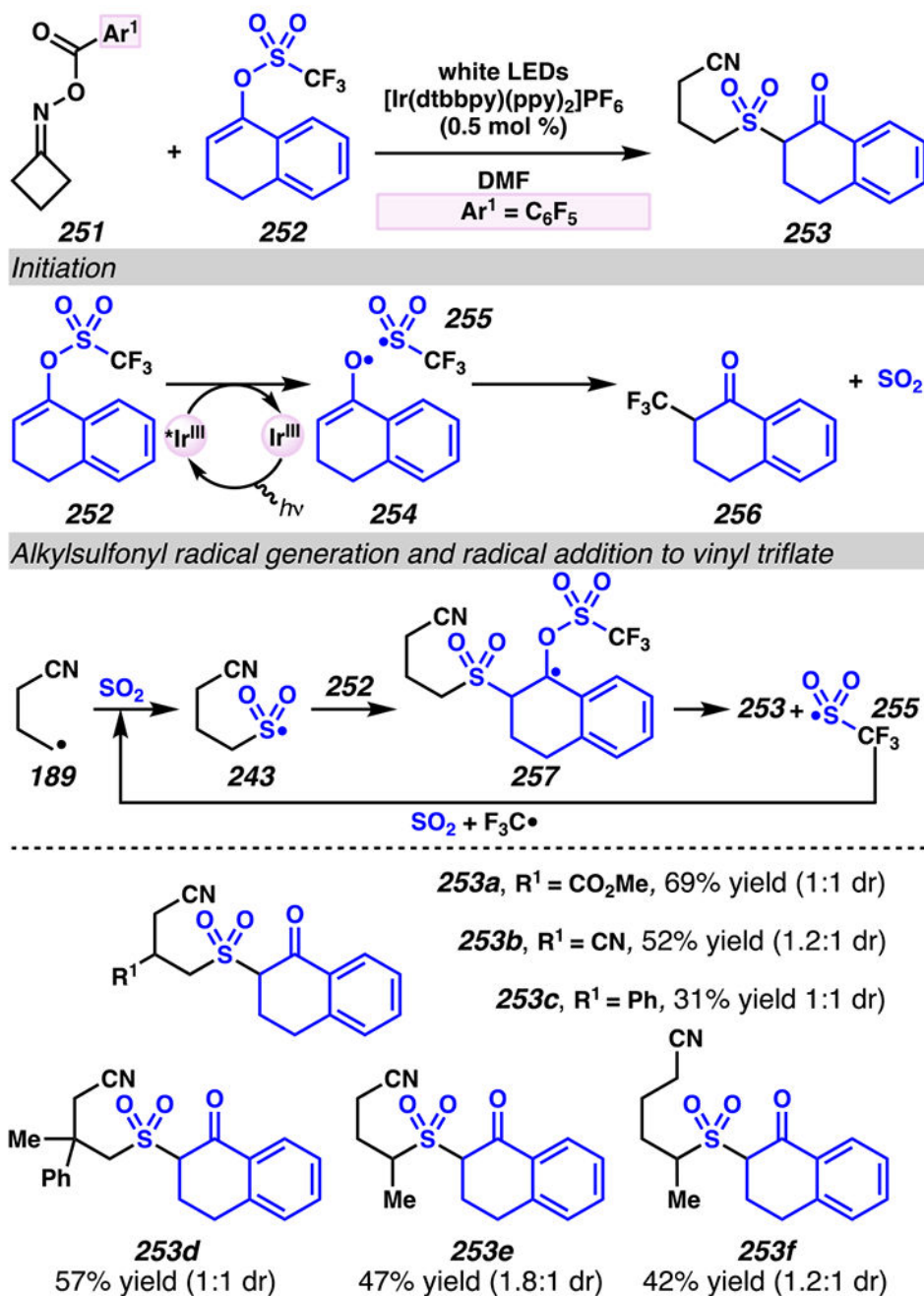


Selected from 40 examples



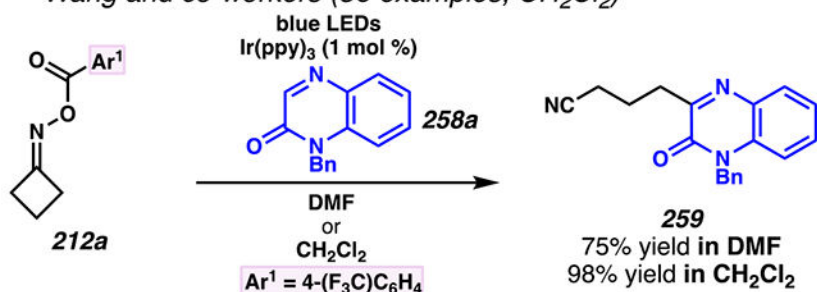
Scheme 61.

Reactions of Alkylsulfonyl Radicals with 2-Aryl-Substituted Methylenecyclopropanes Leads to Cyanoalkylsulfonylated 3,4-Dihydronaphthalene Scaffolds

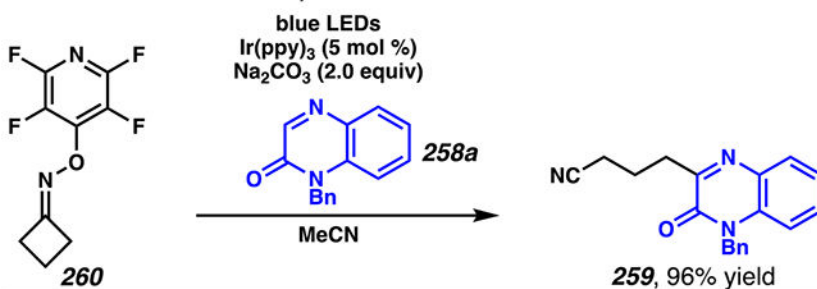
**Scheme 62.**

Oximes and Vinyl Triflate Engage in  $\beta$ -Scission / Radical Addition / Radical Fragmentation to Construct  $\beta$ -Ketonesulfones

(A) Kong, Xu and co-workers (35 examples, DMF)  
Wang and co-workers (36 examples, CH<sub>2</sub>Cl<sub>2</sub>)



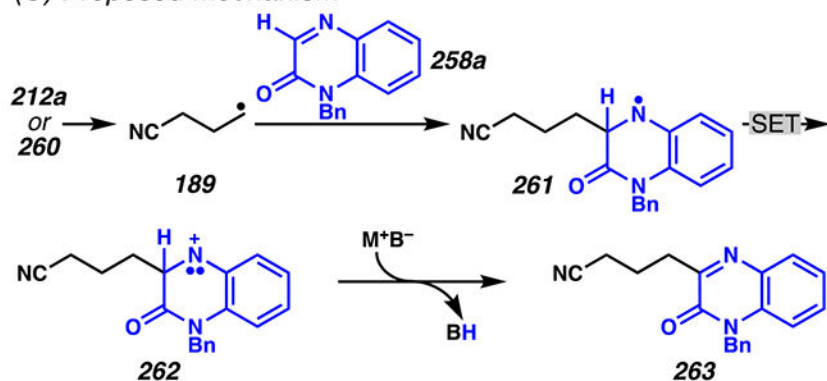
(B) Xiang, Yang and co-workers  
Selected from 22 examples



The impact of Ir(ppy)<sub>3</sub> in this reaction is unclear:

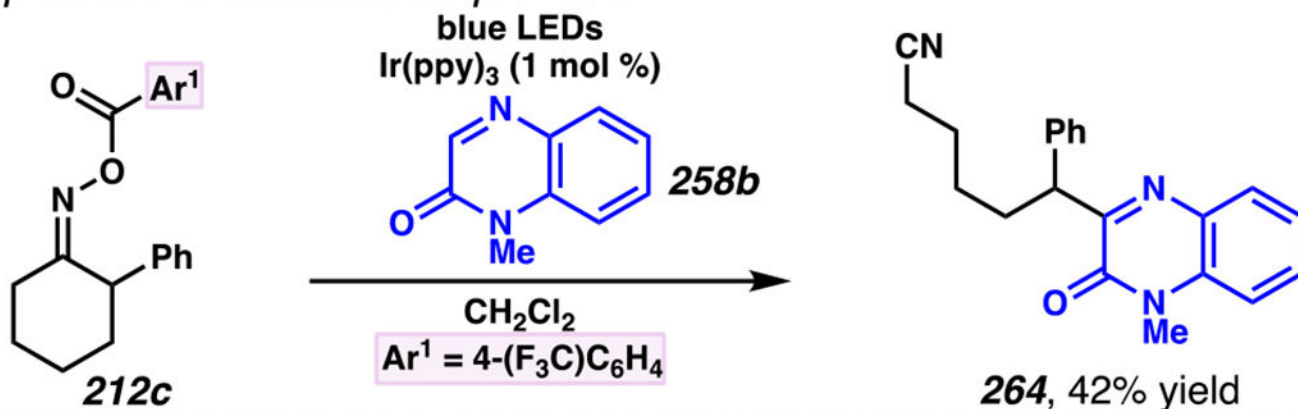
- The reduction of substrate **260** ( $E_{p/2} = -1.49$  V vs. SCE) by Ir(ppy)<sub>3</sub> ( $E_{1/2}[^*Ir^{III}/Ir^{IV}] = -1.73$  V vs. SCE) is thermodynamically feasible.
- In absence of light, the reaction yields 60% of product **259**.
- In absence of Ir(ppy)<sub>3</sub>, the reaction yields trace product **259**.

(C) Proposed Mechanism

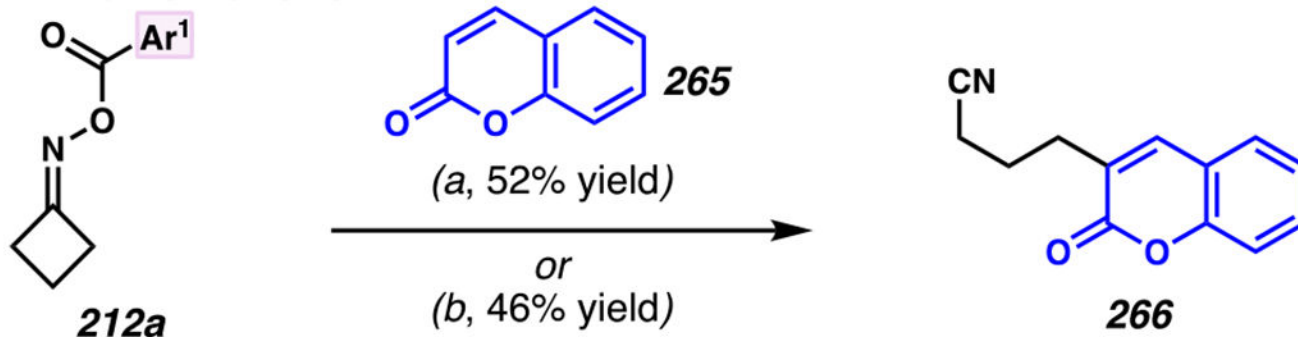


**Scheme 63.**  
Photoredox-Mediated Minisci-Type Reactions Rely on Cyclic Oximes and Quinoxalinones

(A)  $\alpha$ -Phenyl substituted six-membered cyclic oxime engages in productive cascade sequences



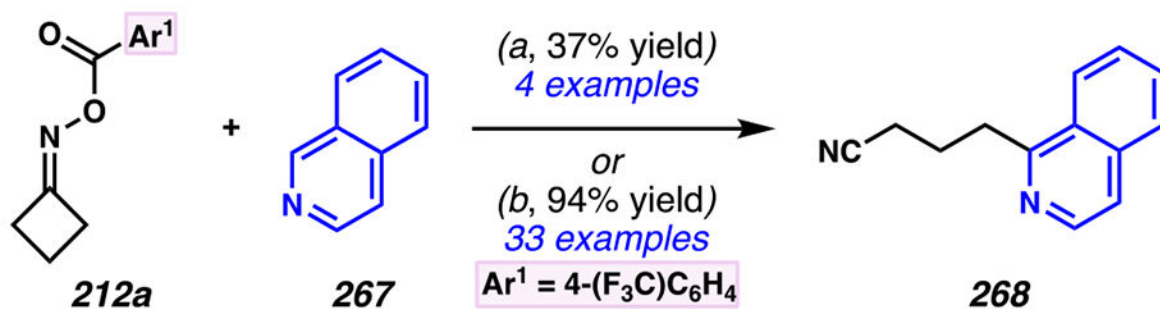
(B) Cyclic oxime can engage in base-free cascade sequences with chromenone



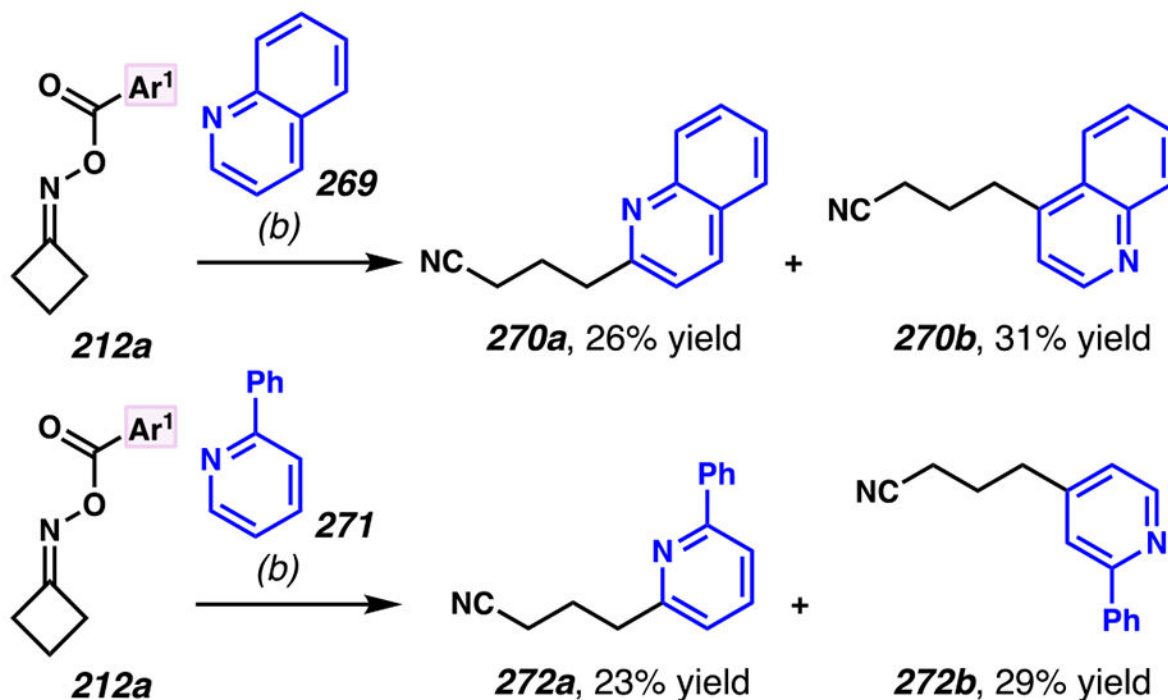
(a) Blue LEDs, Ir(ppy)<sub>3</sub> (2 mol %), Na<sub>2</sub>CO<sub>3</sub> (2.0 equiv), DMF (Wang and co-workers).  
(b) Blue LEDs, Ir(ppy)<sub>3</sub> (1 mol %), DMF (Chen, Xiao and co-workers).

Scheme 64.

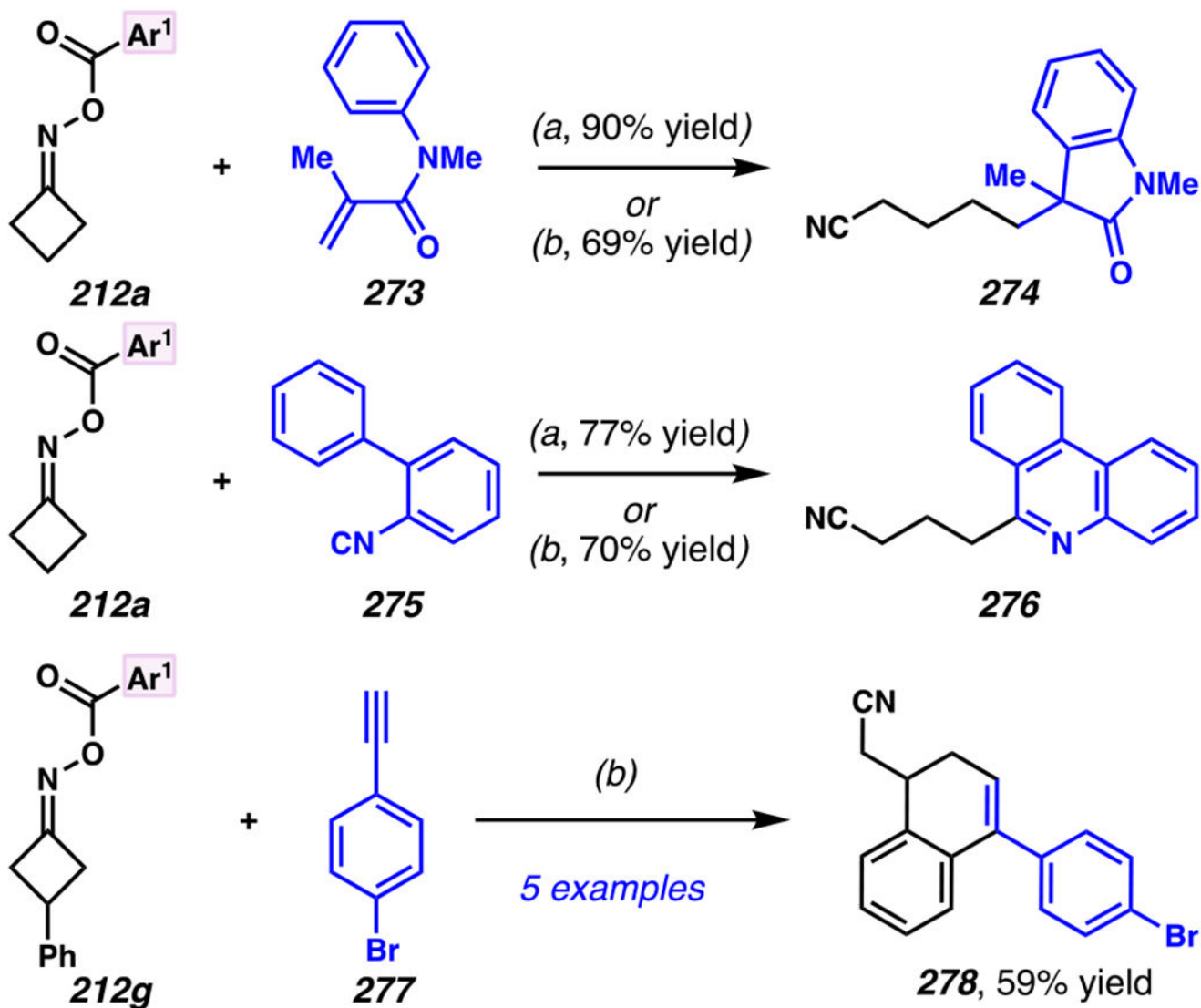
$\alpha$ -Phenyl Substituted Six-Membered Cyclic Oxime and Chromenone are Viable Substrates

**(A) Minisci-type reactions with heterocycles**

(a) Blue LEDs, Ir(ppy)<sub>3</sub> (1 mol %), CH<sub>2</sub>Cl<sub>2</sub> (Wang and co-workers). (b) Blue LEDs, Ir(ppy)<sub>3</sub> (1 mol %), TFA (1.5 equiv), MeCN (Yang, Xia and co-workers).

**(B) Minisci-type reactions with unsubstituted quinoline and 2-phenylpyridine give regioisomeric mixture of products****Scheme 65.**

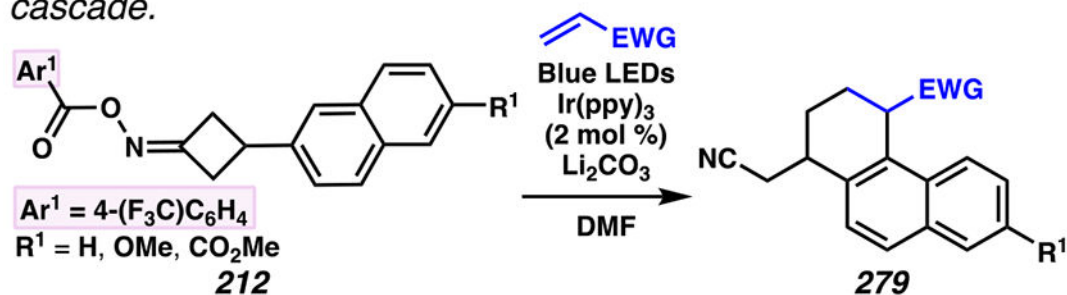
Cyclic Oximes Can Participate in Minisci-Type Reactions with Heterocycles to Furnish Alkylated Isoquinolines, Quinolines and Other Heteroarenes



**Ar<sup>1</sup> = 4-(F<sub>3</sub>C)C<sub>6</sub>H<sub>4</sub>** (a) 5 W blue LEDs, Ir(ppy)<sub>3</sub> (1 mol %), DCE (Zhou and co-workers).  
 (b) 7 W blue LEDs, Ir(ppy)<sub>3</sub> (2 mol %), Na<sub>2</sub>CO<sub>3</sub> (2.0 equiv), DMF (Chen, Xiao and co-workers).

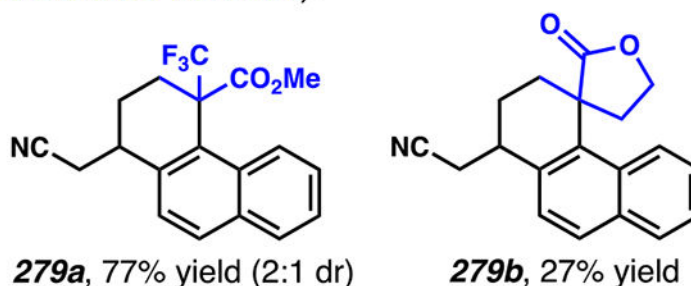
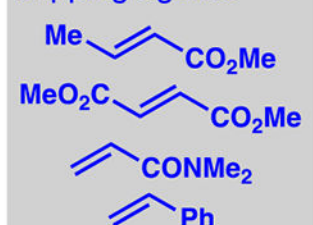
**Scheme 66.**  
 Vinyl Arenes Are Not the Only Radical Acceptors That Engage in Coupling Reactions with *O*-Acyloximes

(A) 3-naphthyl-substituted *O*-acyl oximes and electron-deficient olefins engage in  $\beta$ -scission / radical formal [4+2] cycloaddition cascade.

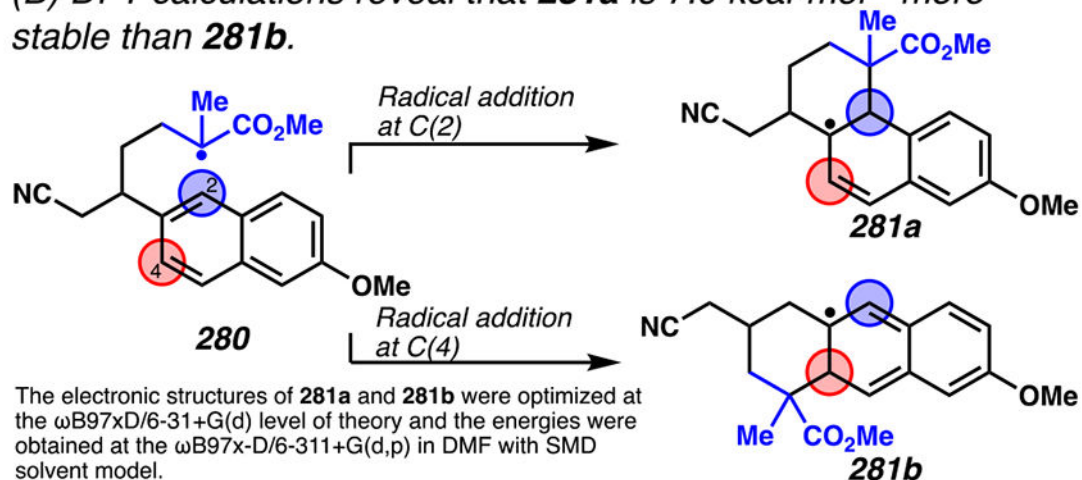


Selected from 19 examples (radical trapping agents include acrylonitrile and  $\alpha,\beta$ -unsaturated ketones).

Unsuccessful radical trapping agents



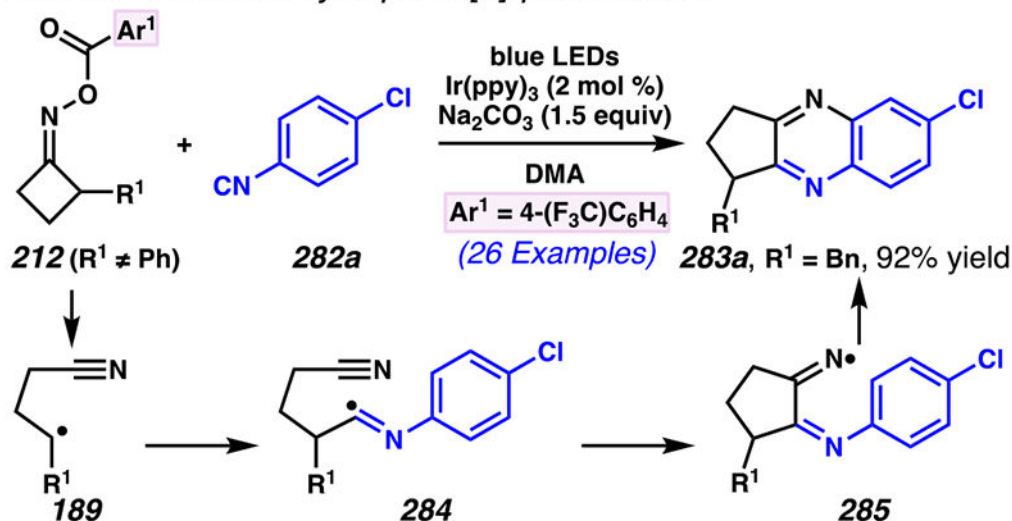
(B) DFT calculations reveal that **281a** is  $7.0 \text{ kcal}\cdot\text{mol}^{-1}$  more stable than **281b**.



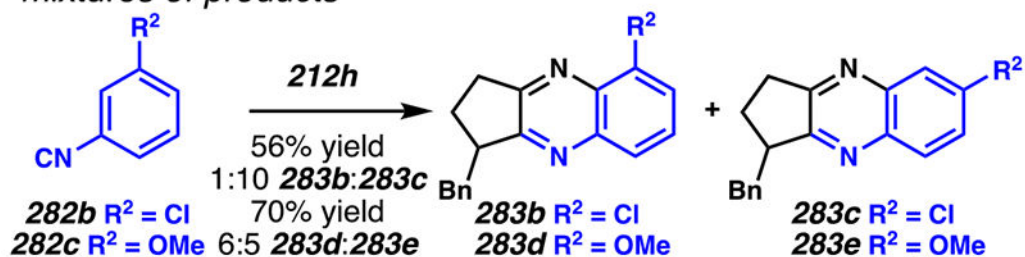
#### Schemes 67.

3-Naphthyl Substituted *O*-Acyl Oximes and Electron-Deficient Olefins Engage in Position-Selective Radical Annulation Cascade to Synthesize 1,2,3,4-Tetrahydrophenanthrene Scaffolds

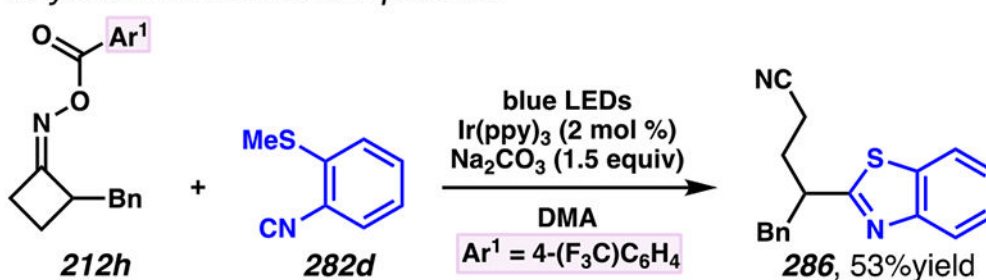
(A) Cyclic oximes and aryl isonitriles undergo radical annulation cascade to furnish cyclopenta[*b*]quinoxalines



(B) Meta-substituted aryl isonitriles give rise to regioisomeric mixtures of products



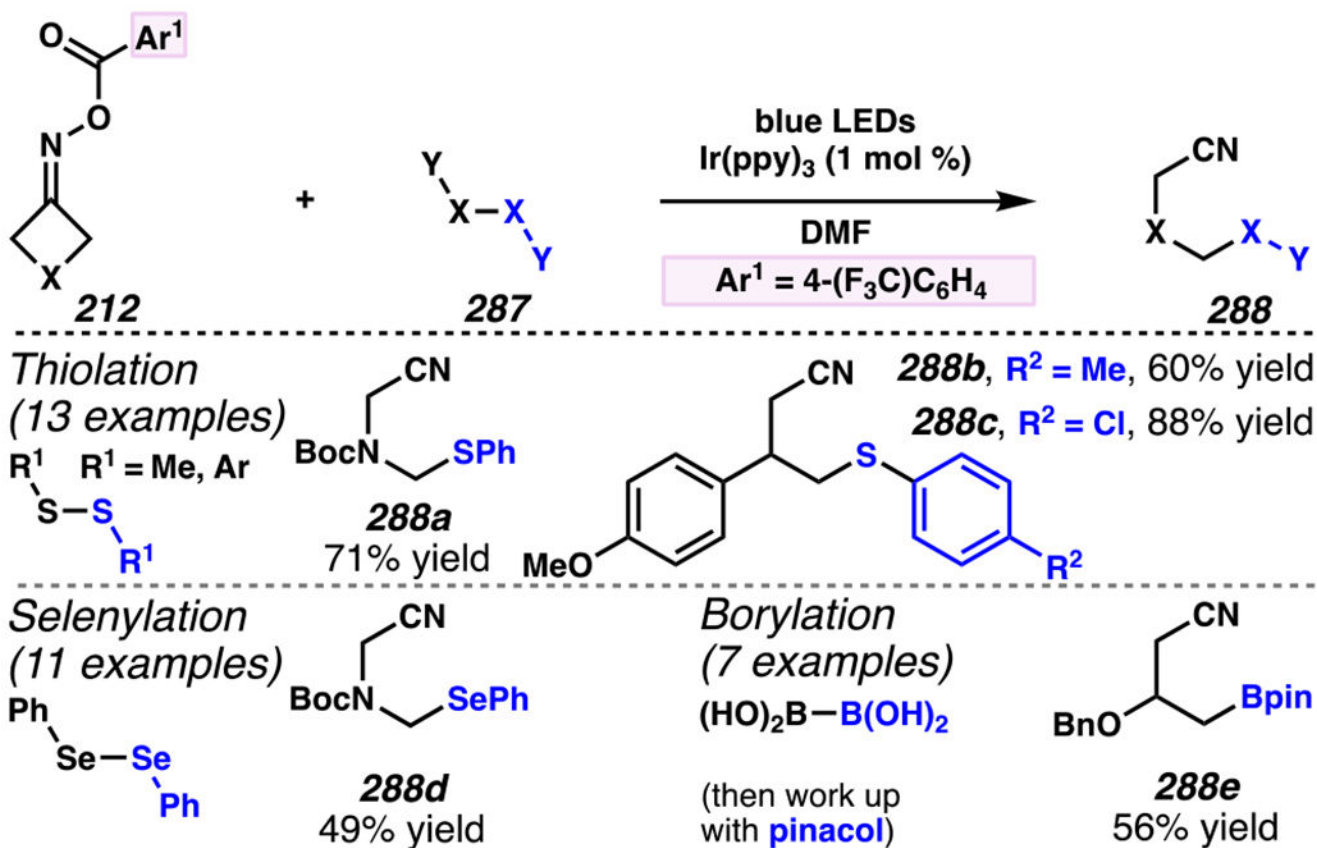
(C) Ortho-thiomethyl substituted aryl isonitrile instead delivers alkylated benzothiazole product



Scheme 68.

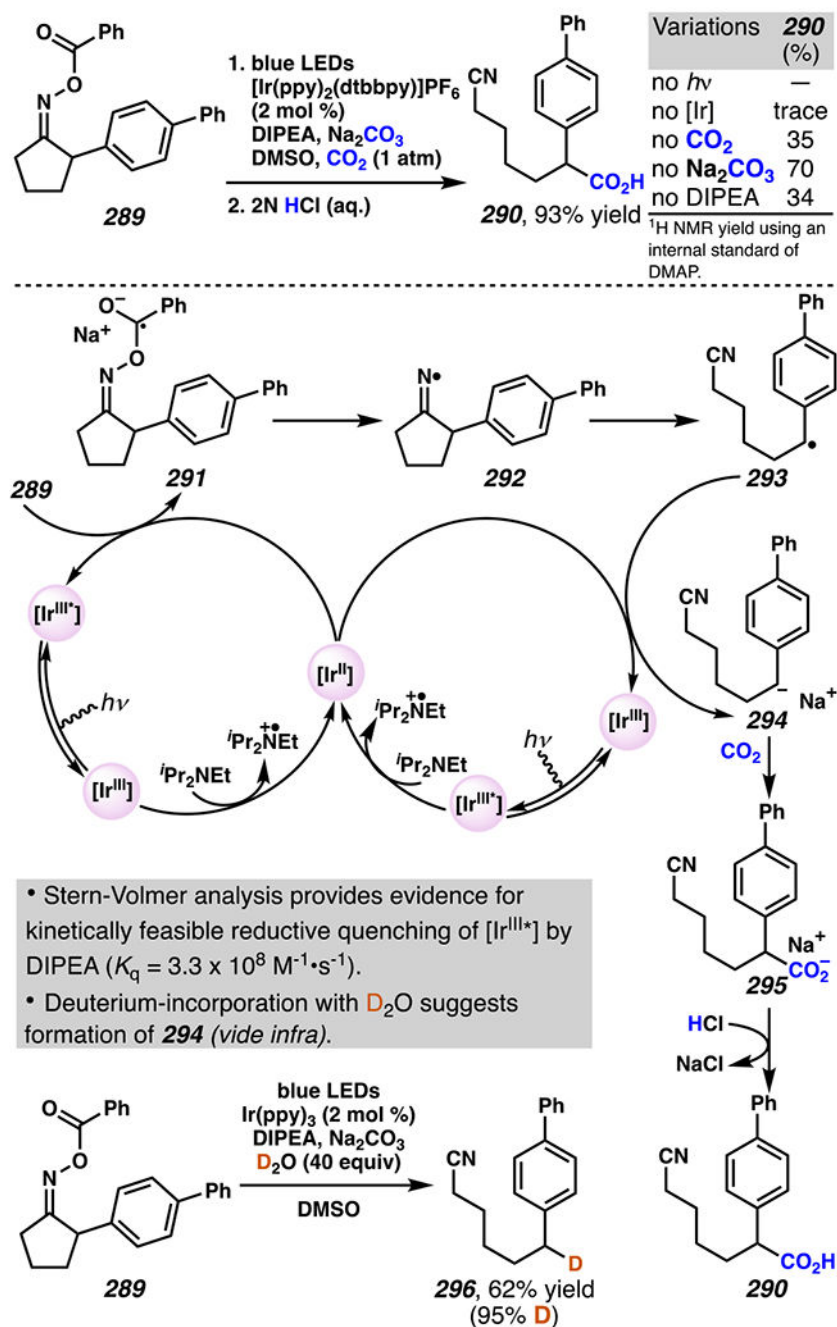
Cyclopenta[*b*]quinoxaline Derivatives Are Synthesized from Radical Annulation Cascade Reaction Between Cyclic Oximes and Aryl Isonitriles, with Well-Documented Limitations



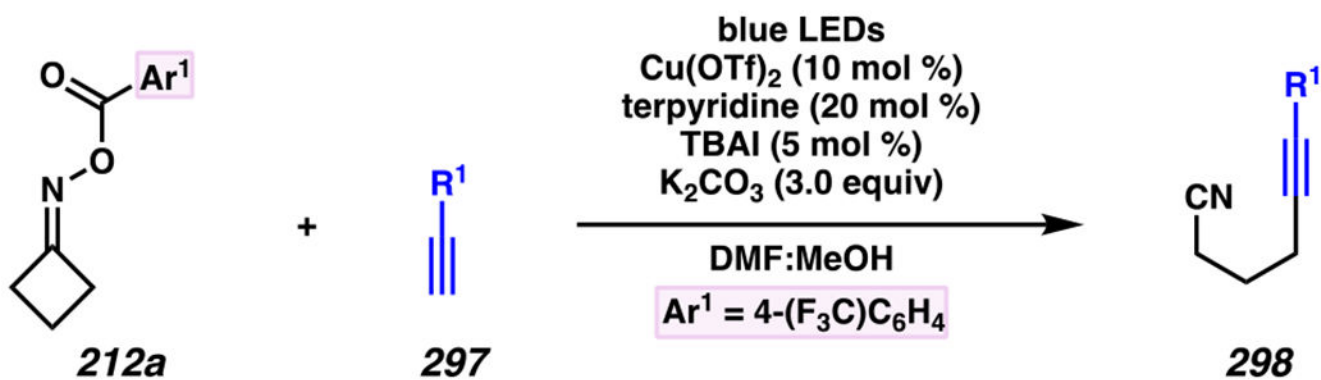


Scheme 69.

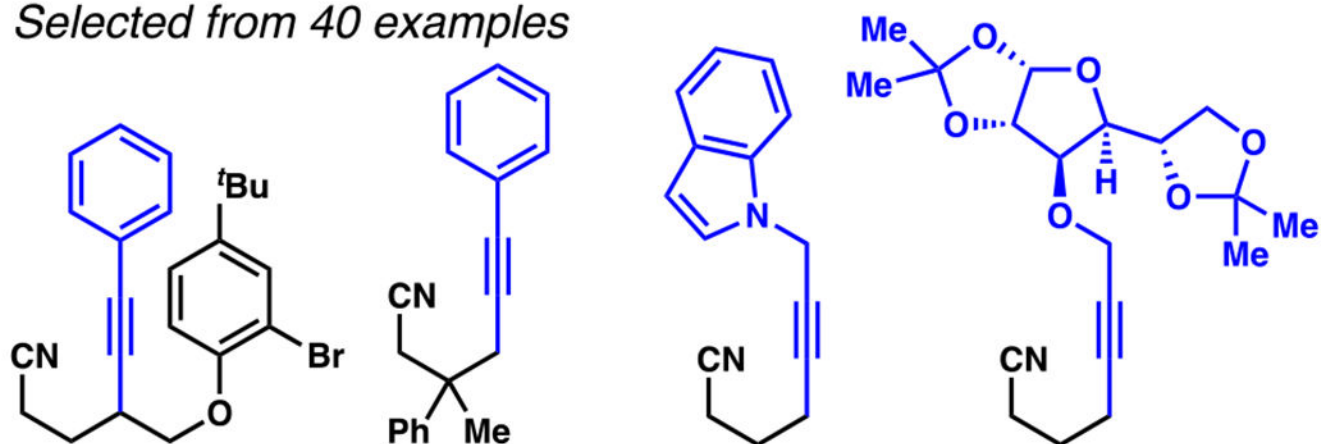
Oximes Participate in Group-Transfer Reactions with Disulfides, Diphenylselenide and Diboronic Acids



**Scheme 70.**  
Oxime Can Engage in Carboxylation Reaction with  $\text{CO}_2$  to Access Carboxylic Acids



*Selected from 40 examples*



**298a**, 77% yield **298b**, 59% yield **298c**, 55% yield **298d**, 43% yield

**Scheme 71.**

In Principle, Copper Can Serve as a Dual Photoredox- and Transition-Metal Catalyst and Both of These Mechanisms Could Be Operative in the C(sp)–C(sp<sup>3</sup>) Cross-Coupling Reaction Between Cyclic Oximes and Terminal Alkynes

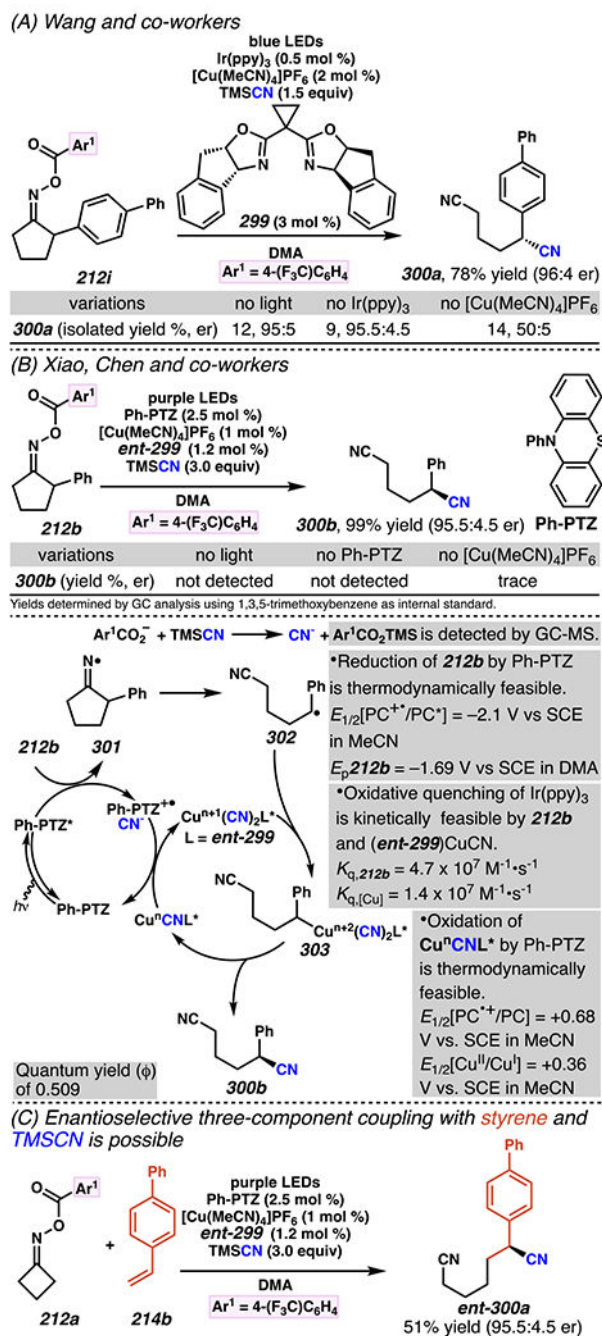
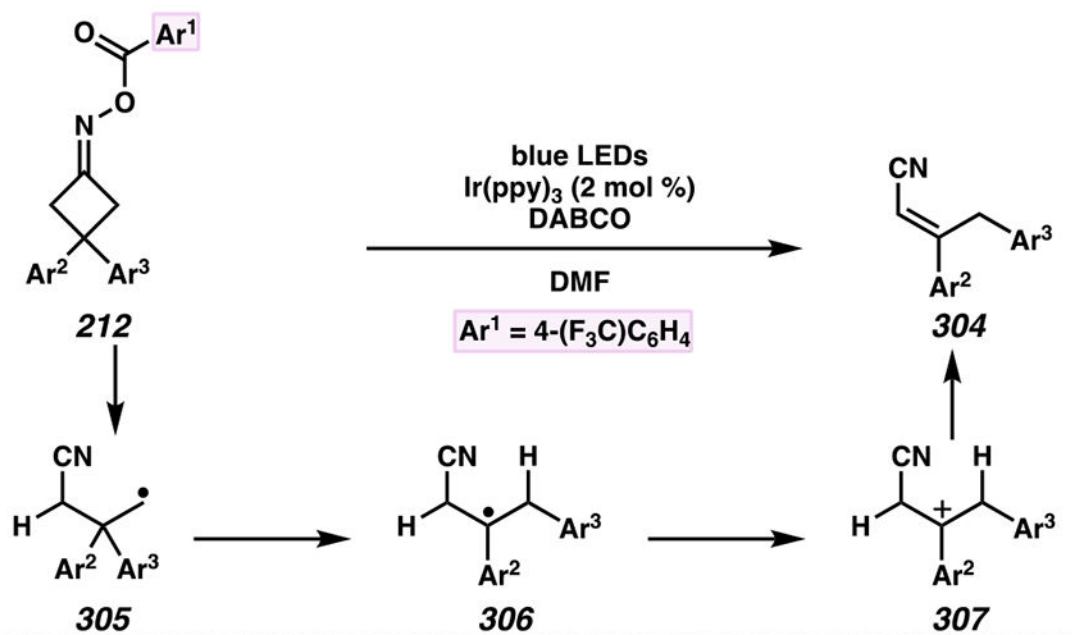
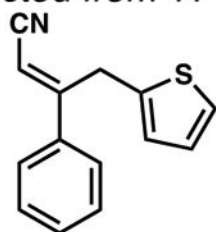
**Scheme 72.**

Photo- and Copper-Mediated Enantioselective Cyanation Reactions Rely on Chiral Bisoxazoline Ligands

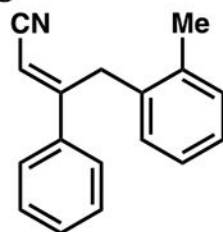


Selected from 11 examples



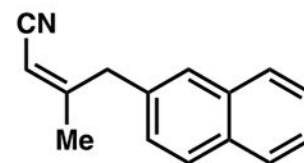
**304a**

55% yield (15:1 *E:Z*)



**304b**

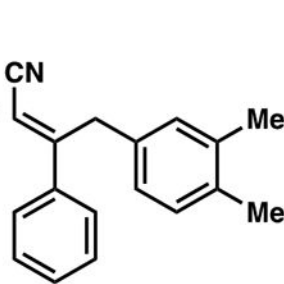
68% yield (6:1 *E:Z*)



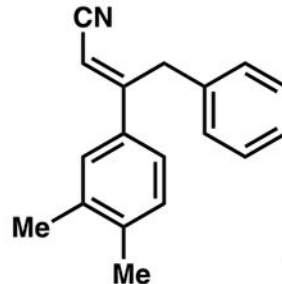
**304c**

48% yield (only *Z*-isomer)

*Aryl groups with similar electronic and steric profiles gives mixture of 1,2-migration products*



**304d**

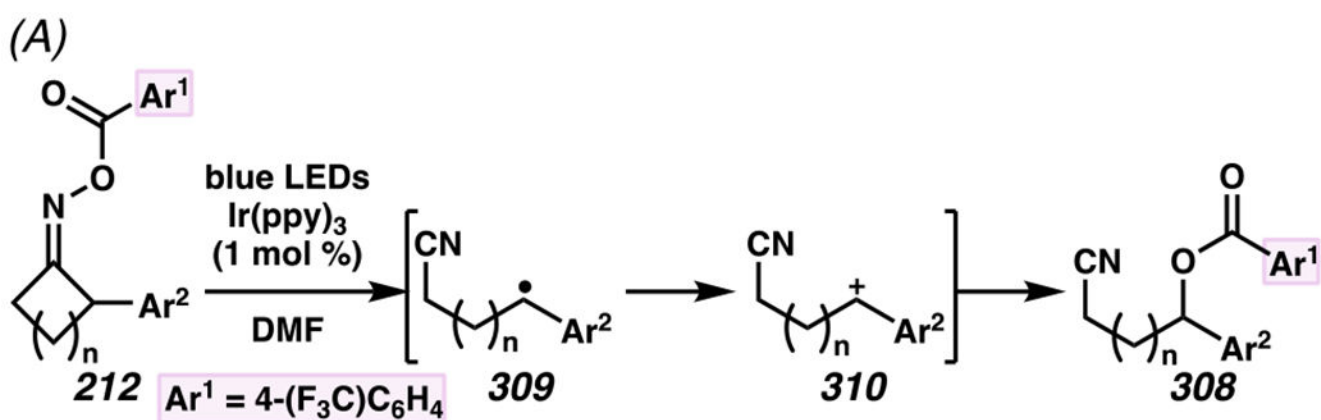


**304d**

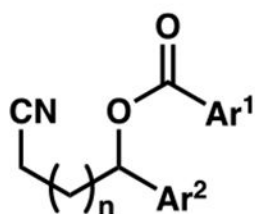
61% yield  
**304d/304e**  
 1:1 (8:1 *E:Z*)

Scheme 73.

Diaryl Substituted Oximes Engage in  $\beta$ -Scission / 1,2-Aryl Migration / Elimination Cascade



Selected from  
15 examples



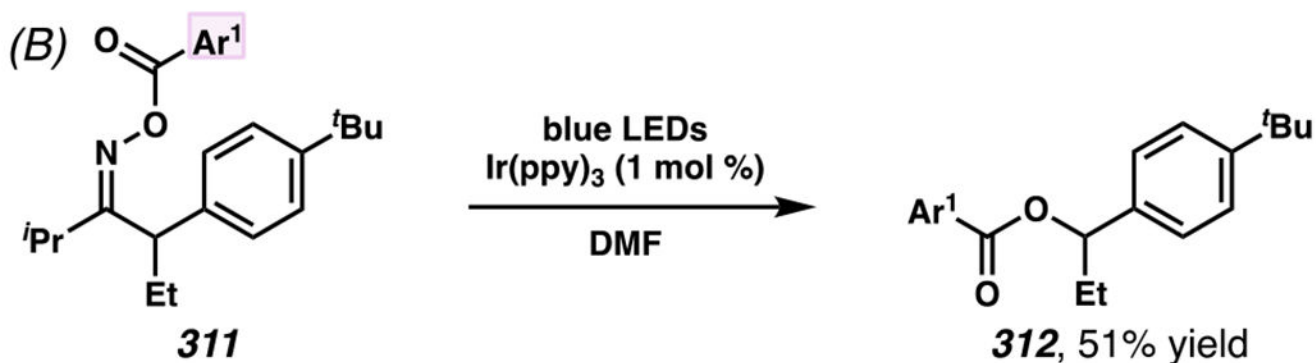
**308a**,  $n = 1$ ,  $\text{Ar}^2 = \text{Ph}$ , 54% yield

**308b**,  $n = 2$ ,  $\text{Ar}^2 = \text{Ph}$ , 81% yield

**308c**,  $n = 3$ ,  $\text{Ar}^2 = \text{Ph}$ , 48% yield

**308d**,  $n = 4$ ,  $\text{Ar}^2 = 4\text{-(OMe)C}_6\text{H}_4$ , 63% yield

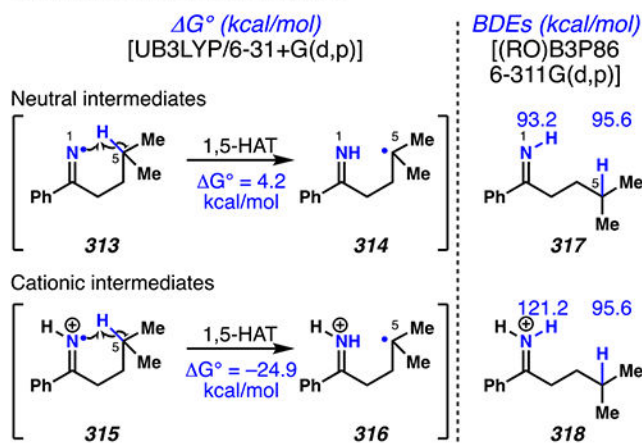
**308e**,  $n = 5$ ,  $\text{Ar}^2 = 4\text{-(OMe)C}_6\text{H}_4$ , 69% yield



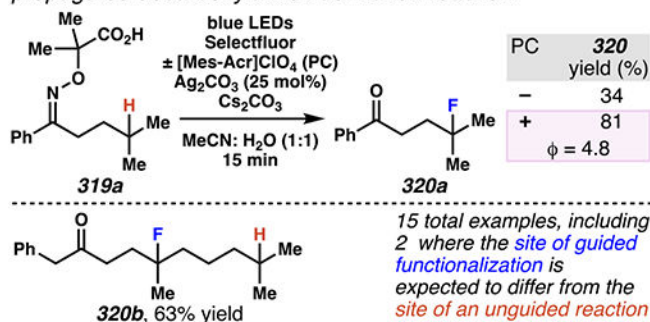
Scheme 74.

Absent Radical Trapping Agents, Aryl Acetate Quenches Carbocationic Intermediates

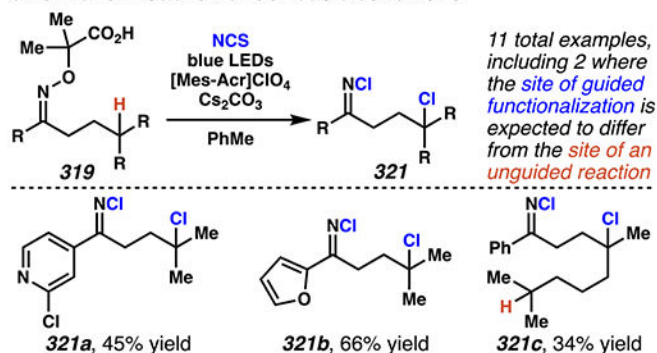
(A) Based on calculations, acidic conditions enable the C–H abstraction step to be exergonic.



(B) Nevertheless, 1,5-HAT is feasible under basic conditions where photocatalyst accelerates turnover in radical chain propagated decarboxylative fluorination reaction

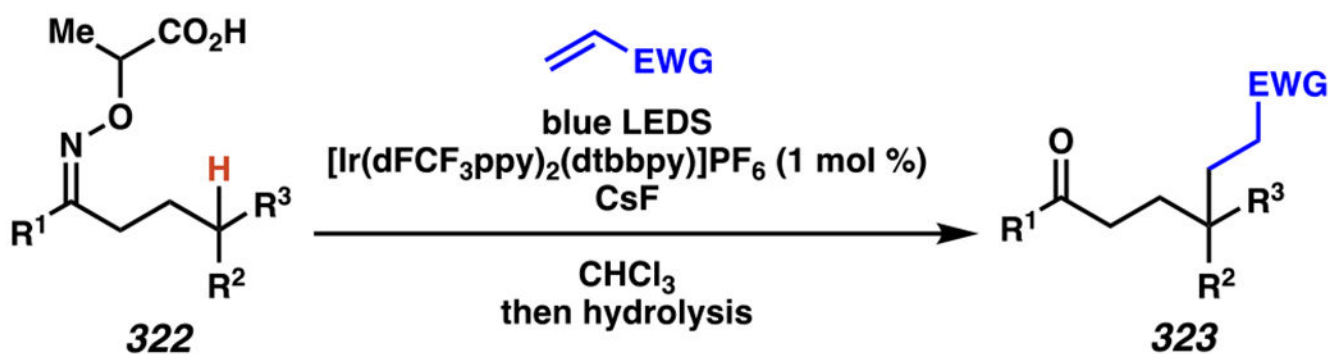


(C) A 1,5-HAT process enables an iminyl-radical guided chlorination reaction under basic conditions

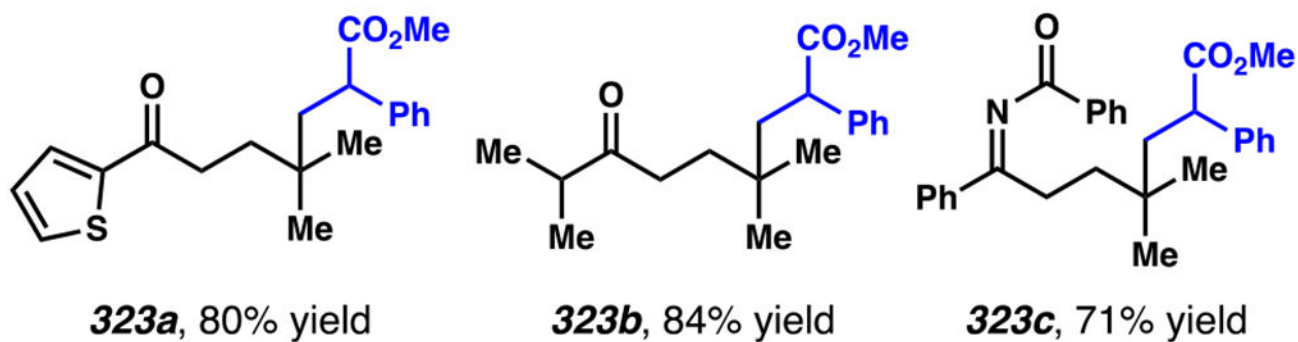


### Scheme 75.

Oximes Are Substrates for C(sp<sup>3</sup>)–H Fluorination and Chlorination Reactions

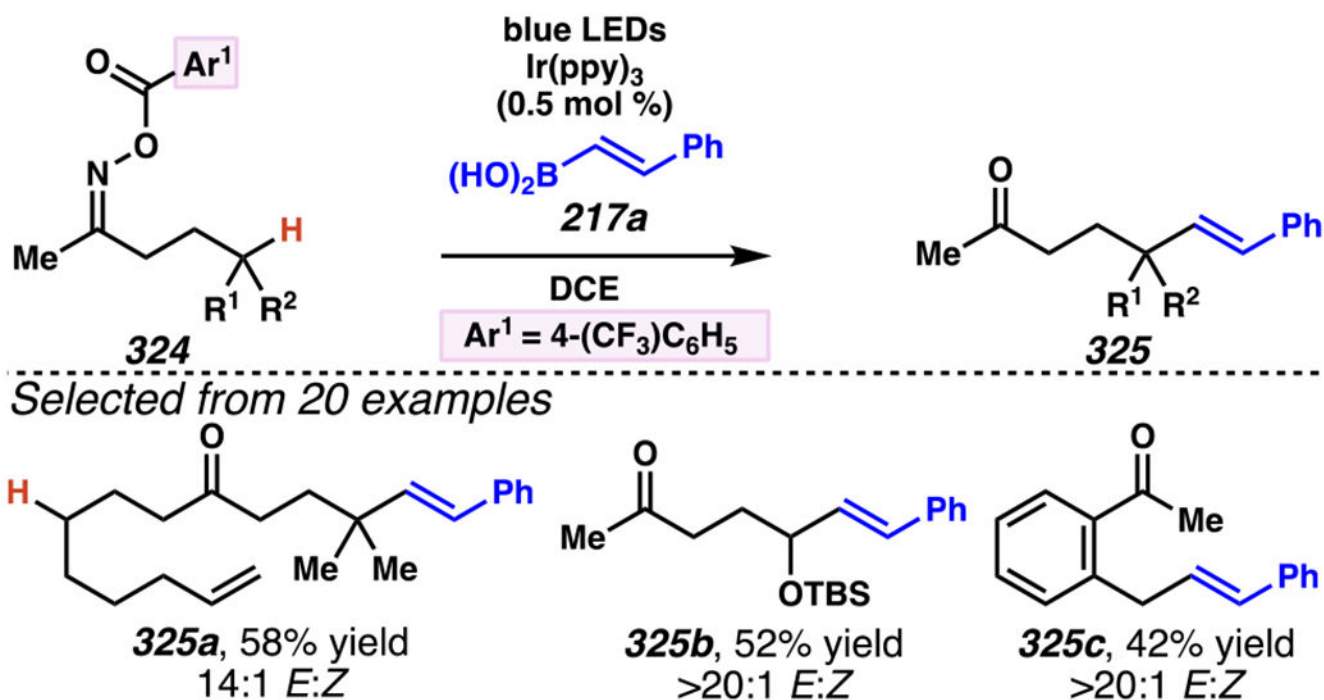


Selected from 33 examples (*radical trapping agents* incorporate esters, and ketones)



Scheme 76.  
Oximes Are Substrates for Guided Giese Reactions





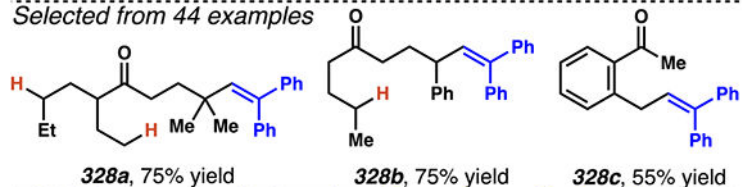
Scheme 77.

Oximes Can Template Guided Vinylation Reactions with Styrenyl Boronic Acids

(A) Acid additive enables guided vinylation reaction between *O*-acyl oxime and styrene derivative



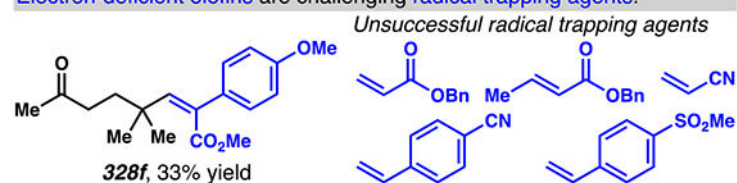
Selected from 44 examples



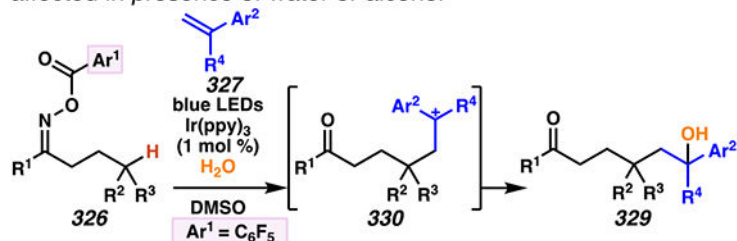
**α-Methyl styrene** as radical trapping agent provides terminal alkene rather than internal alkene. **Coumarin** as radical trapping agent reacts at  $\alpha$ -carbon rather than  $\beta$ -carbon.



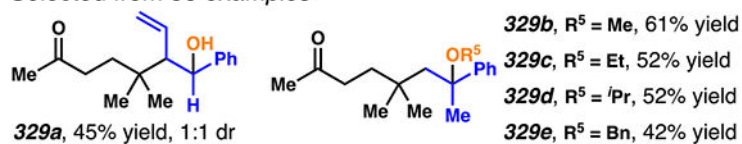
Electron-deficient olefins are challenging radical trapping agents.



(B) Guided carbohydroxylation or carboetherification reaction is affected in presence of water or alcohol



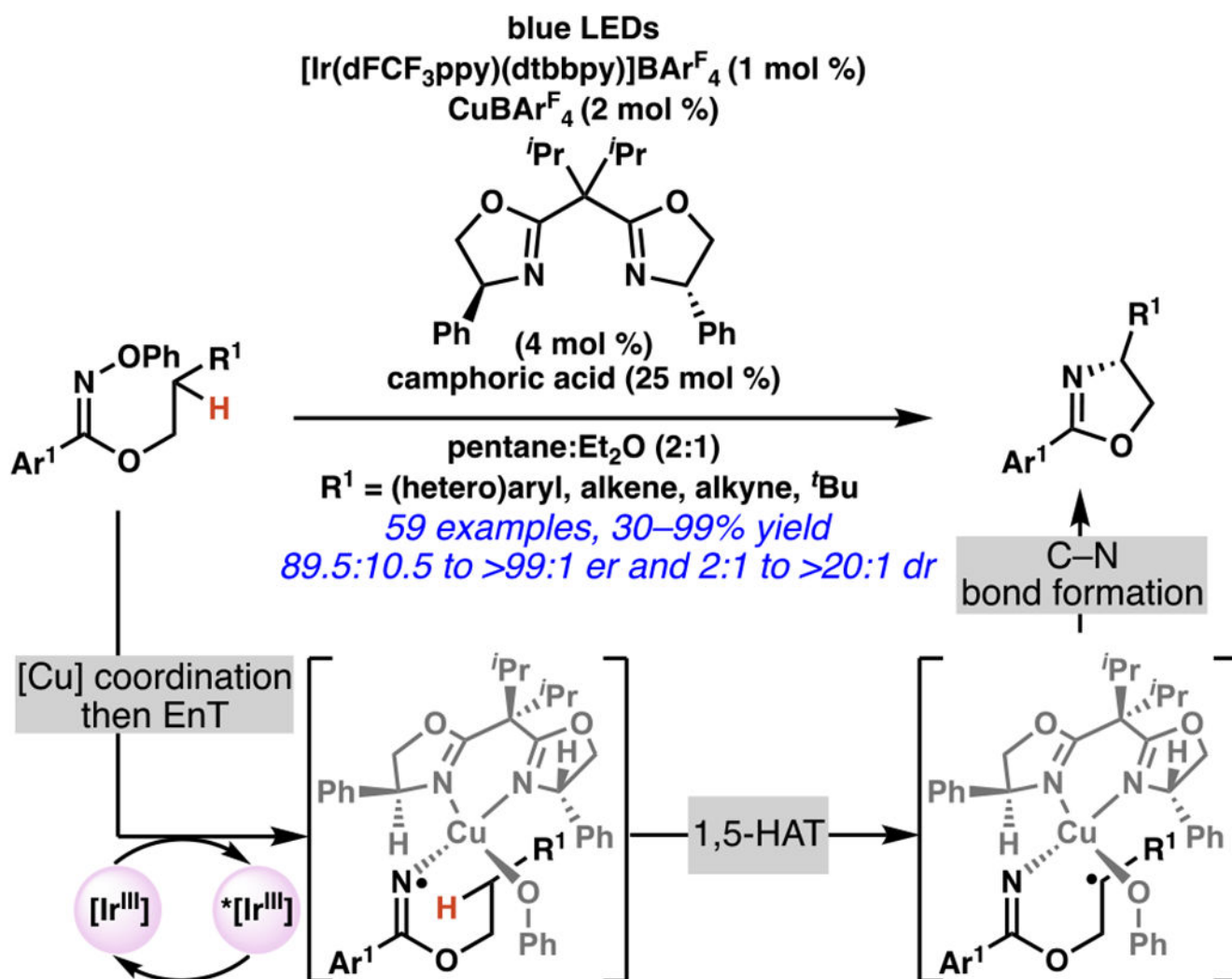
Selected from 38 examples



**329e**, R<sup>5</sup> = Bn, 42% yield

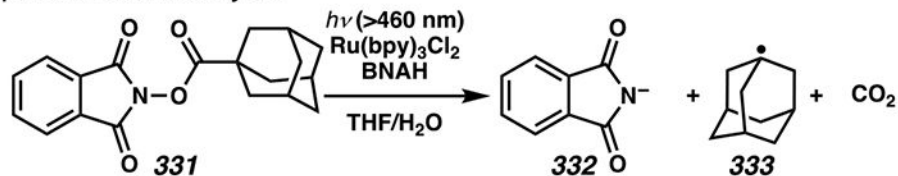
### Scheme 78.

Oximes Guide Vinylation Reactions and Hydroxyalkylation Processes

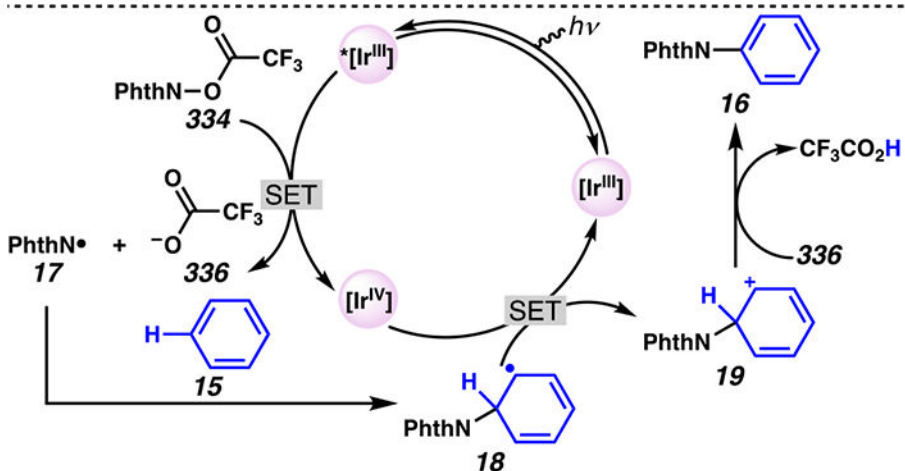


Scheme 79.  
 Guided C(sp<sup>3</sup>)-H Amination Reactions Can Be Enantioselective

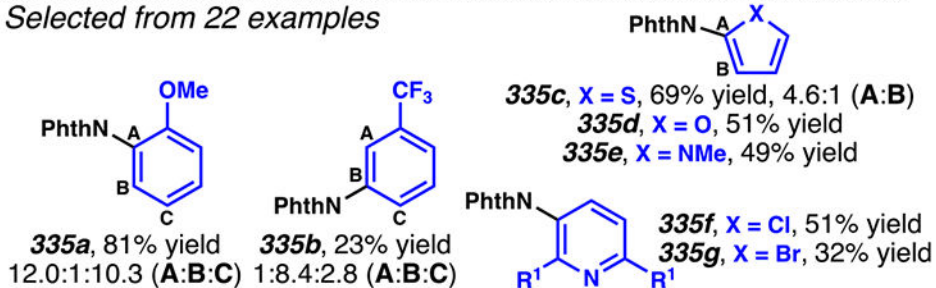
(A) *N*-Acyloxyphthalimide with less electron-deficient acyl group fragments to imidyl anion and alkyl radical under photoredox catalysis



(B) Electron-deficient *N*-acyloxyphthalimides are imidyl radical precursor



Selected from 22 examples



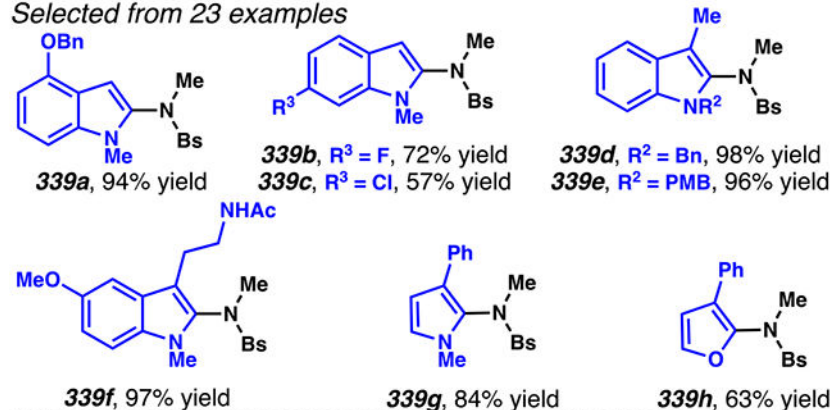
**Scheme 80.**

Electron-Deficient *N*-Acyloxyphthalimides Are Imidyl Radical Precursor for Use in *N*-(Hetero)arylation Reactions

## (A) Benzenesulfonyl radicals react with heteroarenes



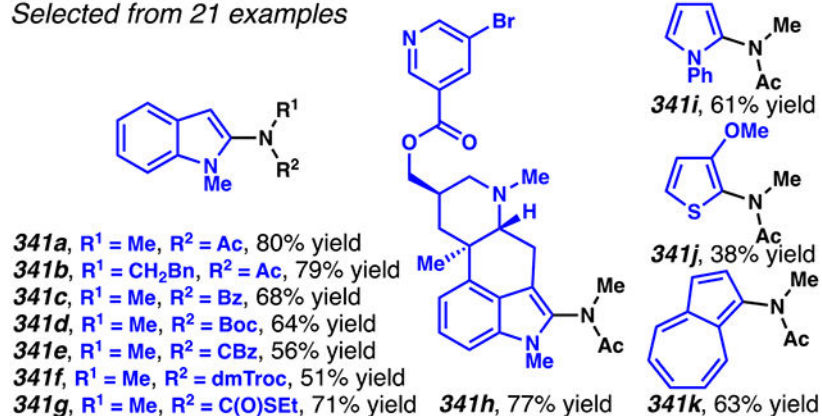
Selected from 23 examples



## (B) Amidyl radicals react with (hetero)arenes



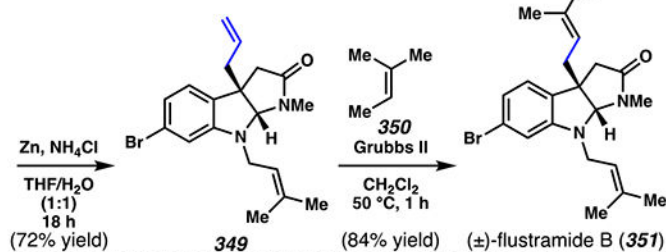
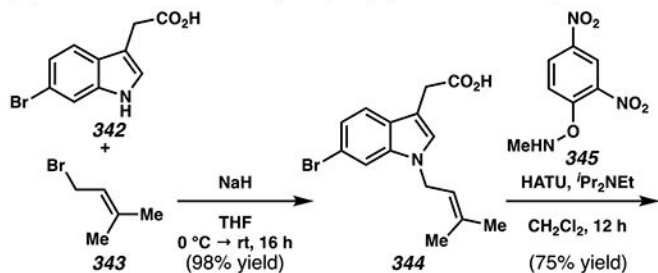
Selected from 21 examples



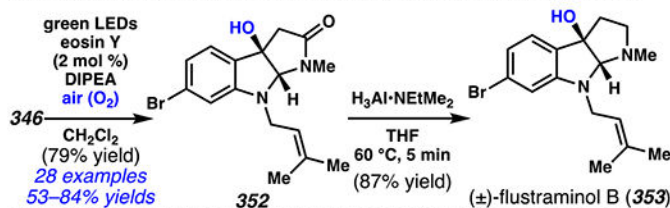
## Scheme 81.

Benzenesulfonyl Radical and Amidyl Radical Intermediates React with Arenes

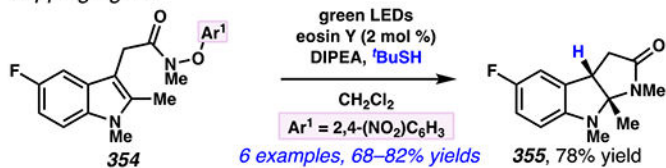
(A) Carboamination is a key-step in ( $\pm$ )-flustramide B synthesis



(B) Hydroxyamination is a key-step to access ( $\pm$ )-flustraminol B



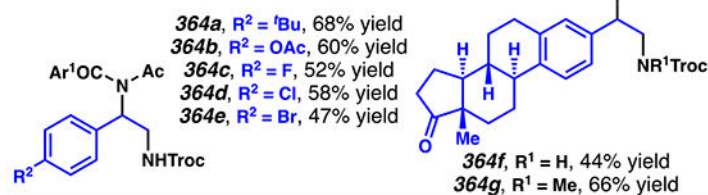
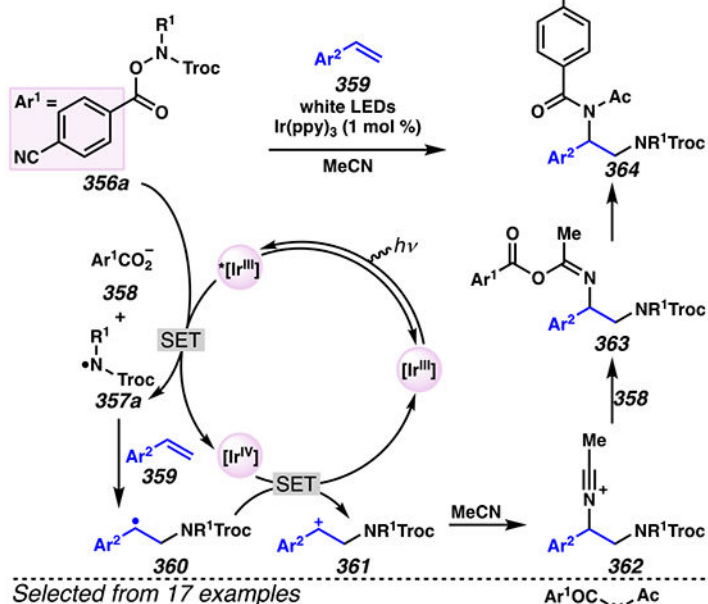
(C) Hydroamination is viable with *tert*-butylthiol as radical trapping agent



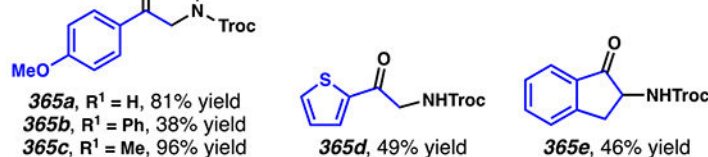
### Scheme 82.

Radical Annulation Sequences Converts Indoles to Higher-Value Products *En Route* to Natural Products

(A) A net diamidation of styrenes is proposed to rely on amidyl radical intermediates

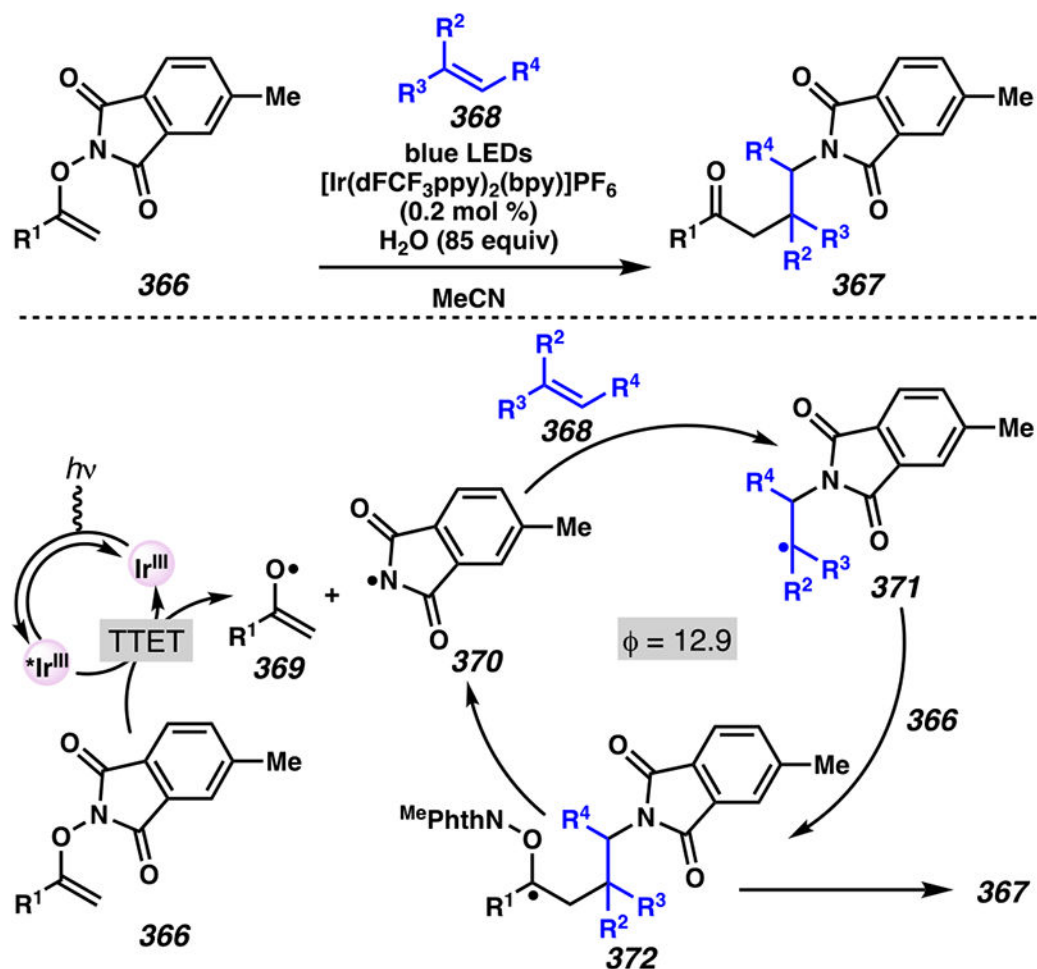


(B) An oxidative amidation of styrenes is hypothesized to rely on amidyl radical intermediates

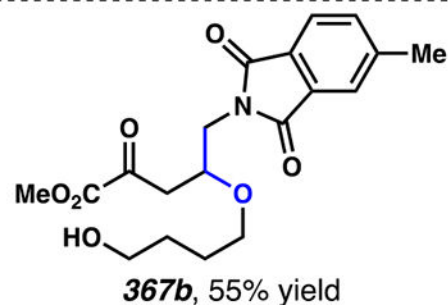
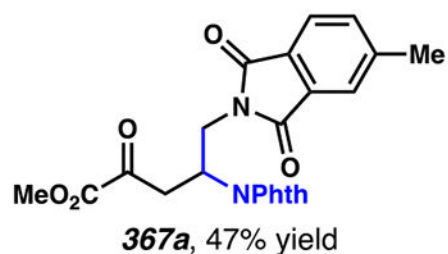


### Scheme 83.

*O*-Aryloxy Amide and Alkenes React with Acetonitrile and DMSO to Synthesize 1,2-Diamides and  $\alpha$ -Amino Ketones



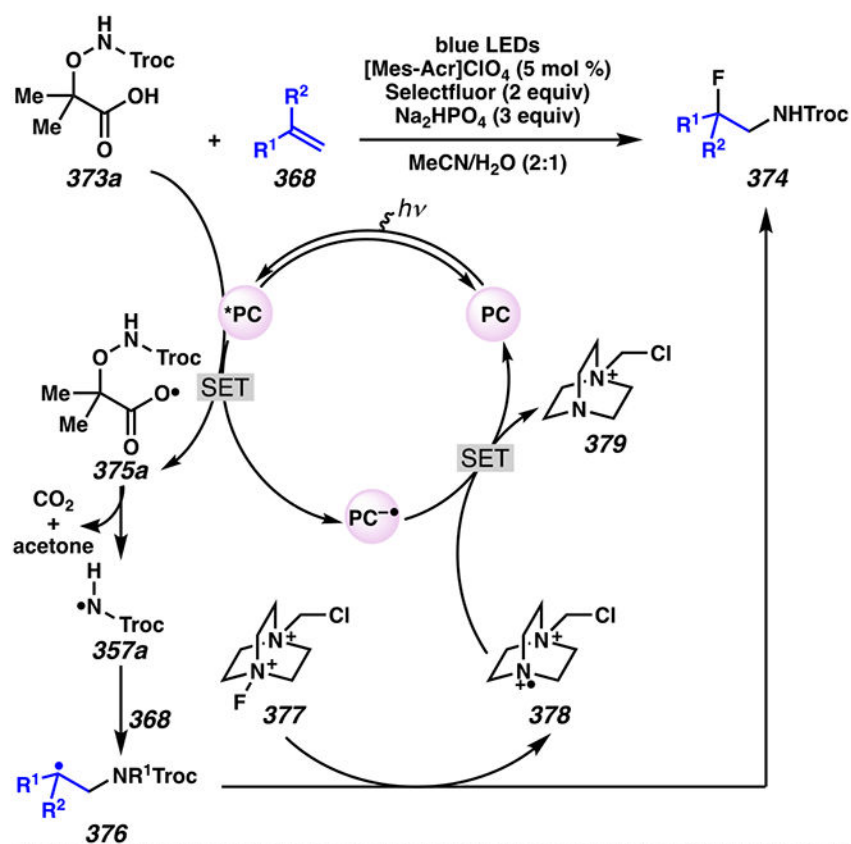
Selected from 53 examples



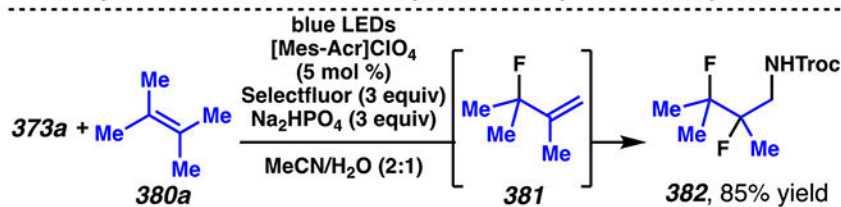
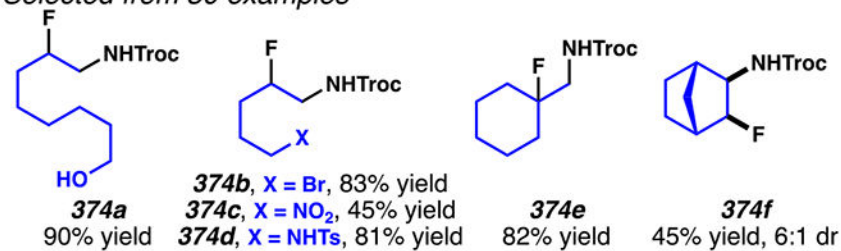
Scheme 84.

*O*-Vinylhydroxylamine Derivative Undergoes Group-Transfer Radical Addition with Alkenes in Presence of Photosensitizer



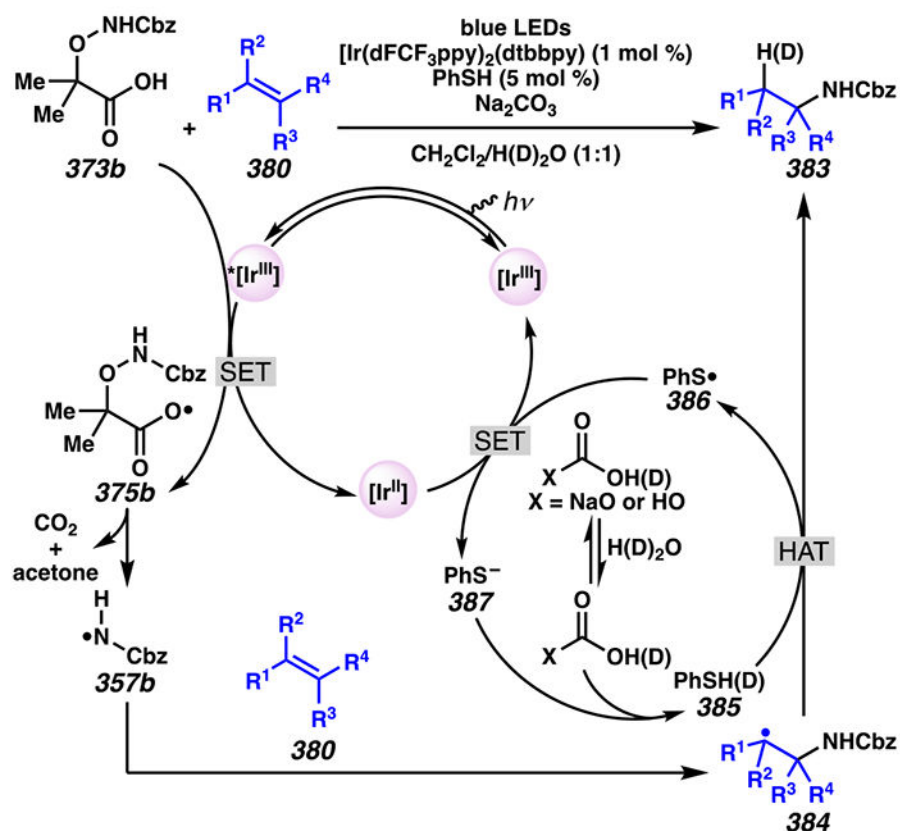


Selected from 30 examples

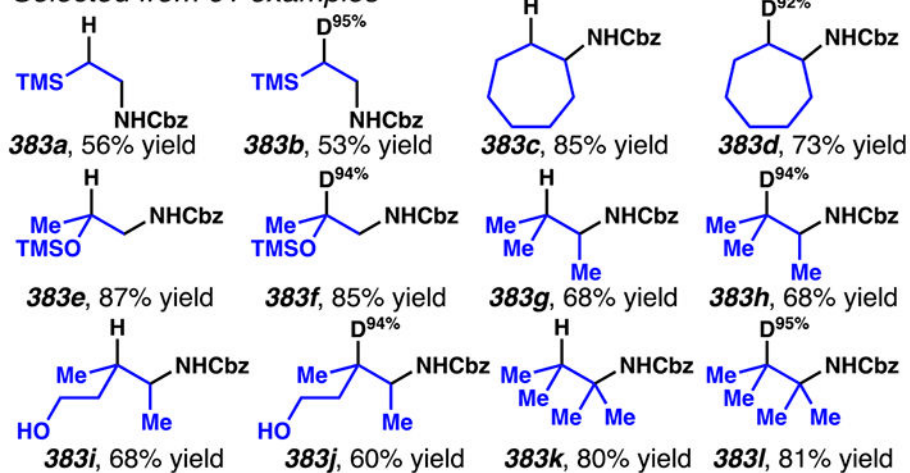


Scheme 85.

$\alpha$ -Amido-oxy Acids React with Olefins and Selectfluor to Provide  $\beta$ -Fluoroamides

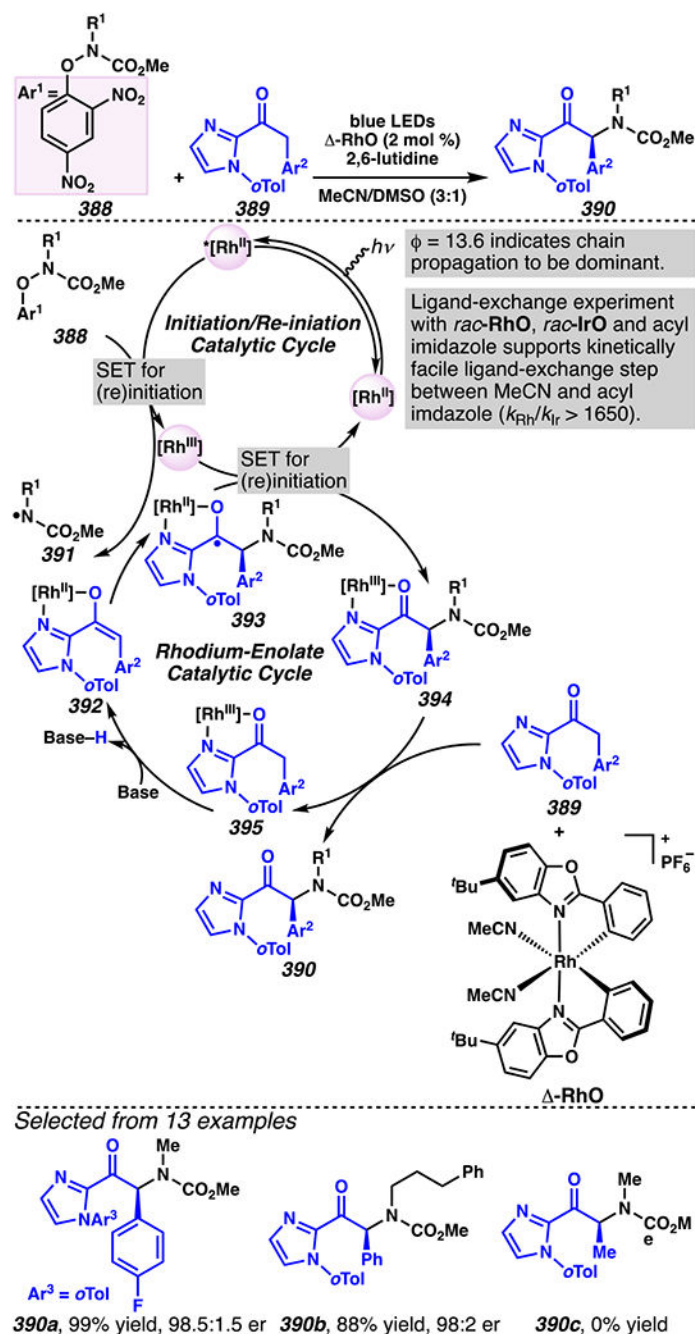


Selected from 61 examples

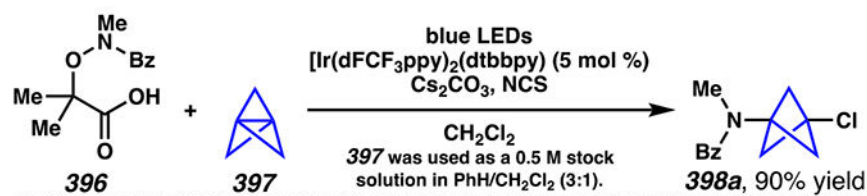


**Scheme 86.**

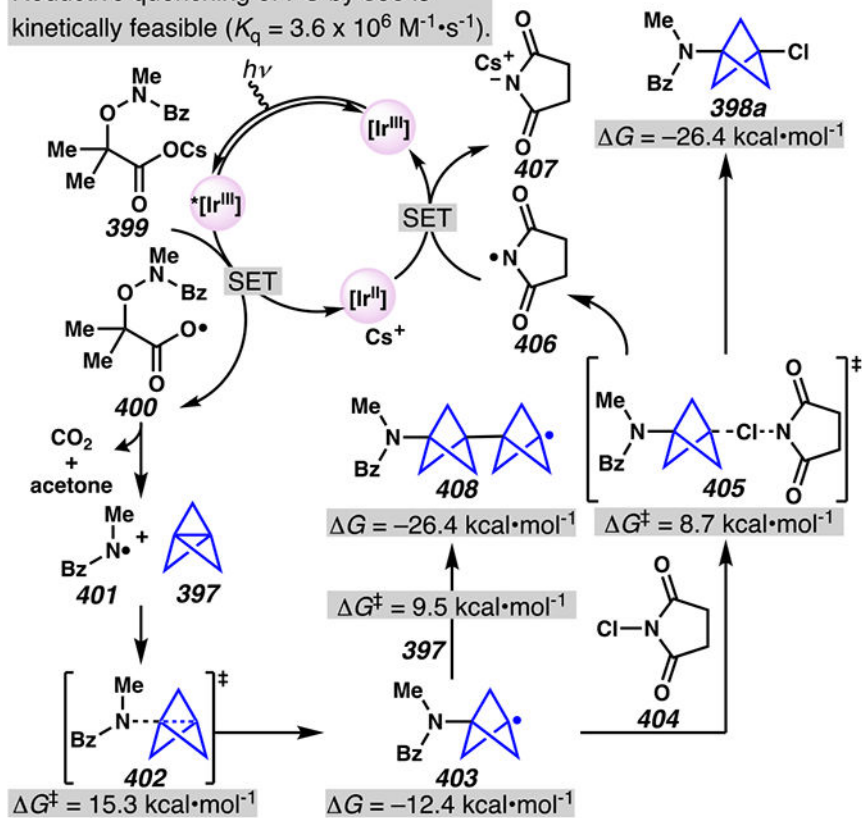
$\alpha$ -Amino-Oxy Acids React with Olefins in Photo-Mediated, Thiol Catalyzed Hydro- and Deuterioamidation Reactions

**Scheme 87.**

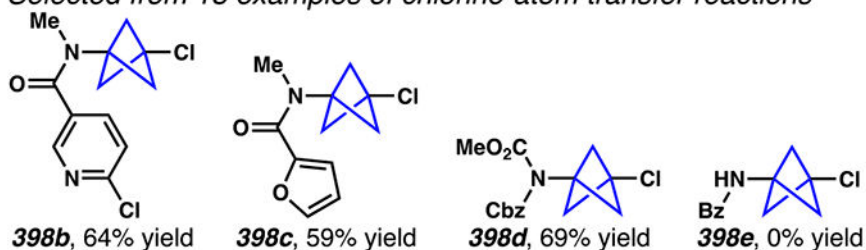
*O*-Aryloxy Amide and 2-Acyl Imidazole React in the Presence of  $\Delta$ -RhO Catalyst to Furnish Enantioenriched Products



Reductive quenching of PC by **396** is kinetically feasible ( $K_q = 3.6 \times 10^6 \text{ M}^{-1} \cdot \text{s}^{-1}$ ).

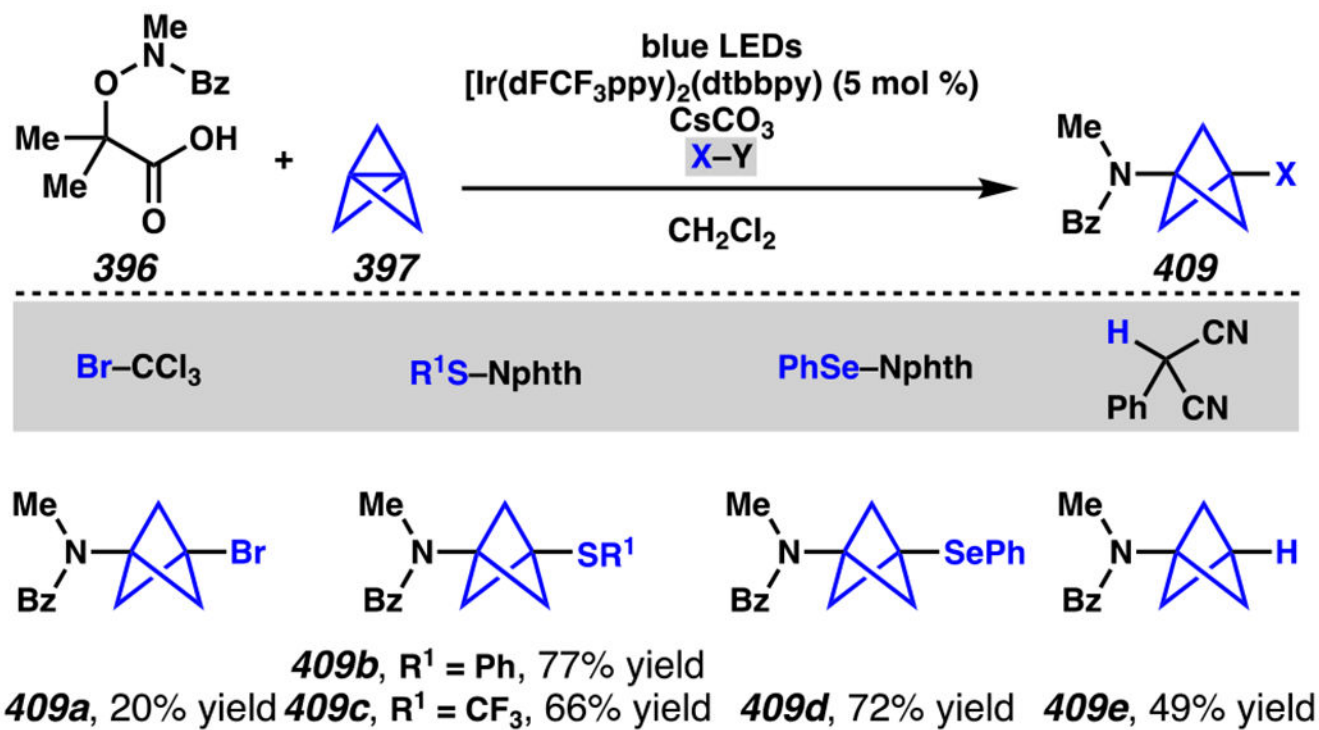


Selected from 18 examples of chlorine-atom transfer reactions



**Scheme 88.**

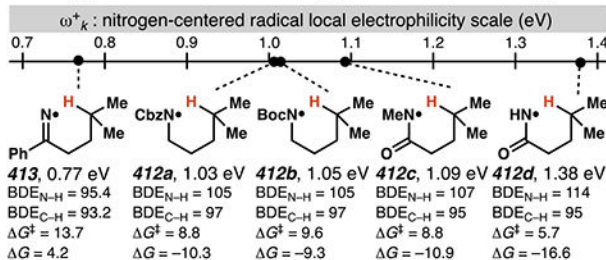
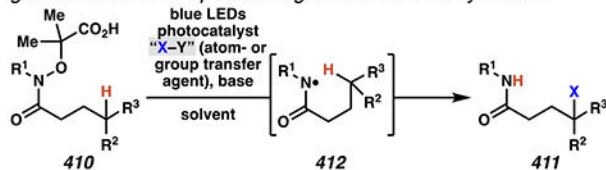
[1.1.1]Propellane Is Converted to Chlorinated Bicyclo[1.1.1]pentylamine Based on Reactions with Amidyl Radical Precursors



Scheme 89.

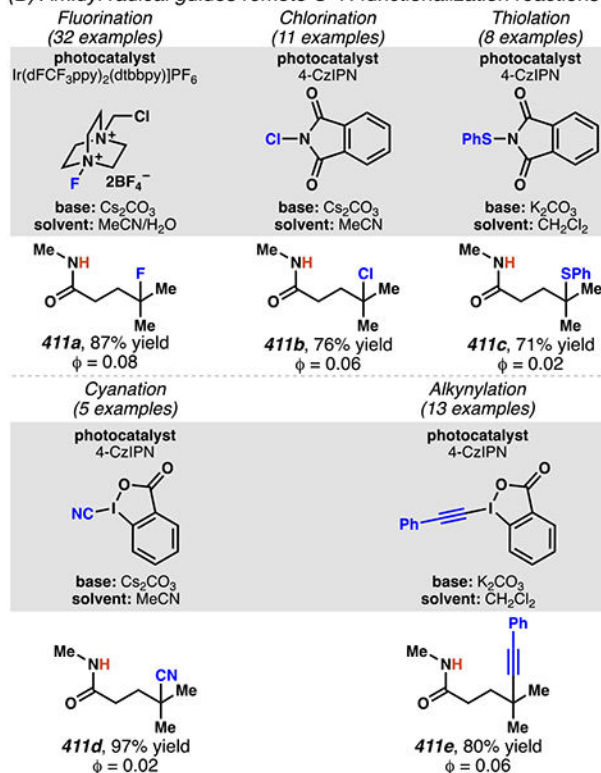
[1.1.1]Propellane Is Converted to Functionalized Bicyclo[1.1.1]pentylamines Based on Reactions with Amidyl Radical Precursors and Atom- and Group-Transfer Agents

(A) Facile generation of nucleophilic carbon radical relies on generation of electrophilic nitrogen-centered amidyl radical



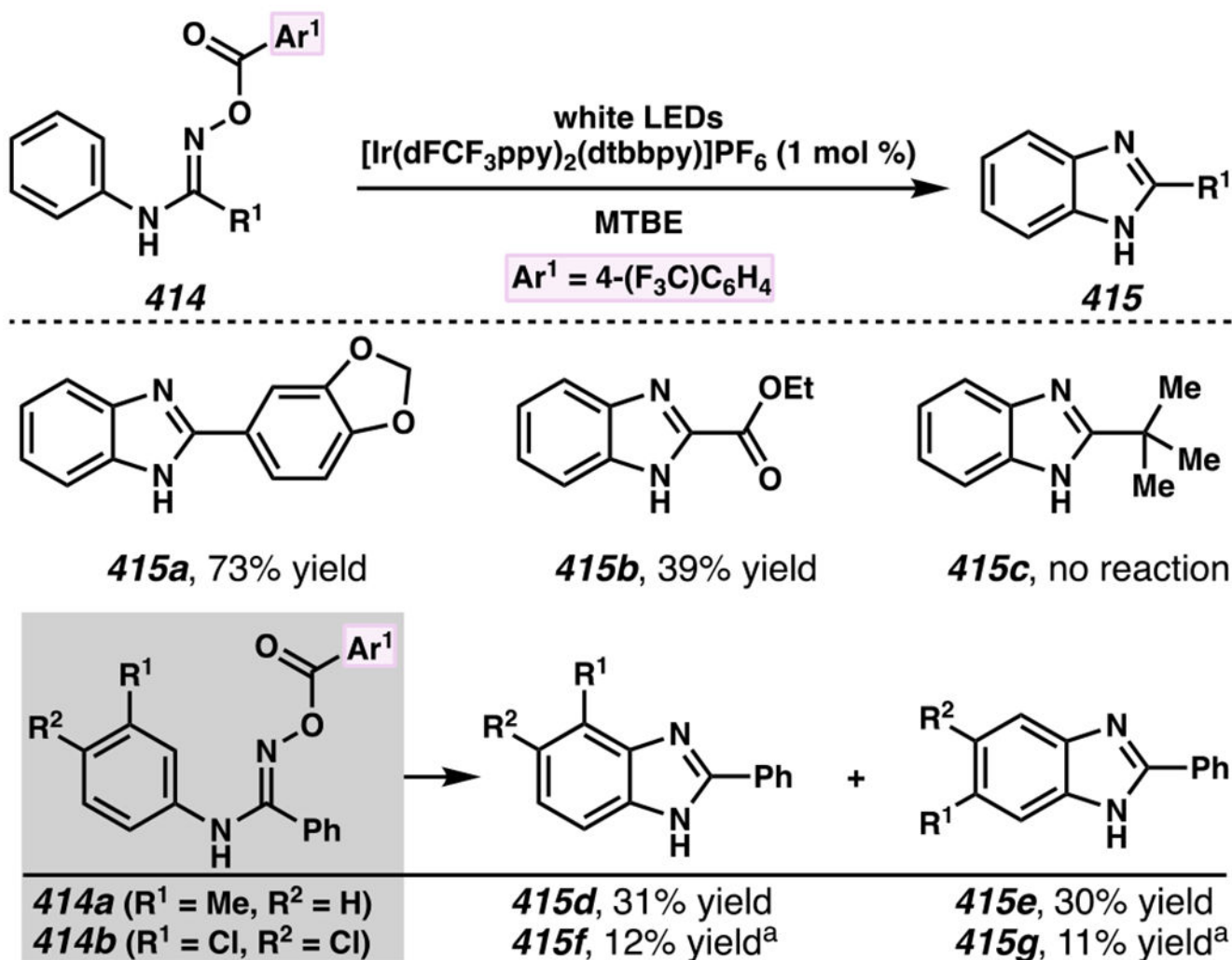
$\omega^*_k$  values were calculated from the UB3LYP/6-311+G(d,p) level of theory. BDEs were estimated from the (RO)B3P86/6-311G(d,p) level of theory and are reported in kcal·mol<sup>-1</sup>.  $\Delta G^\ddagger$  and  $\Delta G$  energies were estimated from the UB3LYP/6-31+G(d,p) level of theory and are reported in kcal·mol<sup>-1</sup>.

(B) Amidyl radical guides remote C-H functionalization reactions



### Scheme 90.

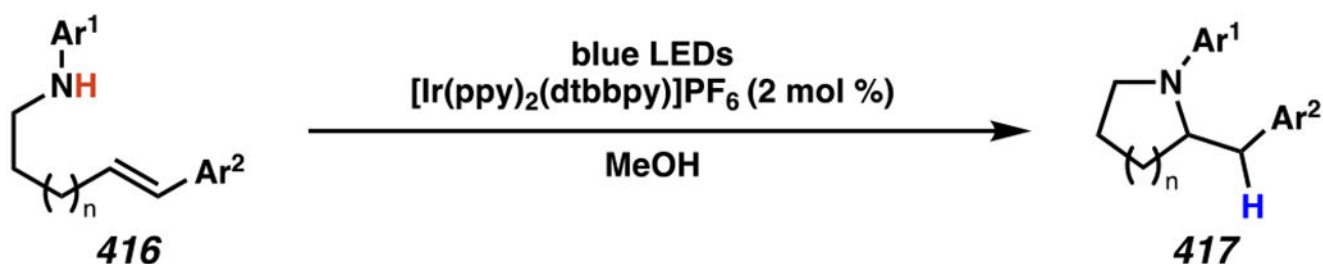
Amidyl Radical Guides Remote Functionalization Reaction to Engage Atom- and Group-Transfer Agents



<sup>a</sup>The yield was derived from the combined yield of the product from **414b**, which contained 1:0.9 mixture of diastereomers **415f**:**415g**, respectively.

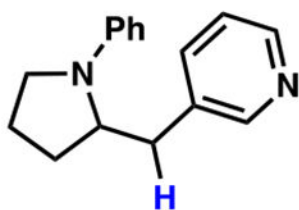
**Scheme 91.**

*N*-Aryl Amidoxime Esters Are Appropriate Precursors to Photo-Mediated Radical Annulation Reactions That Provide 2-Substituted Benzimidazoles

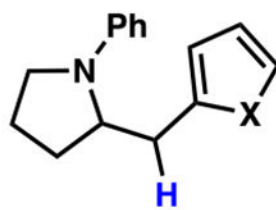


*Selected from 25 examples ( $n = 1$ )*

*Selected from 7 examples ( $n = 2$ )*



**417a**, 86% yield

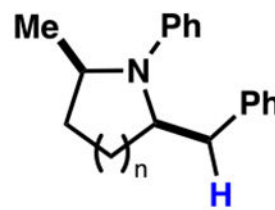


**417b**, X = S

61% yield

**417c**, X = O

76% yield

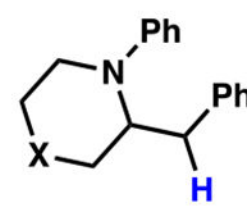


**417d**,  $n = 1$

88% yield, 1:1 d.r.

**417e**,  $n = 2$

64% yield, 4.2:1 d.r.



**417f**, X = NTs

58% yield

**417g**, X = O

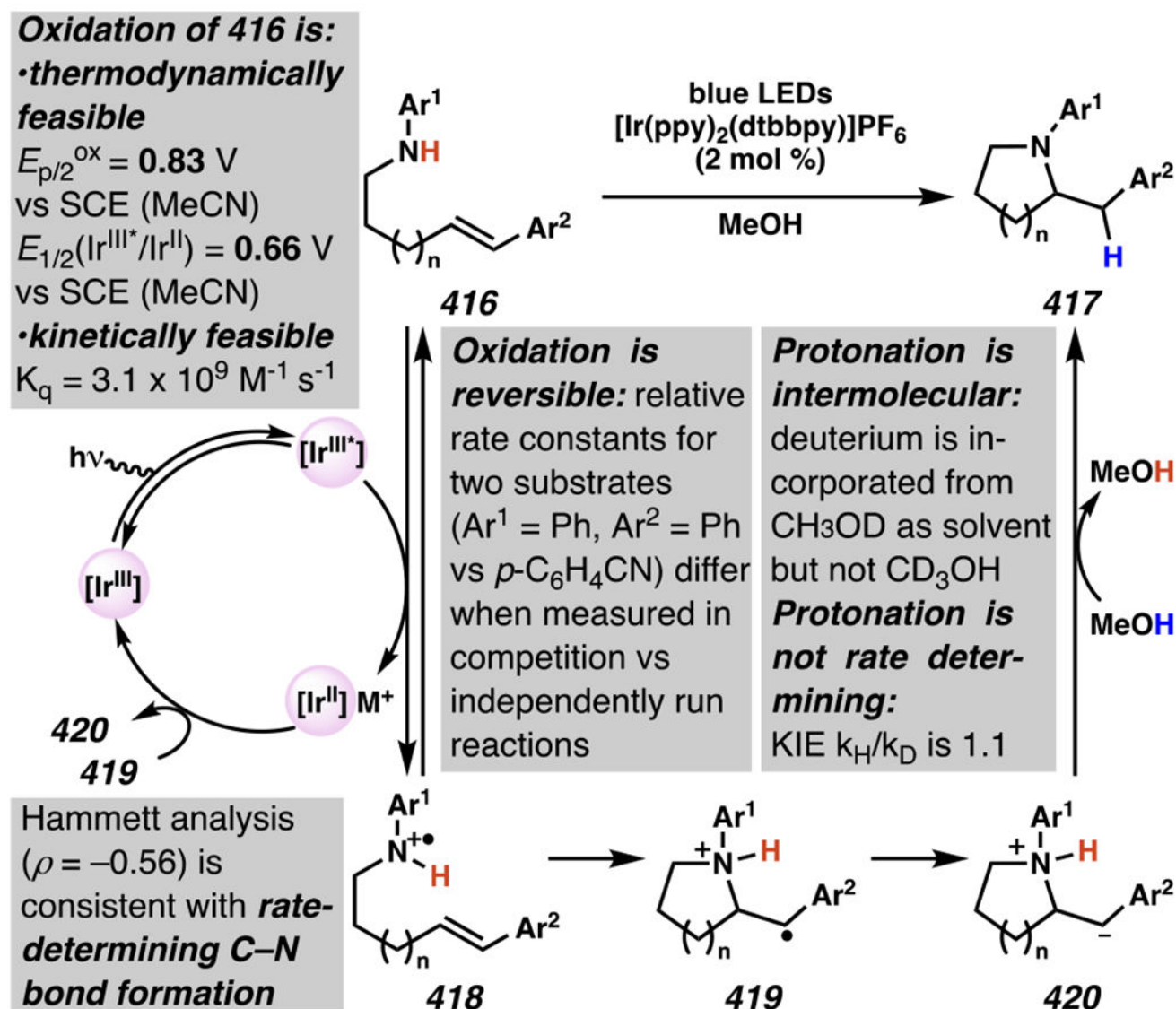
44% yield

**Scheme 92.**

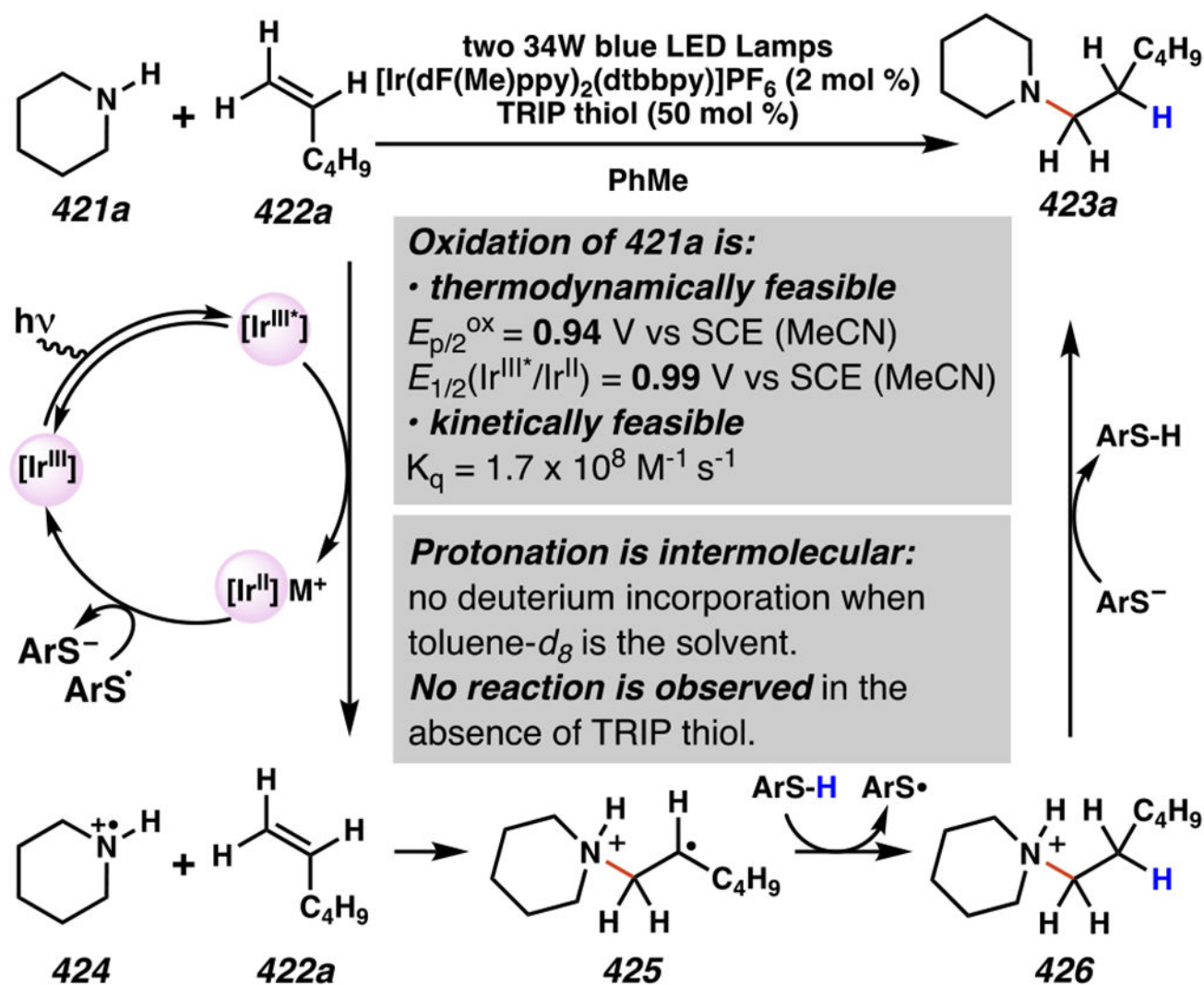
Knowles and Co-workers' Intramolecular, Anti-Markovnikov Hydroamination Reactions

Engage Olefins to Form 5- and 6-Membered, Saturated Heterocycles

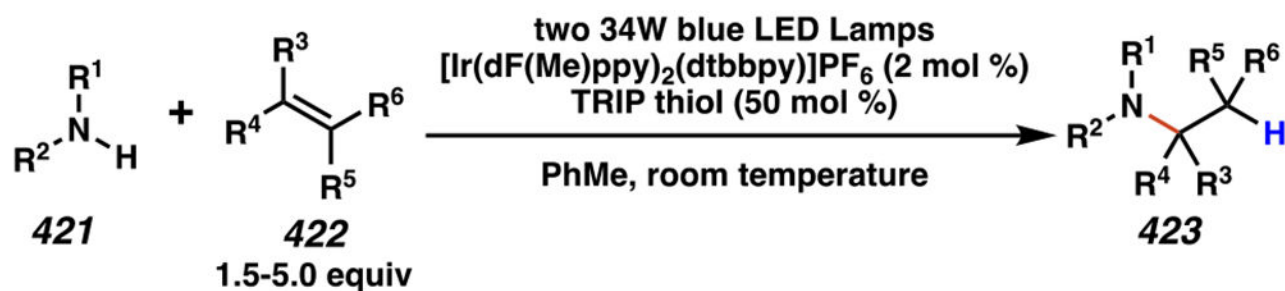




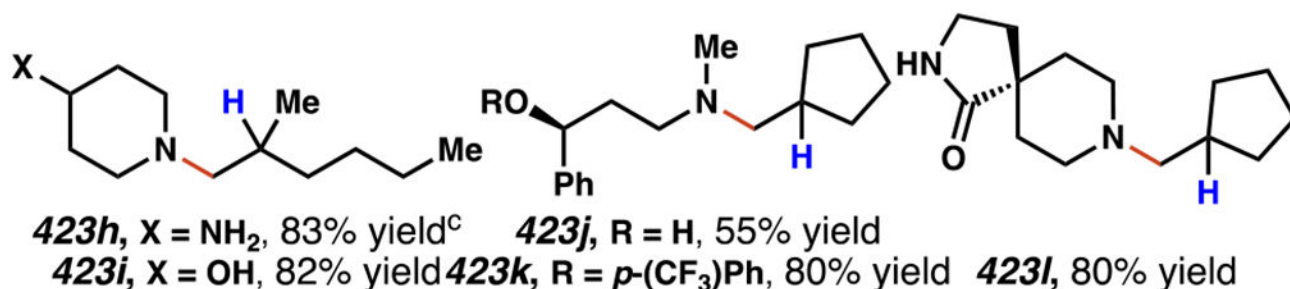
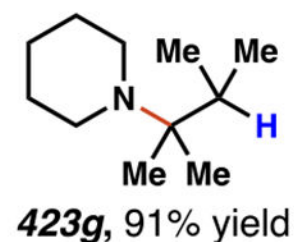
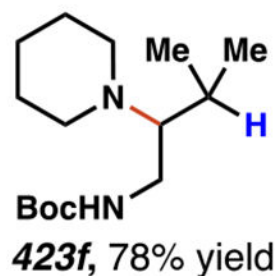
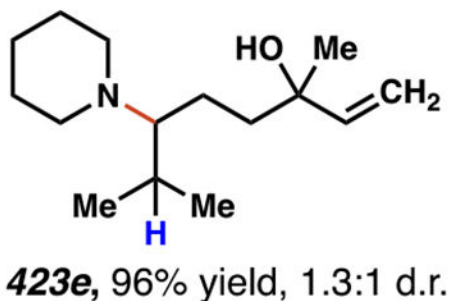
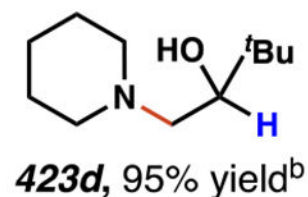
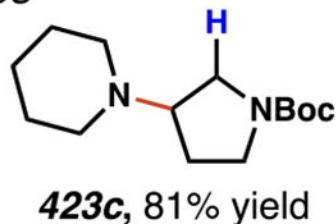
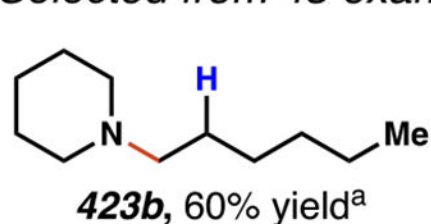
Scheme 93.  
 Photoredox Catalysis Can Be Used to Access *N*-Aryl Aminium Radical Cations That Engage in Intramolecular, Anti-Markovnikov Hydroamination Reactions



**Scheme 94.**  
 Photoredox Catalysis-Generated Aminium Radicals Engage Unactivated Alkenes in Intermolecular, Anti-Markovnikov Hydroamination in the Presence of an Aryl Thiol HAT-Catalyst



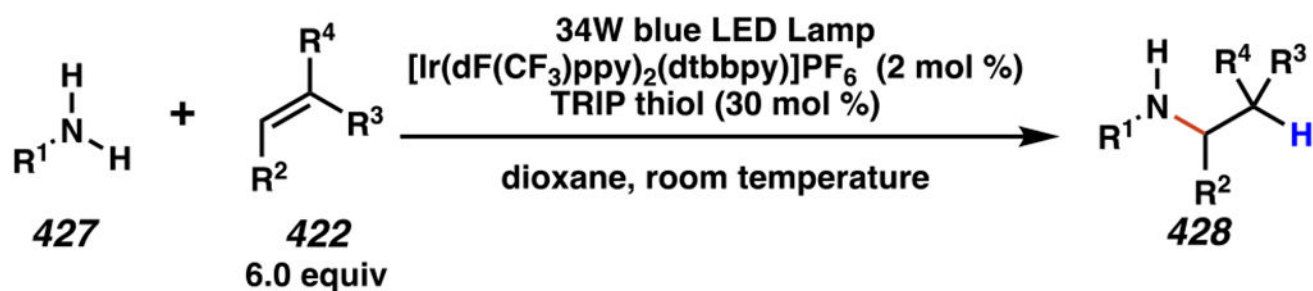
Selected from 43 examples



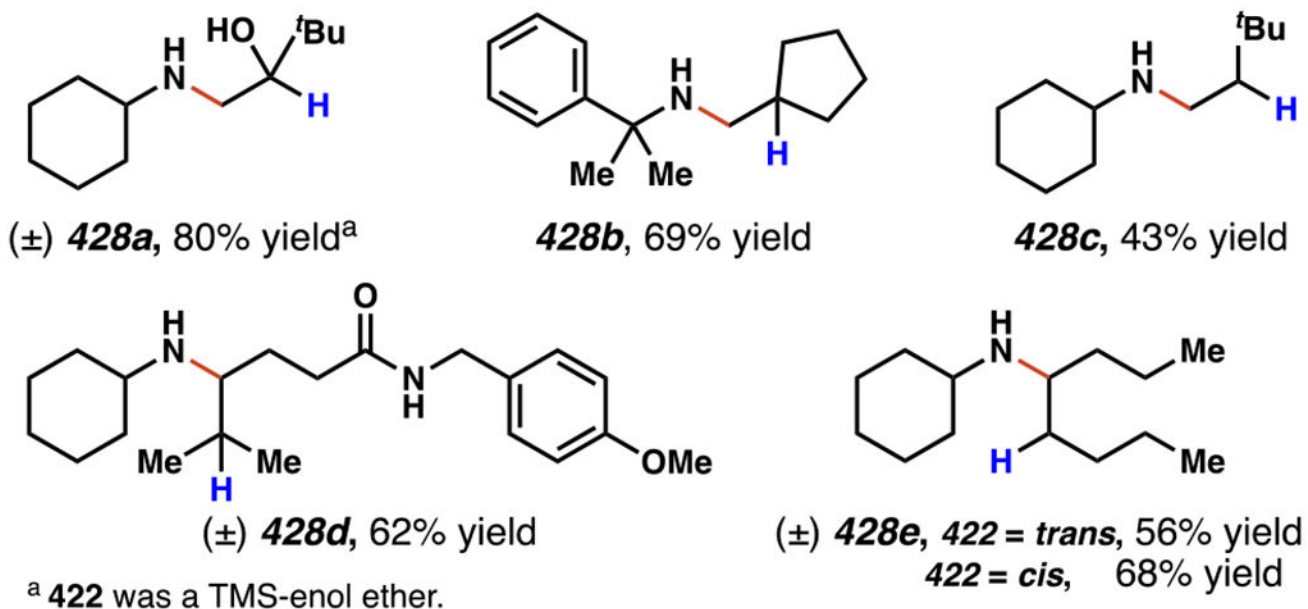
<sup>a</sup> Reaction run at 45 °C. <sup>b</sup> **422** was a TMS-enol ether. <sup>c</sup> Product was isolated after workup with Boc<sub>2</sub>O.

**Scheme 95.**

Secondary Amine-Derived Aminium Radicals Engage Unactivated Alkenes in Intermolecular, Anti-Markovnikov Hydroamination



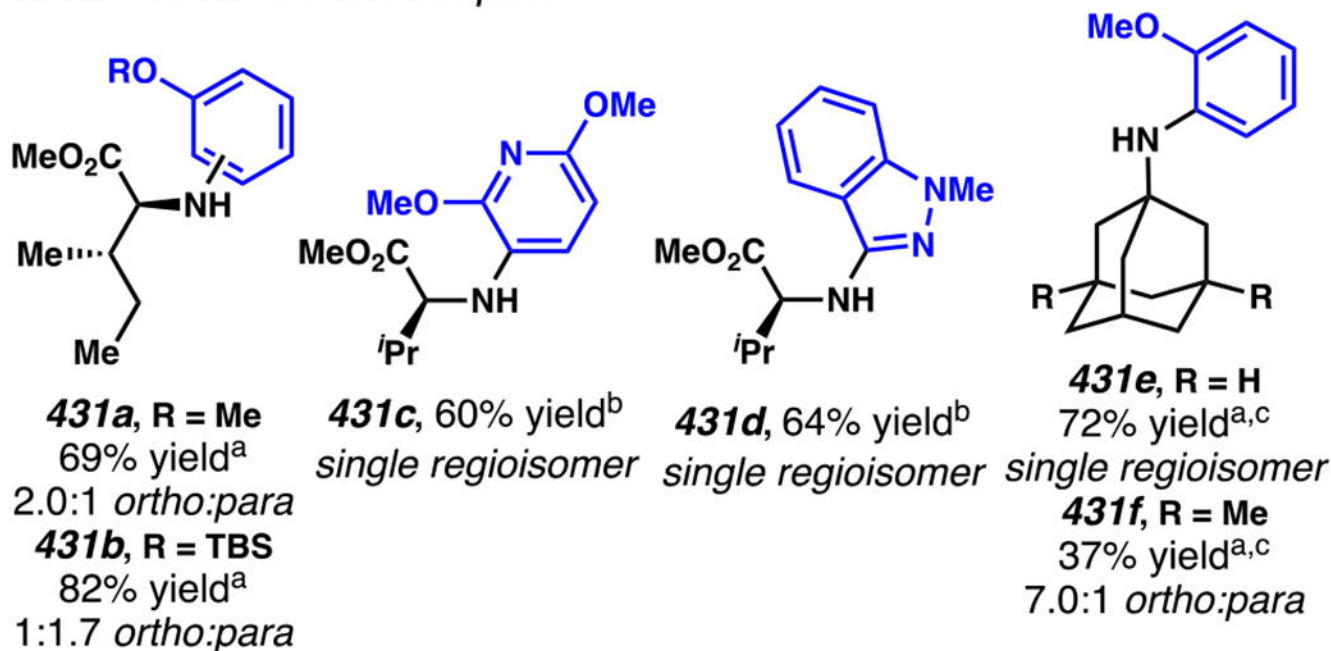
Selected from 31 examples



Scheme 96.  
Primary Amine-Derived Aminium Radicals Engage Unactivated Alkenes in Intermolecular, Anti-Markovnikov Hydroamination Reactions



Selected from 75 examples



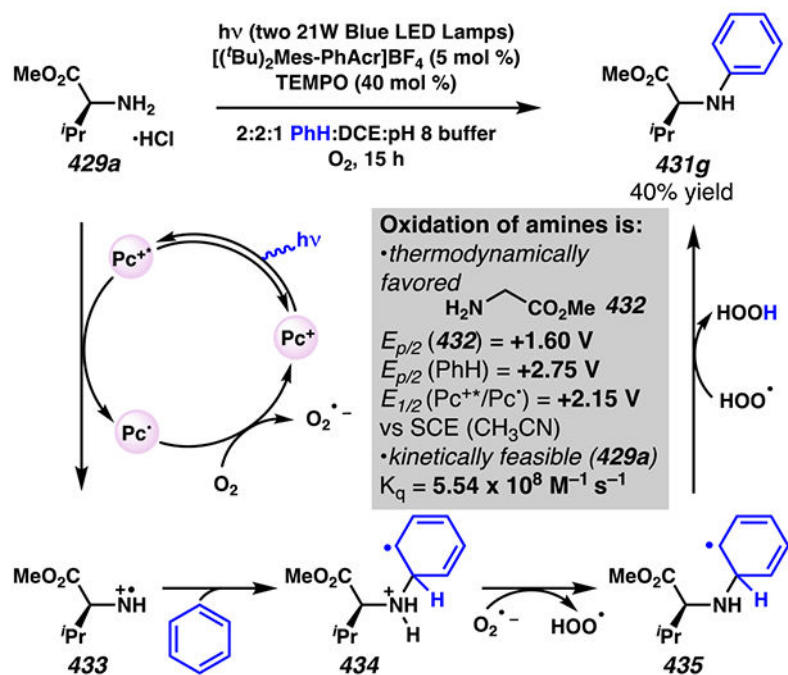
<sup>a</sup>  $\text{R}^3 = \text{Me}$  ( $[(2,7\text{-dMe-Mes-PhAc})\text{BF}_4]$ ). <sup>b</sup>  $\text{R}^3 = \text{tBu}$  ( $[(\text{tBu})_2\text{Mes-PhAc})\text{BF}_4]$ ).

<sup>c</sup> Amine employed as a freebase, and solvent was replaced with DCE (0.1 M) with respect to the arene.

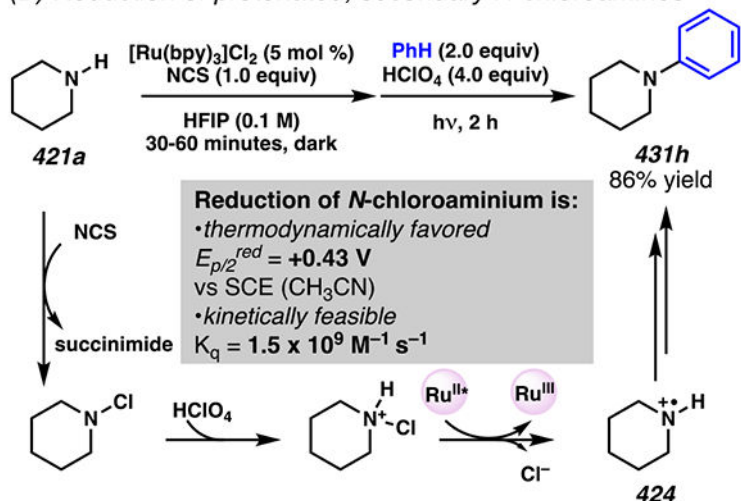
**Scheme 97.**

Varied Amines Efficiently Engage in Photoredox-Mediated C–H Amination of (Hetero)arenes

(A) Oxidation of primary amines in the presence of molecular oxygen



(B) Reduction of protonated, secondary N-chloroamines



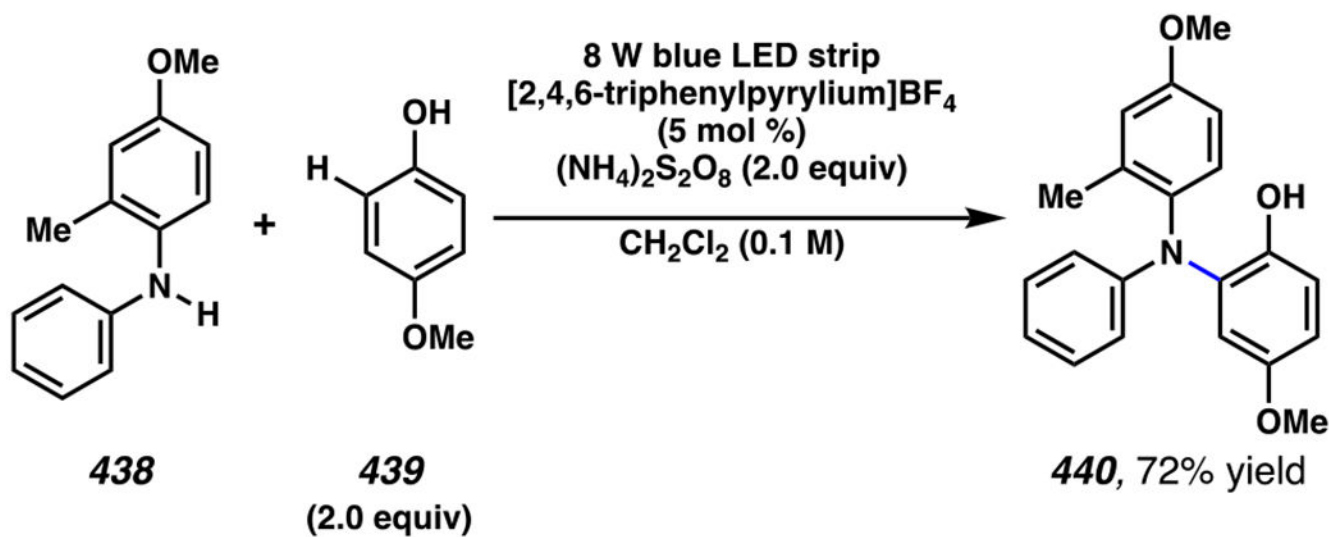
**Scheme 98.**

Aryl C–H Amination Can Be Engaged through Photoredox Generation of Aminium Radical Cations

**Scheme 99.**

Eosin Y Mediates a Dehydrogenative Cross-Coupling Reaction Involving Alkyl Amines and Quinoxalinones

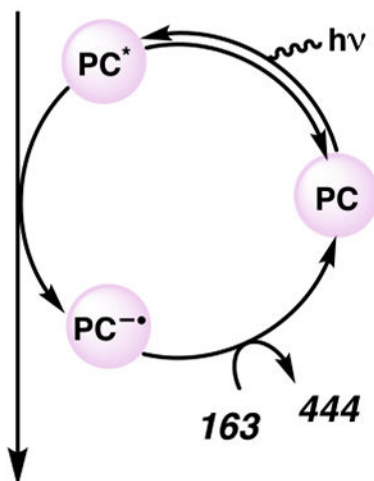
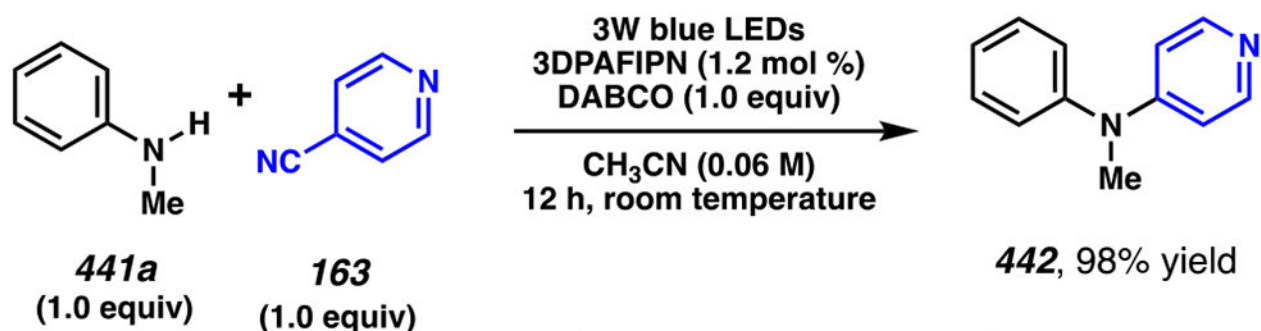
*Selected from 29 examples*



**Scheme 100.**

Dehydrogenative Reaction Enables *ortho*-Selective Coupling of Electron-Dense Diaryl Amines with Electron-Dense Phenols

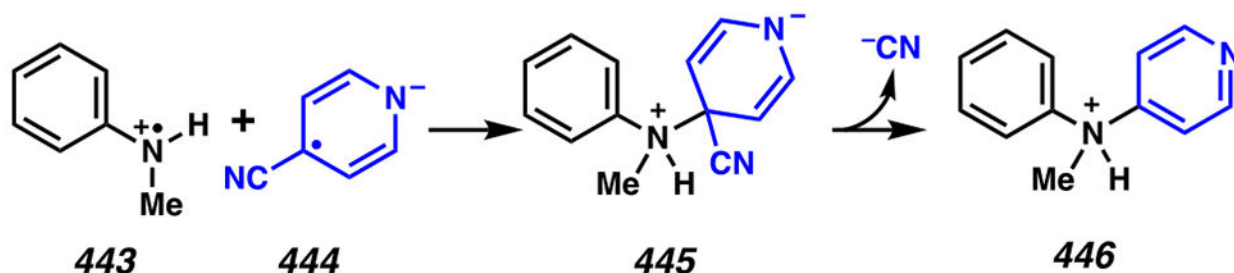
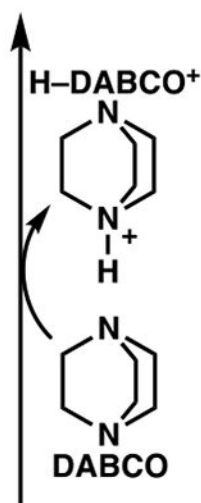




**Oxidation of 441a is:**

- kinetically feasible  
 $K_q = 9.8 \times 10^7 \text{ M}^{-1} \text{ s}^{-1}$
- thermodynamically feasible  
 $E_{p/2}^{\text{ox}}(441a) = +0.92 \text{ V}$   
 $E_{1/2}(\text{Pc}^+/\text{Pc}^{\bullet-}) = +1.09 \text{ V}$   
 vs SCE (CH<sub>3</sub>CN)

**Reduction of 163 by Pc<sup>•-</sup> is observed (TAS)**  
 $K_q = 7.0 \times 10^7 \text{ M}^{-1} \text{ s}^{-1}$

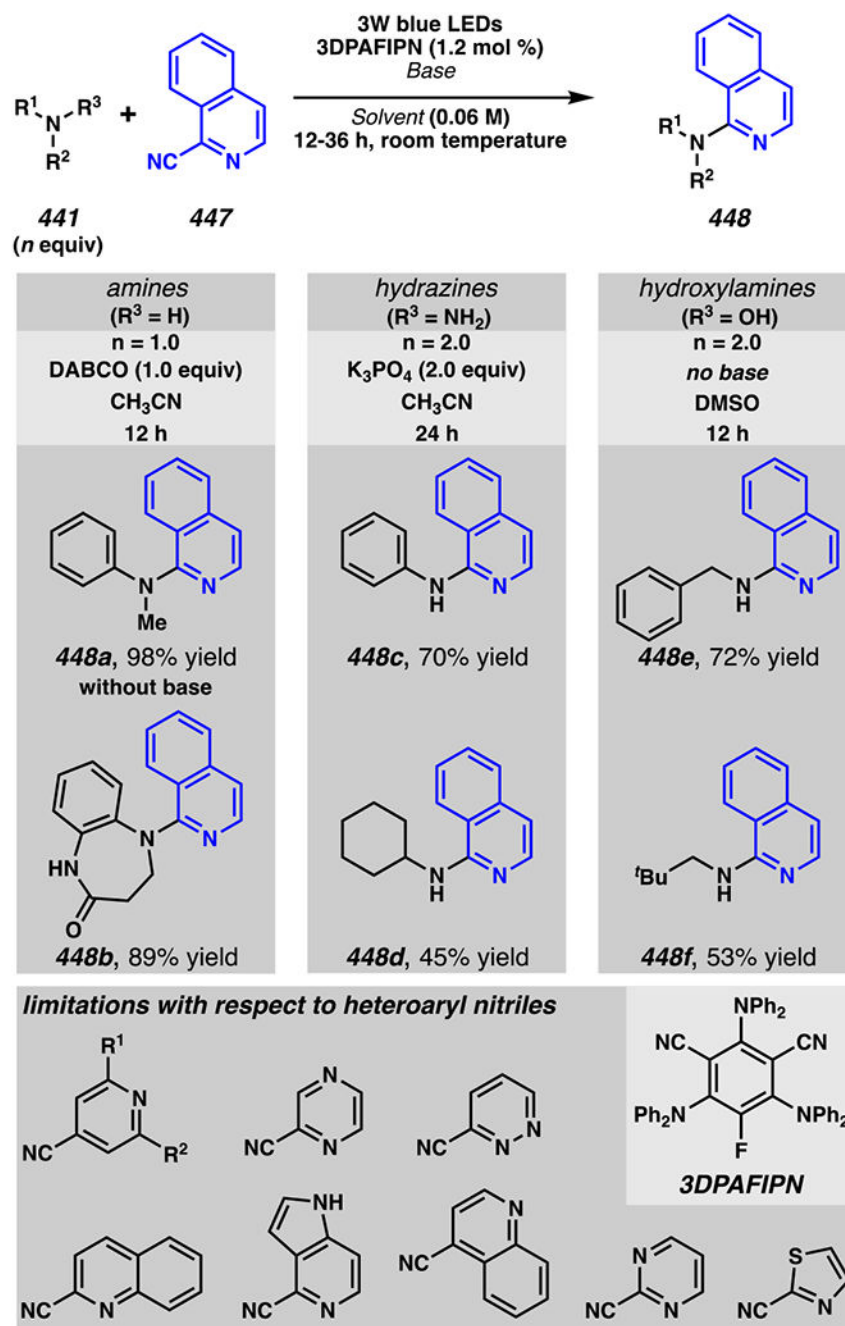


Oxidation of DABCO is competitive with **441a**:  
 $K_q(\text{DABCO}) = 5.3 \times 10^8 \text{ M}^{-1} \text{ s}^{-1}$

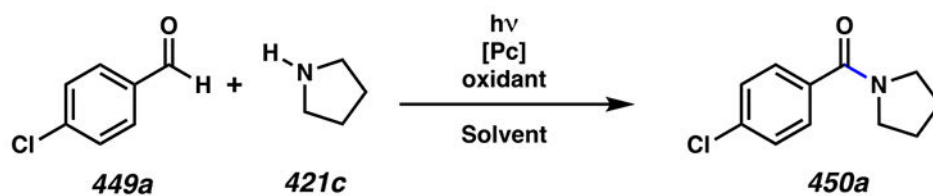
As above: **442**, without base, 21% yield  
 Na<sub>2</sub>CO<sub>3</sub> instead of DABCO, 85% yield  
 NaHCO<sub>3</sub> instead of DABCO, 82% yield

**Scheme 101.**

Proposed Photoredox-Catalyzed, Radical-Radical Heteroaryl Amination Relies on Loss of Hydrogen Cyanide

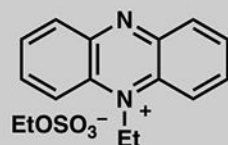
**Scheme 102.**

Amine and Amine-Analogues Engage Heteroarenes to Form New C–N Bonds

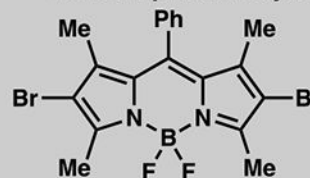


	<i>D. Leow</i> <i>Org. Lett.</i> <b>2014</b>	<i>D. Xue</i> & co-workers <i>Org. Biomol.</i> <i>Chem.</i> <b>2016</b>	<i>V. C.-C. Wang</i> & co-workers <i>Angew. Chem.</i> <i>Int. Ed.</i> <b>2018</b>	<i>V. Bhalla</i> & co-workers <i>RSC Adv.</i> <b>2018</b>
<b>% yield:</b>	87% yield	72% yield	91% yield	75% yield
<b>amine equiv:</b>	2.5 equiv	3.0 equiv	3.0 equiv	3.0 equiv
<b>light source:</b>	24 W CFL	3 W Blue LED	23 W CFL	Incandescent bulb
<b>[Pc]:</b>	<b>Phenazinium</b> (1.0 mol %)	<b>BODIPY</b> (2.0 mol %)	<b>Palladium dicarbene</b> (0.5 mol %)	<b>Hemicyanine</b> (1.0 mol %)
<b>oxidant:</b>	Oxygen	Oxygen BHT (2 equiv)	Oxygen	Oxygen
<b>solvent:</b>	THF inhibitor-free	1,4-dioxane	DMF	1:1 DMSO:H <sub>2</sub> O

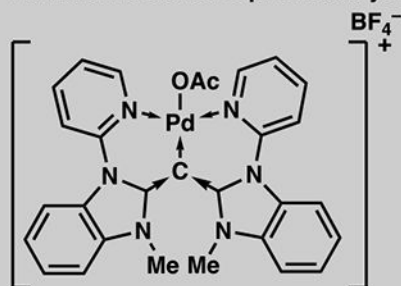
Phenazinium photocatalyst



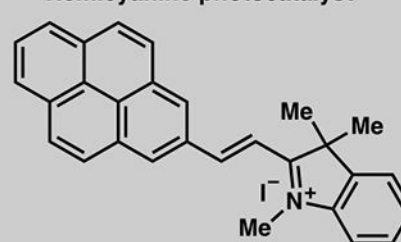
BODIPY photocatalyst



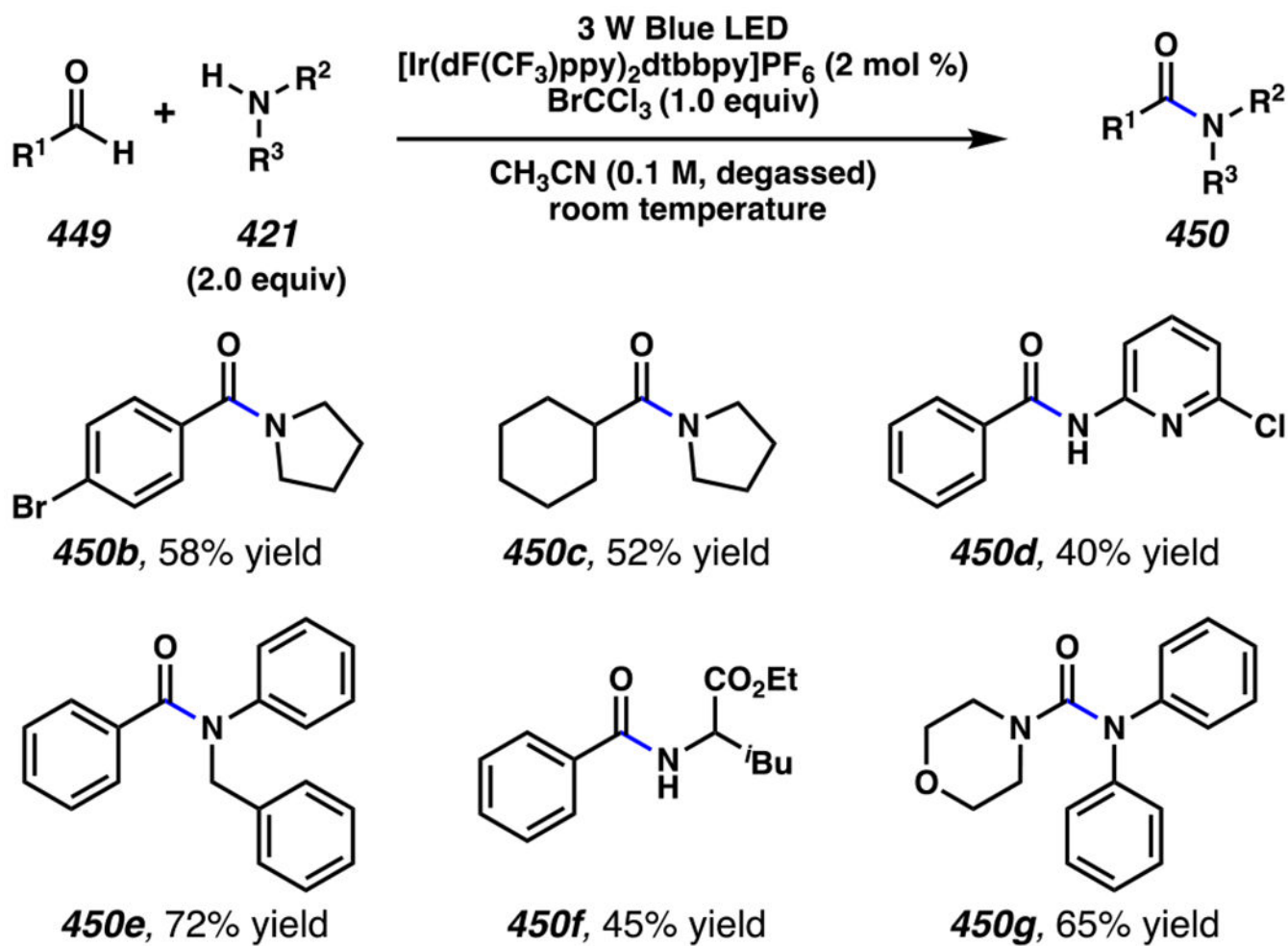
Palladium dicarbene photocatalyst



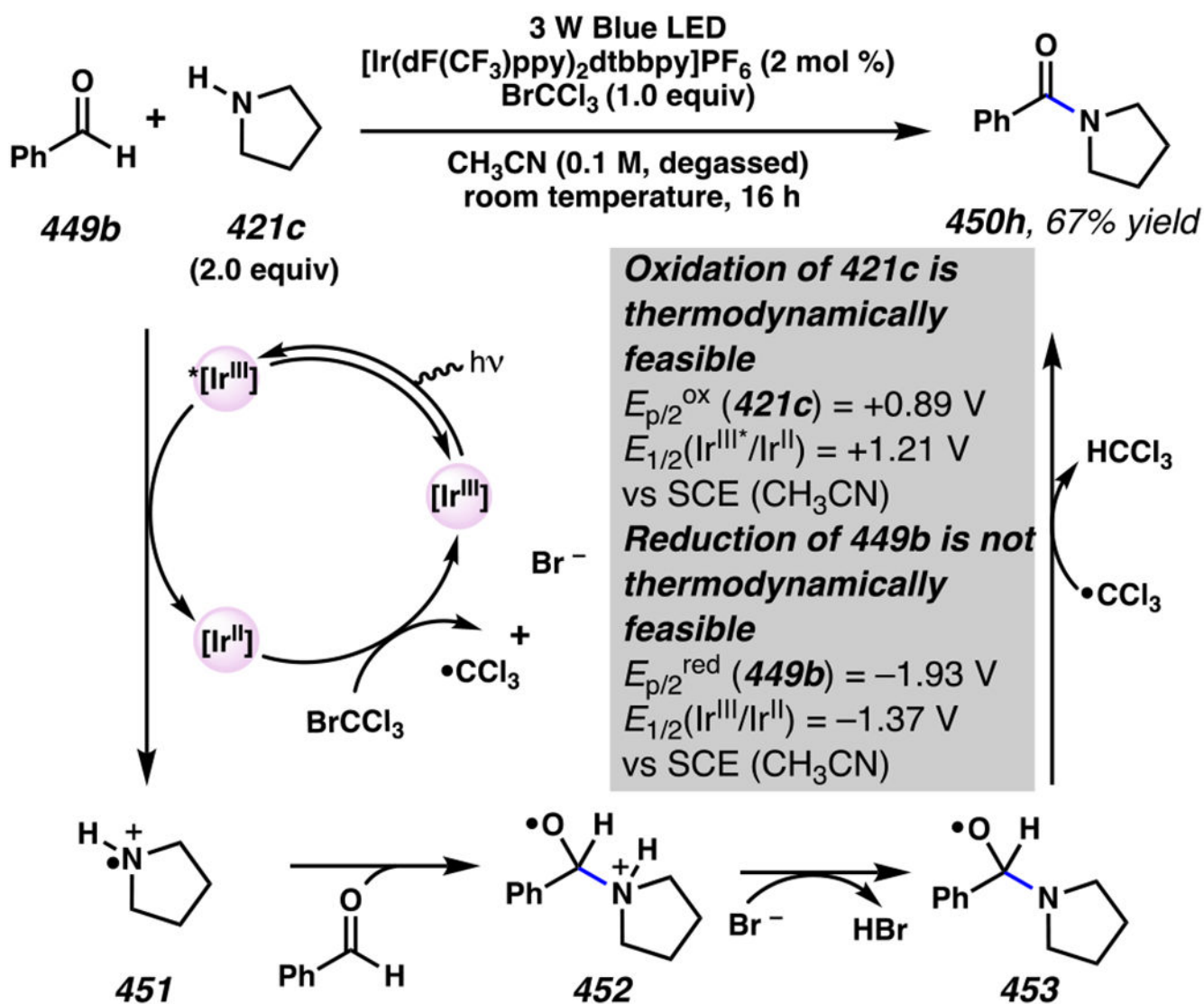
Hemicyanine photocatalyst

**Scheme 103.**

Advances in Amide Bond Formation Reactions Rely on Ambient Molecular Oxygen as an Oxidant



**Scheme 104.**  
 Photo-Driven Reaction Engages Alkyl and Aryl Aldehydes with Primary and Secondary Amines and Anilines to Form Amide Bonds

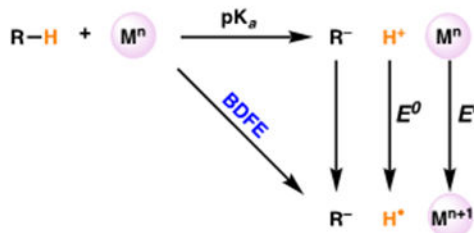


Scheme 105.  
Photo-Driven Reaction Enables Amide Bond Formation from Amines and Aldehydes

(A) Amidyl radicals can be accessed directly from amide by PCET



(B) Qualitatively, the capacity of a given base/oxidant pair to function as hydrogen-atom acceptors can be understood based on a *BDFE* calculation popularized by Mayer



(C) *BDFE* of optimal base/oxidant pair is near that of *N-H* bond

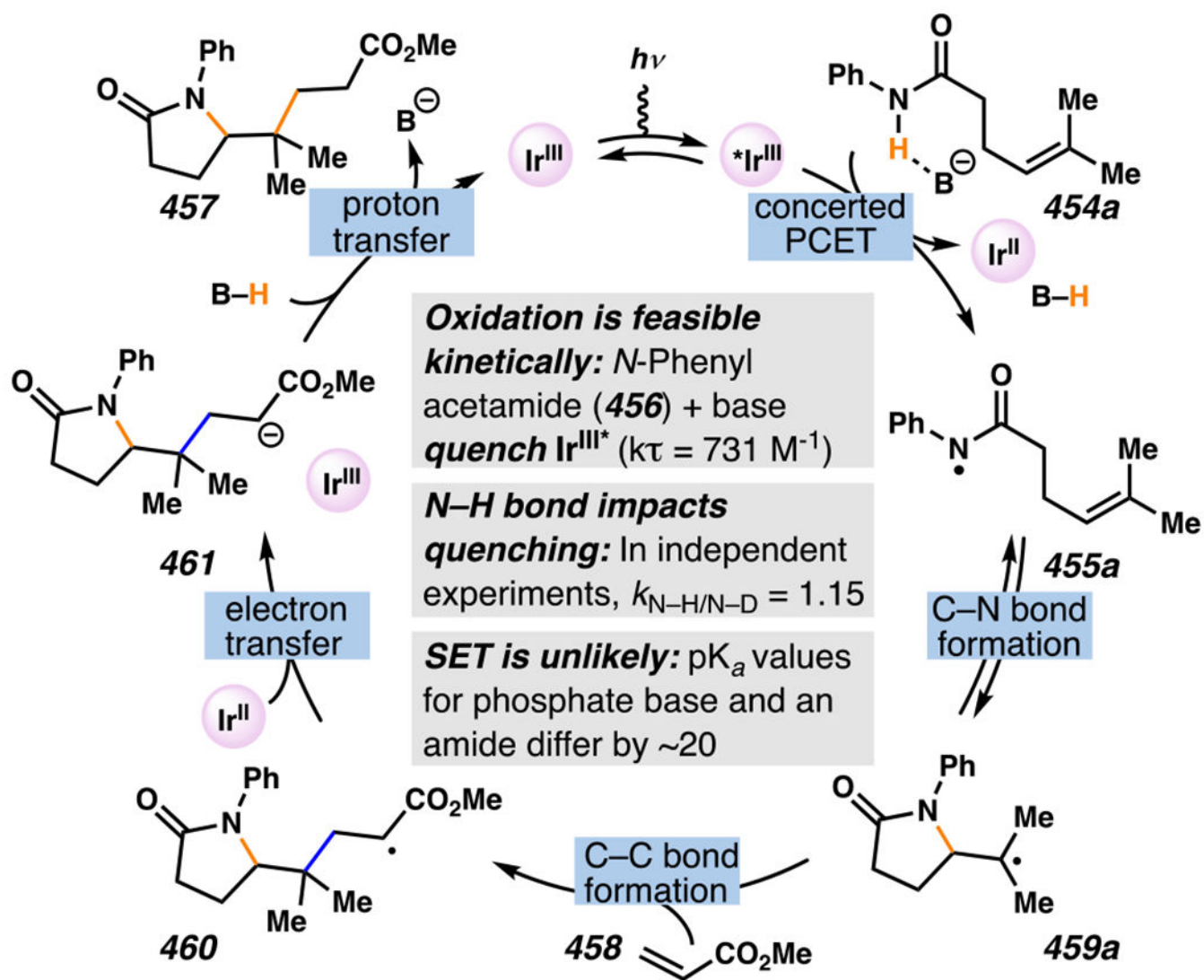


entry	photocatalyst	base	pK <sub>a</sub>	E <sup>0</sup> (vs Fc)	BDFE <sup>a</sup>	yield (%) <sup>b</sup>
1	Ir(Fmppy) <sub>2</sub> (dtbbpy)PF <sub>6</sub>	NBu <sub>4</sub> O <sub>2</sub> P(OBu) <sub>2</sub>	13	0.39	82	0
2	Ir(dF(CF <sub>3</sub> )ppy) <sub>2</sub> (dtbbpy)PF <sub>6</sub>	NBu <sub>4</sub> O <sub>2</sub> P(OBu) <sub>2</sub>	13	0.83	92	76
3	Ir(Fmppy) <sub>2</sub> (dtbbpy)PF <sub>6</sub>	NBu <sub>4</sub> OBz	21.5	0.39	93	56
4	Ir(dF(CF <sub>3</sub> )ppy) <sub>2</sub> (bpy)PF <sub>6</sub>	NBu <sub>4</sub> O <sub>2</sub> P(OBu) <sub>2</sub>	13	1.04	97	92
5	Ir(dF(CF <sub>3</sub> )ppy) <sub>2</sub> (dtbbpy)PF <sub>6</sub>	NBu <sub>4</sub> OBz	21.5	0.83	104	76
6	Ir(dF(CF <sub>3</sub> )ppy) <sub>2</sub> (bpy)PF <sub>6</sub>	NBu <sub>4</sub> OBz	21.5	1.04	108	50

<sup>a</sup> BDFE (kcal/mol) = 1.37 pK<sub>a</sub>(B-H) + 23.06 E<sup>0</sup>(M<sup>n</sup>/M<sup>n+1</sup>) + C<sub>solv</sub>; C<sub>solv</sub> = 54.9 kcal/mol (MeCN). <sup>b</sup> Yield determined by <sup>1</sup>H NMR analysis of the crude reaction mixture relative to an internal standard.

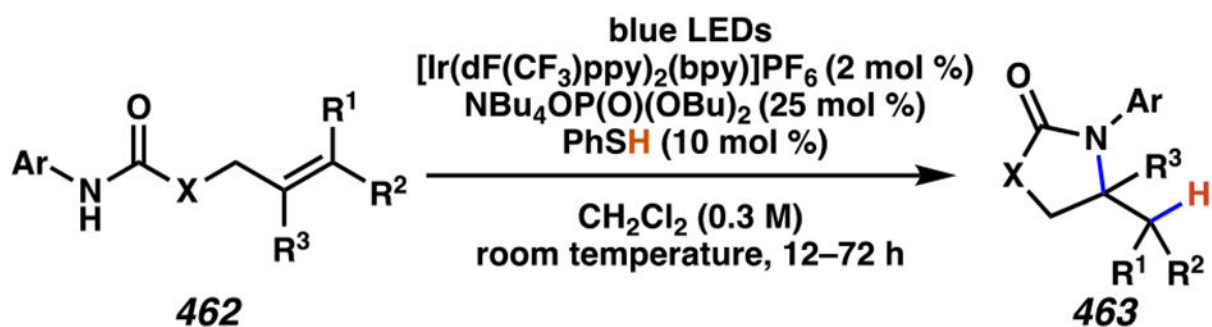
#### Scheme 106.

Photo-driven Proton-Coupled Electron Transfer (PCET) Processes Can Provide Access to Amidyl Radicals, Critical Intermediates in Alkene Carboamination Reactions

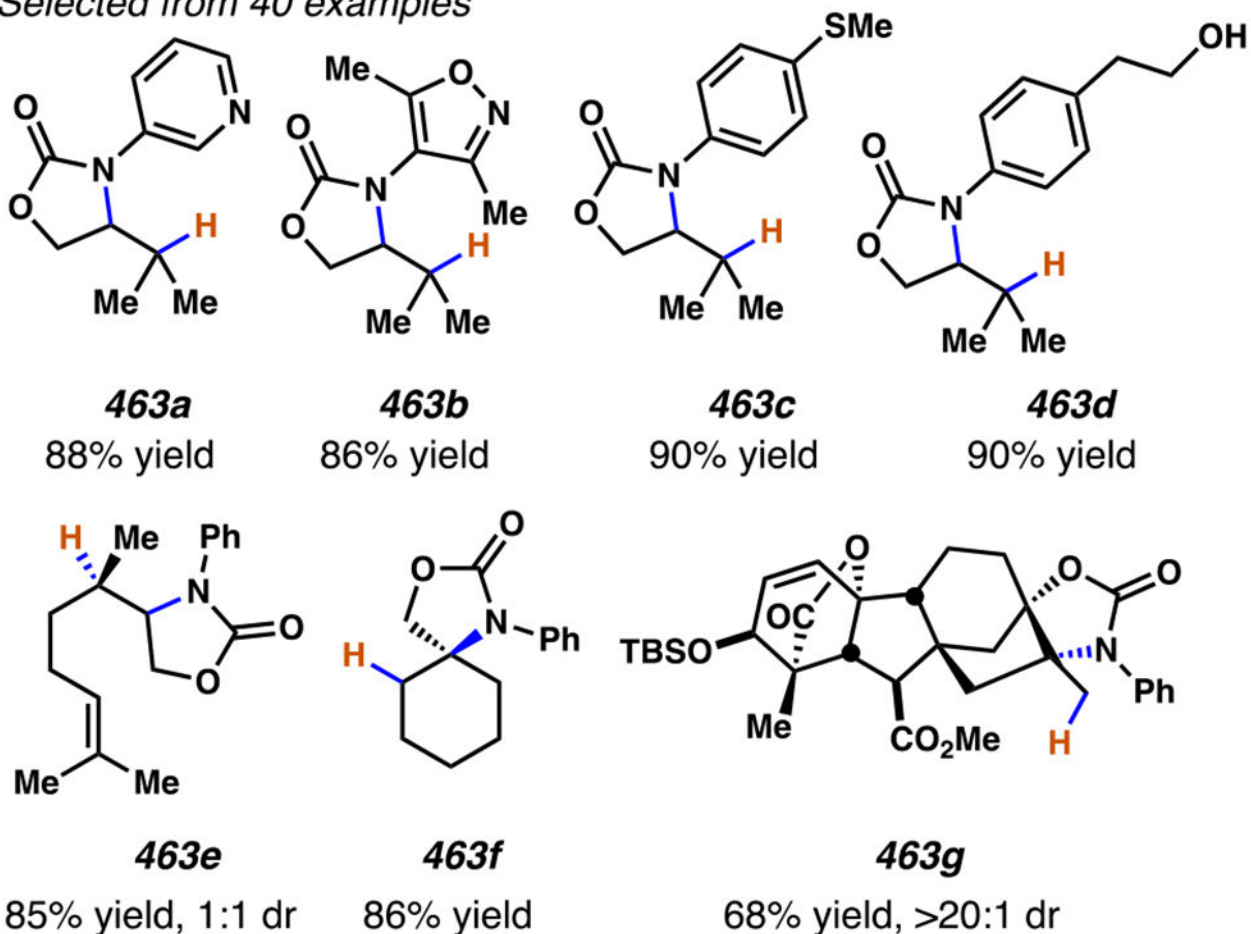


Scheme 107.

Evidence Is Consistent with the Proposed PCET Mechanism



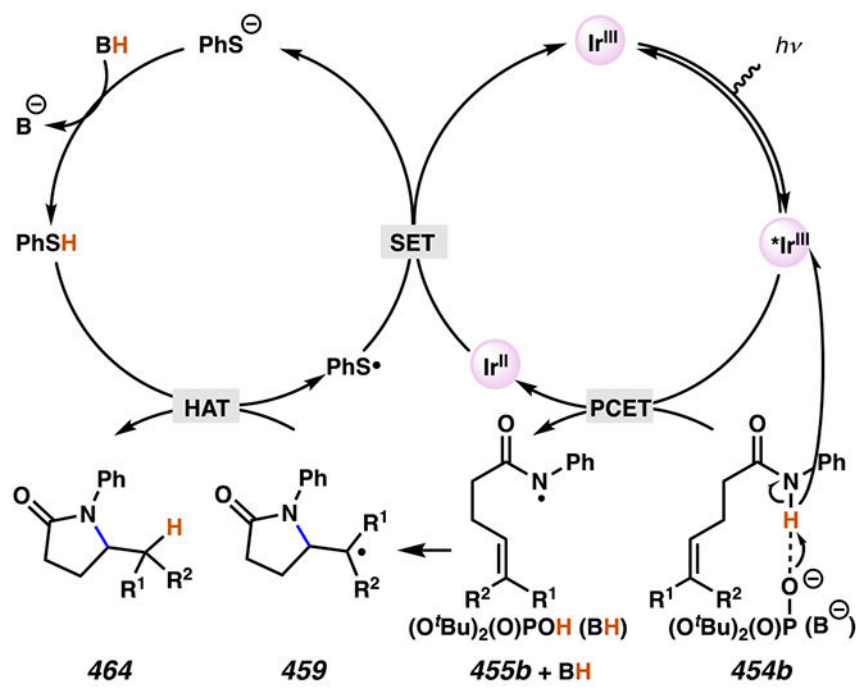
Selected from 40 examples



**Scheme 108.**

Olefin Hydroamidation is Enabled by Selective Amidyl Radical Generation in the Presence of Thiophenol





**Thermodynamic Challenge: An amidyl N–H bond is stronger than the S–H bond of PhSH:** BDFE (CH<sub>3</sub>CN): c.a. 98.9 vs. 79.1 kcal/mol  
**Kinetically: Amide oxidation is feasible and appears to be the dominant pathway for radical generation:**

In solutions with phosphate base, thiophenol and acetanilide, oxidative quenching rates exhibit a first-order dependence on acetanilide concentration ( $k\tau = 1250 \text{ M}^{-1}$ ), and a zeroth order dependence on PhSH.

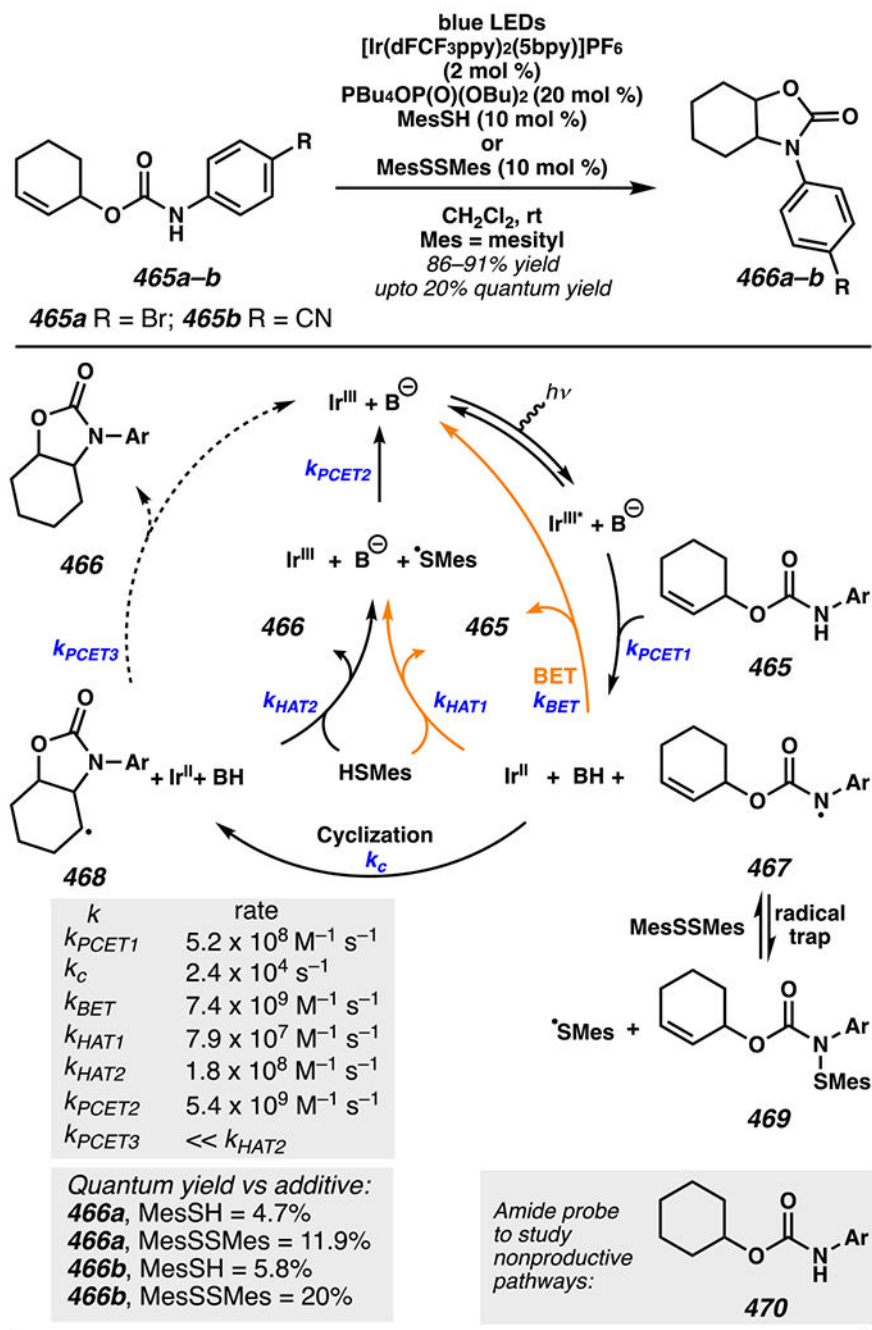
**Rationale:** Computationally, it's 5.2 kcal/mol *more favorable to form a hydrogen bonding complex between phosphate and an amide rather than a thiophenol* ( $\omega\text{B97XD 6-31G}++(2\text{d},2\text{p})\text{CPCM}=\text{CH}_2\text{Cl}_2$ ).

**H-bonding ability dictates chemoselectivity in the PCET process:**

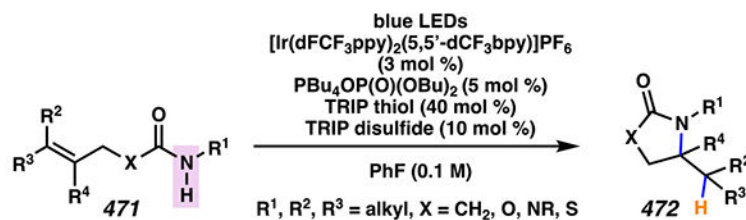
substrate	BDFE <sub>N–H/S–H</sub> (kcal/mol)	$K_A$ (M <sup>-1</sup> )	$k_{\text{PCET}}$ (M <sup>-1</sup> s <sup>-1</sup> )
N-phenylacetamide	98.9	1050	$8.4 \times 10^9$
thiophenol	79.1	200	$9.5 \times 10^9$

**Scheme 109.**

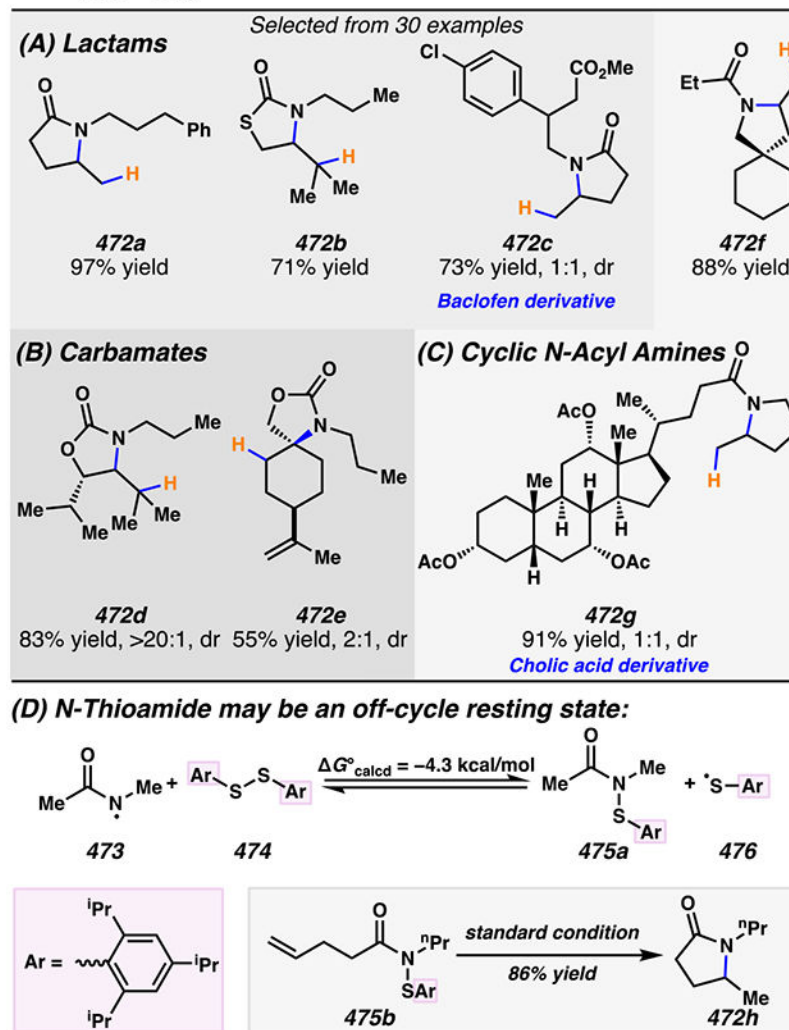
While an Amidyl N–H Bond Is Stronger Than A Thiyl S–H Bond, the Greater Hydrogen-Bonding Ability of an Amide Relative to a Thiol Enables Chemoselective Activation of An Amide to An Amidyl Radical



**Scheme 110.** The Off-Cycle Reversible Trapping of Amidyl Radical Intermediates Disrupts Energy-wasting Pathways and Improves the Reaction Quantum Efficiency

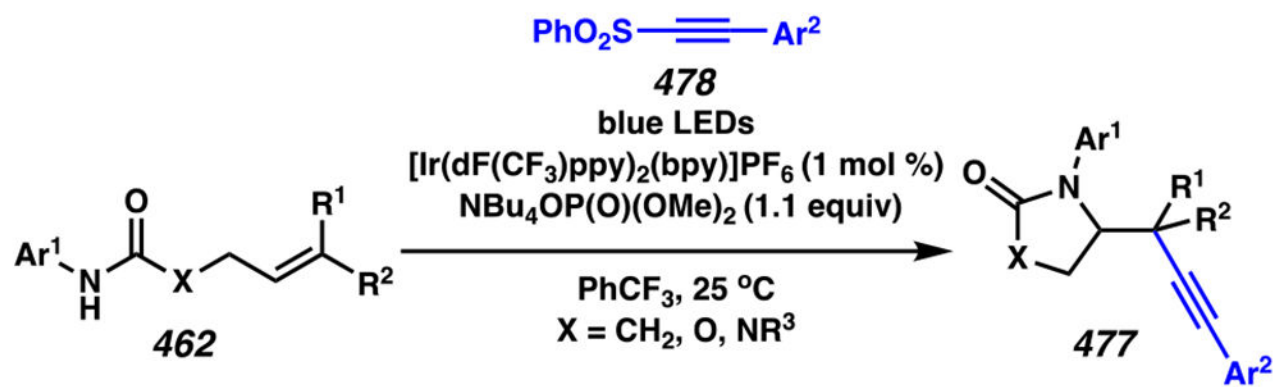


N-H BDFE ~110 kcal/mol  
for X = CH<sub>2</sub>

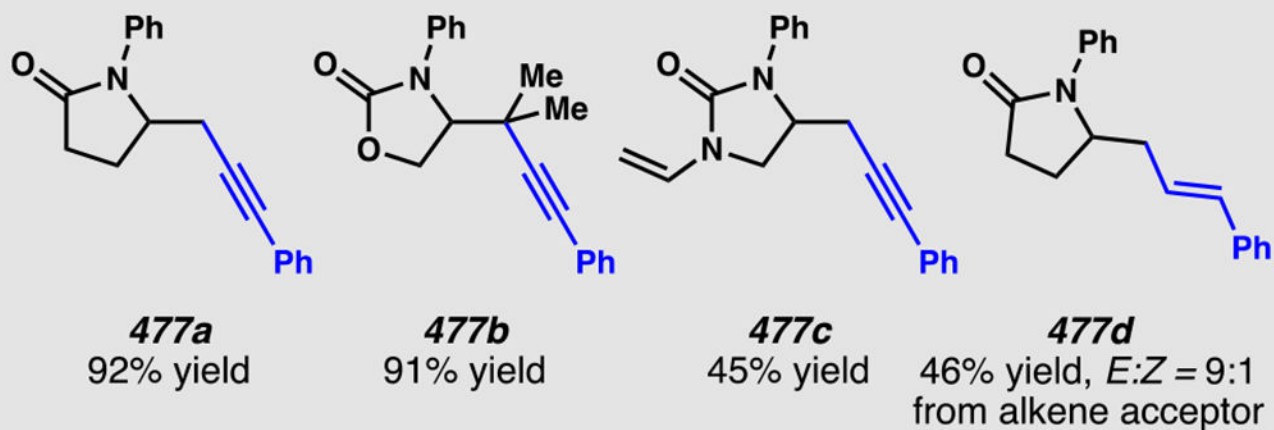


**Scheme 111.**

Amidyl Radicals Form from the Strong N-H Bonds of Unactivated *N*-Alkyl Amides by Excited-State PCET Process and Can Be Employed in Syntheses of Lactams, Cyclic *N*-Acyl Amines and Carbamates



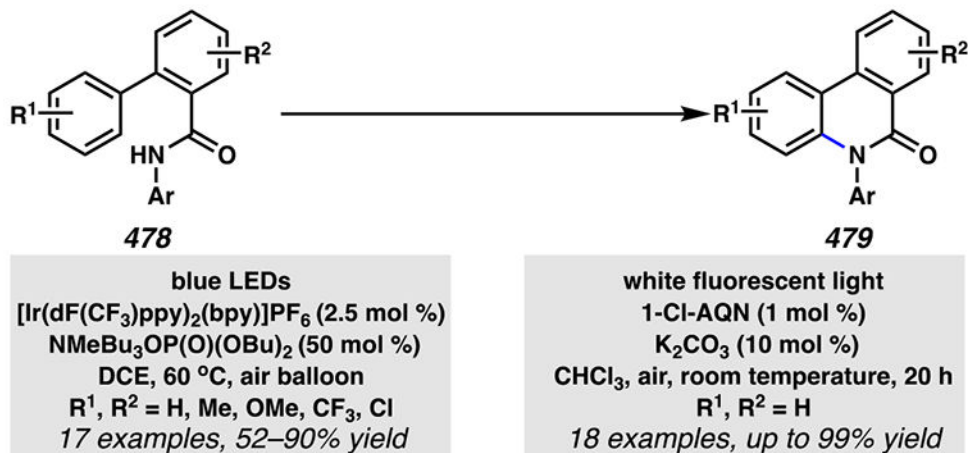
*Selected from 21 examples*



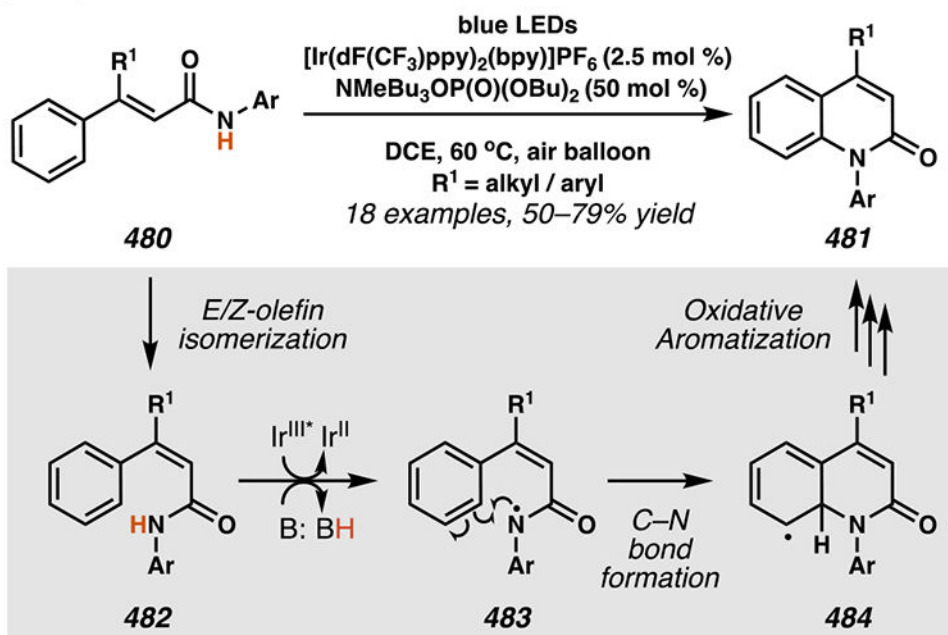
**Scheme 112.**

Alkynyl Sulfones Can Be Used as Acceptors in PCET-Mediated Processes

(A) Amidyl radical direct arene annulation to effect the synthesis of phenanthridinones.

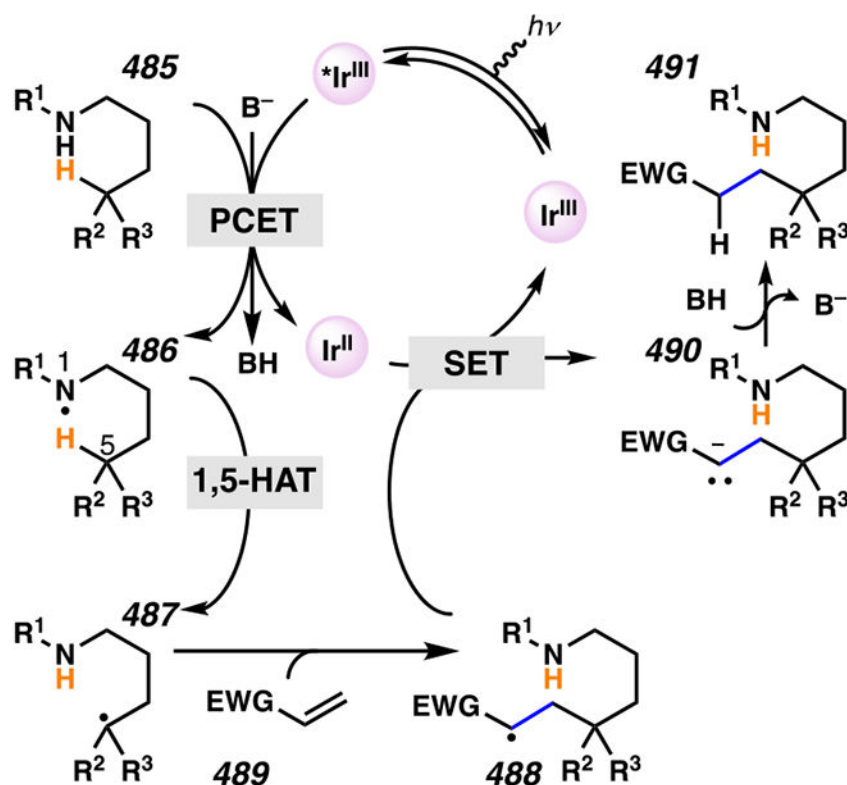


(B) Plausible mechanism to explain the participation of (Z)-N-phenylcinnamamide in intramolecular C–H amidation



**Scheme 113.**

A Cascade Sequence Accesses Phenanthridinones and Quinolinones in a PCET-mediated Process



**Base is necessary to activate amide to PCET:**

Amide ( $E_p = +1.48$  V vs Fc/Fc<sup>+</sup> in MeCN) does not quench <sup>\*</sup>Ir<sup>III</sup> ( $E_{1/2} = +1.30$  V vs Fc/Fc<sup>+</sup> in MeCN).

**Base assisted H-bonding activates PCET.**

**PCET is kinetically favored:** First order kinetics amide ( $k_{SV} = 46$  M<sup>-1</sup>) in the presence of base in luminescence quenching.

**Thermochemical constraints discounts stepwise**

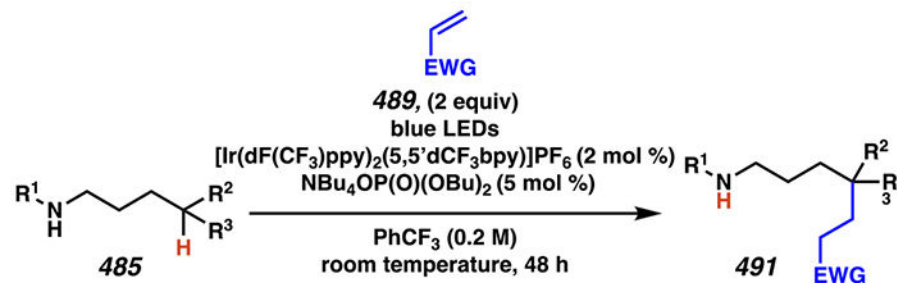
**proton-transfer then SET mechanism:** Large  $pK_a$  difference between amide and base ( $pK_a \sim 20$  in MeCN).

$pK_a$  (amide)  $\sim 23$  in DMSO;  $pK_a$  (HOP(O)(OBu)<sub>2</sub>)  $\sim 1.7$  in H<sub>2</sub>O

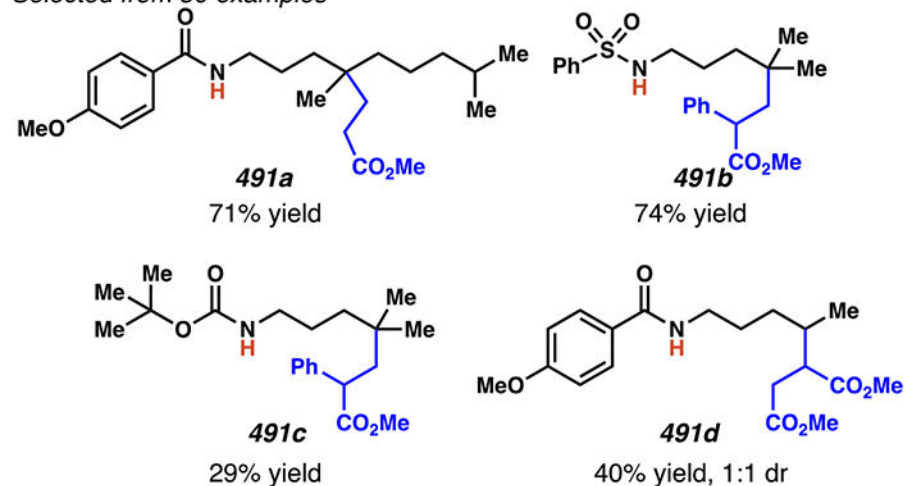
**Scheme 114.**

PCET Provides Access to Amidyl Radicals That Guide Alkylation of Remote C–H Bonds

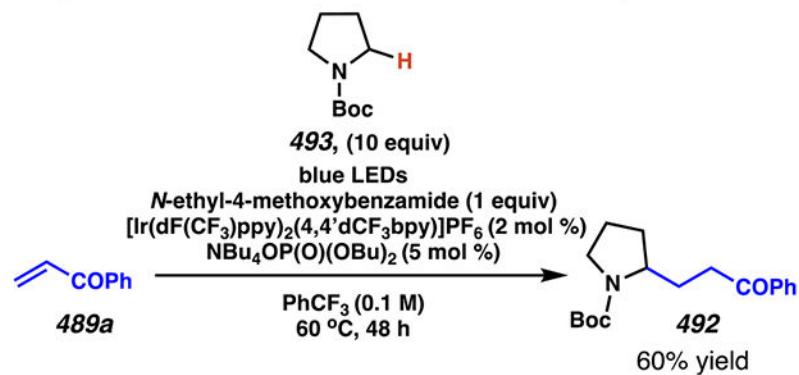
## (A) Amidyl radical mediates alkylation of remote C–H bonds



Selected from 30 examples

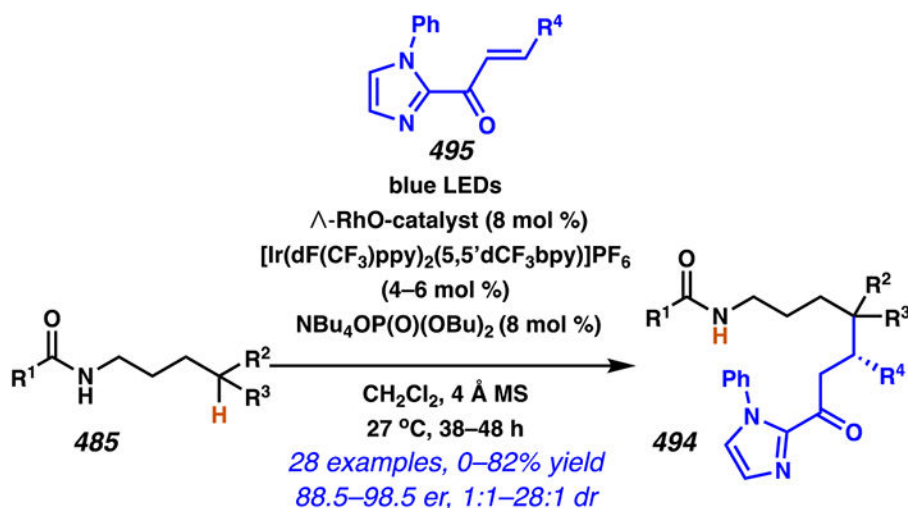


## (B) Amidyl radical mediates intermolecular C–H alkylation reaction

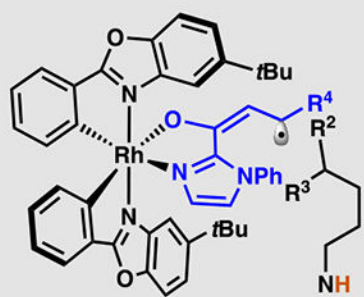


## Scheme 115.

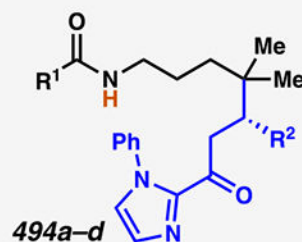
Amidyl Radicals Mediate Alkylation of Remote C–H Bonds



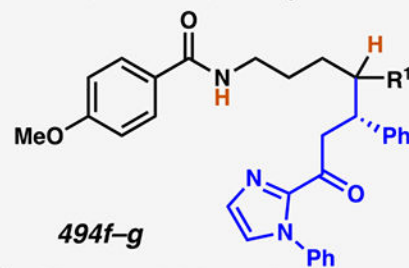
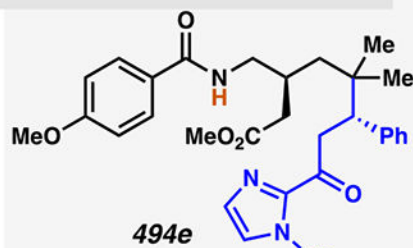
*Proposed model for asymmetric induction by  $\Delta$ -RhO-catalyst*



*Scope of asymmetric C–H alkylation*



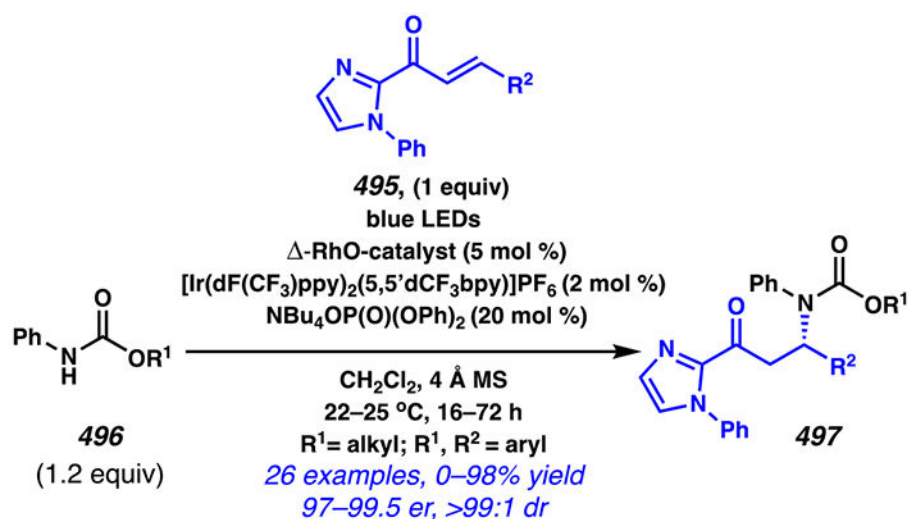
**494a** R<sup>1</sup> = PMP, R<sup>2</sup> = Ph, 80% yield, 97:3 er  
**494b** R<sup>1</sup> = Ph, R<sup>2</sup> = Ph, 0% yield  
**494c** R<sup>1</sup> = PMP, R<sup>2</sup> = PMP, 0% yield  
**494d** R<sup>1</sup> = PMP, R<sup>2</sup> = Me, trace yield



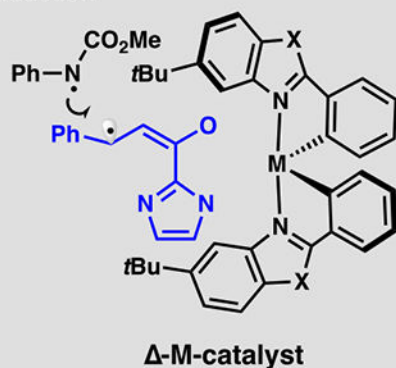
**Scheme 116.**

Asymmetric Alkylation of Remote C–H Bonds Proceeds Based on Amidyl Radical Directed 1,5-HAT and Chiral Rh-Controlled Asymmetric Induction

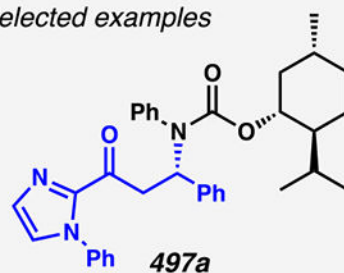




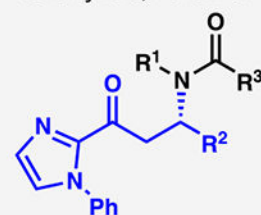
Proposed model for asymmetric induction



Selected examples



85% yield, >99:1 dr



**497b**, R<sup>1</sup> = Me, 0% yield

**497c**, R<sup>2</sup> = Me, trace yield

**497d**, R<sup>3</sup> = Me, 0% yield

Potential substrate will have

R<sup>1</sup> = R<sup>2</sup> = aryl, R<sup>3</sup> = O-alkyl/CH<sub>2</sub>Ar

sed quant.

**$\Delta$ -RhS** (M = Rh, X = S) used <10

**$\Delta$ -IrO** (M = Ir, X = O) used trace

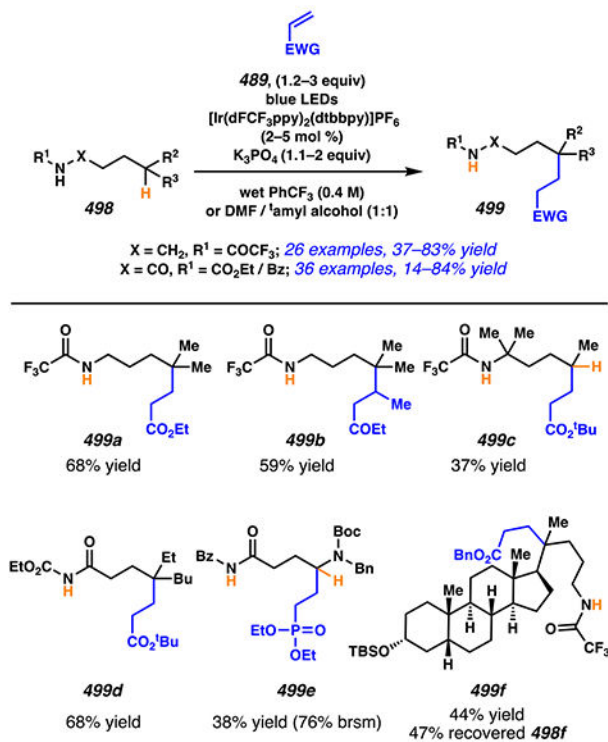
**$\Delta$ -RhO** (M = Rh, X = O) none 39%

<sup>a</sup>Conversion measured by crude <sup>1</sup>H NMR.

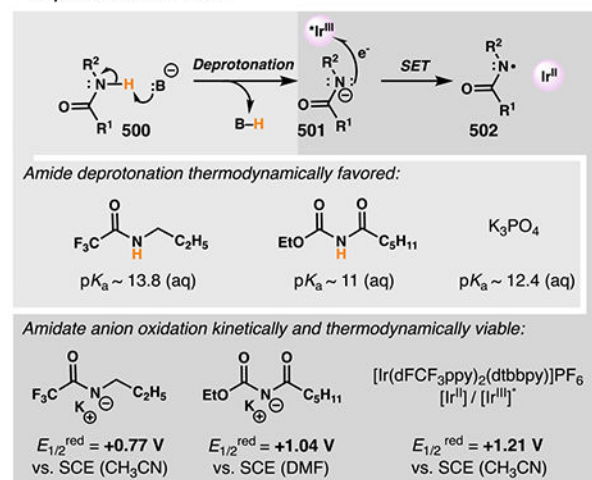
### Scheme 117.

The PCET Enabled Carbamyl Radical Participates in Intermolecular Chiral Rh-Catalyst Controlled Enantioselective  $\beta$ -Amination Reaction

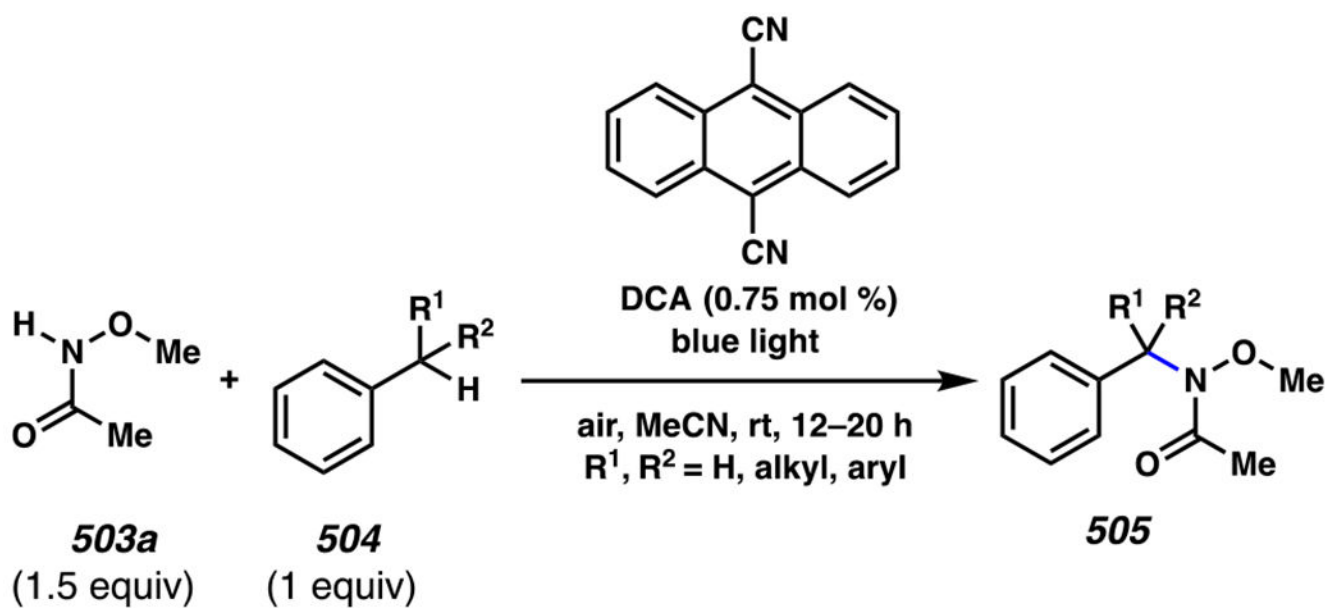
## (A) Amides direct Giese reaction



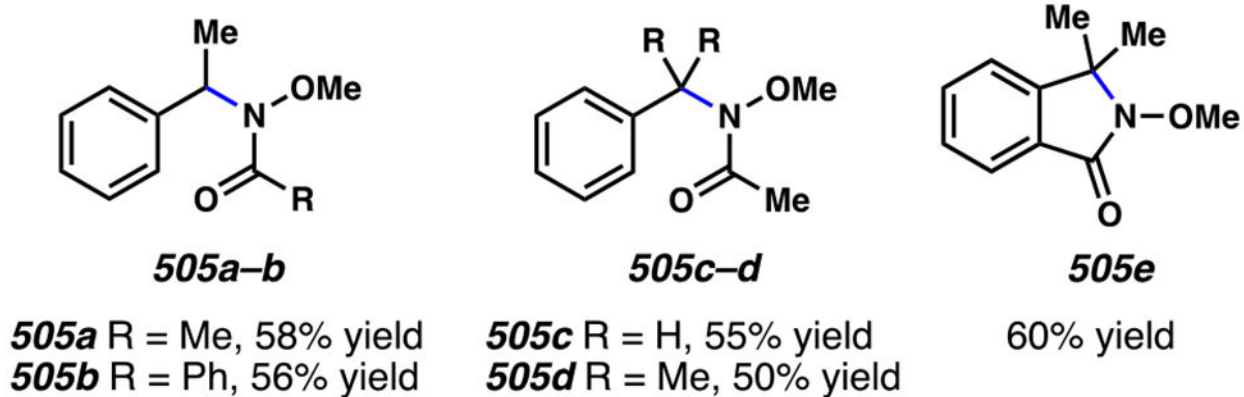
## (B) Rovis and co-workers access amidyl radicals via stepwise deprotonation and SET

**Scheme 118.**

Sequential Proton Transfer and SET Can Provide Access to Amidyl Radicals That Guide Giese Reactions at Unactivated C(sp<sup>3</sup>)-H Bonds

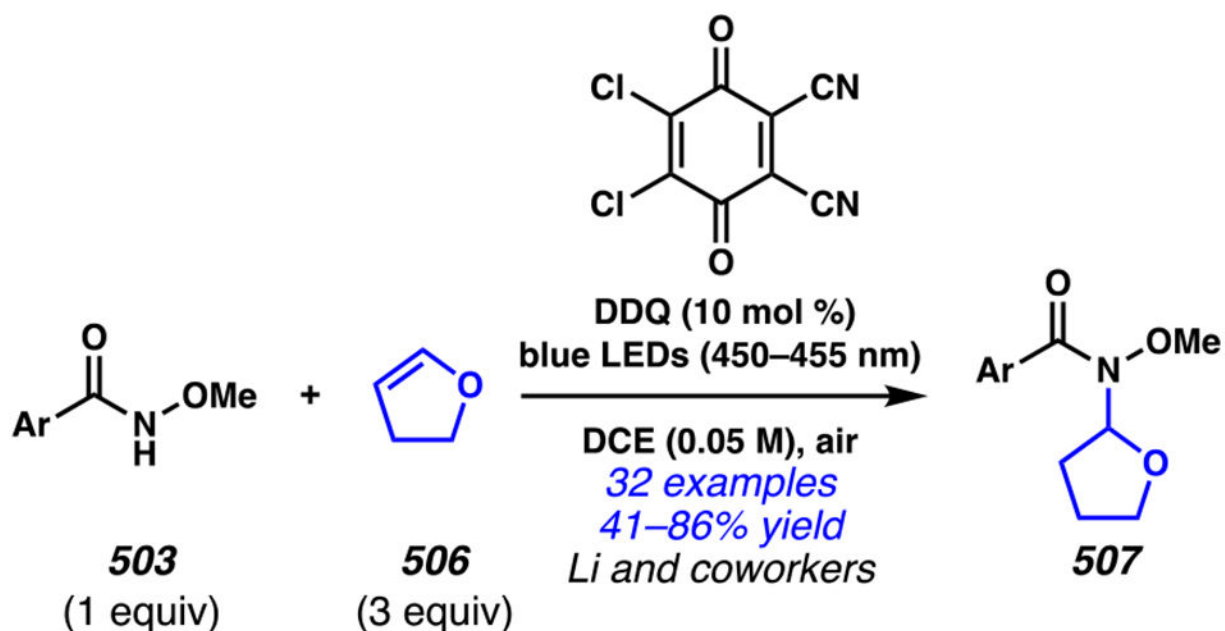


*Selected from 30 examples*



Scheme 119.

DCA Mediates Radical Reaction Involving Weinreb Amides



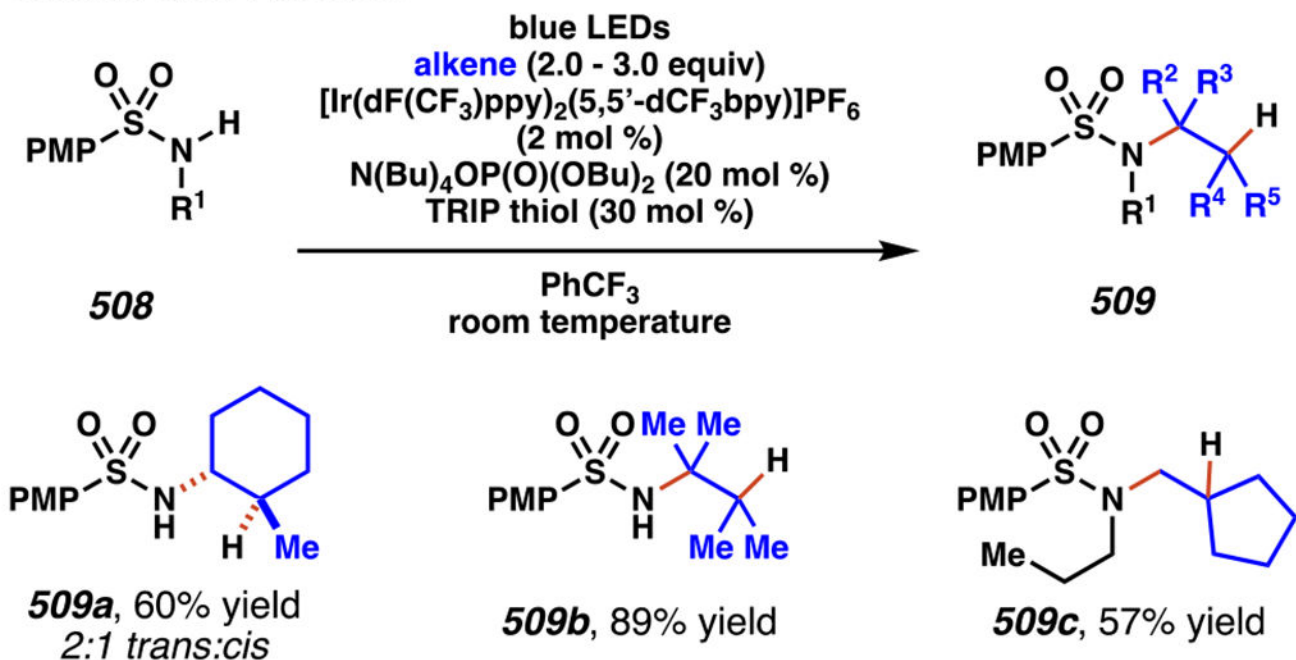
What excites DDQ		EDG provide better yield	Acyclic vinyl ethers
Light source	Yield <sup>a</sup>		
450–455 nm	86%	<b>507a–c</b>	<b>507d</b>
365–370 nm	19%	<b>507a</b> R = H, 86% yield	41% yield
395–405 nm	30%	<b>507b</b> R = OMe, 85% yield	
420–425 nm	28%	<b>507c</b> R = CN, 56% yield	
530–535 nm	35%		

<sup>a</sup>Isolated yield for Ar = Ph

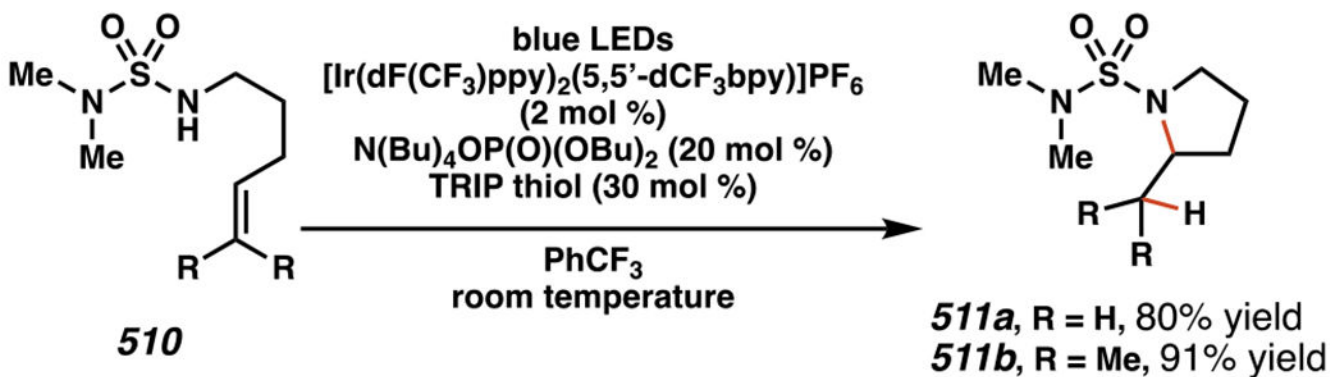
Scheme 120.

DDQ-Mediated Radical Reaction Involves Weinreb Amides as Substrates

(A) Intermolecular Hydroamination Reactions Involving Unactivated Alkenes

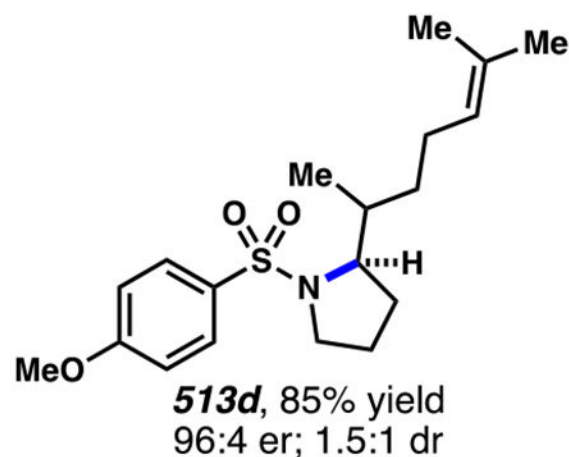
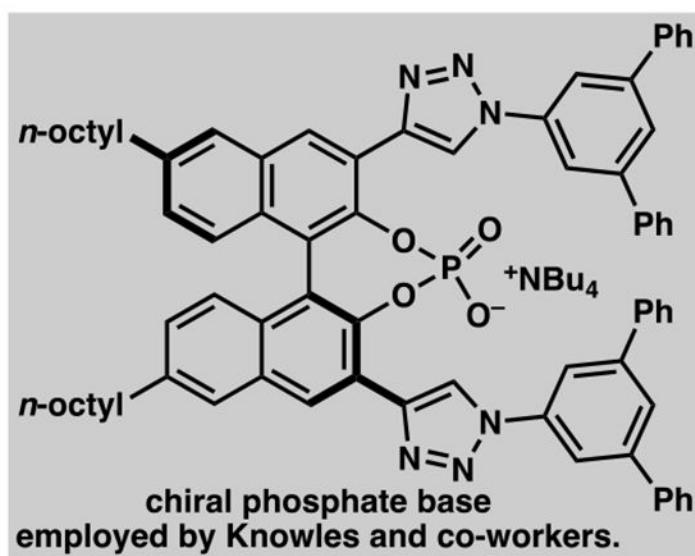
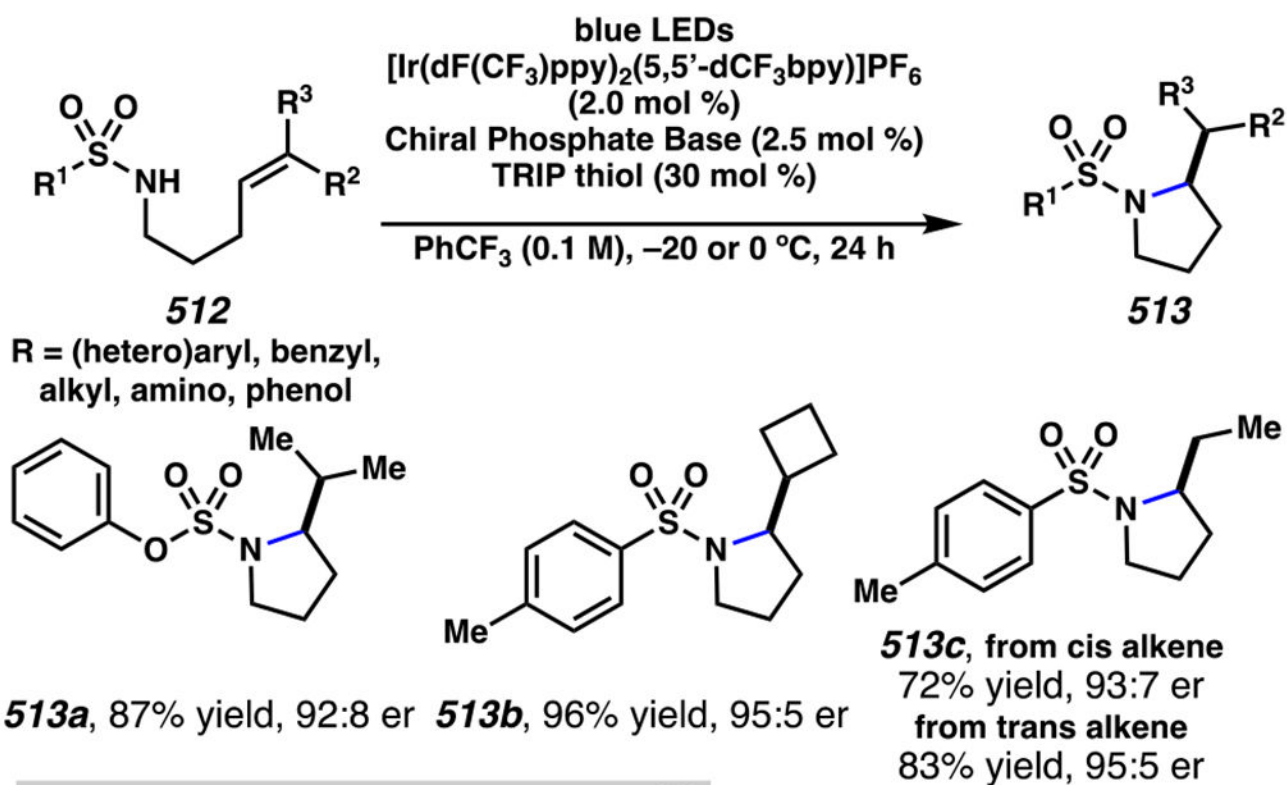


(B) Intramolecular 5-Exo-trig Cyclization Reactions with Sulfamides

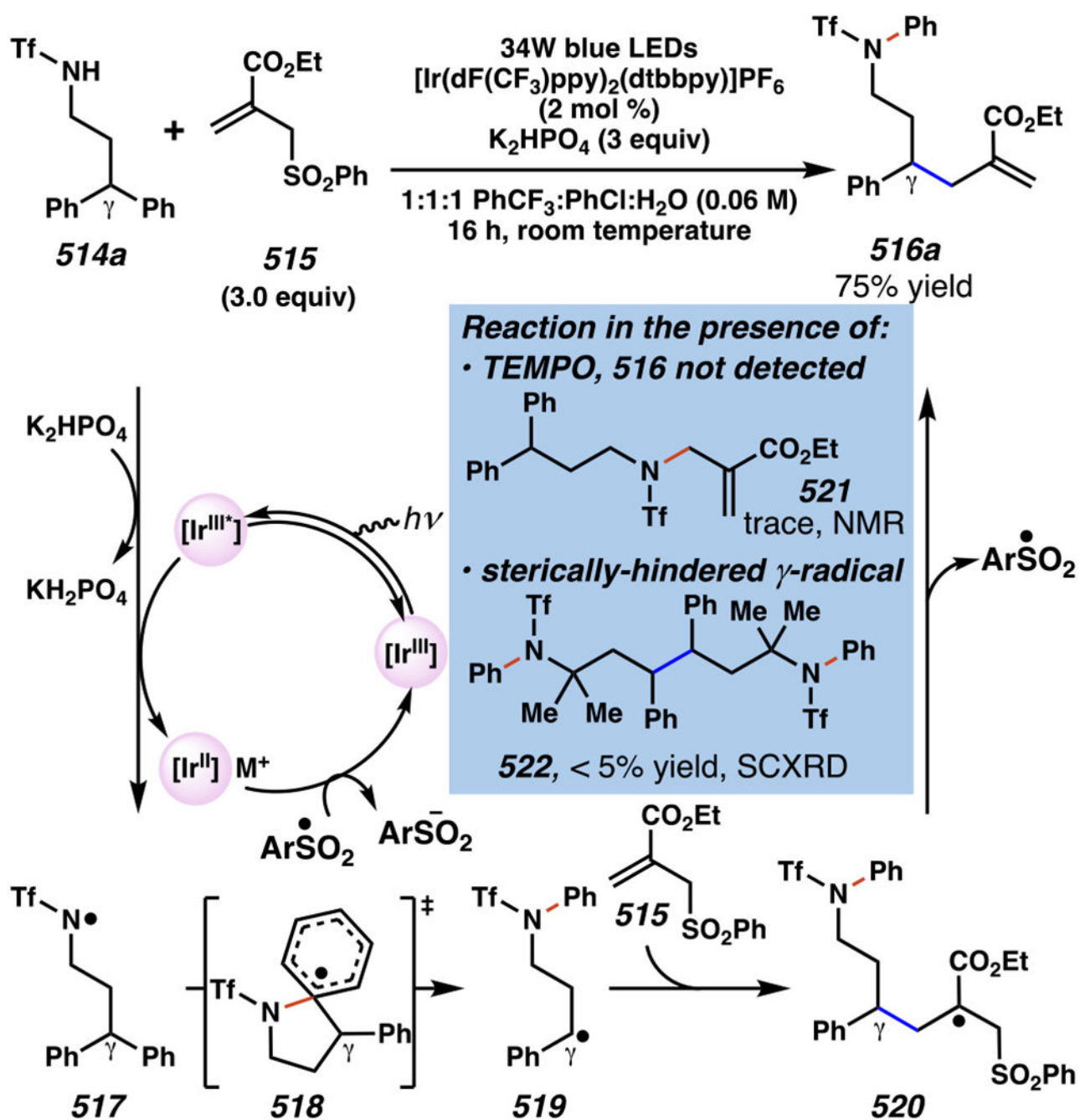


Scheme 121.

Photoredox Conditions Enable (A) Intermolecular Hydroamination Reactions Involving Unactivated Alkenes and (B) Intramolecular 5-*exo*-Trig Cyclization Reactions with Sulfamides

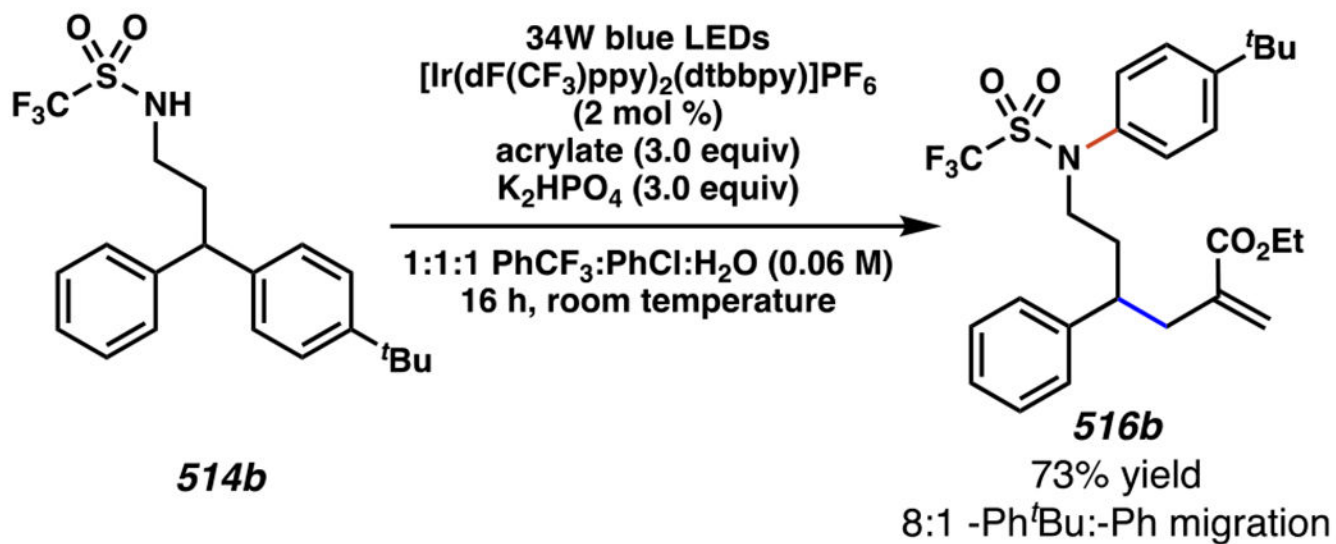


**Scheme 122.**  
 Chiral Phosphate Bases Enable Enantioselective Intramolecular Cyclization Reactions  
 Involving Sulfamyl Radicals



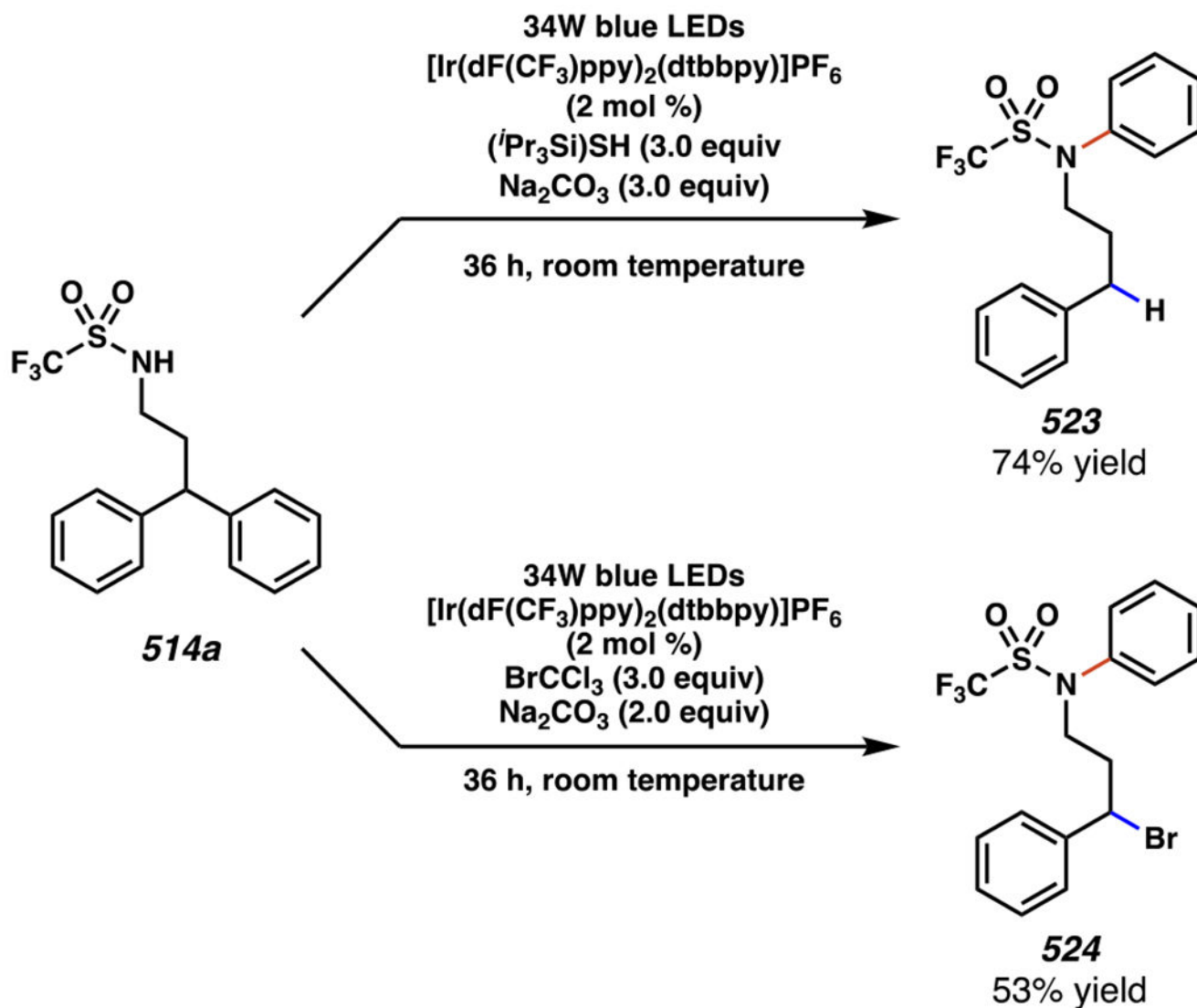
Scheme 123.

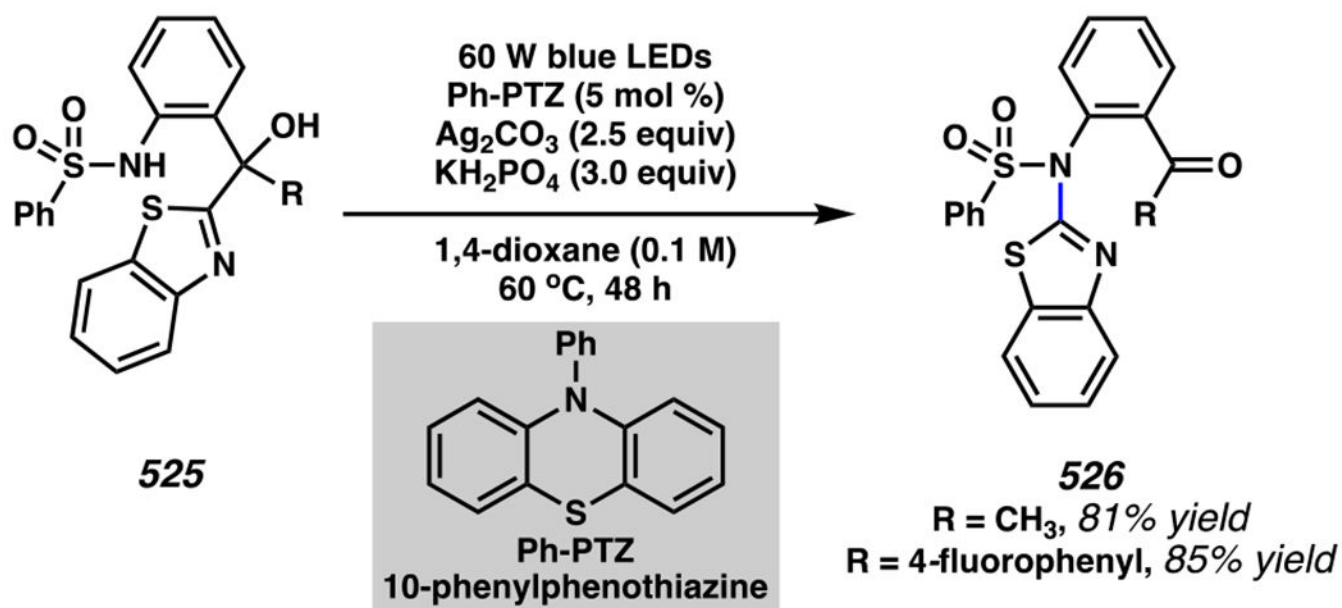
Photoredox Catalysis Enables  $\gamma$ -C(sp<sup>3</sup>) Functionalization through Aryl C–N Migration, Likely Mediated by *N*-Centered Sulfamyl Radicals

**Scheme 124.**

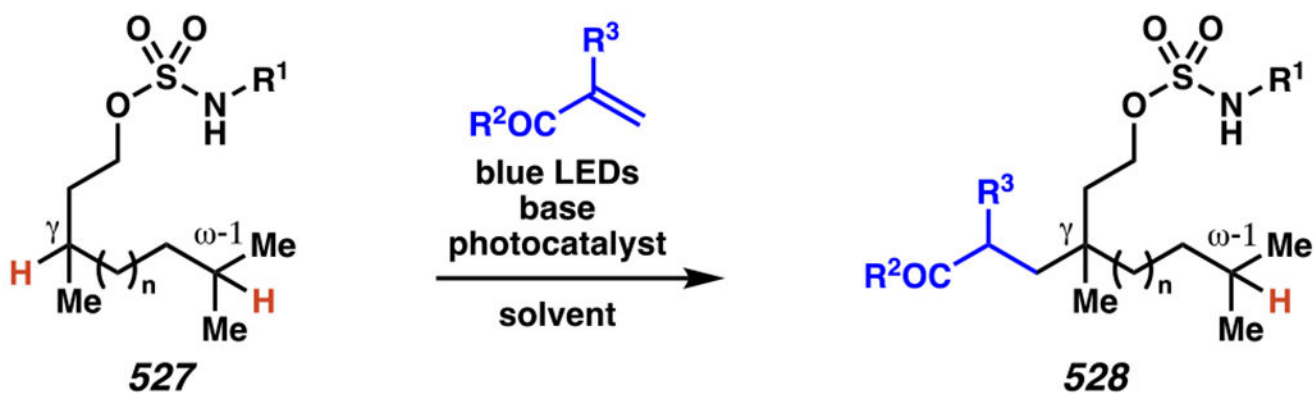
Aryl Migration Is Strongly Biased toward More Electron-Rich Aryl Groups, as Would Be Expected in a Radical Mediated Process



**Scheme 125.**Closely Related Conditions Enable  $\gamma$ -Protodearylation and  $\gamma$ -Bromodearylation Processes



**Scheme 126.**  
Photoredox Catalysis Enables Remote Heteroaryl Migration from Benzylic Alcohols

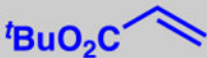
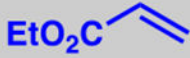
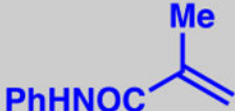


*Authors*

*(examples susceptible to competitive site-selectivity / total examples)*

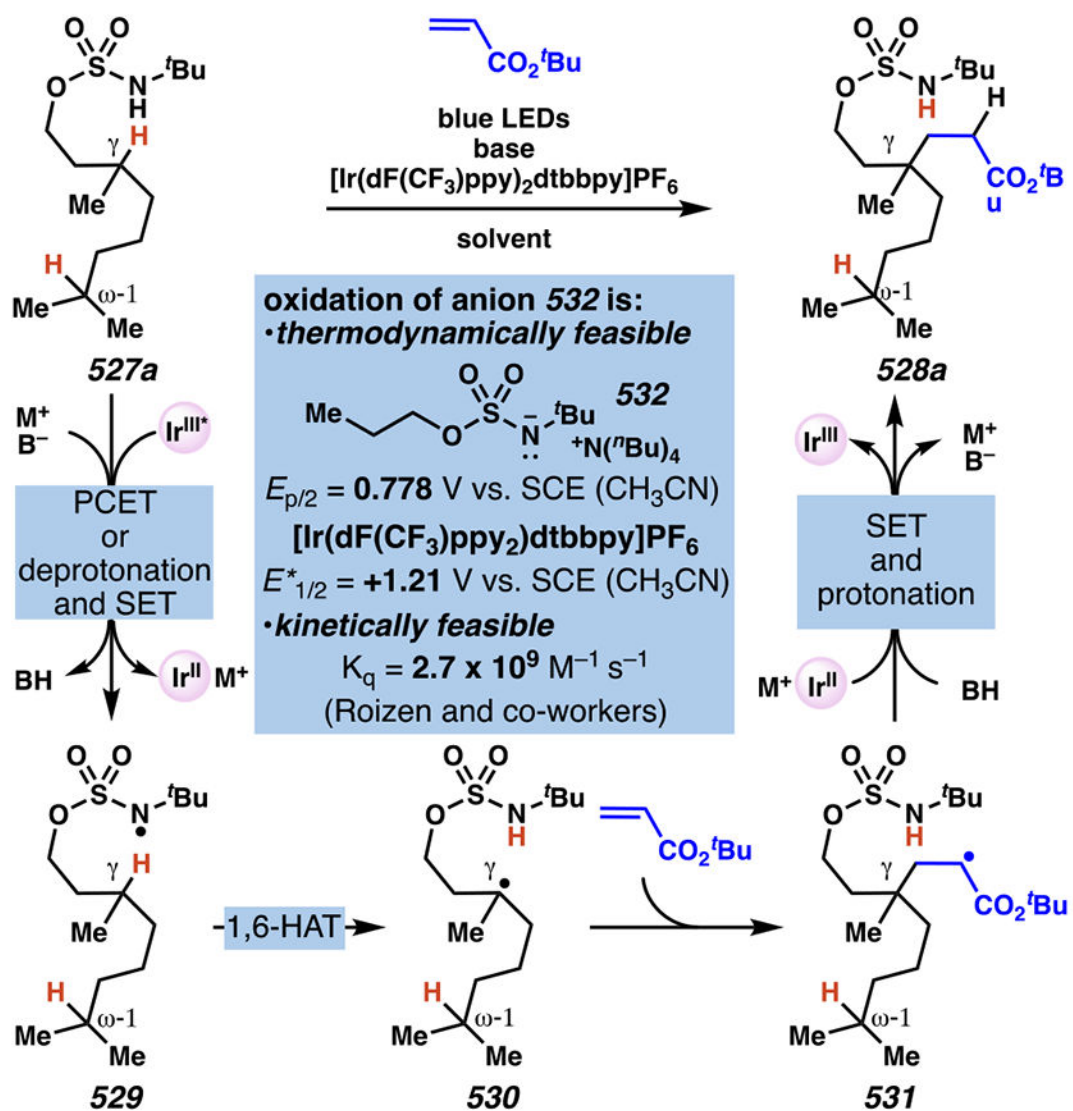
*Roizen and co-workers* (24 / 37)    *Shu and co-workers* (5 / 49)    *Duan and co-workers* (4 / 49)

**528a**,  $\text{R}^1 = \text{tBu}$ ,  $n = 2$     **528b**,  $\text{R}^1 = \text{CH}_2\text{CF}_3$ ,  $n = 1$     **528c**,  $\text{R}^1 = \text{tBu}$ ,  $n = 2$   
 96% yield                      70% yield                      78% yield

<b>trapping agent:</b>	 $\text{tBuO}_2\text{C}$ -alkene (2.2 equiv)	 $\text{EtO}_2\text{C}$ -alkene (2.0 equiv)	 $\text{PhHNOC}$ -Me-alkene (4.0 equiv)
<b>[Ir<sup>III</sup>]PF<sub>6</sub> PC:</b>	[Ir(dF(CF <sub>3</sub> )ppy) <sub>2</sub> dtbbpy] (1.0 mol %)	[Ir(dF(Me)ppy) <sub>2</sub> dtbbpy] (1.0 mol %)	[Ir(dF(CF <sub>3</sub> )ppy) <sub>2</sub> dtbbpy] (2.0 mol %)
<b>base:</b>	K <sub>2</sub> CO <sub>3</sub> (1.0 equiv)	Na <sub>2</sub> HPO <sub>4</sub> (3.0 equiv)	K <sub>3</sub> PO <sub>4</sub> ·3(H <sub>2</sub> O) (1.0 equiv)
<b>solvent:</b>	CH <sub>3</sub> CN (0.2 M)	2:1 <i>p</i> -chlorotoluene:H <sub>2</sub> O (0.03 M)	wet DMF (0.1 M)

**Scheme 127.**

Roizen and Co-workers, Shu and Co-workers, and Duan and Co-workers Develop Sulfamate-Ester Guided Giese Reactions to Selectively Functionalize  $\gamma\text{-C}(\text{sp}^3)\text{-H}$  Bonds

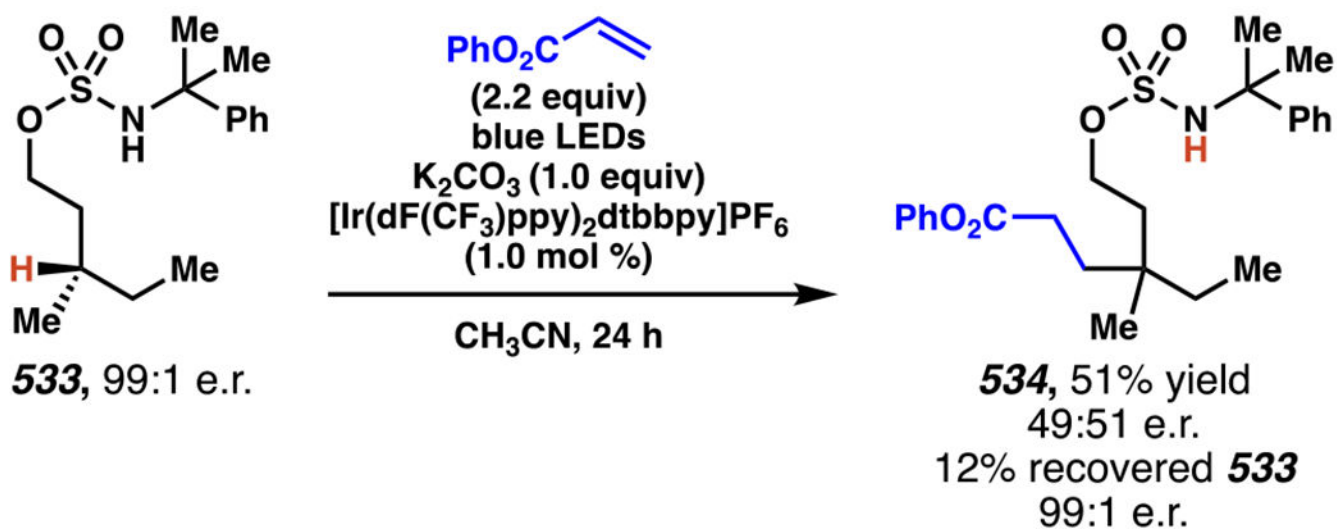


**C–H abstraction is rate-determining:**  $k_H/k_D=4.69$   
 (Shu and co-workers in parallel reactions)

**Protonation occurs intermolecularly:**  $\text{D}_2\text{O}$  labels product **528b**  
 (Shu and co-workers)

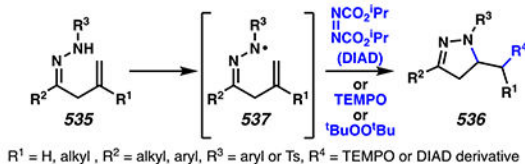
**Scheme 128.**

In the Proposed Mechanism, Sulfamyl Radicals Engage in a 1,6-HAT Process to Generate Carbon-Centered Radicals Capable of Trapping Electron-Deficient Alkenes

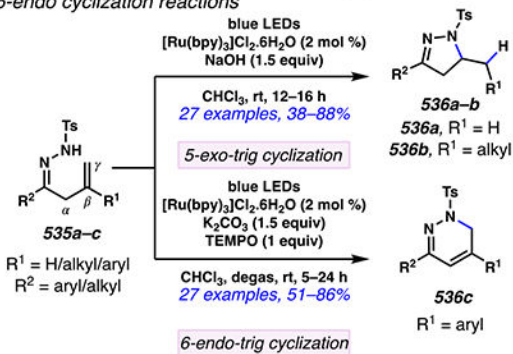
**Scheme 129.**

Under Conditions Developed by Roizen and Co-workers, Carbon-Centered Radicals Are Generated Irreversibly

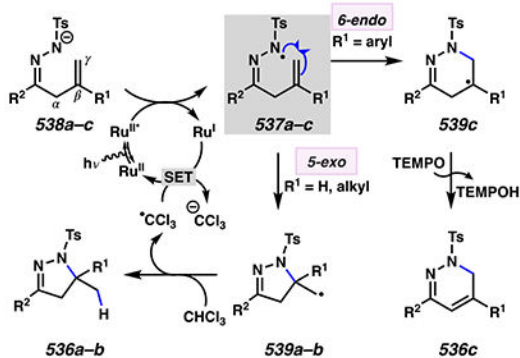
(A) Hydrazonyl radical intermediates can be prepared using copper catalysts or stoichiometric oxidants



(B) Photoredox catalysts can furnish access to hydrazonyl radical intermediates that engage in 5-*exo* or 6-*endo* cyclization reactions



(C) Plausible mechanisms to generate hydrazonyl radical intermediates



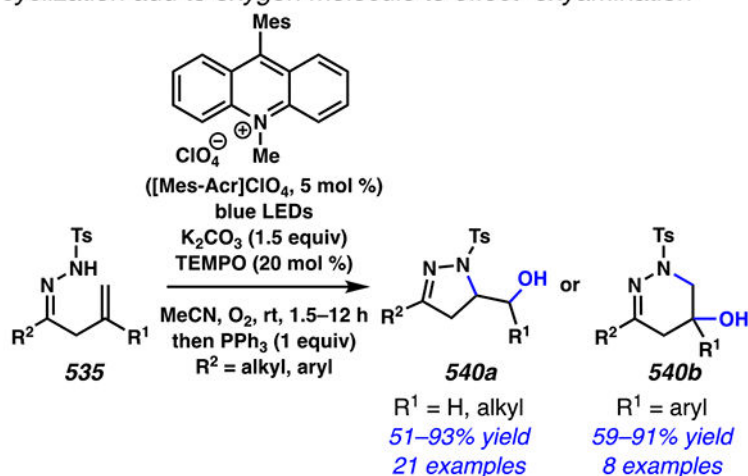
(D) Free energies for the regioselective radical cyclization

537	R <sup>1</sup>	ΔG (kcal/mol) <sup>a</sup>	
		5- <i>exo</i>	6- <i>endo</i>
537a	H	8.8	13.5
537b	Me	7.5	11.2
537c	Ph	11.4	8.7

<sup>a</sup>Gibbs free energies calculated in CHCl<sub>3</sub> using N-12/6-311pG(d, p)/B3 LYP/6-31G(d)

**Scheme 130.**  
Hydrazonyl Radicals Can Engage in 5-*Exo*-trig and 6-*Endo*-trig Cyclization Reactions

(A) Alkyl radical form from the hydrazonyl radical 5-exo or 6-endo cyclization add to oxygen molecule to effect oxyamination

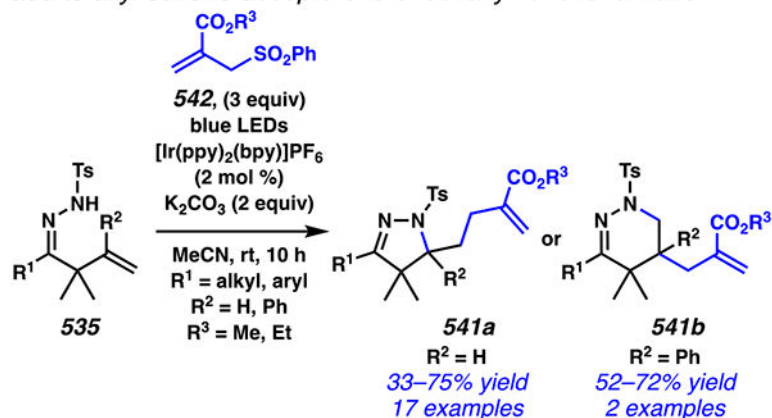


Photocatalyst, air, TEMPO and light need for hydrazone oxyamination

entry	deviation from the standard condition	time (h)	yield (%) <sup>a</sup>
1	-	1.5	85
2	no TEMPO	5	32
3	no $\text{K}_2\text{CO}_3$	4 <sup>b</sup>	86 <sup>b</sup>
4	No PC or no $\text{O}_2$ or No light	12	0

<sup>a</sup>Isolated yield. <sup>b</sup>Addition of  $\text{K}_2\text{CO}_3$  shorten the reaction time and improve the yield.

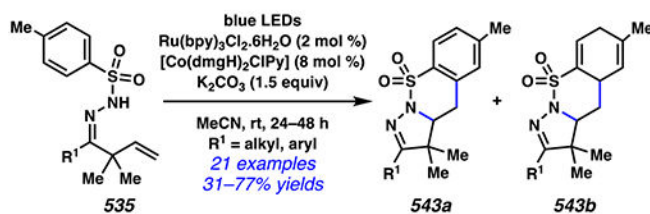
(B) Alkyl radical form from the hydrazonyl radical cyclization add to allyl sulfone acceptors to effect allyl functionalization



### Scheme 131.

Hydrazonyl Radicals Can Engage In Olefin Functionalization Reactions

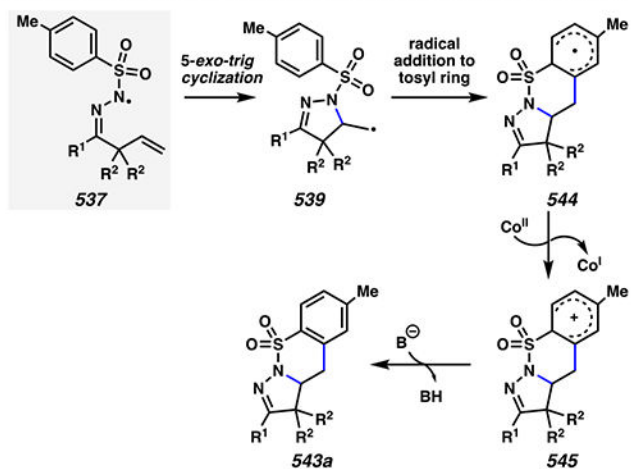
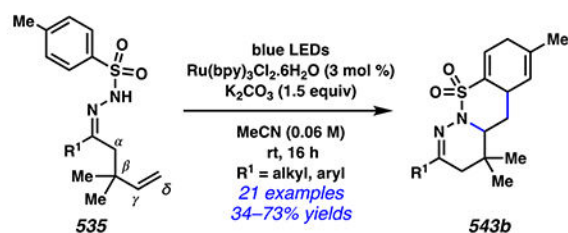
## (A) Photoredox/Co-dual catalysis for benzosultam synthesis

Additive effect on aromatization: Co-catalysts efficiently form sultam **543a**

entry	photocatalyst	additive	<b>543a</b> (%) <sup>a</sup>	<b>543b</b> (%)
1	$[\text{Ir}(\text{ppy})_2\text{bpy}]\text{PF}_6$	No additive	trace	85 <sup>a</sup>
2	$[\text{Ir}(\text{ppy})_2\text{bpy}]\text{PF}_6$	1,3-dinitrobenzene	49	trace
3	$[\text{Ir}(\text{ppy})_2\text{bpy}]\text{PF}_6$	<i>tert</i> -butyl perbenzoate	31	trace
4	$[\text{Ir}(\text{ppy})_2\text{bpy}]\text{PF}_6$	$[\text{Co}(\text{dmgH})_2\text{ClPy}]$	58	trace
5	$\text{Ru}(\text{bpy})_3\text{Cl}_2 \cdot 6\text{H}_2\text{O}$	$[\text{Co}(\text{dmgH})_2\text{ClPy}]$	73	trace

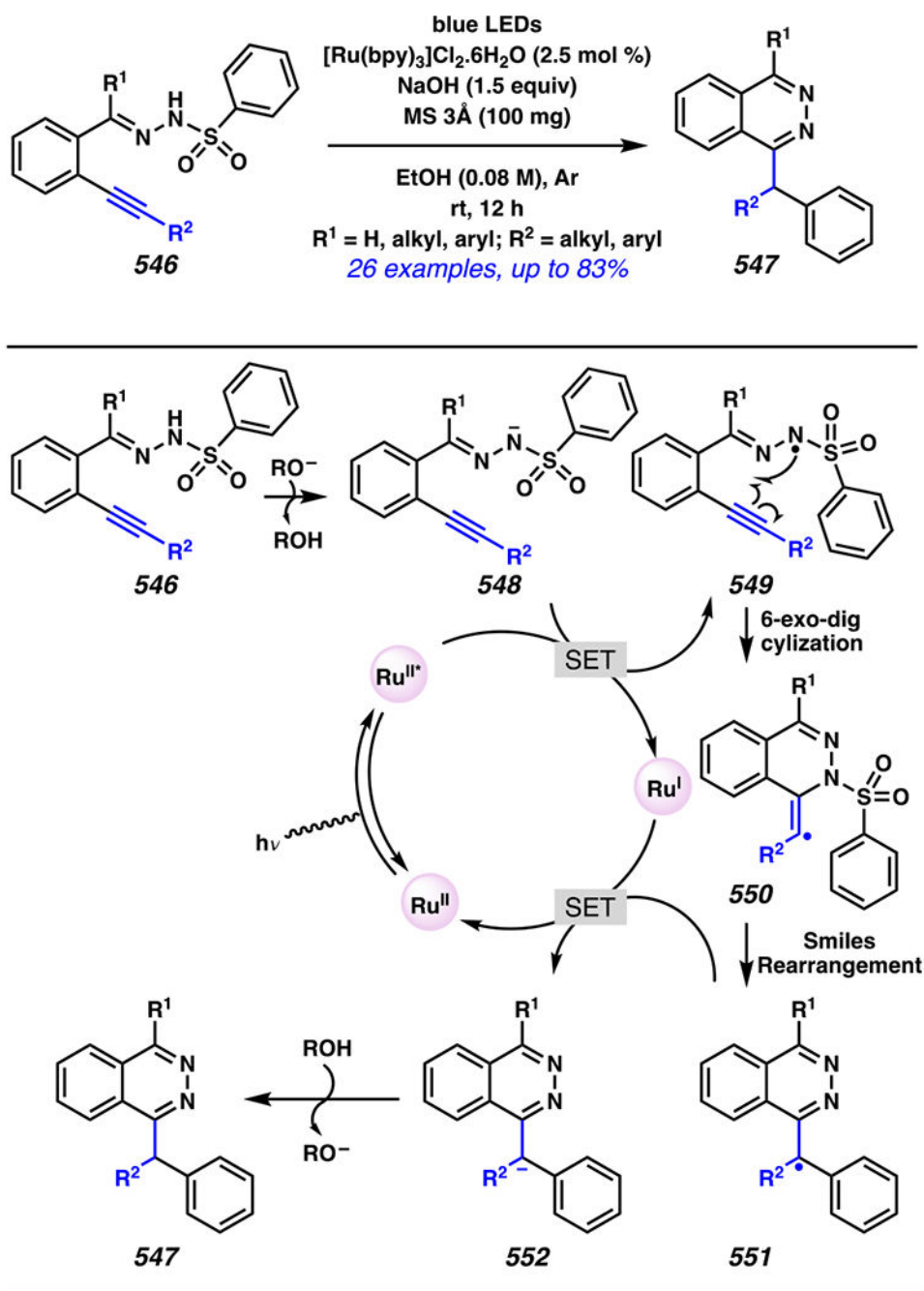
<sup>a</sup>isolated yield.

## (B) Alkyl radical adds to aromatic ring then Co-assisted aromatization

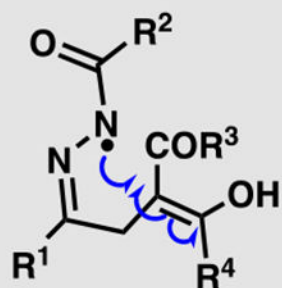
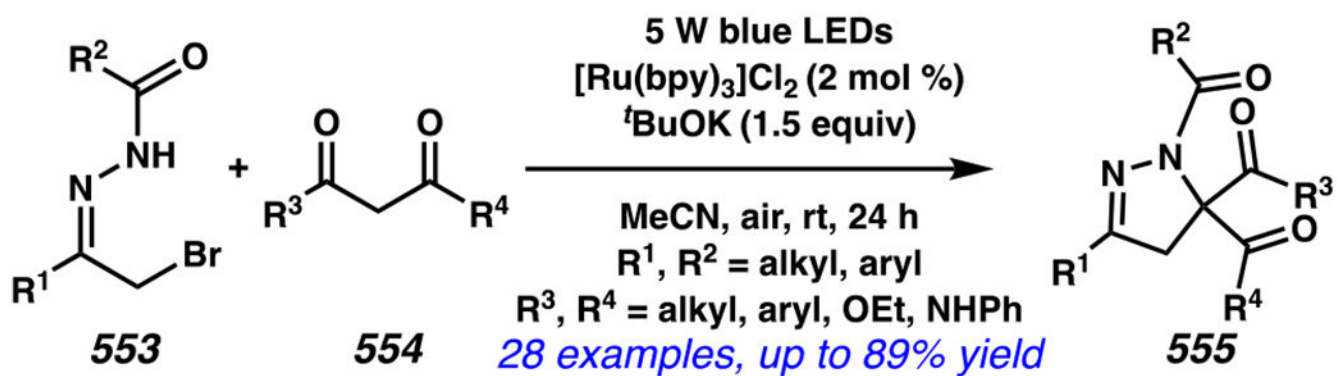
(C) Radical cyclization of  $\beta$ -hindered  $\gamma,\delta$ -unsaturated hydrazones**Scheme 132.**

A Sequential Intramolecular 5-*Exo*-trig Cyclization, Radical Addition, and Aromatization Cascade for the Preparation of Benzosultams

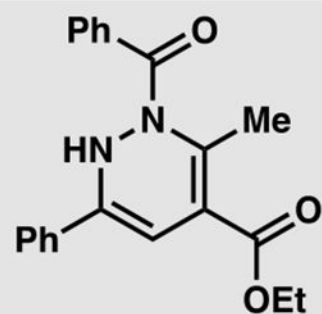


**Scheme 133.**

Hydrazonyl Radical Are Proposed to Engage Sequential Intramolecular 6-*Exo-dig* Cyclization and Radical Smiles Rearrangement



5-*exo*-trig cyclization  
of hydrazonyl radical



product isolated  
absent [Ru] and light

**Scheme 134.**

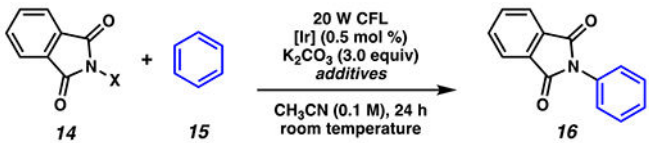
*In Situ*-Generated Hydrazonyl Radical Provides Access to Dihydropyrazoles

Table 1.

C(sp<sup>2</sup>)-H Amination Relies on *N*-Chlorinated Amine

Reaction scheme showing the C(sp<sup>2</sup>)-H amination of benzoxazole (1.0 equiv) with N-chloromorpholine (2.0 equiv) under the following conditions: 3W blue LEDs, (+/-) [Ir(ppy)<sub>2</sub>dtbbpy]PF<sub>6</sub> (1.0 mol %), Ph<sub>3</sub>N (2.0 equiv), CH<sub>2</sub>Cl<sub>2</sub> (0.1 M), room temperature. The product is N-(benzoxazol-2-yl)morpholine.

entry	[Ir(dtbbpy)(ppy) <sub>2</sub> ]PF <sub>6</sub> (present/absent)	yield (%)
1	present	80
2	absent	trace

**Table 2.**C(sp<sup>2</sup>)-H Imidation Proceeds with *In Situ*-Generated *N*-Chlorophthalimide-Derived Radicals


entry	X	[Ir]	additives	yield (%)
1	Cl	Ir(ppy) <sub>3</sub>	–	43
2	Cl	Ir(dFppy) <sub>3</sub>	AcOH (20 mol %)	65
3	H	Ir(dFppy) <sub>3</sub>	<sup>t</sup> BuOH, <sup>t</sup> BuOCl (1 equiv each)	50
4	H	Ir(dFppy) <sub>3</sub>	<i>aq.</i> NaOCl, <sup>t</sup> BuOH, AcOH (1 equiv each)	47
5	OAc	Ir(ppy) <sub>3</sub>	–	n.r.
6	OTs	Ir(ppy) <sub>3</sub>	–	22
7	OTf	Ir(ppy) <sub>3</sub>	–	13
8	OMs	Ir(ppy) <sub>3</sub>	–	20
9	Br	Ir(ppy) <sub>3</sub>	–	4
10	I	Ir(ppy) <sub>3</sub>	–	n.d.